Investigating the impact of the 2D mechanical environment on skin cells cultured in vitro

EVE FLOYD HUNTER-FEATHERSTONE

Department of Biosciences

Investigating the impact of the 2D mechanical environment on skin cells cultured *in vitro*

Eve Floyd Hunter-Featherstone

December 2021

A thesis submitted for the degree of Doctor of Philosophy

Abstract

Mechanotransduction describes a cell's ability to sense mechanical stimuli imparted by its surroundings and translate them into biochemical signals. These signals subsequently influence cell behaviour by promoting remodelling of the cytoskeleton, changes to gene expression and tumour suppression. This is particularly important for tissues with a high cell turnover like the skin. Fibroblasts and keratinocytes, the skin's predominant cell populations, have been shown to respond to physical stimuli such as stretch, compression and shear forces, leading to changes in collagen deposition, and proliferation and migration.

During *in vitro* cell culture it is conventional to use extremely stiff substrates that do not reflect the physiological microenvironment (e.g., plastic and glass). Whilst there have been attempts to limit this issue with the development of 3D tissue models, cells are still first being cultured, or "primed", on a highly stiff surface.

The aim of this project was to investigate keratinocyte and fibroblast behaviour, phenotype, and genotype expression when cultured on biomimetic hydrogel-coated dishes with similar mechanical properties to their *in vivo* environment. It was hypothesised that optimisation of this 2D culture environment would facilitate the development of 3D skin equivalents that better reflected *in vivo* tissue than current models grown from cells primed on plastic.

This study showed that primary keratinocytes and fibroblasts cultured on biomimetic substrates were more reminiscent of cells in quiescent skin rather than the activated phenotype observed on plastic. Keratinocytes exhibited reduced nuclear and cytoplasmic stiffness in response to a 4 kPa culture substrate, and changes were observed in the expression of proliferation and differentiation markers, and proteins involved in mechanosensing. Epidermal 3D models produced using keratinocytes primed on 50 kPa dishes were thicker and better organised. Fibroblasts cultured on soft 2D substrates of 1 kPa and 4 kPa were observed to have fewer reactive oxygen species and expressed fewer DNA damage markers following irradiation to induce senescence.

Dedication

For Charlie, who provided the unjudgmental emotional support that only a dog can, and who sat under my desk for the countless hours it took to put this thesis together.

Acknowledgements

I would like to start by acknowledging the BBSRC and Procter & Gamble for funding this project. I thank my supervisory team, Dr. Akis Karakesisoglou, Dr. Martin Goldberg, Dr. Adam Benham and Dr. Gabrielle Saretzki for supporting me at various stages over the past five years and for allowing me to learn from them. Thank you to Miss Joanne Robson for her assistance with imaging the biomimetic coverslips, and to Dr. Pablo Cubillas for his assistance with the AFM work.

To the former and current members of the ACAS postgraduates who made this experience so enjoyable (and bearable) on a day-to-day basis. Thank you Bek (for always being the calming voice of reason at any time of day or night), Lydia (for being a shining ray of positivity and for always lending a sympathetic ear), Kleo (for being my partner in crime and the best of drinking buddies), Matt (for your sarcasm, down to earth mentality, and 9 years of friendship [give or take a few arguments]), Melissa (for being with me every step of this journey and for always cheering me up), Steve (for the hugs, the gossip, and the prosecco evenings), Kirsty (for always listening and offering sage advice), and Kat (for being a rock of support and motivating me during my final months). Thanks also go to Alex, Ra'ad, Dan, Caroline, Alexia, Ben, Henry, Claire, Nicole and Lucy.

Thank you to Prof. Pali Hungin for offering his assistance at a time when I was struggling most with thesis writing, and for providing motivational pep talks, writing tips, and achievable deadlines to help me find my momentum again.

To Mum and Dad, without whom I would never have made it this far in my academic career. Thank you for the years of unwavering support, for providing a space for me to grow into my own interests, for riding the rollercoaster of career U-turns over the years (you were right, I probably would have gotten sick of being a zookeeper), and for latterly helping to push me over the final hurdle of thesis writing. Thank you to my grandma, Maeve Floyd, for giving me a safe place to escape to when things got tough, and for providing me with copious amounts of wine and quiet, non-pushy support during my thesis writing journey. Thank you to Miles, for always having my

back and for being the only person who spoke to me about normal things and never once asked how my PhD/thesis was going (you have no idea how much that meant). To Mairi and Pete, thank you for always taking an interest in my work, and for your steadfast belief that I would make it to the end. To Bella, for unlimited dog cuddles when I needed them most.

Fiona. For being my best friend for the past 20 years and for always offering your unwavering love and support. Having you there throughout this process has meant the world and I hope one day I can repay the favour ten-fold.

Finally, my endless love and appreciation goes to my husband Ian. For never once doubting me, for never ever pushing me, for putting up with me being a penniless student for 9 years, and for dealing with the many emotional mood swings this PhD has engendered. I could not have done this without you.

Declaration

The work described herein was carried out in the Department of Biosciences, University of Durham between October 2016 and March 2021. All of the work is my own, except where specifically stated otherwise. No part has previously been submitted for a degree at this or any other university.

Statement of Copyright

Publications arising from this work

Papers

Hunter-Featherstone, E., Young, N., Chamberlain, K., Cubillas, P., Hulette, B., Wei, X., Tiesman, J.P., Bascom, C.C., Benham, A.M., Goldberg, M.W., Saretzki, G., Karakesisoglou, I. (2021). Culturing Keratinocytes on Biomimetic Substrates Facilitates Improved Epidermal Assembly In Vitro. *Cells*, 10(5):, 1177. https://doi.org/10.3390/cells10051177

Oral presentations

Hunter-Featherstone, E. (2019). The Role of Extracellular Mechanics in Skin Tissue Engineering and Ageing. Newcastle Liverpool Durham BBSRC-DTP Conference. Durham, UK.

Hunter-Featherstone, E. (2019). The Role of Extracellular Mechanics in Skin Tissue Engineering and Ageing. Durham University Biosciences Postgraduate Conference. Durham, UK.

Hunter-Featherstone, E. (2020). The Role of Extracellular Mechanics in Skin Tissue Engineering and Ageing. Summer Biomechanics, Bioengineering, & Biotransport Virtual Conference. US.

Poster presentations

Hunter-Featherstone, E. (2017). The Role of Extracellular Mechanics in Skin Tissue Engineering and Ageing. Newcastle Liverpool Durham BBSRC-DTP Conference. Durham, UK.

Hunter-Featherstone, E. (2018). The Role of Extracellular Mechanics in Skin Tissue Engineering and Ageing. Durham University Biosciences Research Away Day. Durham, UK.

Hunter-Featherstone, E. (2018). The Role of Extracellular Mechanics in Skin Tissue Engineering and Ageing. Durham University Biosciences Postgraduate Conference. Durham, UK.

Hunter-Featherstone, E. (2019). The Role of Extracellular Mechanics in Skin Tissue Engineering and Ageing. Physics Of Living Matter Symposium 14th Edition. Cambridge, UK.

Hunter-Featherstone, E. (2020) The Role of Extracellular Mechanics in Skin Tissue Engineering and Ageing. Durham University Biosciences Research Away Day. Durham, UK.

Table of Contents

ABSTRACT I

DEDICATION II

ACKNOWLEDGEMENTS III

DECLARATION V

STATEMENT OF COPYRIGHT V

PUBLICATIONS ARISING FROM THIS WORK VI

Papers ..... **vi**

Oral presentations ..... **vi**

Poster presentations ..... **vi**

TABLE OF CONTENTS VIII

LIST OF TABLES XXIII

ABBREVIATIONS XXIV

1 INTRODUCTION 1

1.1 Overview of Thesis **1**

1.2 Background **5**

1.2.1 Mechanotransduction and the mechanosensing machinery of the skin ... 6

1.2.1.1 Ion Channels 6

1.2.1.2 Cell adhesion complexes 9

1.2.1.3 Cytoskeletal proteins 11

1.2.1.4 The LINC complex 13

1.2.1.5 The Hippo signalling pathway 14

1.2.2 The biomechanical environment of human skin 16
1.2.3 Culturing cells in 2D and the negative impacts of tissue culture plastic 19
1.2.4 Methods of 3D skin model production and their limitations 21
1.3 Project aims and objectives 23
1.3.1 Aims 23
1.3.2 Objectives 24
2 MATERIALS AND METHODS 26
2.1 2D Cell culture 26
2.1.1 Human immortal keratinocyte cell line, HaCaT 26
2.1.2 Human epidermal keratinocytes, neonatal 27
2.1.3 Human dermal fibroblasts, neonatal 27
2.2 3D cell culture 28
2.2.1 Hanging drop spheroid models, full thickness 28
2.2.2 BRANDplates® epidermal equivalents, HEKn 29
2.3 Characterisation of cell function and phenotype 29
2.3.1 Cell density measurements 29
2.3.2 EdU proliferation assay 30
2.3.3 Repeat propagations on biomimetic dishes 31
2.3.4 Flow cytometry to measure mitochondrial reactive oxygen species 31
2.3.5 WaferGen 32
2.4 Assessment of nuclear and cytoskeletal mechanics 33
2.4.1 Immunocytochemistry 33
2.4.2 western blotting 35
2.4.3 Osmotic shock assay 38
2.4.4 Atomic force microscopy 39

2.5 Characterisation of 3D skin models 40

2.5.1 OCT embedding hanging drops 40

2.5.2 Paraffin embedding BRANDplates® epidermal equivalents 40

2.5.3 Haematoxylin and Eosin (H&E) staining of BRANDplates® epidermal equivalents 41

2.5.4 Immunohistochemistry of 3D skin models 41

2.5.5 Lucifer yellow barrier permeability assay 42

3 INVESTIGATING THE EFFECTS OF SUBSTRATE STIFFNESS ON KERATINOCYTE FUNCTION 44

3.1 Introduction 44

3.1.1 The role of biomechanics in epidermal assembly 45

3.1.2 Changes in mechanical stimuli between the epidermal layers 46

3.1.3 The use of biomimetic substrates in cell culture 48

3.1.4 Considerations for selecting the appropriate substrate stiffness for culturing epidermal keratinocytes 49

3.1.5 Considering the use of HaCaT cells versus primary keratinocytes for *in vitro* epidermal investigation 50

3.2 Hypotheses and Aims 52

3.3 Objectives 53

3.4 Results 53

3.4.1 Technical challenges faced when working with biomimetic hydrogel cultureware 53

3.4.1.1 Trypsin EDTA does not dissociate cells from hydrogel-coated dishes 53

3.4.1.2 Primary keratinocytes cannot be propagated beyond one passage on very soft hydrogels 57

3.4.1.3 Petrisoft™ hydrogel-coated dishes exhibited batch variability that affected cell growth 59

3.4.1.4 HEKn cultured on BM coverslips were difficult to image by confocal microscopy 61

3.4.1.5 HEKn protein yield for lysates was initially poor 66

3.4.2 Keratinocytes cultured on softer substrates exhibited increased cell density 67

3.4.2.1 HaCaT cells had a more 3D appearance on BM hydrogels 67

3.4.2.2 HEKn cultured on BM hydrogels exhibited greater cell density and cobblestone morphology 70

3.4.3 Culturing keratinocytes on softer substrates led to decreased proliferation and a shift towards differentiation 73

3.4.3.1 HaCaTs cultured on BM hydrogels exhibited decreased proliferative activity 73

3.4.3.2 HEKn cultured on BM hydrogels exhibited signs of decreased proliferation as a direct result of substrate stiffness 75

3.4.3.3 HEKn cultured on very soft hydrogels exhibited increased expression of epidermal differentiation markers 81

3.5 Discussion 93

3.5.1 HaCaTs on biomimetic hydrogels required an alternative dissociating factor for cell passaging 93

3.5.2 Hydrogel-coated dishes did not always promote the growth of primary HEKn 95

3.5.3 Hydrogel-coated coverslips posed problems for microscopy imaging 97

3.5.4 Harvesting of protein lysates for HEKn was adapted to improve protein yield 100

3.5.5 Keratinocytes cultured on BM hydrogels exhibited increased cell density and reduced proliferation 101

3.5.6 HEKn cultured on soft hydrogels showed greater Hippo pathway activation 103

3.5.7 HEKn cultured on softer substrates exhibited a more differentiated genotype 106

3.6 Conclusions 110

4 INVESTIGATING THE EFFECTS OF SUBSTRATE STIFFNESS ON CYTOSKELETAL ORGANISATION AND NUCLEAR MECHANICS IN KERATINOCYTES 112

4.1 Introduction 112

4.1.1 The role of the cytoskeleton in mechanotransduction 113

4.1.2 Cytoskeletal reorganisation through the epidermal layers 115

4.1.3 Nuclear mechanics and mechanosensing through the LINC complex 117

4.1.4 The LINC complex in the epidermis 118

4.2 Hypotheses and Aims 119

4.3 Objectives 120

4.4 Results 120

4.4.1 HaCaTs cultured on softer substrates exhibited changes in cytoskeletal and LINC protein expression 121

4.4.1.1 HaCaT cells exhibited some changes in core cytoskeletal components when cultured on soft substrates 121

4.4.1.2 HaCaT cells exhibited decreased levels of LINC complex proteins when cultured on softer substrates 123

4.4.2 Deeper investigation into Hippo pathway components could not be easily carried out in keratinocytes 125

4.4.3 Cytoskeletal and cell junctional proteins were altered in HEKn cultured on BM hydrogels 128

4.4.3.1 HEKn cultured on BM hydrogels exhibited changes in cytoskeleton and cell junction protein levels and localisation 129

4.4.3.2 HEKn cultured on BM hydrogels exhibited changes in the gene expression of cytoskeletal and cell junction components 137

4.4.4 HEKn cultured on BM hydrogels exhibited changes in LINC complex protein levels and gene expression 142

4.4.4.1 western blot analysis revealed reduced levels of core LINC proteins in HEKn on softer substrates 142

4.4.4.2 Gene expression of LINC complex and Nuclear Pore Complex proteins changed in response to culturing HEKn on BM dishes..... 147

4.4.5 HEKn cultured on BM hydrogels were observed to be softer..... 154

4.4.5.1 HEKn on BM hydrogels exhibited greater nuclear deformation in response to osmotic shock 154

4.4.5.2 AFM analysis revealed HEKn cultured on 4 kPa hydrogels had softer nuclei and cytoplasm..... 155

4.4.5.3 Keratinocyte differentiation induces changes in some LINC complex proteins..... 157

4.5 Discussion 158

4.5.1 HaCaTs exhibited some changes in cytoskeletal protein levels in response to softer culture dishes..... 159

4.5.2 HaCaTs cultured on hydrogel-coated dishes exhibited reduced protein levels of core LINC complex components 162

4.5.3 Exploration of Hippo pathway protein levels met with complications..... 165

4.5.4 HEKn cultured on softer substrates exhibited changes in cytoskeletal and cytoskeletal associated protein levels and organisation..... 168

4.5.5 HEKn cultured on BM hydrogels exhibited gene expression changes in cytoskeletal and cytoskeletal-associated proteins 173

4.5.6 HEKn exhibited reduced protein levels of core LINC complex and LINC associated proteins in response to softer substrates 177

4.5.7 HEKn cultured on BM hydrogels exhibited gene expression changes in NE proteins 180

4.5.8 HEKn tuned their nuclear and cytoplasmic stiffness based on the rigidity of their culture dish 183

4.5.9 HEKn cultured in high calcium medium exhibited changes in some LINC complex proteins suggesting an association with differentiation 185

4.6 Conclusions 186

5 INVESTIGATING THE EFFECTS OF 2D SUBSTRATE STIFFNESS ON THE DEVELOPMENT OF 3D EPIDERMAL MODELS *IN VITRO* 189

5.1 Introduction 189

5.1.1 *In vitro* 3D skin models and their role in epidermal research 190

5.1.2 The limitations of current 3D epidermal models 191

5.2 Hypotheses and Aims 192

5.3 Objectives 193

5.4 Results 193

5.4.1 Early EE development encountered many technical problems that affected model quality 196

5.4.2 Hanging drop spheroid models provided new insight into the effects of substrate stiffness on HEKn behaviour in 3D culture 203

5.4.3 HEKn primed on 50 kPa BM dishes produced thicker and more organised EEs 210

5.4.4 Assessing barrier function proved difficult with the BRAND*plates*™ system 215

5.4.5 HEKn primed on 50 kPa dishes were more responsive to extended time at ALI during EE development 217

5.4.6 Combining 50 kPa and 4 kPa primed HEKn did not produce optimal EEs 218

5.5.7 Pre-screening HEKn for basal phenotype cells greatly improved organisation of TCP primed EEs 220

5.5 Discussion 223

5.5.1 Early experiments focused on troubleshooting the development of EEs produced from TCP primed HEKn 224

5.5.2 Culturing TCP and 4 kPa primed HEKn in hanging drops provided new insights into how 2D stiffness affects model development 226

5.5.3 HEKn primed on 50 kPa BM dishes in 2D produced far superior 3D epidermal models 229

5.5.4 Barrier function in an unchallenged epidermis did not differ between TCP and 50 kPa primed EEs 232

5.5.5 Suboptimal EEs produced from 50 kPa primed HEKn exhibited improved appearance following extended culture time 233

5.5.6 The mixing of 50 kPa and 4 kPa primed cells to produce EEs requires further optimisation 234

5.5.7 TCP primed HEKn screened for a basal phenotype prior to model set-up produced EEs similar to 50 kPa primed 235

5.6 Conclusions 237

6 INVESTIGATING THE EFFECTS OF *IN VITRO* SUBSTRATE STIFFNESS ON FIBROBLAST BEHAVIOUR AND SENESCENCE 239

6.1 Introduction 239

6.1.1 The dermal ECM and the mechanical changes induced by skin ageing 240

6.1.2 Fibroblast senescence and the effects on external and internal mechanics 241

6.1.3 The effects of substrate stiffness on fibroblast activation *in vitro* 243

6.2 Hypotheses and Aims 244

6.3 Objectives **245**

6.4 Results **245**

6.4.1 HDFn cultured on BM dishes appeared more proliferative and had reduced nuclear area 246

6.4.2 HDFn cultured on BM dishes did not appear as susceptible to x-ray irradiation as those on TCP 252

6.4.3 HDFn cultured on BM dishes were observed to have fewer ROS 258

6.4.4 Technical challenges arose when culturing HDFn on hydrogel-coated dishes

6.5 Discussion **264**

6.5.1 Early differences observed between HDFn on hydrogel-coated dishes versus TCP 265

6.5.2 HDFn cultured on BM dishes differed to those on TCP following irradiation 268

6.5.3 HDFn cultured on BM dishes exhibited reduced levels of ROS 271

6.5.4 The use of BM dishes presented technical problems that hindered the culture of HDFn 272

6.5.5 Additional experiments that could not be completed 274

6.6 Conclusions **274**

7 SUMMARY AND FINAL DISCUSSION 277

7.1 Skin cells cultured on BM dishes could be more reflective of their *in vivo* counterparts 277

7.2 Priming skin cells in a more realistic mechanical environment could be used to produce superior 3D skin models 279

7.3 Culturing HEKn and HDFn on BM cultureware required adaptation of standard 2D cell culture techniques 281

8 REFERENCES 284

List of Figures

Figure 1.1 Schematic illustration of models of mechanical gating in ion channels 8
Figure 1.2 Schematic illustration of cell adhesion complexes. 10
Figure 1.3 Schematic illustration of the LINC complex 14
Figure 1.4 Schematic illustration of Hippo signalling pathway activation 15
Figure 1.5 Histology image of human skin 17
Figure 1.6 Schematic illustration showing the average Young's Modulus values of different human tissues 20
Figure 3.1 HaCaTs cultured on 4 kPa hydrogels do not dissociate with trypsin-EDTA 54
Figure 3.2 BM hydrogels absorbed medium during culture and acquired a high serum content 55
Figure 3.3 HaCaTs cultured on 4 kPa hydrogels were successfully dissociated using TrypLE™ Express Enzyme. 56
Figure 3.4 HEKn could not be cultured on 4 kPa hydrogels beyond one passage 57
Figure 3.5 HEKn cultured on 4 kPa hydrogels were able to reattach for a second passage if seeded back onto TCP 59
Figure 3.6 HEKn were observed not to attach or proliferate when seeded onto certain batches of BM dishes 60
Figure 3.7 Coverslips coated with hydrogel had an increased distance between the microscope objective and cells 61
Figure 3.8 Confocal images taken of HEKn on BM coverslips were unfocused 62
Figure 3.9 Mounting BM coverslips on glass bottom dishes improved confocal image quality 63
Figure 3.10 Using an objective with a greater free working distance improved confocal image quality for BM coverslips 65
Figure 3.11 HEKn lysates had a better protein yield when cells were incubated with lysis buffer on ice 66
Figure 3.12 HaCaTs cultured on BM hydrogels exhibited increased cell density within colonies 68

Figure 3.13 HEKn cultured on BM hydrogels had a greater cell density 71
Figure 3.14 HEKn cultured on BM dishes under high calcium conditions still exhibited greater cell density. 72
Figure 3.15 HaCaTs cultured on BM hydrogels exhibited decreased proliferative activity. 73
Figure 3.16 HEKn cultured on BM substrates exhibited decreased proliferative activity. 75
Figure 3.17 HEKn cultured on glass coverslips showed a greater Integrated Density of YAP1 staining 77
Figure 3.18 RNA analysis of the Hippo signalling pathway revealed changes in expression when HEKn were cultured on BM hydrogels 81
Figure 3.19 HEKn cultured on 4 kPa hydrogels showed increased expression of the differentiation marker cytokeratin 10 82
Figure 3.20 HEKn cultured on BM hydrogels exhibited a downregulation of TP63 after 4 days of culture 84
Figure 3.21 HEKn cultured on BM hydrogels exhibited downregulation of the basal stem cell markers ITGA6 and ITGB1 85
Figure 3.22 HEKn cultured on BM hydrogels exhibited downregulation of ROCK1 and ROCK2 87
Figure 3.23 HEKn cultured on BM hydrogels exhibited a downregulation in AKT1 expression 89
Figure 3.24 HEKn cutured on BM hydrogels exhibited upregulated expression of HES1 91
Figure 3.25 HEKn cultured on BM hydrogels exhibited downregulation of PTCH192
Figure 4.1 HaCaTs cultured on BM hydrogels exhibited changes in cytoskeletal protein levels 121
Figure 4.2 HaCaTs cultured on BM hydrogels exhibited changes in LINC protein levels 124
Figure 4.3 HaCaTs assessed for YAP1 levels through western blotting presented with bands of the incorrect molecular weight. 125

Figure 4.4 Mouse brain and neuronal lysates confirmed that the Santa Cruz anti-KIBRA antibody SC-133374 showed specificity for multiple known KIBRA isoforms 126
Figure 4.5 KIBRA was observed to localise at the Golgi apparatus in HEKn 128
Figure 4.6 HEKn cultured on soft hydrogels had lower β-actin levels 129
Figure 4.7 HEKn cultured on glass coverslips showed a greater number of basal actin fibres..... 131
Figure 4.8 No change in microtubule organisation was observed between HEKn cultured on glass and 4 kPa coverslips 133
Figure 4.9 HEKn cultured on 4 kPa coverslips exhibited perinuclear plectin staining 134
Figure 4.10 HEKn cultured on 4 kPa coverslips exhibited linear E-cadherin staining rather than punctate 135
Figure 4.11 HEKn cultured on 4 kPa coverslips exhibited perinuclear E-cadherin staining 136
Figure 4.12 RNA analysis revealed significant downregulation of actin and vinculin when HEKn were cultured on BM hydrogels..... 138
Figure 4.13 RNA analysis revealed significant downregulation of tubulin when HEKn were cultured on BM hydrogels 140
Figure 4.14 RNA analysis revealed some downregulation of adhesion proteins when HEKn were cultured on BM hydrogels 141
Figure 4.15 HEKn cultured on BM hydrogels exhibited decreased Lamin levels ..143
Figure 4.16 HEKn cultured on BM hydrogels exhibited decreased levels of multiple nesprin-1 isoforms 144
Figure 4.17 HEKn cultured on BM hydrogels showed some reduction in nesprin-2 levels 147
Figure 4.18 RNA analysis revealed no statistically significant change in emerin expression in HEKn cultured on BM hydrogels..... 148
Figure 4.19 RNA analysis revealed significant downregulation of Lamins in HEKn cultured on BM hydrogels 149

Figure 4.20 RNA analysis revealed no statistically significant changes in SUN1 and SUN2 expression in HEKn cultured on BM hydrogels. 150
Figure 4.21 RNA analysis revealed significant changes in nesprin expression in HEKn cultured on BM hydrogels 151
Figure 4.22 RNA analysis revealed significant changes in the expression of NPC components in HEKn cultured on BM hydrogels 154
Figure 4.23 HEKn cultured on 4 kPa dishes exhibited more nuclear deformation following osmotic shock 155
Figure 4.24 HEKn cultured on 4 kPa hydrogels had a lower Young's Modulus than those on TCP 156
Figure 4.25 Differentiated HEKn exhibited changes in emerin and Lamin B1 levels 158
Figure 5.1 Schematic outlining the key methodologies used to generate 3D EEs for this thesis 196
Figure 5.2 Early EE models were poorly developed and showed abnormal differentiation 196
Figure 5.3 Neutral red staining of EEs showed that HEKn adhered to PET membrane regardless of the presence of coating matrix 198
Figure 5.4 A reasonable proportion of HEKn were observed to be binucleated. During 2D culture of Gibco™ HEKn it was observed that many of the cells were binucleated 199
Figure 5.5 HEKn cultured on BRANDplates™ PC inserts produced superior EEs 200
Figure 5.6 HEKn showed superior epidermal assembly in the presence of Matrigel® 201
Figure 5.7 HEKn primed on TCP and 4 kPa BM dishes showed different aggregation patters when transferred into hanging droplets 204
Figure 5.8 HEKn primed on 4 kPa BM dishes were unable to coat a dermal spheroid when transferred into hanging droplets 205
Figure 5.9 Immunofluorescence analysis of hanging droplets confirmed HEKn primed on 4 kPa did not coat dermal spheroids 206

Figure 5.10 HEKn cultured in hanging droplets of high calcium medium were better able to coat a dermal spheroid 207
Figure 5.11 Culturing TCP and 4 kPa primed HEKn in the same hanging droplet may lead to organised epidermal assembly under high calcium conditions..... 209
Figure 5.12 HEKn primed on 50 kPa BM dishes produced thicker EEs than TCP and 4 kPa dishes..... 210
Figure 5.13 HEKn primed on 50 kPa dishes had more columnar basal cells than those on TCP in EEs 213
Figure 5.14 HEKn primed on 50 kPa dishes had more defined epidermal layers and clearer E-cadherin staining in EEs 214
Figure 5.15 Lucifer Yellow barrier function assay was difficult using the BRANDplates™ culture system..... 216
Figure 5.16 HEKn primed on 50 kPa dishes had the same barrier function as TCP217
Figure 5.17 HEKn primed on 50 kPa BM dishes showed greater improvement following longer culture time at the ALI 218
Figure 5.18 Mixing 50 kPa and 4 kPa primed HEKn produced an EE of intermediate quality 219
Figure 5.19 EEs produced from TCP primed HEKn pre-screened for basal cell phenotype cells produced more organised models that were reminiscent of 50 kPa primed 222
Figure 5.20 HEKn primed on 50 kPa dishes did not seem affected by pre-screening for basal cells..... 223
Figure 6.1 HDFn cultured on 1 kPa dishes appeared denser than those on TCP after 5 days of culture 246
Figure 6.2 HDFn cultured on BM dishes had a greater average PDL after one passage than cells on TCP..... 248
Figure 6.3 HDFn cultured on BM coverslips had fewer ki67 positive nuclei than cells on glass. HDFn were cultured on glass and BM coverslips and immunostained for the proliferation marker ki67..... 249
Figure 6.4 HDFn cultured on BM coverslips had reduced nuclear area and perimeter compared to those on glass..... 251

Figure 6.5 HDFn cultured on BM dishes did not appear to alter appearance following irradiation.....253
Figure 6.6 HDFn cultured on BM dishes had fewer DNA damage foci following irradiation than those on TCP.....254
Figure 6.7 HDFn cultured on BM dishes may have had more DNA damage foci than TCP 10 days after irradiation.....255
Figure 6.8 HDFn cultured on BM dishes may have had higher p21 expression than TCP 10 days after irradiation.....256
Figure 6.9 Immunofluorescence staining of p16INK4a could not be optimised 258
Figure 6.10 HDFn cultured on BM dishes exhibited reduced mitochondrial mass and ROS compared to TCP.....259
Figure 6.11 HDFn were difficult to dissociate from BM dishes.....262
Figure 6.12 A significant proportion of BM dishes developed a stain within the hydrogel on which HDFn would not grow.....263

List of Tables

Table 2.1 Probes and dyes used for flow cytometry of irradiated HDFn 32

Table 2.2 Primary (top) and secondary (bottom) antibodies used for the immunostaining of cells cultured in 2D or 3D environments. 34

Table 2.3 Primary (top) and secondary (bottom) antibodies used in western blotting 37

Abbreviations

2D – Two-Dimensional

3D – Three-Dimensional

AFM – Atomic Force Microscope

ALI – Air-Liquid Interface

APS – Ammonium Persulfate

BM – Biomimetic

BSA – Bovine Serum Albumin

$CaCl_2$ – Calcium Chloride

CK – Cytokeratin

DAPI – 4′,6-Diamidine-2′-phenylindole dihydrochloride

DDR – DNA Damage Response

DHE – Dihydroethidium

DHR – Dihydrorhodamine123

diH_2O – Deionised Water

DMEM – Dulbecco's Modified Eagle Medium

DMSO – Dimethyl Sulfoxide

DNA – Deoxyribonucleic Acid

DPBS – Dulbecco's Phosphate Buffered Saline

ECM – Extracellular Matrix

EEs – Epidermal Equivalents

FACS – Fluorescence-Activated Cell Sorting

FBS – Fetal Bovine Serum

GAGs – Glycosaminoglycans

GPa – Gigapascal

HDFn – Human Dermal Fibroblasts, neonatal

H&E – Haematoxylin and Eosin

HEKn – Human Epidermal Keratinocytes, neonatal

HKGS – Human Keratinocyte Growth Supplement

KASH – Klarsicht/ANC-1/Syne Homology

KGF – Keratinocyte Growth Factor

KIBRA – Kidney/Brain Protein

kPa – Kilopascal

LATS – Large Tumour Suppressor

LDH – Lactate Dehydrogenase

LINC - Linker of Nucleoskeleton and Cytoskeleton

MMPs - Matrix Metalloproteases

MST – Mammalian Sterile Twenty

NAO – 10-*n*-nonyl-acridine

NE – Nuclear Envelope

NPC – Nuclear Pore Complex

OCT – Optimal Cutting Temperature Compound

p63 – Tumour Protein 63

PBG – Immunofluorescence Blocking Solution

PBS – Phosphate Buffered Saline (prepared in the laboratory)

PC – Polycarbonate

PDL – Population Doubling Level

PEG – Poly(Ethylene Glycol)

PET – Polyester

PFA – Paraformaldehyde

P&G – Procter and Gamble

Rap1 – Ras-associated protein-1

RLT – RNeasy Lysis Buffer

ROCK – Rho-associated Kinase

rpm – Revolutions Per Minute

SASP – Senescence-Associated Secretory Phenotype

SAV – Salvador

SDS – Sodium Dodecyl Sulfate

SHH – Sonic Hedgehog

SMA – Smooth Muscle Actin

SUN – Sad1p UNC-84

TAZ – Transcriptional Coactivator with PDZ-binding motif

TBS-(T) – Tris Buffered Saline-(+ 0.1% Tween 20)

TCP – Tissue Culture Plastic

TEMED – Tetramethylethylenediamine

YAP – Yes-Associated Protein

1 Introduction

1.1 Overview of Thesis

The research presented in this thesis focuses on investigating the effects of two-dimensional (2D) culture surface stiffness on the behaviour, morphology, gene, and protein expression of human epidermal keratinocytes and dermal fibroblasts. Early studies using micropatterning approaches to alter the topology of 2D surfaces first enabled scientists to investigate how changes to the microenvironment affects cell morphogenesis and function (Ito, 1999). These findings later led to the development of membranes and scaffolds that facilitated the production of three-dimensional (3D) tissue models. These were designed to provide cells with a mechanical environment similar to their native tissue, and enabled the investigation of cell attachment, growth, and extracellular matrix (ECM) formation in a 3D setting (Melchels et al., 2011; Zeltinger et al., 2001; Hollister, Maddox and Taboas, 2002; Van Bael et al., 2012).

However, whilst 3D tissue engineering is clearly a vital tool for the future of cell culture, it is a slower and less cost-effective technique than 2D culture. As such, the fact remains that the majority of *in vitro* cell work is still performed using traditional 2D techniques that rely on materials such as tissue culture plastic (TCP) and glass. The implications of this are two-fold; firstly, that all studies performed on cells cultured on TCP cultureware *in vitro* have the potential to have altered gene and protein expression compared to their *in vivo* counterparts as a result of an inappropriate mechanical environment. Secondly, cells subsequently used to set up 3D tissue models may already have altered gene expression to *in vivo* cells, which could impact model development as the cells acclimatise to the different external mechanical signals. Consequently, this calls into question the reliability of all data that TCP or glass cultureware have played a role in the production of.

The skin is a high turnover tissue that is subject to both macroscopic mechanical changes, resulting from physical manipulation of the tissue, and microscopic mechanical changes caused by factors such as remodelling of the dermal ECM, and migration of epidermal cells away from the stiff basement membrane. Fibroblasts and

keratinocytes, the skin's predominant cell populations, have been shown to respond to physical stimuli such as stretch, compression, and shear forces, leading to changes in collagen deposition, and proliferation and migration respectively (Wong, Longaker and Gurtner, 2012). The development and characterisation of *in vitro* 3D skin models is a large field given their use as an alternative to animal models for dermopharmaceutical testings, and their potential in a clinical setting for producing skin grafts for patients such as burn sufferers (Jean, Garcia-Pérez and Pouliot, 2011). However, the study of skin cells is subject to the same culture limitations as mentioned in the previous paragraph.

The basis of this thesis is to explore three main questions regarding biomimetic (BM) substrate utilisation in the 2D culture of skin cells; firstly, does BM cultureware offer a comparable ease of use and cost-effectiveness to TCP thus making it a viable alternative? Secondly, what impact does the culturing of skin cells on BM cultureware have on their behaviour, gene expression, and phenotype in comparison to TCP? And thirdly, does culturing skin cells on BM cultureware prior to setting up 3D skin models improve model appearance and development? Individual literature reviews have been conducted for each focused area of research to determine clear rationales for each step in the process. This work is broad in scope and provides a preliminary foundation that supports a more widespread implementation of mechanically relevant cultureware into 2D cell culture techniques. The general introduction introduces the mechanisms by which cells detect their mechanical environment and begins to examine the relevance of mechanics in *in vivo* skin during both quiescent tissue maintenance, and in skin ageing. This is underpinned by explorations into current culture practices when working with skin cells *in vitro*.

Chapter 3 begins by introducing the cultureware chosen for this project which were TCP dishes/plates and glass coverslips coated with a very thin layer of a polyacrylamide hydrogel. Through changing the concentration of polyacrylamide, it is possible to alter the stiffness of the hydrogel, and thus a range of stiffnesses aimed at replicating the epidermal mechanical environment were used. The literature review explores the rationale behind the dishes chosen, the cell types selected, and

draws attention to the role of mechanical cues in the epidermis. This chapter then goes on to provide an early comparison between primary keratinocytes cultured on TCP versus BM hydrogel-coated dishes. It first highlights parts of the standard cell culture protocol for which the hydrogel coating posed an issue, and how these problems were troubleshooted. The main bulk of the results in this chapter are then focused on exploring the shift keratinocytes underwent from being highly proliferative on TCP dishes, to less proliferative on BM dishes with the upregulation of some differentiation markers. This chapter highlights that BM dishes do have the potential to provide a viable alternative to TCP in standard 2D cell culture and draws attention to the highly activated phenotype of keratinocytes cultured on TCP.

Chapter 4 begins to expand on the molecular differences between keratinocytes cultured on TCP and BM dishes, with particular focus on proteins associated with mechanotransduction. The literature review explores the changes in cytoskeletal expression in keratinocytes undergoing terminal differentiation and looks at the role of the cytoskeleton in mechanosensing. It then goes on to introduce the role of the Linker of Nucleoskeleton and Cytoskeleton (LINC) complex in the epidermis and how changes to LINC protein expression can affect keratinocyte behaviour. The chapter directly compares the gene expression, protein expression, and localisation of key cytoskeleton and LINC complex proteins in keratinocytes cultured on TCP and BM cultureware. The implication of these altered expressions on the stiffness of the cells themselves was investigated through atomic force microscopy (AFM) which revealed that the keratinocytes adapted their nuclear and cytoplasmic stiffness in response to the mechanics of their culture dish. This chapter concludes by beginning to investigate whether the changes observed in cytoskeletal and LINC proteins are a direct reflection of the mechanical environment, or if they are an effect of the change in the balance between proliferation and differentiation presented in chapter 3.

Chapter 5 turns the attention towards the development of 3D epidermal models, and the effects of priming keratinocytes on 2D BM dishes prior to model set up. The literature review introduces the current techniques for producing 3D epidermal equivalents, and then explores the limitations of these techniques. These largely

include a prolonged culture time and lack of reproducibility across laboratories due to complex in-house media recipes and lack of protocol transparency (Bertolero et al., 1984; Faller and Bracher, 2002; Ng and Ikeda, 2011). The literature review concludes by highlighting the potential impact of mechanical memory, and the possibility of a lag period in which cells primed on TCP have to adjust to their new mechanical environment before being able to fully initiate epidermal assembly. This chapter goes on to present the results of this study in which it was demonstrated that culturing keratinocytes on a BM dish of similar mechanics to the basement membrane does in fact produce 3D epidermal models with superior thickness and organisation. This provides a novel insight into how relatively simple changes to 2D culture could be used to further improve the development of 3D tissue models.

Finally, chapter 6 moves away from keratinocytes to provide a preliminary insight into the effects of culturing fibroblasts on 2D BM cultureware. The literature review explores the mechanical environment in the dermis, with particular emphasis on skin ageing, and introduces the effects of senescence on internal cell mechanics. This section then concludes by discussing the observations of previous studies when culturing fibroblasts on softer substrates *in vitro* and highlights the lack of similar work focusing on senescent cells. The chapter continues by presenting the early observable differences between fibroblasts cultured on TCP and BM dishes, and highlights changes in reactive oxygen species (ROS) levels and differences in deoxyribonucleic acid (DNA) damage markers and cell appearance following irradiation to induce senescence. The results of this chapter are not sizeable, but they do provide a striking insight into how even aspects of cell biology not directly linked to mechanosensation may be being influenced by the use of TCP in cell culture.

This work consolidates previous studies exploring the effects of hydrogels on proliferation, differentiation, cell morphology in skin cells cultured *in vitro*. However, this project significantly expands on previous investigations, by providing a novel insight into the effects of hydrogel-coated dishes on the expression and organisation of core mechanoproteins in skin cells. Moreover, this work places an emphasis on the use of BM cultureware for all 2D cell culture work, regardless of whether

biomechanics are the focus of the research. Finally, this study aims to bridge the gap between 2D and 3D culture by recognising and highlighting the impact that mechanical memory might have on the development of tissue models using cells first primed on TCP cultureware.

1.2 Background

Mechanotransduction describes a cell's ability to sense mechanical stimuli from its surroundings, such as stiffness of the ECM, and translate them into biochemical signals (Dupont et al., 2011). These signals subsequently control cell behaviour by influencing remodelling of the cytoskeleton, gene expression and suppression of tumour development (Dupont et al., 2011). The main signalling route involved in this process is the Hippo pathway, which plays a vital role in skin biology and epidermal proliferation (Schlegelmilch et al., 2011). Two key downstream components of the Hippo signalling pathway, are the transcription factors YAP (Yes-associated protein) and TAZ (transcriptional coactivator with PDZ-binding motif) (Dupont et al., 2011). YAP/TAZ are observed to localise in the cytoplasm and nucleus, with nuclear accumulation being key to their functionality (Piccolo, Dupont and Cordenonsi, 2014). This subcellular localisation is mainly controlled through phosphorylation of YAP/TAZ serine residues by Lats1/2 kinases, creating a binding consensus for protein complexes, and thus sequestering the transcription factors to the cytoplasm. Activation of the Hippo pathway has been shown to be controlled by mechanical stimuli. Where the ECM provides a soft substrate, cells and their nuclei are round in shape, reducing the mechanical stimulus and thus resulting in phosphorylation of YAP/TAZ and arrest of cell growth. However, when the ECM is stiff, cells become stretched, which increases the mechanical stimulus and results in YAP/TAZ activation (Piccolo, Dupont and Cordenonsi, 2014). In this instance the transcription factors are not phosphorylated and translocate to the nucleus where they upregulate genes involved in cellular proliferation.

Whilst the Hippo signalling pathway plays a role in all cells, it is particularly important in controlling epidermal proliferation (Schlegelmilch et al., 2011). As a highly proliferative cell type, keratinocytes have an increased risk of becoming

cancerous, and as such YAP/TAZ have an important function in controlling cell growth and suppressing tumour formation (Piccolo, Dupont and Cordenonsi, 2014). Moreover, changes in skin biomechanics are fundamental in inducing age-associated alterations in cell behaviour during the ageing process. Unlike some other tissues, skin undergoes both intrinsic and extrinsic ageing as a result of exposure to UV radiation (Mancini et al., 2014). Aged skin is characterised by dramatic remodelling of the ECM, and a build-up of senescent cells, leading to thinning of the epidermis (Naylor et al., 2011). These changes inevitably affect the mechanical stimuli cells experience, and studies into human skin have shown that ageing results in a loss of ECM stiffness in the dermis due to the degradation of its components (Achterberg et al., 2014). Softening of a substrate causes cells to undergo cell cycle arrest and apoptosis which are both key hallmarks of ageing.

Research into the production of young and aged skin is becoming increasingly prevalent, and as science begins to seek alternatives to animal research, the development of skin models has become an important aspect of this field. However, current skin models fail to take into account the significance of the fact that cells are still being cultured on TCP cultureware prior to model set-up. TCP is known to be significantly stiffer than the *in vivo* mechanical environment (Landry, Rattan and Dixon, 2019) and this has a direct impact on the behaviour and expression profile of cells. Moreover, there is evidence that cell possess "mechanical memory" which means the 2D mechanical environment can influence the behaviour of cells in 3D (Yang et al., 2014). Consequently, the physiological relevance of current tissue models will always be in question as long as prolonged exposure to TCP plays a role in the cell culture process.

1.2.1 Mechanotransduction and the mechanosensing machinery of the skin

1.2.1.1 Ion Channels

The concept of cellular mechanotransduction is reasonably novel, and the mechanism behind it is yet to be fully understood as there are many different layers to mechanosensation. The process itself can be simply explained as external

biomechanical forces being translated into biological cues within a cell, thus impacting its overall behaviour (Wong et al., 2012). Unlike other tissues, the skin possesses a sensory element that allows the brain to detect stimuli outside of the body, such as changes in temperature and objects that come into physical contact with the skin. Whilst it is widely accepted that neurons in the skin detect these stimuli through mechanosensing, it is unclear as to how these signals are translated to the cell, and thus sent to the brain. However, studies into the ion channels involved in neurotransmission, have produced three main models (Figure 1.1) (Lumpkin and Caterina, 2007). Ion channels are well established as key players in cellular activity and have been linked to mechanosensing due to their position as membrane-spanning proteins, providing them with access to both the external and internal environment of a cell (Jiang et al., 2002). It has already been mentioned that in the presence of a stiff ECM, cells become stretched which increases mechanical stimulation (Piccolo et al., 2014). One theory is that when cells flatten, tension in the lipid bilayer is altered which applies force to the ion channels, resulting in conformational changes that facilitate activation of the channel and ion binding/passage through the membrane (Jiang et al., 2002). These are known as stretch-activated ion channels (Figure 1.1A).

A second, similar theory is that the ion channels are physically connected to both the ECM and cytoskeleton, and thus directly detect mechanical changes in ECM proteins (Lumpkin and Caterina, 2007). Studies into sensory hair cells in the ear have found that in order for calcium channels to open and close, they must be connected to crosslinks known as tip links. These tip links directly connect the actin filaments at the tip of a shorter stereocilium, to the lateral wall of an adjacent, taller stereocilium. Destruction of these tip links was observed to completely inactivate ion channels (LeMasurier and Gillespie, 2005), thus suggesting that the crosslinks connected directly to the channels themselves and stimulated opening and closing by transmitting mechanical signals (Figure 1.1B). However, the final model suggests that

in some cells, it is mechanosensitive proteins situated adjacent to the ion channels, that are in fact responsible for detecting mechanical changes, and regulating channel activation (Lumpkin and Caterina, 2007). A study into *Caenorhabditis elegans* found that the absence of long chain polyunsaturated fatty acids, synthesized from dietary precursors, leads to sensory deficits in neurons reliant on transient receptor potential

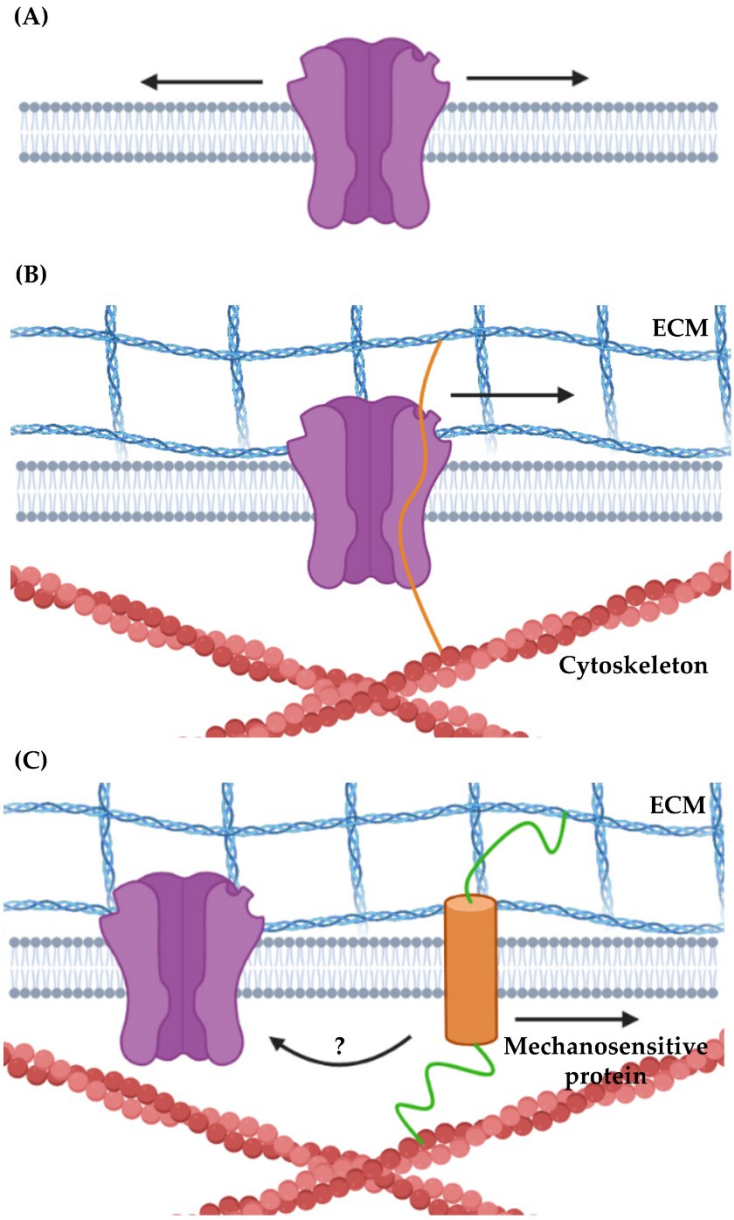

Figure 1.1 Schematic illustration of models of mechanical gating in ion channels. **(A)** *Stretch-activated ion channels open and close in response to changes in lipid bilayer tension.* **(B)** *Tethered ion channels possess crosslinks that connect them to ECM and cytoskeletal proteins. Changes in the tension of these crosslinks causes ion channels to open and close.* **(C)** *Indirect gated ion channels possibly involve a mechanosensitive protein adjacent to the ion channel that regulates its opening through a signalling intermediate. Adapted from Lumpkin and Caterina, 2007. Created using BioRender (https://biorender.io).*

ion channels (Kahn-Kirby et al., 2004). However, this final mechanism leads to significantly slower activation of ion channels than those subject to direct mechanical stimulation, and thus is not deemed the prevalent model used for neural mechanosensing (Lumpkin and Caterina, 2007).

1.2.1.2 Cell adhesion complexes

Mechanosensation is not just important for the action of neurons and detecting physical manipulation of the skin. All cell types are able to detect changes in mechanical stimuli such as alterations in ECM stiffness, and this plays a vital role in controlling cell behaviour and fate. Mechanotransduction involves a complex collection of proteins beginning with those in direct contact with the external environment.

Integrins are formed as heterodimers at the cell membrane and provide the cell with a connection to the surrounding ECM through one of two adhesion complexes: focal adhesions or hemidesmosomes (Figure 1.2A). Focal adhesions supply cells with a direct link between the ECM and the actin cytoskeleton, whilst hemidesmosomes link the ECM, specifically the basement membrane, to intermediate filaments such as keratins (Duperret and Ridky, 2013). In the epidermis, integrin expression is normally confined to the basal layer, with integrin $\alpha 6\beta 4$ primarily concentrated at the basement membrane where it is part of a hemidesmosome complex binding laminin-332 (Watt, 2002). Other integrins are reportedly found over the basal, lateral and apical surfaces of basal cells, and complementary roles have been proposed for $\alpha 3\beta 1$ and $\alpha 6\beta 4$ in mediating keratinocyte adhesion and migration (Watt, 2002).

Cell-cell interactions are formed by cadherin molecules, specifically P-cadherin and E-cadherin in the epidermis, though P-cadherin is only found in the basal layer (Furukawa et al., 1997). E-cadherin plays a vital role in maintaining the epidermal barrier function by forming the adhesive component of cell-cell interactions (Figure

1.2B), and ablation of the E-cadherin gene in the postnatal epidermis of mice has been shown to result in severe disruption of adherens junctions (Young, 2003).

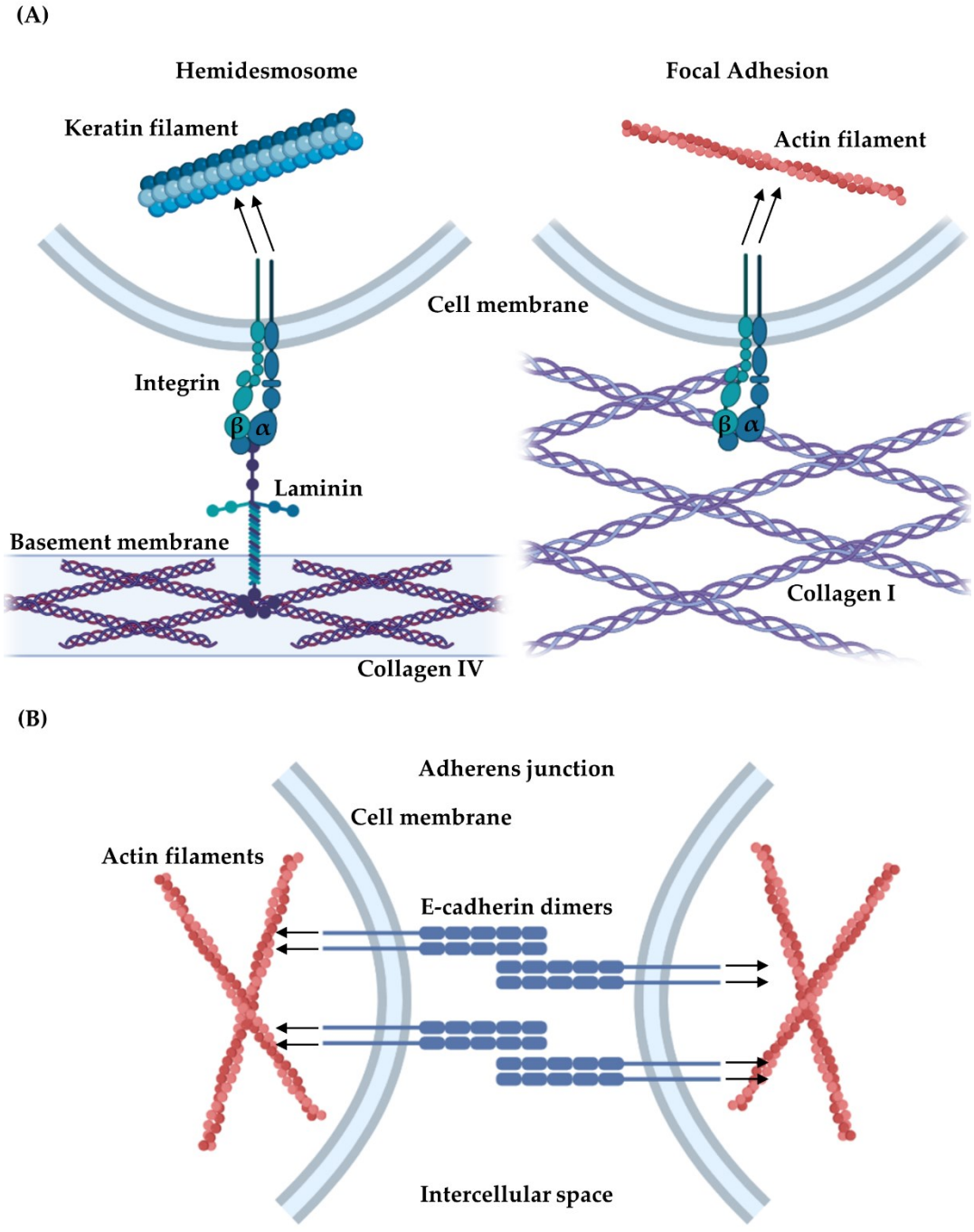

Figure 1.2 Schematic illustration of cell adhesion complexes. (A) *Integrins provide cell-ECM interactions either through hemidesmosomes (α6β4) which bind the basement membrane to intermediate filaments, or focal adhesions (α3β1) which bind the ECM to actin filaments.* **(B)** *E-cadherin provides cell-cell adhesions at adherens junctions. Created using BioRender (https://biorender.io).*

Mechanotransduction begins when integrins and cadherins come into contact with either the ECM or neighbouring cells, and the rigidity of their binding partner is

assessed through the deployment of localised contractions (Ghassemi et al., 2012). The level of resistance provided by the binding partner then provides cells with mechanical information that is translated into signals. Hemidesmosomal integrin $\alpha 6\beta 4$ has been shown to regulate several intracellular signalling pathways, including the Hippo pathway (Wang et al., 2020). Cadherin-catenin complexes also play a role in regulating major intracellular signalling pathways, including the Wnt and Hedgehog pathways (Klezovitch and Vasioukhin, 2015), both of which are critical in maintaining epidermal homeostasis (Abe and Tanaka, 2017).

1.2.1.3 Cytoskeletal proteins

The cytoskeleton is composed of filamentous proteins which provide cells with mechanical support and enable them to maintain their shape and internal organisation. Microtubules are the largest of these filaments and are composed of a protein called tubulin; a dimer made up of α-tubulin and β-tubulin polypeptides. Microtubules consist of thirteen linear protofilaments of α-tubulin and β-tubulin that are assembled around a hollow core and arranged head-to-tail in parallel, thus inferring polarity (Cooper, 2000). The classic roles of microtubules are to provide structural support and facilitate the trafficking of intracellular components around the cell, the latter of which relies on the polymer specific motor proteins kinesin and dynein (Fletcher and Mullins, 2010). However, perhaps the most vital role of microtubules is during cell division, where formation of the mitotic spindle is required for the segregation of chromosomes (Prosser and Pelletier, 2017). The role of microtubules in cell architecture and mechanotransduction is contested, with recent work suggesting that microtubule organisation is more reactionary to changes in cell shape rather than being a key driver (Gomez et al., 2016). However, it has been suggested that due to their rigidity, linearity, and cell-spanning nature, microtubules may be well placed to play a role in tuning cytoskeletal stiffness in response to external tension (Hamant et al., 2019).

Actin filaments are highly abundant across all eukaryotic cell types, and also play a role in the maintenance of cell shape; high rates of actin polymerisation and depolymerisation are used to generate directed forces that alter cell shape and

promote motility (Fletcher and Mullins, 2010). Actin filaments are composed of actin proteins which polymerise to form thin, flexible fibres that can be up to several micrometres long. The filaments are arranged in a highly organised 3D network which possses the properties of a semisolid gel (Cooper, 2000). The relationship between actin filaments and mechanotransduction is much more defined than that of microtubules, and it has been reported that actin organisation is dependent on both ECM stiffness and the shape of a cell (Gupta et al., 2019). Additionally, as mentioned in the previous section, actin filaments are the binding partner of numerous cell adhesion complexes and as such play a key role in the localised contractions used by cells to assess the rigidity of their binding partners. In a similar mechanism to sarcomere shortening in skeletal muscle, cells use myosin IIB to contract adhesion molecules along the actin filaments and use the amount of force required to displace the adjacent cell or ECM to infer the stiffness of their surroundings (Moore, Roca-Cusachs and Sheetz, 2010; Yang et al., 2018). The highly non-linear nature of actin filaments, their ability to stretch and bend, and the organisational constraints imposed by crosslinkers have all been determined as signs that the mechanical behaviour of the cytoskeleton is highly dependent on network architecture (Fletcher and Mullins, 2010). In fact, it has been shown that variation in crosslinker length and the spacing between actin-binding domains has a significant effect on the macroscopic properties of a cell including the elastic Modulus (Wagner et al., 2006). The elastic, or Young's, Modulus describes a measure of the resistance of a cell to deformation (Fletcher and Mullins, 2010), with a high elastic Modulus indicating increased cell stiffness, and a low elastic Modulus indicating reduced stiffness.

The third and final filament group included in the cytoskeleton are intermediate filaments, which are strong and rope-like in appearance, and commonly work in tangent with microtubules to provide strength and support. The composition of intermediate filaments varies with cell type, but one of the most prevalent types are keratins which play an important role in the regulation of epidermal homeostasis through variable expression across the different layers. Intermediate filaments are able to resist tensile forces, and often their assembly is in response to shear stress (Flitney et al., 2009), suggesting a role in spatial redistribution of tension to ensure

the structural integrity of a cell is maintained. Moreover, crosstalk between keratins and the actin cytoskeleton has been identified as a staple component of mechanotransduction; external mechanical strain triggers keratins to activate the ROCK signalling pathway which promotes actin stress fibre formation and increased cell stiffness (Bordeleau et al., 2012).

1.2.1.4 The LINC complex

Whilst the primary interface for mechanosensation is between the external environment and the cytoskeleton via adhesion complexes, the information must be relayed to the nucleus in order for cells to translate stimuli into reactionary gene expression changes. The LINC complex describes a collection of proteins found at the nuclear envelope (NE) which together span from the outer to the inner nuclear membrane (Figure 1.3). At its core, the LINC complex is composed of two protein domains; the SUN (Sad1p, UNC-84) domain which spans the inner nuclear membrane, and the C-terminal KASH (Klarsicht/ANC-1/Syne Homology) domain which is expressed by nesprin proteins and spans the outer nuclear membrane (Bouzid et al., 2019). The nesprin KASH domain extends into the perinuclear space where it interacts with the SUN domain of SUN proteins; variations in KASH and SUN domain interactions enable multiple LINC complex isoforms to exist (Bouzid et al., 2019).

The engagement of adhesion molecules at the cell membrane transfers tension to the nucleus through the cytoskeleton which is bound to the LINC complex. Nesprin-1 and nesprin-2 both possess giant isoforms that have an N-terminal actin-binding domain (Mellad, Warren and Shanahan, 2011), whilst the nesprin-3 N-terminal binds plectin which in turn binds to core cytoskeletal components (Wilhelmsen et al., 2005), and nesprin-4 indirectly binds to microtubules via kinesin (Roux et al., 2009). In contrast, the N-termini of SUN domain proteins at the opposite end of the LINC complex bind to nuclear lamina, thus providing the final link between external mechanical stimuli and the nuclear interior (Cartwright and Karakesisoglou, 2014).

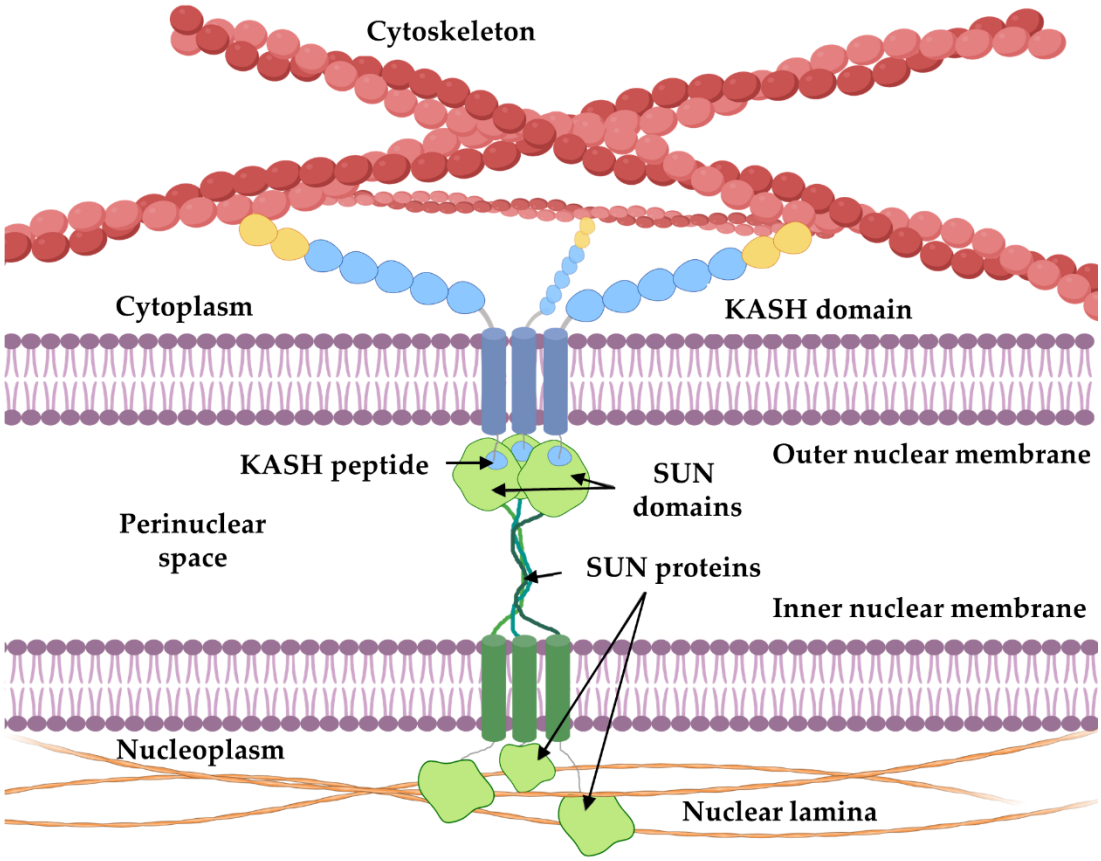

Figure 1.3 Schematic illustration of the LINC complex. *The LINC complex is composed of two protein domains, the KASH domain which binds to the cytoskeleton at the outer nuclear membrane, and the SUN domain which spans the perinuclear space and bind the nuclear lamina. Created using BioRender (https://biorender.io).*

1.2.1.5 The Hippo signalling pathway

Whilst the LINC complex is responsible for directly linking the external environment to the chromatin within the nucleus, not all mechanotransduction relies on this connection. As mentioned previously, relayed tension to the cytoskeleton can trigger signal cascades that provide a specific cell response to mechanical stimuli. One of the key pathways regulated in this way is the Hippo signalling pathway (Figure 1.4). At its core, the Hippo pathway is a kinase cascade that has been linked to the control of cell differentiation, proliferation, and death (Yu & Guan, 2013). In its simplest form, the pathway begins with the F-actin binding proteins merlin and expanded, which upon detection of reduced cytoskeletal tension, phosphorylate MST1/2 (mammalian Ste20-like) kinases, which phosphorylate LATS1/2 (large tumour suppressor) kinases, SAV1 (Salvador 1), and MOB1 (Mps1-binder-related) proteins (Chang et al.,

2020). When activated by phosphorylation, LATS1/2 in turn act to phosphorylate YAP/TAZ; the key transcription factors involved in mediating gene expression and cell behaviour as a result of the Hippo pathway (Hong & Guan, 2012). When they are phosphorylated, YAP/TAZ are inhibited, due to the creation of a binding site for 14-3-3 proteins which sequester YAP/TAZ in the cytoplasm (Hong & Guan, 2012). In this instance cells are directed towards cell cycle arrest, apoptosis or differentiation. However, when upstream kinases are inactive, hypophosphorylation of YAP/TAZ enables them to translocate to the nucleus, where they upregulate transcription of key genes by binding to their promoters (Yu & Guan, 2013) (Figure 1.4). Expression of these genes leads to increased proliferation. Nuclear YAP1 localisation has been

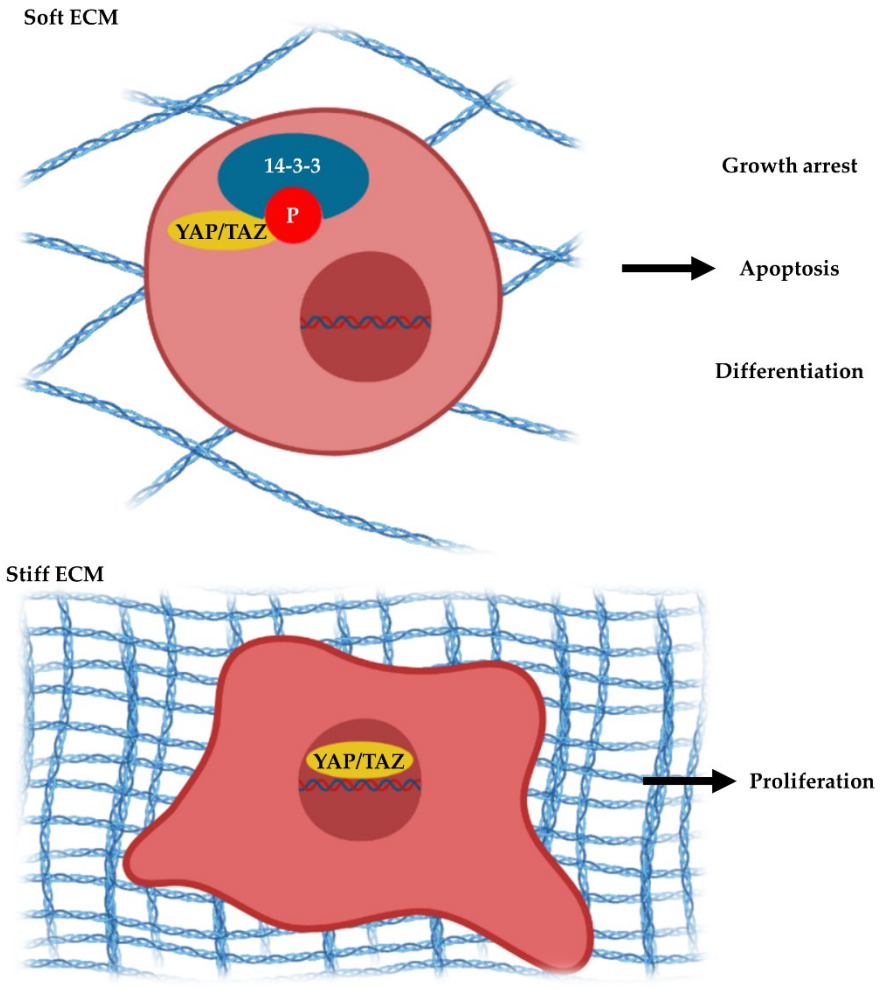

Figure 1.4 Schematic illustration of Hippo signalling pathway activation. *On a soft ECM cells are under less tension and the Hippo pathway is active, meaning the transcription factors YAP/TAZ are phosphorylated and sequestered in the ECM through binding to 14-3-3 protein. On a stiff ECM, cells are under high tension and the Hippo pathway is inactive allowing YAP/TAZ to translocate to the nucleus. Created using BioRender (https://biorender.io).*

linked to increased ECM stiffness as a result of high cell spreading and actin cytoskeletal tension (Cai, Wang and Meng, 2021).

In the skin, the link between external mechanical stimuli, and regulation of the Hippo pathway is extremely important. As mentioned previously, the Hippo signalling pathway plays a key role in controlling proliferation and remodelling of the cytoskeleton (Piccolo et al., 2014). The epidermis is composed of layers of keratinocytes that gradually move to the surface of the skin as they differentiate, before eventually being shed (Candi, Schmidt and Melino, 2005). This means that the epidermis must undergo rapid self-renewal in order to be maintained; a process that relies heavily on the cells knowing when they need to proliferate, where they need to migrate to fill any gaps, and when to stop if the gaps have been filled (Schlegelmilch et al., 2011).

1.2.2 The biomechanical environment of human skin

The skin is composed of two main compartments, the epidermis and the dermis, which both have strikingly different cell and ECM compositions that provide each with its own distinct mechanical environment. The dermis is split into two additional regions, the papillary and reticular dermis, whilst the epidermis is composed of multiple cell layers between the basement membrane and the upper stratum corneal layer (Figure 1.5). These additional niches within the dermis and epidermis exhibit different mechanical environments that are further open to change as a result of wounding and the skin ageing process. Consequently, cells within the skin are subjected a variety of mechanical stimuli to which they must respond appropriately to ensure tissue homeostasis.

The epidermis is composed of keratinocytes that are assembled in multiple layers, each with distinct mechanical properties that play an important role in maintaining the balance between the proliferation and differentiation required for epidermal homeostasis. The basement membrane represents the stiffest component of the epidermis (Biggs et al., 2020), with evidence suggesting that the epidermal side of the basement membrane is significantly stiffer than the dermal as a result of either

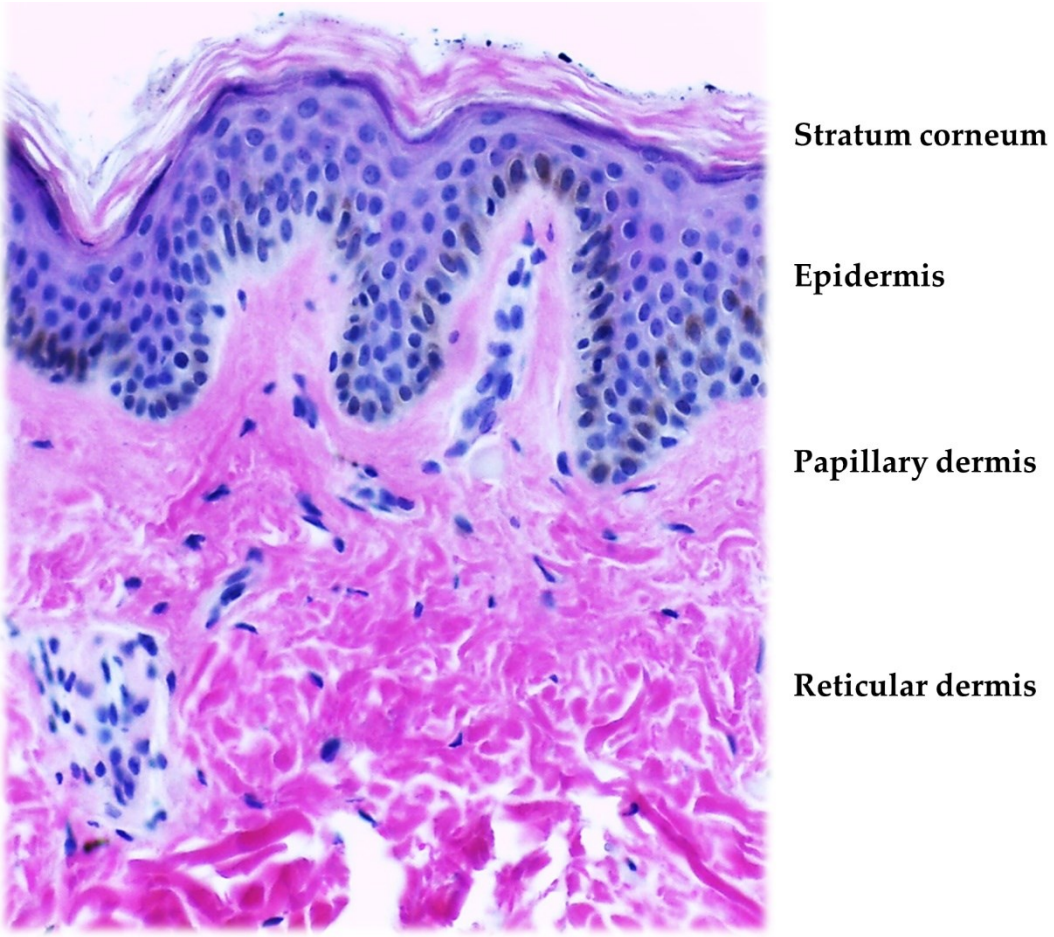

Figure 1.5 Histology image of human skin. *Brightfield microscopy image shows an H&E stained section of human skin taken from an arm biopsy of a young adult. Image taken from Masters thesis http://etheses.dur.ac.uk/12341/.*

different protein composition or tighter packaging and greater compression (Halfter et al., 2013). As cells differentiate and migrate upwards away from it, they are exposed to a variety of force changes influenced by variations in cell shape and keratin composition (Biggs et al., 2020). Cells in the basal layer of the epidermis are anchored to the basement membrane via hemidesmosomes which facilitate their stable adhesion and provides the epidermis with a foundation of mechanical stability. Mutations in which a component of the hemidesmosome is affected result in a variety of skin blistering disorders (Walko, Castañón and Wiche, 2015). The suprabasal cell layers are considered the most important for barrier function in an epithelium (Sosnova-Netukova, Kuchynka and Forrester, 2007), and thus the spinous and granular layers of the epidermis possess more complex cell-cell adhesions and cytoskeletal networks than the basal layer, providing the tissue with high mechanical resistance (Broussard et al., 2017; Rübsam et al., 2017b). Tight junctions are observed

in the third granular layer only, which has been attributed to the presence of tension-high cadherin-based lateral adherens junctions which are specific to the granular layer (Rübsam et al., 2017a).

Finally, changes to epidermal mechanics throughout the cell layers are associated with altered expression and organisation of the actin and keratin cytoskeletons (Laly et al., 2021). Human keratinocyte stem cells cultured *in vitro* exhibit short actin bundles located radially, whilst keratinocytes that have stopped proliferating present with a well-developed circumferential actin network (Nanba et al., 2013). Moreover, as keratinocytes differentiate the composition of keratins changes (Biggs et al., 2020), contributing to shifts in cell stiffness and thus the level of resistance that neighbouring cells encounter when contracting their adhesion molecules to assess the mechanics of their external environment.

Whilst the variations in the epidermal mechanical environment are important in ensuring the balance of keratinocyte proliferation and terminal differentiation, it is the dermis that is responsible for providing skin tissue with its main mechanical properties. This is due to the vast amount of ECM contained within the dermis that is remodelled in response to both wounding and skin ageing. Collagens I and III are the most abundant ECM proteins in the dermis and co-polymerise to provide the tissue's tensile strength. In a relaxed state, collagen fibres have no clear organisational arrangement, but when skin is stretched, the fibres shift and become aligned in parallel to one another (Hussain, Limthongkul and Humphreys, 2013). Skin elasticity (resilience and compliancy) is provided by the presence of an elastic fibre system which comprises 4% of the fat-free dry weight of skin. Elastin is responsible for the ability of skin to recoil following the application of deforming stresses due to their long-range elastic extendability (Hussain, Limthongkul and Humphreys, 2013). Skin hydration is supported by a group of carbohydrates collectively referred to as glycosaminoglycans (GAGs) (Naylor, Watson and Sherratt, 2011). Another factor influencing the mechanical properties of the dermis is the location on the body, as variation in ECM composition means that some skin is thicker, stiffer, less tense, and

less elastic than in other parts of the body (e.g., forehead versus forearm skin) (Hussain, Limthongkul and Humphreys, 2013).

However, the major driver of mechanical changes to the skin is ageing. Unlike other tissues, skin undergoes both an intrinsic and extrinsic ageing process. Intrinsic ageing of the skin over time, results in the gradual degradation of collagens I, III and IV, and elastic fibres, as well as the loss of oligosaccharides which impacts the skin's ability to retain water. In conjunction, these changes produce the aged phenotype of wrinkled, stiffened skin that is less able to recoil (Naylor, Watson and Sherratt, 2011). Extrinsic ageing is triggered as a result of exposure to ultraviolet (UV) radiation, and results in a distinctly different remodelling event including both catabolic and anabolic mechanisms (Takeuchi and Rünger, 2013). These events are dose dependent; severe photoageing results in the additional loss of collagen VII at the dermal-epidermal junction, and the increase and redistribution of GAG's to co-localise with the elastic fibre system. The elastic network is also remodelled, with severe photoageing leading to the accumulation of disorganised elastic fibre proteins in the reticular dermis (Kohl et al., 2011). The dermal compartment of aged skin has been shown to be softer than that of young skin, demonstrating the significant effect that ageing has on the mechanical properties of skin (Achterberg et al., 2014).

1.2.3 Culturing cells in 2D and the negative impacts of tissue culture plastic

To summarise the preceding sections, the external mechanical environment to which a cell is exposed provides stimuli that are transmitted internally via a multitude of proteins, and which ultimately dictate cell behaviour and fate. Given the variations in the mechanical environment observed even within different compartments of the skin, it is of no surprise that tissues throughout the body exhibit a vast range of stiffnesses. However, despite this, culturing cells on TCP and glass in a 2D format still remains the most common cell culture practice. TCP has been shown to have a Young's Modulus of around 3 GPa (Landry, Rattan and Dixon, 2019), which far surpasses the stiffness of the majority of *in vivo* tissues (Figure 1.6). Whilst growing cells on TCP is an appealing technique due to the ease and speed with which it

supports *in vitro* cell study, it comes with the caveat that cells behave aberrantly, displaying abnormal differentiated phenotypes, flattened shape, abnormal polarisation, and responses to pharmaceutical reagents that do not reflect the *in vivo* reaction (Caliari and Burdick, 2016).

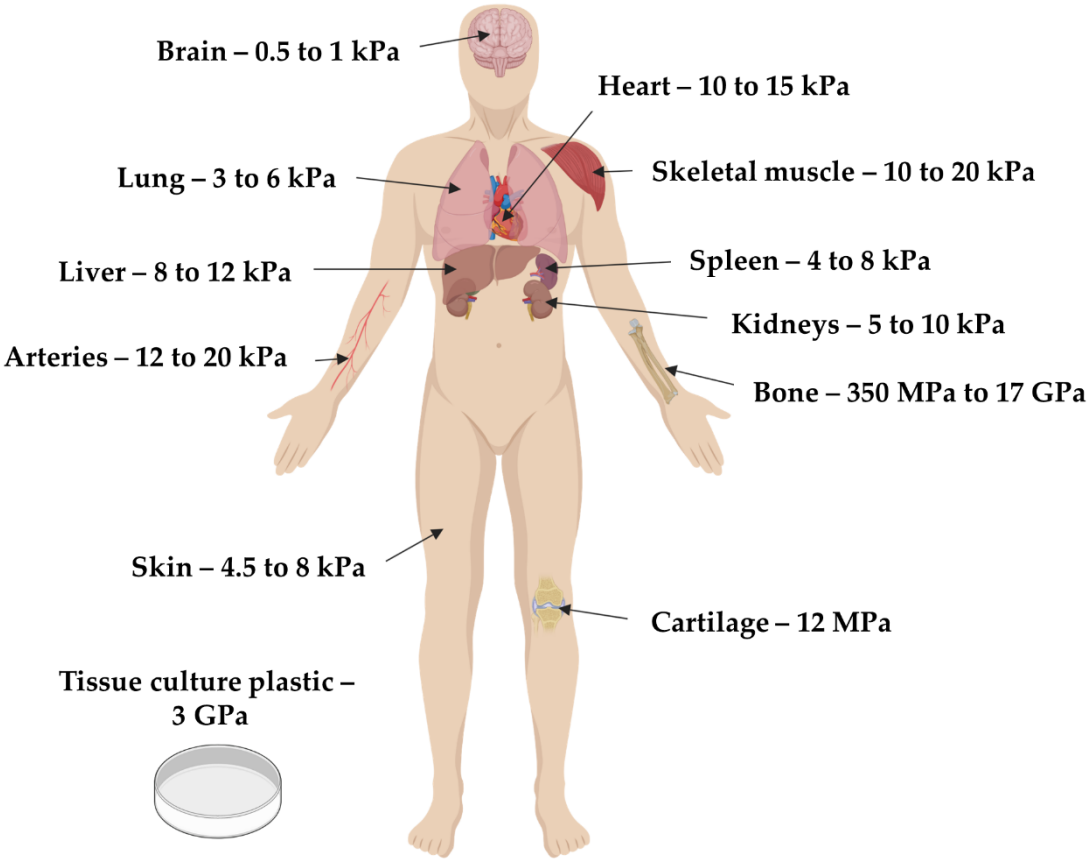

Figure 1.6 Schematic illustration showing the average Young's Modulus values of different human tissues. *Most human tissue is significantly softer than the TCP traditionally used to culture cells in vitro. Created using BioRender (https://biorender.io).*

Developments in the field of biomaterials have provided a range of solutions to the 2D culture issue, supplying alternatives such as patterned glass substrates, fibrillar foams, hydroxyapatite ceramics, and elastomeric films (Caliari and Burdick, 2016). However, hydrogels have emerged as the most promising candidate due to their *in vivo*-like mechanics, their ability to interface with biological systems, and the wide variety of applications that they can be used for (Peppas et al., 2006; Saha et al., 2007). Moreover, the ability to develop thin hydrogel films makes them ideal for 2D cell culture application, where they can be used to coat standard TCP and thus maintain

the desired ease of use, whilst providing a more physiologically relevant mechanical environment (Kazi, Yamanaka and Osamu, 2019).

Dermal fibroblasts cultured on silicone substrates with the softness of the dermis have been observed to possess a protein and mRNA profile similar to human skin, which was not seen in fibroblasts cultured on TCP or collagen gels (Achterberg et al., 2014). Moreover, corneal keratinocytes cultured on non-physiologically relevant substrates of 1.74 MPa were seen to undergo significant changes in the gene expression of most tissue-innate biomarkers, but this was not observed to be the case for cells cultured on softer substrates of 40 kPa and 130 kPa (Moers et al., 2013). Neonatal human epidermal keratinocytes cultured on soft and stiff polyacrylamide gels were found to exhibit differences in cell spreading area and migration speeds (Zarkoob et al., 2015). Consequently, it is clear that culturing cells on TCP has a significant effect on cell behaviour and expression profile which could be avoided through the permanent implementation of a BM alternative that better reflects the *in vivo* mechanics of the specific native tissue.

1.2.4 Methods of 3D skin model production and their limitations

Whilst an inappropriate mechanical environment is a major limitation of 2D culture, another significant flaw is that cells growing in a 2D monolayer lack the heterogeneity of *in vivo* tissue, do not exhibit the full transcriptomic and proteomic profiles, and have no surrounding ECM. This has led to the development of 3D cell culture which offers an opportunity to further research more poorly understood areas of skin biology such as wound healing, ageing, and diseases such as psoriasis, eczema, and melanoma, which can all be explored through *in vitro* skin models.

A key pioneer in the early development for 3D culture models was Dr. Mina Bissell, who challenged the long-standing belief that the ECM is merely a cellular scaffold and argued that in order to understand the nature of tissues it was vital to first understand the cellular microenvironment; the biological subtleties of which cannot be observed in a 2D monolayer. In a landmark publication, Bissel and her research group demonstrated that in 3D spheroid models of the epithelial breast cancer cell

line HMT-3522, treatment with an inhibitory β1-integrin antibody led to the reestablishment of E-cadherin-catenin complexes, reorganisation of the cytoskeleton, and reduced malignancy (Weaver et al., 1997). This result had not been observed in 2D cultures, thus demonstrating the significant impact that 3D culture could have on the progression of scientific understanding with regards to *in vivo* tissue.

Today, the four main proposed methodologies of 3D cell culture are animal explants, microcarriers, spheroids, and cellular scaffolds (Haycock, 2010). In the world of skin research, spheroids and scaffold models have become the most prevalent and both rely on a self-assembly technique. Spheroid cultivation methods are well established for a wide range of tissues, perhaps largely due to the relative simplicity of the protocol and the ability to combine multiple cell types to form multi-layered tissues. This technique relies on the self-aggregating ability of cells, keeping them in suspension until they have formed a spheroid organoid structure. However, there are limitations to spheroid cultures, the most prevalent being the inadequate supply of nutrients and oxygen to the core of the spheroid which prevents them from being maintained long-term (Ryu, Lee and Park, 2019). In addition, due to the cell-only nature of spheroid models, there are no external mechanical stimuli provided to the cells to help them determine what they need to do to replicate an *in vivo* tissue. This has been noted as a significant roadblock in the development of epithelial spheroid models, with cells such as keratinocytes being highly sensitive to surface-detachment and the loss of a basement membrane structure; keratinocytes cultured in the absence of a cell-surface attachment will undergo terminal differentiation (Woappi et al., 2020).

An alternative to spheroid culture is to utilise scaffolds or membranes upon which cells can be seeded. Scaffolds aim to provide cells with a support that allows them to retain a more physiologically relevant morphology, thus encouraging a gene and protein profile that better reflects *in vivo* tissue (Zhong, Zhang and Lim, 2010). Epidermal skin models are often produced by culturing keratinocytes on top of collagen gels or polycarbonate (PC) membranes coated with a collagen layer to promote cell adhesion. However, a limitation of this technique is that there is no

basement membrane structure to provide an appropriate mechanical stimulus which could have an impact on epidermal assembly. In order to combat that, alternative models have been produced that first generate a dermal equivalent within a scaffold onto which keratinocytes can then be seeded. Models produced in this way have been shown to develop their own basement membrane (Roger et al., 2019), making this the most realistic in vitro environment available for epidermal model generation.

Whilst the advances in 3D cell culture have gone a long way towards tackling the issue of the inappropriate mechanical environment of 2D TCP culture, it is important that researchers do not lose sight of the fact that the presence of TCP or glass surfaces at any stage of the culture process poses a problem. It is currently still standard practice to revive and expand cell populations using traditional 2D culture techniques on TCP prior to setting up 3D models. However, there is emerging evidence that cells possess "mechanical memory" and are able to store information on their previous mechanical environment which can impact their behaviour even when they are moved into a new one (Kanoldt, Fischer and Grashoff, 2018). It has been demonstrated that the gene expression profiles of skin models and *in vivo* skin differ, with *in vitro* epidermal models exhibiting a hyperproliferative and activated phenotype more reminiscent of wounded native skin (Simard-Bisson et al., 2018; Smiley et al., 2005; Smiley et al., 2006). As such, current 3D tissue models are unlikely to become more reminiscent of *in vivo* tissue as long as TCP or glass are still being used at the 2D culture stage. With this in mind, it is time that researchers begin to consolidate the lessons learned from 2D hydrogel culture and 3D models rather than viewing them as separate entities. Thus, by controlling the mechanical environment at both the 2D and 3D stage of culture, the optimal cell culture protocol can be developed.

1.3 Project aims and objectives

1.3.1 Aims

This project aims to answer the following questions:

- Does culturing keratinocytes on 2D hydrogels offer the same ease of use as standard TCP?
- Should keratinocytes grow well on hydrogels, does a softer substrate influence cell behaviour?
- Using hydrogels in culture, can we control keratinocyte proliferation and differentiation?
- Does culturing keratinocytes on softer hydrogels induce changes to the cytoskeleton that explain the observed alterations to cell behaviour?
- Do keratinocytes cultured on hydrogels adapt their own Young's Modulus in response to reduced external tension?
- Do keratinocytes cultured on softer substrates alter their expression of LINC protein components?
- Does culturing keratinocytes on hydrogels prior to setting up 3D culture facilitate superior epidermal assembly?
- Should hydrogel primed keratinocytes exhibit superior epidermal assembly, does this translate into changes in protein expression and barrier function?
- Is it possible to produce an epidermal model more quickly by priming keratinocytes on hydrogel-coated dishes first?
- Does culturing fibroblasts on soft 2D hydrogels result in changes to cell proliferation and density compared to those on TCP?
- Do fibroblasts cultured on soft hydrogels exhibit altered levels of senescence and ROS compared to those on TCP?
- Do the mechanics of the underlying 2D substrate affect the DDR of *in vitro* cultured fibroblasts?

1.3.2 Objectives

In order to answer the proposed research questions, the following objectives must be met:

- Determine whether hydrogel-coated cultureware facilitates normal 2D culture practices and analysis.
- Characterise the behaviour and phenotype of keratinocytes cultured on hydrogels in comparison to TCP.

- Determine appropriate stiffnesses of hydrogels to replicate the epidermal basement membrane and suprabasal layers.
- Determine whether culturing keratinocytes on hydrogels leads to changes in cytoskeletal and cytoskeletal-associated proteins.
- Determine how the LINC complex responds when keratinocytes are cultured on softer substrates.
- Calculate the Young's Modulus of keratinocytes cultured on TCP and BM hydrogels to determine whether adaptation occurs.
- Determine whether culturing keratinocytes on hydrogel-coated dishes in 2D, improves the appearance of 3D epidermal models.
- Characterise protein expression in epidermal models produced from keratinocytes primed on TCP and hydrogel-coated dishes.
- Assess barrier function of epidermal models produced from keratinocytes primed on TCP and hydrogel-coated dishes.
- Determine whether priming keratinocytes on hydrogel-coated dishes leads to faster epidermal model development.
- Determine whether soft hydrogels promote a less active fibroblast phenotype reminiscent of their in vivo counterparts.
- Use irradiation to induce DNA damage and determine differences in the DDR of fibroblasts cultured on TCP versus BM dishes.
- Use irradiation to induce cell senescence and determine the prevalence of senescent fibroblasts on TCP versus BM dishes.

2 Materials and methods

2.1 2D Cell culture

2.1.1 Human immortal keratinocyte cell line, HaCaT

HaCaT (human immortal keratinocyte line) cells (T0020001, AddexBio, San Diego, CA, US) were maintained in High Glucose Dulbecco's Modified Eagle Medium (DMEM, Gibco™, Thermo Fisher Scientific, Cramlington, UK) supplemented with 10% Fetal Bovine Serum (FBS, Thermo Fisher Scientific), 2 mM L-Glutamine (Sigma-Aldrich, Irvine, UK) and 1 mg/ml Penicillin/Streptomycin (Sigma-Aldrich) in a humidified atmosphere with 5% CO_2 at 37°C. Cells were passaged at a maximum of 80% confluency by washing with Dulbecco's Phosphate Buffered Saline (DPBS, Thermo Fisher Scientific) and dissociating with TrypLE™ Express Enzyme (Thermo Fisher Scientific). The cell suspension was centrifuged at 1000 rpm for 5 min and resuspended in growth medium. Cells were then transferred to the required cultureware and medium was added.

Cells were sub-cultured at a 1:6 ratio and the medium was changed every 2 to 3 days. Cells were frozen down in cryovials (Sarstedt, Nümbrecht, Germany) in their usual medium supplemented with 10% DMSO (Sigma-Aldrich) and kept at -150°C for long-term storage. For 2D priming on different substrates, HaCaTs were cultured for 4 days on 10 cm dishes of either TCP (Greiner BioOne, Stonehouse, UK) or BM dishes coated with either a 4 or 8 kilopascal (kPa) collagen coated hydrogel (Petrisoft®, Cell Guidance Systems, Cambridge, UK).

2.1.2 Human epidermal keratinocytes, neonatal

Neonatal human epidermal keratinocytes (HEKn, FC-0007, LifeLine Cell Technology, Oceanside, CA, USA) were maintained in EpiLife medium containing 60 μM calcium (Thermo Fisher Scientific), supplemented with 100x Human Keratinocyte Growth Supplement (HKGS, Thermo Fisher Scientific) and 500x Gentamicin/Amphotericin (Thermo Fisher Scientific) in a humidified atmosphere with 5% CO_2 at 37°C. Cells

were passaged at a maximum of 80% confluency by washing with DPBS (Thermo Fisher Scientific) and dissociating with TrypLE™ Express Enzyme (Thermo Fisher Scientific). The cell suspension was centrifuged at 1,000 rpm for 5 min and resuspended in growth medium. Cells were then transferred to the required cultureware and medium was added.

Cells were sub-cultured at a 1:6 ratio and the medium was changed every 2 to 3 days. Cells were frozen down in cryovials (Sarstedt) in Synth-a-freeze (Thermo Fisher Scientific) and kept at -150°C for long-term storage. Cells were used at passage 4 for all 2D work, and passage 5 for all 3D work to ensure optimal cell fitness. For 2D priming on different substrates, HEKn were cultured for 4 days on 10 cm dishes of either TCP (Greiner BioOne) or BM dishes coated with either a 4, 8, or 50 kPa collagen coated hydrogel (Petrisoft®, Cell Guidance Systems).

2.1.3 Human dermal fibroblasts, neonatal

Neonatal human dermal fibroblasts (HDFn, provided by Dr. Gabriel Saretzki, Newcastle University, UK) were maintained in High Glucose DMEM (Thermo Fisher Scientific) supplemented with 10% FBS (Thermo Fisher Scientific), 2 mM L-Glutamine (Sigma-Aldrich, Irvine, UK) and 1 mg/ml Penicillin/Streptomycin (Sigma-Aldrich) in a humidified atmosphere with 5% CO_2 at 37°C. Cells were passaged at 100% confluency by washing with DPBS (Thermo Fisher Scientific) and dissociating with TrypLE™ Express Enzyme (Thermo Fisher Scientific). The cell suspension was centrifuged at 1,000 rpm for 5 min and resuspended in growth medium. Cells were then transferred to the required cultureware, and medium was added.

Cells were subcultured at a 1:3 ratio and the medium was changed every 3 days. Cells were frozen down in cryovials (Sarstedt) in FBS (Thermo Fisher Scientific) containing 10% DMSO (Sigma-Aldrich) and kept at -150°C for long-term storage. For 2D priming on different substrate stiffnesses, HDFn were cultured for 4 days on 10 cm dishes of either TCP (Greiner BioOne) or BM dishes coated with either a 1, 4 or 8 kPa collagen coated hydrogel (Petrisoft®, Cell Guidance Systems).

For irradiation, cells were plated at a density that ensured they reached approximately 80% confluency after 4 days of culture. Cells were treated with either 10 Gy or 20 Gy X-irradiation using an X-rad225 irradiator (Precision x-ray Inc., North Branford, USA). Medium was immediately replaced following irradiation, then cells were cultured as normal for 10 days to allow senescence to occur. Where immediate DNA damage needed to be assessed, cells were dissociated and transferred to glass coverslips (SLS, Wilford, UK) the day before irradiation. Coverslips were then irradiated, and media changed as above, before being fixed in 4% paraformaldehyde (PFA) for 10 min at room temperature and stored in the fridge in PBS until needed. For all experiments, control samples were taken down to the irradiator and media changed afterwards to avoid variability due to prolonged exposure to room temperature or application of fresh medium.

2.2 3D cell culture

2.2.1 Hanging drop spheroid models, full thickness

HDFn were cultured on TCP dishes (Greiner BioOne) and maintained until confluent and dissociated as described in 2.1.3. Cells were then resuspended in High Glucose DMEM (Thermo Fisher Scientific) supplemented with 10% FBS (Thermo Fisher Scientific), 2 mM L-Glutamine (Sigma-Aldrich, Irvine, UK) and 1 mg/ml Penicillin/Streptomycin (Sigma-Aldrich). 10 µl droplets of cell suspension containing 3000 cells were pipetted at equal intervals onto the lid of a 10 cm culture dish and then suspended over the rest of the dish which contained 10 ml of sterile deionised water (diH_2O) to limit evaporation of medium within the droplets. HDFn hanging drops were cultured for 3 days in a humidified atmosphere with 5% CO_2 at 37°C.

HEKn were cultured for 4 days on either TCP (Greiner BioOne) or 4 kPa BM dishes (Cell Guidance Systems) then dissociated as described in 2.1.2. Cells were resuspended in EpiLife medium containing 60 µM calcium (Thermo Fisher Scientific), supplemented with 100x Human Keratinocyte Growth Supplement (HKGS, Thermo Fisher Scientific) and 500x Gentamicin/Amphotericin (Thermo Fisher Scientific). 10 µl of cell suspension containing 6000 cells was pipetted into each

of the 3-day old HDFn hanging drops previously prepared. These combined droplets were cultured for a further 7 days in a humidified atmosphere with 5% CO_2 at 37°C. Medium was changed every 3 days by harvesting the droplets and seeding them into a pool of fresh medium before redistributing them on a clean dish lid. All bright and dark field images were taken using a stereo-dissecting microscope.

2.2.2 BRANDplates® epidermal equivalents, HEKn

3D epidermal cultures were carried out using BRAND® insert strips for 24 x 6-well BRANDplates® (polycarbonate, 0.4 μm pore size, Sigma-Aldrich) with the 6-well BRANDplates® (Sigma-Aldrich). Inserts were coated with human collagen I coating matrix diluted 1:100 (Thermo Fisher Scientific) 30 min prior to use. HEKn were dissociated from their culture dish as described in 2.1.2 and resuspended in EpiLife medium containing 60 μM calcium supplemented with HKGS, 0.25 μg⁄ml Amphotericin B, 10 μg⁄ml Gentamicin, and 10 ng/ml of keratinocyte growth factor (KGF). All cell culture reagents were obtained from Gibco™ (Thermo Fisher Scientific). Cells were seeded at a density of 2.5 x 10^5 cells per insert and incubated at 37 °C in a 5% CO_2 humidified incubator for 4 days, before being raised to the air-liquid interface (ALI) and further supplemented with 25 μg/ml ascorbic acid (Sigma-Aldrich) and 1.5 mM $CaCl_2$ (Sigma-Aldrich) and maintained in this way for an additional 12 days.

2.3 Characterisation of cell function and phenotype

2.3.1 Cell density measurements

To assess cell density changes between cells cultured on TCP versus those on BM dishes, the number of cells per 10,000 μm^2 was quantified. Cells were cultured to the confluency at which they were usually passaged, and phase contrast images were taken using an EVOS XL Core microscope. Images were then analysed in ImageJ where the number of cells were counted within 100 x 100 μm squares.

For HEKn, where cell density measurements were taken at low and high calcium conditions, the cells were cultured up to 80% confluency in standard low calcium medium (EpiLife with 60 μM calcium, Thermo Fisher Scientific) then phase contrast images were taken. The medium was then replaced with EpiLife supplemented with 1.5 mM $CaCl_2$ (Sigma-Aldrich) and cells were returned to culture in a humidified incubator in 5% CO_2 and at 37°C for a further 24 hours before a second round of phase contrast images were taken. These images were analysed as above.

2.3.2 EdU proliferation assay

HaCaTs and HEKn were cultured on either glass (SLS) or BM 12 mm coverslips (Softslip®, Cell Guidance Systems) for a minimum of 4 days until no more than 50 to 60% confluent. The EdU assay was carried out using the Click-iT® EdU Alexa Fluor® 488 kit (Invitrogen, Thermo Fisher Scientific), using the recommended protocol. Half of the culture medium was removed and replaced with the same volume of fresh medium containing 20 μM EdU to create a final concentration of 10 μM EdU. The cells were incubated for 30 min in a humidified atmosphere at 37°C and 5% CO_2. All of the media was then removed and dishes were rinsed with DPBS (Gibco™, Thermo Fisher Scientific). Coverslips were fixed in 10% formalin in PBS then washed twice in 3% bovine serum albumin (BSA, Sigma-Aldrich) in PBS. Coverslips were incubated at room temperature with 0.5% Triton-X-100 in PBS then washed twice in 3% BSA in PBS. Using the recipe provided in the kit protocol, the Click-iT® reaction cocktail was made up, 0.5 ml was added to each coverslip, and they were then covered and incubated at room temperature for 30 min. Coverslips were washed in 3% BSA in PBS then incubated with 2 μg/ml DAPI (Sigma-Aldrich) for a further 60 min in a humidified atmosphere at room temperature. Coverslips were washed 3x 5 min in PBS, before being mounted onto slides using a drop of VECTASHIELD® anti-fade mounting medium

(H1000, Vector Laboratories, Peterborough, UK). Slides were left to dry in a slide book at room temperature for 15 min then kept at 4°C until ready to image. All slides were imaged using a Zeiss LSM 880 with Airyscan.

2.3.3 Repeat propagations on biomimetic dishes

HEKn were cultured for 4 days on TCP (Greiner BioOne), 50 kPa, and 4 kPa BM (Cell Guidance Systems) dishes. Phase contrast images were taken before cells were dissociated as described in 2.1.2, and then seeded onto a new dish of the same stiffness. After a further 4 days, additional images were taken to assess whether cells had continued to grow through a second propagation on the same substrate. All phase contrast images were taken using an EVOS XL Core microscope.

2.3.4 Flow cytometry to measure mitochondrial reactive oxygen species

HDFn cells were cultured on TCP (Greiner BioOne) and BM (Cell Guidance Systems) dishes and irradiated as described in 2.1.3. Cells were maintained in culture for a further 10 days after irradiation, before being dissociated from their respective dishes using TrypLE™ Express Enzyme, centrifuged at 1800 rpm for 3 minutes, and counted using a haemocytometer. Live cells were split into pellets of $2x10^5$ cells for each treatment and incubated with one of four probes/dyes in the absence of light. Concentrations and incubation times are provided in Table 1. Cellular peroxide levels were evaluated using dihydrorhodamine123 (DHR), mitochondrial ROS levels were evaluated using mitoSOX stain, mitochondrial superoxide levels were evaluated using dihydroethidium (DHE), and mitochondrial mass was measured using 10-*n*-nonyl-acridine (NAO). Following incubation, cells were once again centrifuged at 1800 rpm for 3 mins, then the supernatant was removed and cells were resuspended in either DMEM with serum (DHR) or serum-free

DMEM (mitoSOX DHE, NAO) and immediately analysed using a flow cytometer (Partec GmbH, Goerlitz, Germany).

The flow cytometer was calibrated by using 3 μm fluorescent calibration beads (Polysciences Inc., Warrington, USA) to calibrate the laser, optics and stream flow, and the gains were set to 100 for FL1 (green) and 180 for FL3 (red) to ensure comparable measurements. Cell populations were defined using forward and sideways scatter and cells were gated in FSC/SSC, with the median of the gated fluorescence peak used as an estimate of the concentration of peroxides/superoxides. For the FL3 channel, unstained cells were used to subtract any background. Between uses, the flow cytometer was cleaned with 2 ml 1% Triton X-100, followed by 2 ml PBS and 2 ml diH_2O.

Table 2.1 Probes and dyes used for flow cytometry of irradiated HDFn

Probe/Dye	Supplier	Product Code	Concentration	Incubation Time – Temp
mitoSOX	Invitrogen	M36008	5 μM	37° – 15 min
DHR	Invitrogen	D23806	30 μM	37°C – 30 min
DHE	Invitrogen	D11347	10 μM	37°C – 30 min
NAO	Invitrogen	A1372	10 μM	37°C – 10 min

2.3.5 WaferGen

HEKn were initially cultured in TCP T75 flasks (Greiner BioOne) as described in 2.1.2, then were dissociated and seeded onto TCP (Greiner BioOne) or BM (Cell Guidance Systems) 6-well plates at the end of a day, using seeding densities that would ensure approximately 80% confluency at the point of harvest. The morning after seeding, all plates were media changed. Samples were harvested at 24, 48, 72 and 96 hours after seeding (1 plate per stiffness for each time point). Medium was removed from each well and 350 μl Buffer RLT (Qiagen, Manchester, UK) was flushed over the surface multiple times. The Buffer RLT was then removed and placed into an Eppendorf on

ice before being transferred to -80°C for short-term storage. The resulting samples were then shipped on dry ice to Procter & Gamble (P&G, Cincinnati, USA) where they were assessed via WaferGen and statistically analysed.

Upon arrival at P&G, RNA samples were thawed to 4°C, vortexed for 2 seconds, and then transferred into a 96-well, deep well plate (Ritter, Schwabmünchen, Germany). The plate was then transferred onto a Beckman Biomek® FXp (Beckman Coulter Life Sciences, Indianapolis, USA) and isolated using the Agencourt RNAdvance Tissue Kit (Beckman Coulter Life Sciences) according to their protocol for the Biomek FxP. After elution, samples were quantitated using a Nanodrop 8000. Following this, 500 ng of total RNA was loaded into a 96-well plate and converted into cDNA using Life Technologies High Capacity RNA to cDNA Reverse Transcription kit (Thermo Fisher Scientific) and then stored at -20°C until required.

In order to run the WaferGen experiment, cDNA samples were thawed and 1.6 µl of each sample was transferred into a 96-well plate with 18.4 µl of 1.5x qPCR MasterMix (Thermo Fisher Scientific) added to each well. The plate was sealed, vortexed, and centrifuged for 5 mins. Next, 14.4 µl of the mixture was plated into a 384-well plate and transferred to a 5,184 nano-well WaferGen SmartChip (WaferGen Biosystems, California, USA) via a SmartChip Nanodispenser (WaferGen Biosystems). The WaferGen SmartChip contained 50 pre-selected genes of interest and 4 house-keeping genes (*18S*, *GAPDH*, *PGK1*, *RPL13A*). Following transfer, the chip was sealed and centrifuged for 15 mins. The chip was then loaded into the SmartChip qPCR cycler (WaferGen Biosystems), and run using the GeneExpression with UNG protocol.

2.4 Assessment of nuclear and cytoskeletal mechanics

2.4.1 Immunocytochemistry

Sterile 12 mm glass (Greiner BioOne) or BM (Cell Guidance Systems) coverslips were placed into a 24-well plate (Greiner BioOne) and cells were seeded at a density that ensured approximately 70% confluency after 4 days of culture. Cells were maintained in 1 ml of their relevant medium (see 2.1) in a humidified atmosphere with 5% CO_2

at 37°C, and media was changed 48 hours after seeding. At 4 days, cells were rinsed in DPBS (Thermo Fisher Scientific) and fixed in 10% formalin for 15 min at room temperature. The coverslips were then washed three times in PBS for 5 min each and permeabilised in 0.5% Triton-X-100 in PBS for 10 min at room temperature. Coverslips were again washed in PBS before being blocked in PBG blocking solution (1% BSA (Sigma-Aldrich) and 0.1% fish gelatin (Sigma-Aldrich) in PBS) for 15 min at room temperature. Coverslips were incubated with primary antibody (Table 2.2) in a humid atmosphere for either 1 hour at room temperature or at 4°C overnight. Coverslips were washed in TBS (50 mM Tris-HCl, 150 mM NaCl, diH_2O pH 7.6) + 0.1% Tween 20 (TBST) three times 10 min on a slow rocker. Coverslips were incubated for 60 min at room temperature with the secondary antibody (Table 2.2) and 2 μg/ml DAPI (Sigma-Aldrich), then washed a further three 10 min in TBST. Coverslips were mounted onto slides using VECTASHIELD® anti-fade mounting medium (VectorLaboratories). Slides were left to dry in a slide book at room temperature for 15 min then kept at 4°C until ready to image. All slides were imaged using a Zeiss LSM 880 with Airyscan.

Table 2.2 Primary (top) and secondary (bottom) antibodies used for the immunostaining of cells cultured in 2D or 3D environments.

Antibody	Supplier	Product Code	Species	Dilution
Yap 1	Novus Biologicals	NB-110-58358	Rabbit	1:50
Tubulin	Sigma-Aldrich	T8328	Mouse	1:50
E-cadherin	Abcam	ab1416	Mouse	1:100
Plectin	Santa Cruz Biotechnology	sc-7572	Goat	1:200
Lamin B1	Abcam	ab1684	Rabbit	1:400
Ki67	Abcam	ab15580	Rabbit	1:100
Phospho-Histone H2A.X	Cell Signaling Technology	9718	Rabbit	1:400
p16INK4a	CINTEC	9511	Mouse	1:5

Keratin 10	Abcam	ab76318	Rabbit	1:100
Keratin 14	Abcam	ab7800	Mouse	1:100

Phalloidin (Alexa Fluor™ 568)	Invitrogen	A-12380	-	1:1,000
Anti-Mouse (Alexa Fluor™ 488)	Invitrogen	A-21202	Donkey	1:1,000
Anti-Mouse (Alexa Fluor™ 568)	Invitrogen	A-11004	Goat	1:1,000
Anti-Rabbit (Alexa Fluor™ 488)	Invitrogen	A-21441	Chicken	1:1,000
Anti-Rabbit (Alexa Fluor™ 568)	Invitrogen	A-11036	Goat	1:1,000
Anti-Goat (Alexa Fluor™ 555)	Invitrogen	A-21432	Donkey	1:1,000

2.4.2 Western blotting

Protein lysates were made using RIPA buffer containing protease inhibitors.

RIPA buffer:

- 50 mM Tris
- pH 7.5 – 8
- 150 mM NaCl
- 0.1% SDS
- 1% Nonidet P-40
- 0.5% Sodium-deoxycholate
- 1% Protease Inhibitors (Pierce™ mini-tablets, Thermo Fisher Scientific)

All lysates were harvested from a 10 cm TCP (Greiner BioOne) or BM (Cell Guidance Systems) dish. Cells were cultured on the dishes for a minimum of 4 days under standard culture conditions (2.1) then the medium was removed, and dishes were

rinsed three times with DPBS (Thermo Fisher Scientific). Next, 400 µl of RIPA buffer was pipetted onto each dish and they were then placed on ice on a rocker for 30 min before a cell scraper was gently used to dislodge the cells. The resulting lysates were then sheared by passing them through a 27-gauge needle (BD Microlance™, Thermo Fisher Scientific) 20 times (for BM samples it was sometimes necessary to start with a lower gauge due to the presence of small amounts of polyacrylamide in the sample which blocked the needle). Lysates were then spun in a 4°C centrifuge for 10 min at 13,000 rpm. The supernatant was removed and placed in a clean Eppendorf. A BCA Assay (Pierce® BCA Protein Assay Kit, Thermo Fisher Scientific) was used to assess the protein concentration of each lysate, using protein standards of 1 mg, 0.75 mg, 0.5 mg, 0.25 mg, 0.125 mg and 0.025 mg, detergent compatible reagent, and RIPA buffer as a blank. As per product protocol, samples were left to incubate with the reagent in the dark at 37°C for 30 min. After allowing the plate to cool, a needle was used to remove any bubbles from the wells and absorbance was read at 570 nm using a BioTek ELx800 plate reader. Lysate samples of 400 µl were then mixed with 100 µl of 5x Laemmli buffer. Lysates were heated at 99°C for 4 min then cooled on ice, before being stored in the -20°C freezer until required.

Novex™ WedgeWell™ 4 to 12%, Tris-Glycine gradient gels (Thermo Fisher Scientific) were used to run high molecular weight nesprin proteins (Table 2.3). However, for all other proteins the gels were prepared fresh in the laboratory prior to each western blot experiment.

4% stacking gel (100 ml):

- 65.6 ml deionised water (diH_2O)
- 13.3 ml Protogel (30% acrylamide) (National Diagnostics, Thermo Fisher Scientific)
- 20 ml 0.5 M Tris pH 6.8
- 1 ml 10% Sodium Dodecyl Sulfate (SDS)
- 10% Ammonium Persulfate (APS)
- Tetramethylethylenediamine (TEMED)

10% resolving gel (100 ml):

- 34 ml diH2O
- 33.3 ml Protogel (30% acrylamide) (National Diagnostics, Thermo Fisher Scientific)
- 25 ml 1.5 M Tris pH 8.8
- 1 ml 10% SDS
- 10% APS
- TEMED

Equal loading of lysates was confirmed by loading 10 μg of protein using the volumes calculated following the BCA assay, and staining gels overnight with InstantBlue™ (Expedeon, Thermo Fisher Scientific). If necessary, the loading volume was altered until the bands on the gel were observed to be equal. Gels were run at 120 V. Transfer was carried out using either an Invitrogen Power Blotter (Thermo Fisher Scientific) or, for high molecular weight nesprins, using a wet transfer method run at 10 V for 18 hours, followed by 45 V for 2 hours). Immobilon®-P transfer membrane (Merck Millipore, Watford, UK) was used, and the membrane was activated and fixed using methanol. After fixing, membranes were dried in Whatman paper for a minimum of 15 min. They were then blocked for 60 min in 5% milk (semi-skimmed milk powder in TBST) and incubated with the primary antibody (Table 2.3) overnight in a 4°C cold room. The membrane was then washed three times 10 min in TBST before being incubated with the secondary antibody (Table 2.3) at room temperature for 60 min. The membrane was again washed three times 10 min in TBST. The membrane was developed using the Bio-Rad Clarity ECL Western Blotting Substrates (Bio-Rad, Watford, UK) and either exposed to film (GE Healthcare, Chicago, US) or imaged using an iBright1500 imaging system (Thermo Fisher Scientific).

Table 2.3 Primary (top) and secondary (bottom) antibodies used in western blotting.

Antibody	Supplier	Product Code	Species	Dilution
GAPDH	Calbiochem	CB1001	Mouse	1:5,000

Keratin 10	Abcam	ab76318	Mouse	1:5,000
Keratin 14	Abcam	ab7800	Rabbit	1:5,000
β-actin	Sigma-Aldrich	AC-74	Mouse	1:5,000
Tubulin	WA3, kind gift of Dr. U. Euteneuer	-	Mouse	1:5,000
Emerin	Vector Laboratories	VP-E602	Mouse	1:500
Lamin A/C	ImmuQuest	IQ332	Mouse	1:50
Lamin B1	Abcam	ab1684	Rabbit	1:500
Sun 1	Abcam	ab124770	Rabbit	1:1,000
Sun 2	Abcam	ab124916	Rabbit	1:1,000
E-cadherin	Abcam	ab1416	Mouse	1:1,000
Nesprin 1	In-house[1]	N-ABD	Rabbit	1:500
Nesprin 2	In-house[2]	PABK1	Mouse	1:1,000

Anti-Mouse POD	Sigma-Aldrich	A-4416	Goat	1:10,000
Anti-Rabbit POD	Sigma-Aldrich	A-6154	Goat	1:5,000

[1]Padmakumar, VC.; Abraham, S.; Braune, S.; Noegel, A.A.; Tunggal, B.; Karakesisoglou, I.; Korenbaum, E. Enaptin, a giant actin-binding protein, is an element of the nuclear membrane and the actin cytoskeleton. Exp Cell Res 2004, 295, 330-339. doi: 10.1016/j.yexcr.2004.01.014.

[2]Libotte, T.; Zaim, H.; Abraham, S.; Padmakumar, VC.; Schneider, M.; Lu, W.; Munck, M.; Hutchison, C.; Wehnert, M.; Fahrenkrog, B.; Sauder, U.; Aebi, U.; Noegel, A.A.; Karakesisoglou, I. Lamin A/C dependent localization of Nesprin-2, a giant scaffolder at the nuclear envelope. *Mol Biol Cell* **2005**, *16*, 3411–3424, doi: 10.1091/mbc.e04-11-1009.

2.4.3 Osmotic shock assay

HEKn were cultured on either glass (SLS) or 4 kPa BM (Cell Guidance Systems) coverslips for a minimum of 4 days. Medium was removed and replaced with fresh medium containing 640 mM sucrose and cells were incubated for 30 min in a

humidified atmosphere with 5% CO_2 at 37°C. Coverslips were fixed in 10% formalin then washed in PBS before being permeabilized for 10 min in 0.5% Triton-X-100 in PBS and blocked for 15 min in PBG blocking solution (see 2.4.1 for recipe). Coverslips were incubated with the nuclear envelope marker Lamin B1 (Table 2.2) in a humid atmosphere for 1 hour at room temperature, followed by three washes in TBST. Coverslips were incubated for 1 hour at room temperature with the secondary antibody (Table 2) and 2 μg/ml DAPI (Sigma-Aldrich) (Sigma-Aldrich), then washed a further three times in TBST. Coverslips were mounted with VECTASHIELD® anti-fade mounting medium (Vector Laboratories) and imaged using a Zeiss LSM 880 with Airyscan. Cells were then examined for nuclear abnormalities, which were defined as clear folds/creases in the envelope, and the percentage of cells exhibiting these abnormalities was calculated.

2.4.3 Atomic force microscopy

HEKn were cultured on TCP (Greiner BioOne) or 4 kPa Petrisoft® BM dishes for 4 days following the standard protocol described in 2.1.2, then dissociated and transferred to the lids of 6 cm TCP dishes (Greiner BioOne) and allowed to adhere overnight. Dish lids were used rather than the dishes themselves due to the lower height of the sides, which was required to ensure samples fit into the atomic force microscope (AFM). To ensure adequate provision of medium, the lids were placed within a standard 10 cm dish containing 12 ml medium overnight before being removed in order to conduct the experiment. Cells were analysed using a NanoWizard® 3 Bioscience AFM (JPK, Berlin, Germany) fitted with a Silicon Nitride pyramidal probe cantilever with a spring constant of 0.005-0.022 Nm-1 (AppNano, San Jose, USA). Young's Modulus values were then assessed for each cell at 10 randomly selected points in the nucleus and 10 points in the cytoplasm using JPKSPM Data Analysis software and the supplied Hertz-Fit Application Note for biological samples.

2.5 Characterisation of 3D skin models

2.5.1 OCT embedding hanging drops

Dispomoulds were filled with Optimal Cutting Temperature compound (OCT, Thermo Fisher Scientific) and hanging drop models were harvested using a P200 pipette (VWR, Lutterworth, UK). Multiple models were pipetted at once and the pipette was held with the tip facing down to ensure the models were as close to the opening as possible. The tip was inserted to the bottom of the dispomould, and the models were ejected into the OCT, ensuring the pipette was removed as soon as the last model left the tip to reduce contamination of the OCT with medium. The moulds were then placed on a metal plate in a box containing liquid nitrogen. The blocks were left to set for up to 30 min before being wrapped in metal foil and placed in a -80°C freezer until required. They were sectioned at 7 μm using a cryostat and mounted onto Superfrost plus microscope slides (4951PLUS4, Thermo Fisher Scientific). After cutting, sections were left to dry on a hot plate then placed in the -20°C freezer until needed.

2.5.2 Paraffin embedding BRANDplates® epidermal equivalents

BRANDplates® inserts (Sigma-Aldrich) were removed from their culture plate and transferred to a 12-well plate (Greiner BioOne). They were rinsed twice in DPBS (Thermo Fisher Scientific), then fixed in 10% formalin overnight at 4°C. The inserts were washed in PBS three times for 5 min, then dehydrated in 30%, 50%, 70%, 80%, 90% and 95% ethanol for 10 min each. A scalpel was then used to remove the polycarbonate membranes from the inserts, and they were placed within a folded piece of biopsy paper (Thermo Fisher Scientific) before being put into a cassette and further dehydrated in a beaker of 100% ethanol for 30 min. The ethanol was replaced with Histoclear (Thermo Fisher Scientific) before being left for a further 30 min. Half of the Histoclear was emptied and replaced with molten paraffin wax (Thermo Fisher Scientific) and the beaker was incubated in a 65°C oven for 30 min. Finally, the Histoclear:wax mixture was removed and replaced with 100% molten wax, and the beaker was incubated for a further 60 min in the 65°C oven.

The membranes were removed from the cassettes and laid out on tin foil to allow them to dry. Once hardened, a scalpel blade was used to cut each membrane in half. Molten wax was poured into a dispomould, and the membranes were orientated, using forceps, so that the cut edge of the membrane was in contact with the wax. The cassette was then placed over the membranes and molten wax was poured over the top until the mould was full. These were left to set at room temperature overnight. All wax blocks were sectioned at 7 μm using an HistoCore BIOCUT microtome, and mounted onto Superfrost plus microscope slides (4951PLUS4, Thermo Fisher Scientific).

2.5.3 Haematoxylin and Eosin (H&E) staining of BRANDplates® epidermal equivalents

Slides were deparaffinised in Histoclear (Thermo Fisher Scientific) for 5 min, then gradually rehydrated; first being submerged in 100% ethanol for 2 min, then moved to 95% ethanol, 70% ethanol and diH_2O for 1 min each (in rare cases where models were observed to detach from the slide, 1 min in 50% and 1 min in 35% ethanol were added to the hydration step). The slides were soaked in Mayer's Haematoxylin (H1532, Sigma-Aldrich) for 5 min, then submerged in alkaline ethanol for 30 sec. Samples were once again dehydrated through submersion in 70% ethanol and 95% ethanol for 30 sec each. They were then soaked in 0.5% eosin (E4009, Sigma-Aldrich) in 95% ethanol for 15 - 20 sec and further dehydrated through submersion in 95% ethanol for two rounds of 10 sec, 100% ethanol for 15 sec, 100% ethanol for 30 sec, then Histoclear (Thermo Fisher Scientific) for two rounds of 3 min. Slides were mounted with a glass coverslip using DPX (VWR) and brightfield images were taken using an EVOS XL Core microscope.

2.5.4 Immunohistochemistry of 3D skin models

For hanging drop models in OCT, slides were thawed on the bench then washed twice in PBS and fixed in 10% formalin for 30 min at room temperature. Models were then washed in PBS and permeabilised in 0.5% Triton X-100 in PBS for 30 min before

being washed in PBS again and blocked in 2% BSA in PBS for 30 min at room temperature.

Paraffin embedded BRANDplates® models were submerged in Histoclear (Thermo Fisher Scientific) for 10 min to deparaffinise them. Samples were then rehydrated for 5 min in 100% ethanol, 5 min in 70% ethanol and 5 min in diH_2O. Antigen retrieval was carried out through submersion in citrate buffer (Sodium Citrate Dyhydrate, Tween 20, diH_2O, pH 6.0) for 15 min at 98°C. Slides were gradually cooled then transferred to a humidified box and blocked for 60 min at room temperature. Blocking solution was made up of 10% goat serum (Abcam, Cambridge, UK) and 0.1% BSA (Sigma-Aldrich) in PBS.

All models were incubated with primary antibody (Table 2.2) at 4°C overnight, with antibodies diluted in 1:60 goat serum and 0.1% BSA in PBS. Slides were washed in TBST three times 10 min on a gentle rocker. Slides were incubated for 60 min at room temperature with secondary antibody and 2 μg/ml DAPI (Sigma-Aldrich) in 1:60 goat serum and 0.1% BSA in PBS, before again being washed 3 times 10 min in TBST. Slides were mounted using VECTASHIELD® anti-fade mounting medium (VectorLaboratories). Slides were left to dry in a slide book at room temperature for 15 min then kept at 4°C until ready to image. All slides were imaged using a Zeiss LSM 880 with Airyscan.

2.5.5 Lucifer yellow barrier permeability assay

BRANDplates® epidermal equivalents were cultured using the standard protocol with 12 days at the ALI (2.2.2). On day 12, models were transferred to an empty well and 200 μl of 1 mg/ml lucifer yellow (Lucifer Yellow CH dilithium salt, Sigma-Aldrich) was applied to the surface of the membrane. The models were then incubated in a humidified atmosphere with 5% CO_2 at 37°C for 2 hours before being removed and rinsed 3 times with DPBS (Thermo Fisher Scientific). Models were fixed overnight at 4°C in 10% formalin and paraffin embedded (2.5.2). Sections on slides were then processed using the immunohistochemistry protocol (2.5.4) and nuclei were labelled with 2 μg/ml DAPI (Sigma-Aldrich). Samples were imaged using a

Zeiss LSM 880 with Airyscan, and the lucifer yellow stain was observed using an Argon-Ion laser of 488 nm wavelength.

3 Investigating the effects of substrate stiffness on keratinocyte function

3.1 Introduction

Biomechanics is fast becoming a vital consideration in the world of *in vitro* cell culture and tissue engineering. In recent years, it has become apparent that external mechanical stimuli play a significant role in cell behaviour and function, influencing proliferation, cell differentiation, growth arrest, and even apoptosis (Dupont et al., 2011). Despite the fact that tissues within the body vary drastically in stiffness, cells have traditionally been cultured *in vitro* on glass or plastic cultureware, which greatly exceeds the stiffness of the vast majority of human tissues (Landry, Rattan and Dixon, 2019). Given what we now know about mechanotransduction, this begs the question as to how much of science's previous *in vitro* data has been skewed by abnormal gene expression changes associated with culturing cells in an inappropriately stiff environment.

The introduction of micropatterning approaches to alter the topology of 2D surfaces first enabled scientists to investigate how changes to the microenvironment affects cell morphogenesis and function (Ito, 1999). This was followed by the development of synthetic scaffolds enabling the growth of multi-layered 3D tissue in an *in vitro* setting and creating a more realistic environment in which to investigate cell behaviour (Guyot et al., 2014). The role of scaffolds in cell culture will be fully explored in chapter 5, but alone they do not entirely negate the issue of plastic cultureware due to "mechanical memory" and the long-lasting effects of the prior mechanical environment on cell behaviour. Moreover, 3D models do not provide the same ease of use which has long made 2D *in vitro* work so appealing. It was therefore necessary to find a solution that bridged the gap between traditional 2D culture and a 3D environment. One such solution has been to coat cultureware with a thin biomimetic hydrogel, the composition of which can be altered so that it matches the stiffness of a variety of different tissues within the body. In this way, it is possible to

culture cells in a 2D setting, whilst ensuring that the mechanical cues imbued by the underlying substrate are as *in vivo*-like as possible (Caliari and Burdick, 2016).

3.1.1 The role of biomechanics in epidermal assembly

Keratinocytes are the predominant cell type in the epidermis, which as the upper layer of the skin, is subject to a host of external stressors including mechanical manipulation. One of the key features of epidermal biology is a high cell turnover and the ability to tip the balance between proliferation and differentiation to maintain constant self-renewal and ensure efficient wound healing (Schlegelmilch et al., 2011; Sotiropoulou and Blanpain, 2012). Consequently, mechanotransduction plays a key role in the regulation of the epidermal niche, with sheer forces, stretch, and compression having been shown to induce changes in keratinocyte proliferation, migration, and differentiation rates (Wong, Longaker and Gurtner, 2012).

In order to maintain a normal tissue turnover, keratinocytes are able to actively respond to mechanical stimuli. The mechanosensory ability of cells begins with the cell adhesion complexes, namely integrins and cadherins, which are the first point of contact with the external environment. Integrins are physically attached to the extracellular matrix (ECM), whilst E-cadherin molecules, the primary cadherin found in the epidermis, participate in cell-cell binding and have an important function in maintaining epidermal barrier function (Müller et al., 2008). When integrins and cadherins come into contact with either the ECM or neighbouring cells, they assess the rigidity of their binding partner by deploying localised contractions (Ghassemi et al., 2012).

It has been well established that during normal epidermal homeostasis, the integrin β1 subunit plays a pivotal role in maintaining the balance between proliferation and terminal differentiation (Kenny and Connelly, 2015). Grose et al. observed that β1-null mice exhibited decreased proliferative capacity and keratinocyte migration, and instead terminal differentiation was stimulated (Grose et al., 2002). Moreover, though the mechanism is not completely understood, E-cadherin has been highlighted as an essential molecule for epithelial layer formation by regulating monolayer

organisation (Yang et al., 2018). Collins et al. demonstrated that altering the stiffness of polyacrylamide gel substrates led to alterations in epithelial cell spreading and actin organisation that were attributed to E-cadherin-dependent adhesion (Collins et al., 2017). Though this study used MDCK cells rather than keratinocytes, the results paint a striking picture as to the role of E-cadherin proteins in responding to external mechanical stimuli.

In addition to cell adhesion complexes, homeostasis of the epidermis relies on the Hippo signalling pathway (Rognoni and Walko, 2019). Activation of the Hippo pathway relies on mechanotransduction, with "soft" substrates providing a low mechanical stimulus and thus initiating pathway activation. When active, the transcription factors YAP and TAZ are sequestered in the cytoplasm or tagged for degradation, leading to growth arrest and the pushing of cells towards terminal differentiation. When the external environment is "stiff", YAP and TAZ move into the nucleus and upregulate genes associated with cell proliferation (Dupont et al., 2011; Piccolo, Dupont and Cordenonsi, 2014). The reason that the Hippo signalling pathway plays such a crucial role in epidermal biology is that the proliferative cells of the epidermis are located in the basal layer, where they sit on a stiff basement membrane. As the cells migrate into the suprabasal layers the mechanical stimuli provided by the surroundings changes, leading to a switch from a proliferative phenotype towards terminal differentiation (Biggs et al., 2020). Consequently, the Hippo pathway is a key component ensuring epidermal homeostasis.

3.1.2 Changes in mechanical stimuli between the epidermal layers

The epidermis is composed of multiple layers, each with distinct mechanical properties that play an important role in maintaining the balance between proliferation and differentiation required for epidermal homeostasis. The basement membrane represents the stiffest component of the epidermis, and as cells differentiate and migrate upwards away from it, they are exposed to a variety of force changes influenced by variations in cell shape and keratin composition (Biggs et al., 2020).

Engagement of adhesion molecules relays tension to the nucleus via the LINC complex and ultimately the nuclear interior (Hieda, 2019), which in turn manipulates nuclear positioning, actin dynamics, cell adhesion and cell migration (Chang et al., 2015; Stewart et al., 2015). Carley et al. cultured mouse keratinocytes on fibronectin-coated dishes and observed that integrin-associated tension on the nuclear lamina via the LINC complex, such as that caused by basal cell attachment to the basement membrane, represses differentiation and helps to maintain the progenitor state of epidermal basal keratinocytes (Carley et al., 2020). This suggests that the mechanical properties of the basement membrane have a significant role in controlling the function of the cells attached to it.

As a high turnover epithelium, the keratinocytes of the epidermis are constantly migrating upward until they are eventually shed from the skin's surface as corneocytes (Maeda, 2017). The exact mechanism by which epidermal stem and progenitor cells differentiate and migrate away from the basement membrane is still under debate. It is widely believed that the reality is a combination of delamination, where cells detach themselves from the basement membrane and migrate upwards (Nekrasova et al., 2018), and cell divisions that use perpendicular spindle orientations to directly position one daughter cell into the suprabasal layers (Gonzales and Fuchs, 2017). The suprabasal cell layers are considered the most important for barrier function in an epithelium (Sosnova-Netukova, Kuchynka and Forrester, 2007), and thus the spinous and granular layers possess more complex cell-cell adhesions and cytoskeletal networks than the basal layer, providing the tissue with high mechanical resistance (Broussard et al., 2017; Rübsam et al., 2017b).

Though all layers express the necessary components to form tight junctions, these are only found in the third granular layer, with the spinous layers favouring strong desmosome-intermediate filament complexes (Broussard et al., 2017; Rübsam et al., 2017b). This absence of tight junctions lower down in the epidermis is attributed to the lack of tension-high cadherin-based lateral adherens junctions which are specific to the granular layer (Rübsam et al., 2017a). These features highlight the important role that the distribution of layer-specific mechanical tension plays in epidermal

tissue morphogenesis, both in terms of junctional protein expression and overall barrier maintenance.

Alterations in epidermal mechanics throughout the layers appears to revolve around changes to the expression and organisation of the actin and keratin cytoskeletons (Laly et al., 2021), and the associated effect that this has on the types of cell-cell junctions present (Jacob et al., 2018). This aspect of keratinocyte biology will be explored in greater depth in chapter 4.

3.1.3 The use of biomimetic substrates in cell culture

Traditionally, cells have been cultured *in vitro* on 2D surfaces that offer a simple and quick method of studying them. However, this comes with the caveat that cells behave aberrantly, displaying abnormal differentiated phenotypes, flattened shape, abnormal polarisation and responses to pharmaceutical reagents that do not reflect the *in vivo* reaction (Caliari and Burdick, 2016). Whilst 3D culture is a useful tool to study cells in a more tissue-like environment, it does not provide the same ease of use as 2D, nor does it facilitate the rapid propagation and expansion of cells.

Developments in the field of biomaterials have provided a range of solutions to the 2D culture issue, supplying alternatives such as patterned glass substrates, fibrillar foams, hydroxyapatite ceramics, and elastomeric films (Caliari and Burdick, 2016). However, hydrogels have emerged as the most promising candidate due to their *in vivo*-like mechanics, their ability to interface with biological systems, and the wide variety of applications that they can be used for (Peppas et al., 2006; Saha et al., 2007). The crosslinked, hydrophilic polymers that make up hydrogels have a similar molecular architecture to the ECM, making them excellent biological mimetics (Lutolf and Hubbell, 2005). They are able to replicate tissue viscoelasticity, support diffusive transport, and can be incorporated with a number of other biological characteristics which further improve their resemblance to *in vivo* tissue (Tibbitt and Anseth, 2009). Moreover, the ability to develop thin hydrogel films makes them an ideal for 2D cell culture application, where they can be used to coat standard TCP so that cells can be grown on top, thus maintaining the desired ease of use, whilst providing a more

physiologically relevant mechanical environment (Kazi, Yamanaka and Osamu, 2019).

3.1.4 Considerations for selecting the appropriate substrate stiffness for culturing epidermal keratinocytes

As mentioned previously, keratinocytes are exposed to a variety of mechanical stimuli during their migration through the epidermis, which plays a key role in their differentiation and expression of different junctional proteins at different layers (Biggs et al., 2020). This immediately posed an initial challenge in that there is no specific Young's Modulus value that can be attributed to the epidermis as a whole. A core aim of this project was to use BM hydrogels to improve epidermal assembly once cells were moved into a 3D model. Consequently, it was deemed prudent to narrow the stiffness down to that of the basement membrane, thereby promoting a basal cell phenotype. However, this again presented problems as isolating an intact epidermal basement membrane is very technically challenging.

The values for skin stiffness vary greatly in the literature. This is largely due to its anisotopic nature, meaning that the direction at which force is applied can give different measurements (Kvistedal and Nielsen, 2007). Moreover, skin behaves viscoelastically, meaning that any initial deformation in response to an applied force is followed by a slower subsequent deformation (Akiyama et al., 2008). There are also a variety of techniques used to measure skin stiffness, ranging from non-invasive *in vivo* biophysical skin analysis, to *in vitro* mechanical measurements of biopsies (Limbert, 2017). Additionally, anatomical site, donor age, and degree of skin hydration can all impact the value obtained, meaning that skin Young's Modulus values in the literature can vary by up to three orders of magnitude (Graham et al., 2019).

In order to ensure that substrates were as standardised as possible throughout this project, it was decided that hydrogel-coated dishes would be purchased, rather than made in the laboratory (see chapter 2). This meant that the substrate stiffness chosen had to be selected from the available choices of 0.2, 0.5, 1, 2, 4, 8, 12, 25 and 50 kPa. In

the early stages of the project 50 kPa was initially deemed too stiff given its association with the Descemet's membrane of the corneal endothelium, which is a significantly harder tissue than the skin (Last et al., 2012). Moreover, literature providing values below 2 kPa for the dermal Young's Modulus suggested that these substrates would be too soft to replicate the epidermal basement membrane (Achterberg et al., 2014).

Given that a stiffness value for the epidermal basement membrane could not be found in the literature, it was decided to begin by culturing keratinocytes on 4 kPa and 8 kPa substrates. This matched with literature values for the skin stiffness as a whole (Pailler-Mattei, Bec and Zahouani, 2008), and also aligned with a previous PhD project within the laboratory in which it was observed that the innate Young's Modulus of HaCaT cells was approximately 5 to 7 kPa (Carthew, 2015). Moreover, whilst the Descemet's membrane has a stiffness of around 50 kPa, the anterior basement membrane of the cornea has been observed to be around 7.5 kPa (Last et al., 2012), suggesting that 4 to 8 kPa is not an unreasonable stiffness range for a basement membrane. Nonetheless, the hydrogels used in this project were later expanded to include the 50 kPa substrate after 4 and 8 kPa were deemed too soft to replicate the basement membrane, instead appearing to promote differentiation, as will be discussed further in this chapter. That 50 kPa hydrogels were an appropriate addition to the project was consolidated by the discovery of a publication from 2016, in which Young's Modulus measurements of the dermal-epidermal interface of dermal explants revealed that the stiffness was around 48.09 kPa (Kao, Connelly and Barber, 2016).

3.1.5 Considering the use of HaCaT cells versus primary keratinocytes for *in vitro* epidermal investigation

When studying keratinocytes and epidermal assembly *in vitro*, the first thing to consider is whether the investigation would be better served by working with human primary cells or the spontaneously immortalised human keratinocyte cell line, HaCaT. The obvious benefit of working with primary keratinocytes is that the cells remain as representative of their *in vivo* counterparts as possible. However, there are

also multiple caveats, chief of these being that keratinocytes exhibit proliferative decline during *in vitro* culture and can only be propagated a finite number of times before undergoing terminal differentiation (Ramirez, 2001). Not only does this mean that primary keratinocytes can differ from passage to passage, but it necessitates the use of cells harvested from multiple donors. This in turn presents new problems as donor-to-donor variability can lead to erratic results that make experimental conclusions difficult (Wong et al., 2019). Additionally, donor variability can have a significant impact on epidermal assembly in 3D models, with some cells readily forming a 3D epidermal equivalent, whilst others do not have the proliferative capacity to assemble an epidermis in an *in vitro* setting.

In contrast, HaCaT cells offer an unrestricted culture time given their immortalised nature, and thus come with none of the variability concerns highlighted with regards to primary keratinocytes. This is particularly appealing for 2D culture where repeated passaging is required, and improves the cost effectiveness of a project as cells can be used for a much longer period. Nonetheless, HaCaTs also possess their limitations, one of the most striking being that the standard culture of HaCaT cells uses 10% FBS in DMEM, which induces a partially to fully differentiated phenotype due to the high calcium content in both the medium and the serum (Wilson, 2013). Whilst reducing the calcium content of HaCaTs has been shown to induce a more basal cell phenotype (Colombo et al., 2017; Wilson, 2013), the gene transcription profile of differentiated HaCaTs has been shown to be different to that of primary keratinocytes (Seo et al., 2012). This raised concerns as to their viability for 3D model development.

Based on these pros and cons, it was decided that HaCaT cells would be used for the initial investigations into 2D culture on BM hydrogels so as not to waste primary keratinocytes should any problems be encountered. Primary keratinocytes would then be used for the rest of the 2D analysis and the 3D models to ensure that the results were as representative of the *in vivo* situation as possible. To reduce variability, neonatal keratinocytes were used to ensure that donors were of a similar age, and the same passage number was utilised for all experiments (see 2.1.2).

3.2 Hypotheses and Aims

This chapter aims to investigate potential changes in keratinocyte behaviour and phenotype in the context of proliferation, cell density, and expression of differentiation markers in response to culture on biomimetic hydrogels. In addition, this chapter will assess the ease with which keratinocytes were propagated and analysed when cultured on hydrogel-coated dishes versus standard TCP. This was completed using 10 cm dishes, 6-well plates, and coverslips that were bound with collagen pre-coated hydrogels made of polyacrylamide cross-linked with bisacrylamide (see chapter 2 for purchase details). It was hypothesised firstly, that culturing keratinocytes on softer substrates could replicate the changes in mechanical tension experienced by cells within the epidermis as they migrate away from the basement membrane. The stiffness of the hydrogels on which the keratinocytes were cultured could then be refined in order to promote either more basal or differentiated cell phenotypes. This would be important in providing a more physiologically relevant environment for the keratinocytes. Finally, it was hypothesised that using this approach may facilitate longer term maintenance of primary keratinocytes in culture.

To summarise, the key hypothesis behind this chapter was that soft BM dishes would replicate the mechanical environment of the epidermis, and thus facilitate control over the balance between keratinocyte proliferation and differentiation. This chapter therefore aims to answer the following questions:

- Does culturing keratinocytes on 2D hydrogels offer the same ease of use as standard TCP?
- Should keratinocytes grow well on hydrogels, does a softer substrate influence cell behaviour?
- Using hydrogels in culture, can we control keratinocyte proliferation and differentiation?

3.3 Objectives

- Determine whether hydrogel coated cultureware facilitates normal 2D culture practices and analysis.
- Characterise the behaviour and phenotype of keratinocytes cultured on hydrogels in comparison to TCP.
- Determine appropriate stiffnesses of hydrogel to replicate the epidermal basement membrane and suprabasal layers.

3.4 Results

3.4.1 Technical challenges faced when working with biomimetic hydrogel cultureware

One of the most desirable qualities for BM hydrogel coatings is that they offer users the same ability to easily propagate and analyse cells as traditional 2D cell culture; something 3D culture systems have yet to achieve. Consequently, this chapter begins by exploring the technical challenges faced when culturing cells on BM hydrogel-coated dishes versus standard TCP.

3.4.1.1 Trypsin EDTA does not dissociate cells from hydrogel-coated dishes

The initial work using BM hydrogels was carried using HaCaT cells, and after being revived into TCP flasks they were then passaged and seeded onto 10 cm dishes of either standard TCP or coated with 8 kPa or 4 kPa BM hydrogels. The cells adhered and grew readily on the hydrogel substrates (see 3.4.2) but the first technical difficulty encountered came when the cells reached the appropriate confluency for passage. Typically, adherent cells are dissociated using trypsin-EDTA, but it was observed that HaCaTs cultured on 4 kPa remained completely adherent, whilst their TCP counterparts began to dissociate after 2 minutes incubation with trypsin-EDTA and were entirely dissociated by 7 minutes incubation (Figure 3.1). It should be highlighted that significantly longer trypsin exposures of up to 60 minutes were

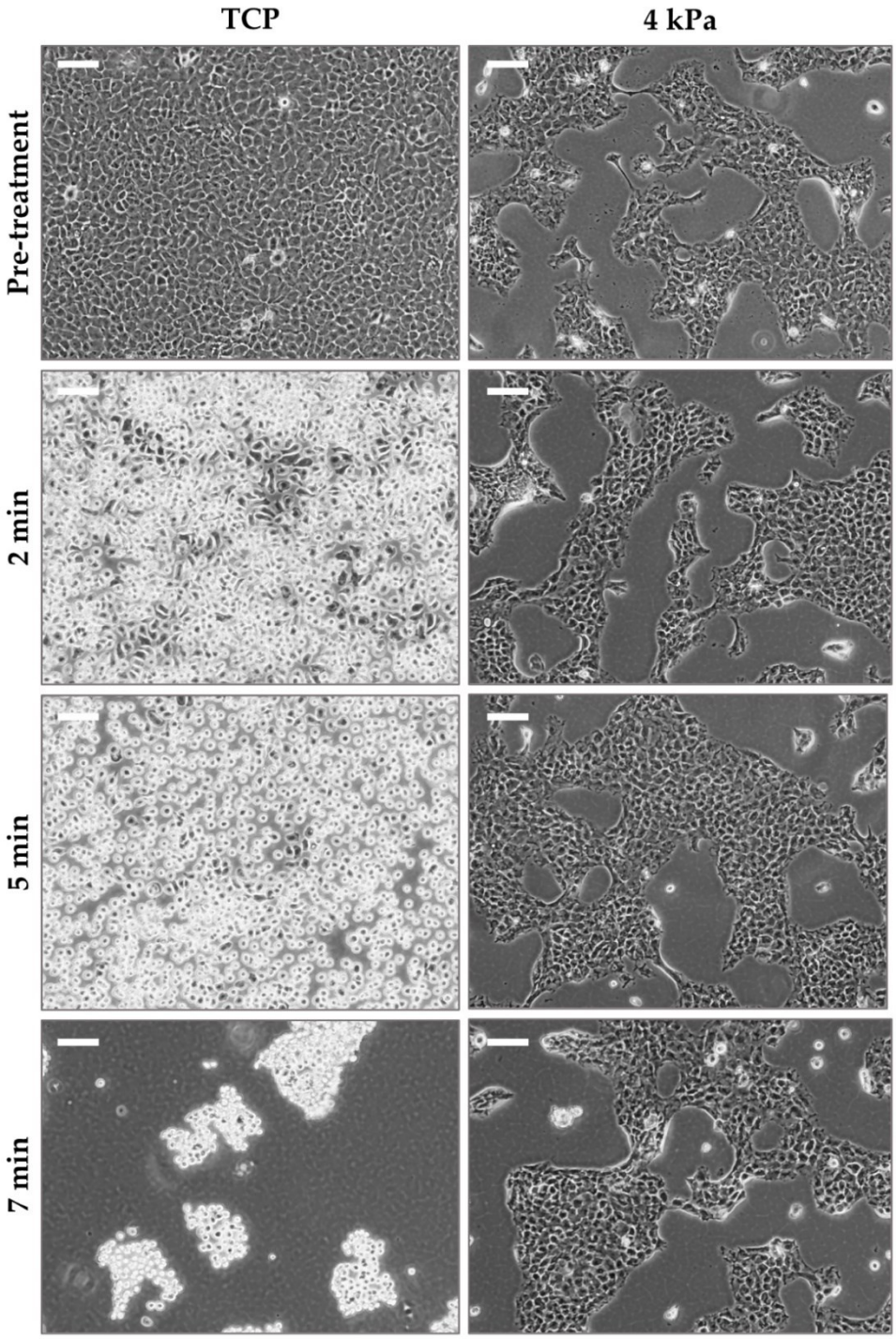

Figure 3.1 HaCaTs cultured on 4 kPa hydrogels do not dissociate with trypsin-EDTA. *HaCaT cells were cultured on TCP and 4 kPa hydrogel-coated 10 cm dishes then incubated at 37°C with trypsin-EDTA. Phase contrast microscopy displays that HaCaTs on 4 kPa dishes remained adhered to the substrate in the presence of trypsin-EDTA, whilst those on TCP had dissociated by 7 minutes. Scale bars = 100 μm.*

tested but increased time did not improve dissociation. It was noted that when the medium was removed from BM dishes, the hydrogels had acquired a red tinge

(Figure 3.2A) which suggested that the medium was absorbed by the gel during culture. Extensive washing with PBS did not appear to remove the medium from the gel as they remained stained.

Protein lysates were prepared from the HaCaTs and assessed using SDS-PAGE gels. The polyacrylamide gels were stained with InstantBlue®, which revealed that HaCaTs cultured on BM hydrogels possessed a very strong protein band beneath the 70 kDa marker on the ladder that was strikingly absent from the TCP cultured cells (Figure 3.2B). The molecular weight of albumin is approximately 66 kDa and it was thus concluded that the strong protein band observed in the BM cultured HaCaT samples was likely albumin from the FBS used to supplement the culture medium. The medium had been observed to be retained by the hydrogels even after extensive

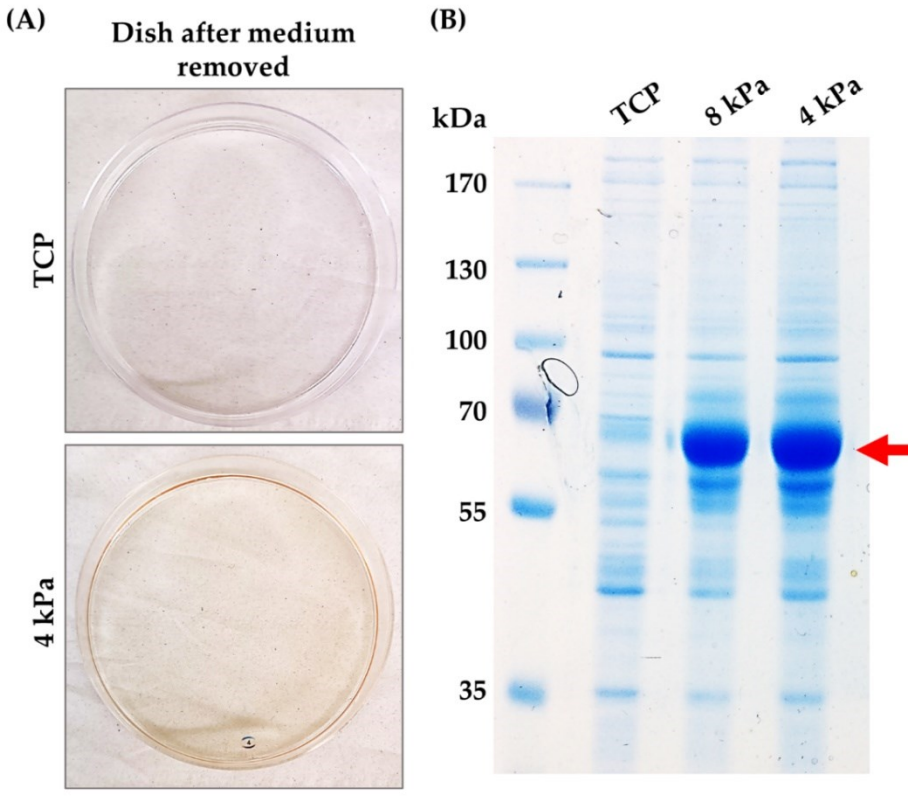

Figure 3.2 BM hydrogels absorbed medium during culture and acquired a high serum content. (A) *BM hydrogel-coated dishes retained a red hue following removal of the culture medium, suggesting that medium had been absorbed.* **(B)** *Protein lysates taken from HaCaT hydrogel cultures and analysed following SDS-PAGE and InstantBlue™ staining were observed to possess a strong protein band (red arrow) consistent with the weight of albumin which is found in the medium supplement FBS.*

washes and lysate samples were stained pink following use of the cell scraper, thus it was concluded that serum absorbed by the gels was inactivating the trypsin during the dissociation process.

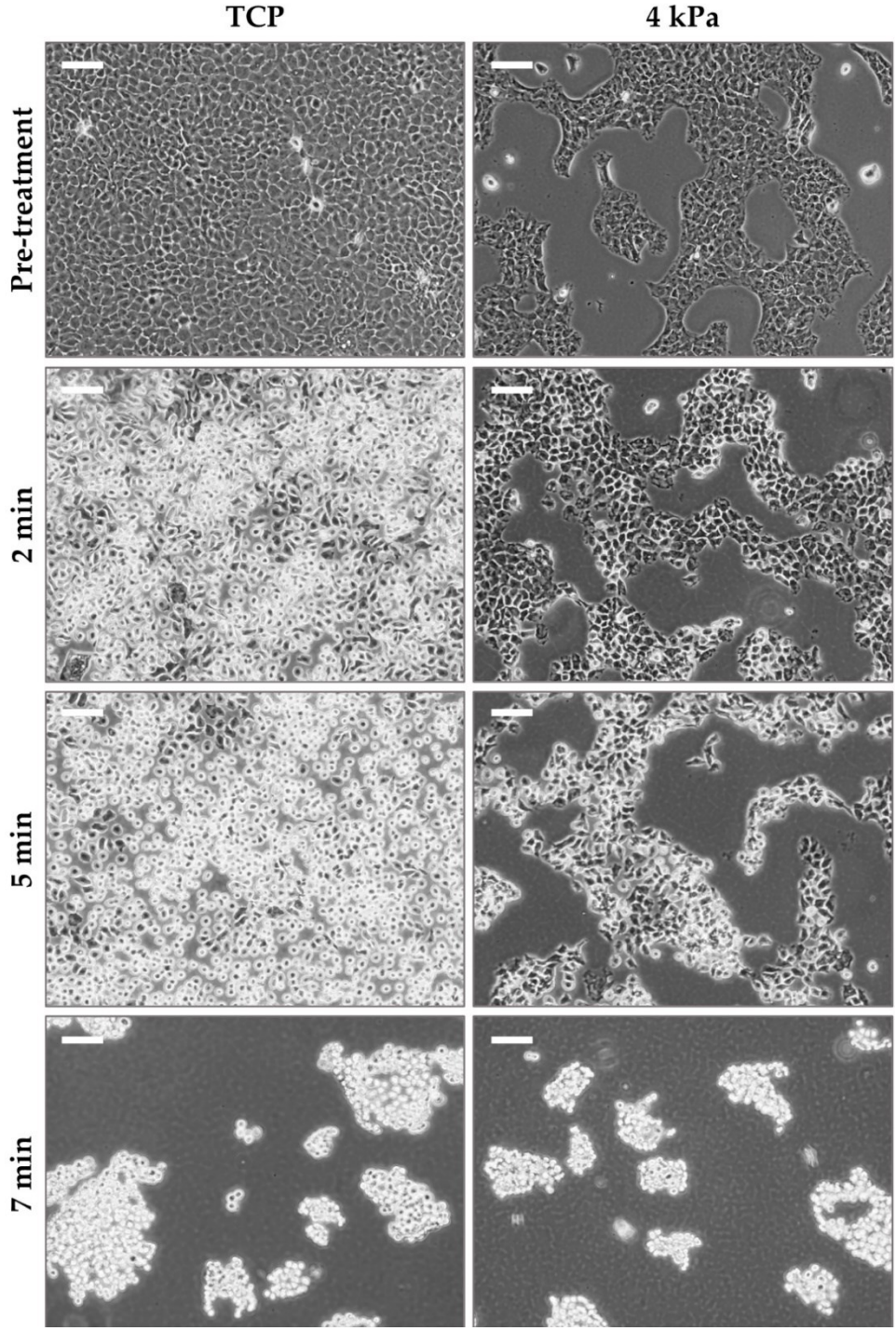

Figure 3.3 HaCaTs cultured on 4 kPa hydrogels were successfully dissociated using TrypLE™ Express Enzyme. *HaCaT cells were cultured on TCP and 4 kPa hydrogel-coated 10 cm dishes then incubated at 37°C with TrypLE™ Express Enzyme. Phase contrast microscopy displays that HaCaTs on both TCP and 4 kPa dishes had dissociated by 7 minutes of incubation time. Scale bars = 100 μm.*

With the ultimate goal being to use primary keratinocytes, it was deemed inappropriate to increase the concentration of trypsin given that primary cells are very sensitive. TrypLE™ Express Enzyme is a trypsin alternative produced by Gibco (Thermo Fisher Scientific) that has been shown to have greater specificity than trypsin and has been demonstrated to dissociate cells in serum supplemented systems (TrypLE Express User Guide, 2020). It was decided that this was a viable alternative to trypsin and would not jeopardise sensitive primary keratinocytes should incubation time or volume of the enzyme be increased. It was subsequently observed that HaCaTs cultured on BM hydrogels could be dissociated using TrypLE™ Express Enzyme (Figure 3.3), and this was therefore the dissociation agent used for all further cell culture work.

3.4.1.2 Primary keratinocytes cannot be propagated beyond one passage on very soft hydrogels

Another benefit of culturing cells in 2D is that they can be easily and rapidly expanded, providing a large amount of material to work with and thus making it a cost-effective method. These are features that are not translated well into 3D culture, and so it was a point of interest whether keratinocytes could be cultured for multiple passages using hydrogel-coated dishes. HEKn were revived and cultured in a TCP flask before initially being seeded onto 10 cm TCP or 4 kPa hydrogel-coated dishes. They were cultured for 4 days to allow acclimatisation to their substrate, then dissociated and seeded onto a new substrate of the same stiffness and cultured for a further 4 days. It was observed that HEKn cultured on TCP readily adhered and proliferated on a second dish (Figure 3.4). However, whilst HEKn grew well on 4 kPa dishes during the first passage, when they were seeded onto a second dish, they failed to adhere and consequently propagation could not continue.

Figure 3.4 (overleaf) HEKn could not be cultured on 4 kPa hydrogels beyond one passage. *HEKn were cultured on TCP and 50 kPa and 4 kPa hydrogel-coated dishes for one passage before being dissociated and seeded onto a second dish of the same stiffness. Phase contrast microscopy displays that HEKn adhered and grew as normal on a second TCP and 50 kPa dish but were unable to reattach when seeded onto a second 4 kPa dish. Scale bars = 100 μm.*

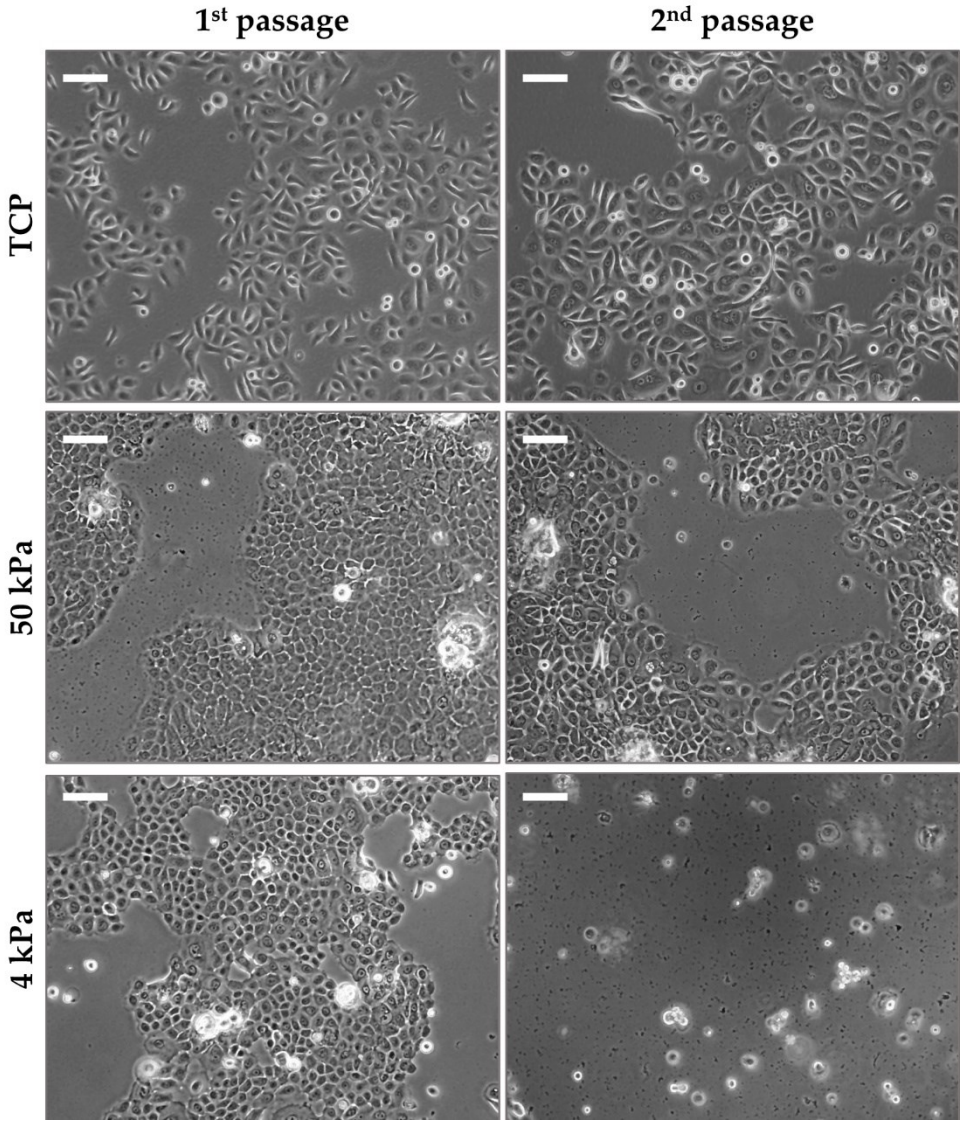

To check that this was a result of substrate stiffness rather than an effect of the hydrogels themselves, the experiment was repeated to include 50 kPa hydrogel-coated dishes which are over 10 times stiffer than the 4 kPa substrates. It was observed that HEKn cultured on 50 kPa were able to adhere and proliferate on a second dish in a similar way to those cultured on TCP (Figure 3.4). Consequently, it was hypothesised that 4 kPa hydrogels were potentially too soft to promote a basal cell phenotype and thus cells did not readily express the necessary adhesion molecules to reattach following acclimatisation to the soft substrate. The veracity of this supposition will be explored later in this chapter. However, it was observed that when HEKn cultured on 4 kPa were seeded back onto a TCP dish for the second passage, some cells were able to adhere and continue growing (Figure 3.5). This

further implied that it is the stiffness of the 4 kPa hydrogels that affects the ability of HEKn to reattach and continue their propagation.

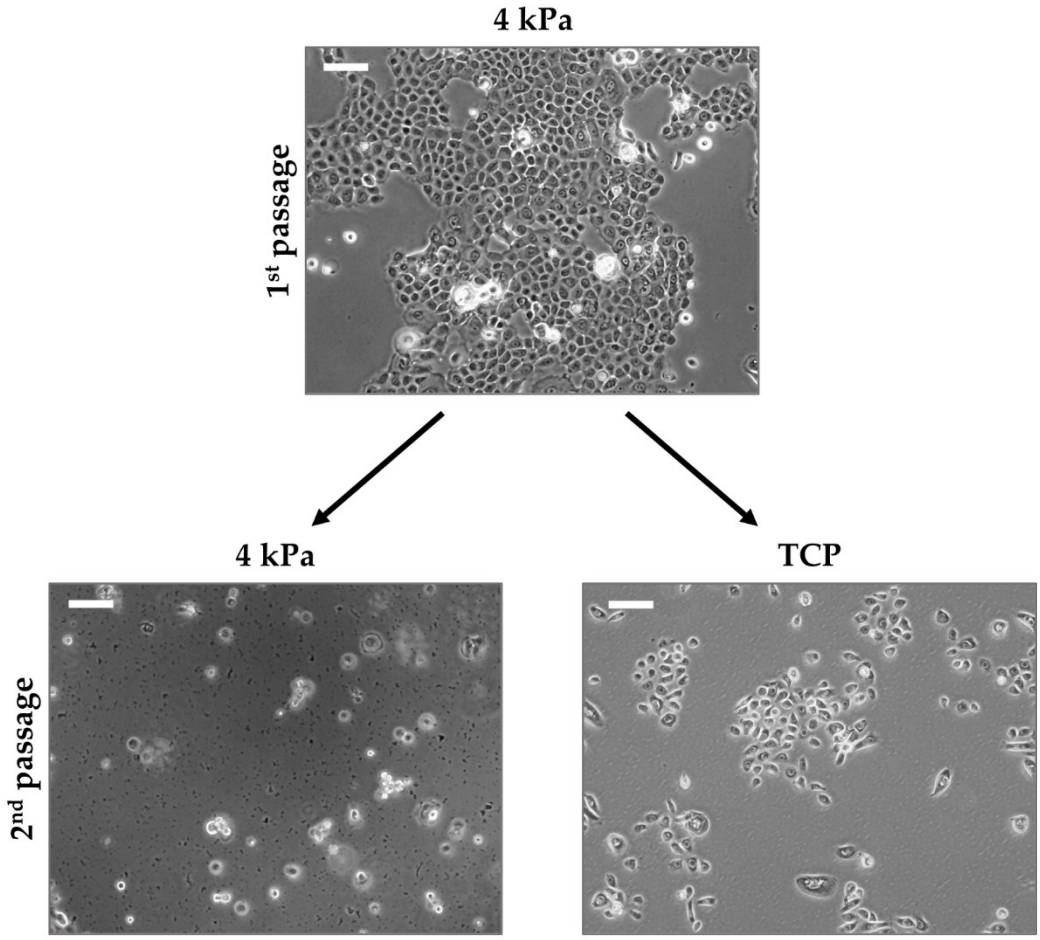

Figure 3.5 HEKn cultured on 4 kPa hydrogels were able to reattach for a second passage if seeded back onto TCP. *HEKn were cultured on 4 kPa hydrogel-coated dishes for one passage, before being dissociated and seeded onto either a second 4 kPa dish or a TCP dish. Phase contrast microscopy displays that HEKn did not reattach when seeded onto a 4 kPa dish, but they were able to adhere to TCP. Scale bars = 100 μm.*

3.4.1.3 Petrisoft™ hydrogel-coated dishes exhibited batch variability that affected cell growth

One of the main reasonings behind choosing to purchase hydrogel-coated dishes for this project rather than make them was to reduce variability that could impact results. However, on several occasions batches of Petrisoft™ dishes were received that did not appear to support cell adhesion or growth (Figure 3.6). These defective dishes were observed across all stiffness ranges so did not appear linked to a particular

substrate. Moreover, multiple dishes received in the same box were found to exhibit the same problem rather than single dishes here and there, suggesting that the issue arose from the recipe used for the entire batch (Figure 3.6). Given that these were commercially purchased, no further investigations were carried out regarding this observation, but it is worth noting the implication that variability between dishes is unavoidable even when obtained from a regulated source.

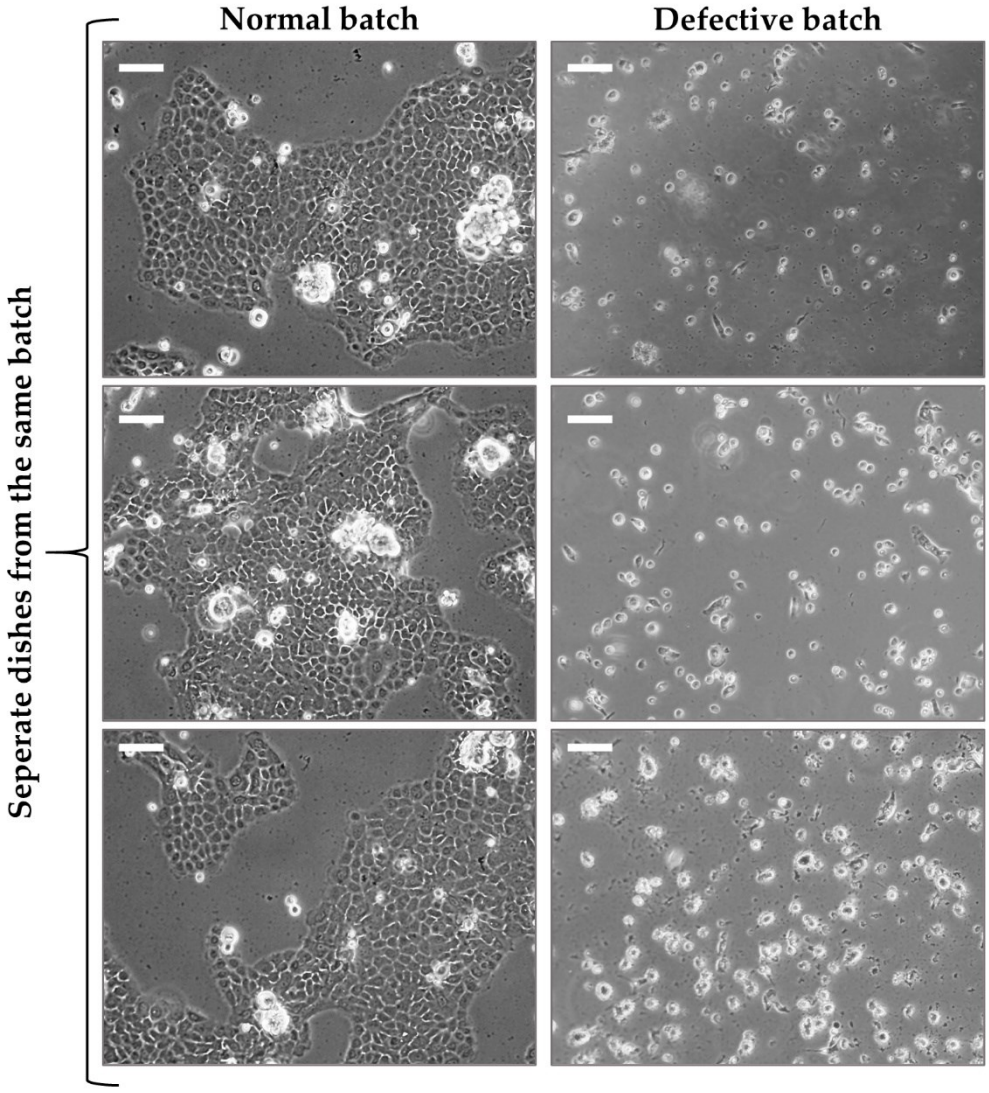

Figure 3.6 HEKn were observed not to attach or proliferate when seeded onto certain batches of BM dishes. *Phase contrast microscopy displays that when seeded onto defective Petrisoft™ hydrogel-coated dishes, HEKn did not exhibit normal attachment or proliferation and appeared to have undergone apoptosis by the end of 4 days, as evidenced by cell crenation, detachment, and the presence of debris. Scale bars = 100 μm.*

3.4.1.3 HEKn cultured on BM coverslips were difficult to image by confocal microscopy

Aside from general day-to-day culture challenges, working with biomimetic hydrogels presented technical obstacles at various stages of cell analysis. One of the most striking of these was discovered whilst attempting to image immunofluorescently stained cells through confocal microscopy. HEKn were cultured on glass and BM substrates for 4 days to allow acclimatisation of the cells, then they were fixed and stained as detailed in 2.4.1. Coverslips were mounted onto glass slides and viewed on a Zeiss LSM 880 with Airyscan. The majority of images were taken using a Plan-Apochromat 63x/1.4 Oil DIC M27 objective, and it quickly became apparent that the hydrogel layer coating the coverslips created too great a distance between the objective and the cells to view them with clarity (Figure 3.7).

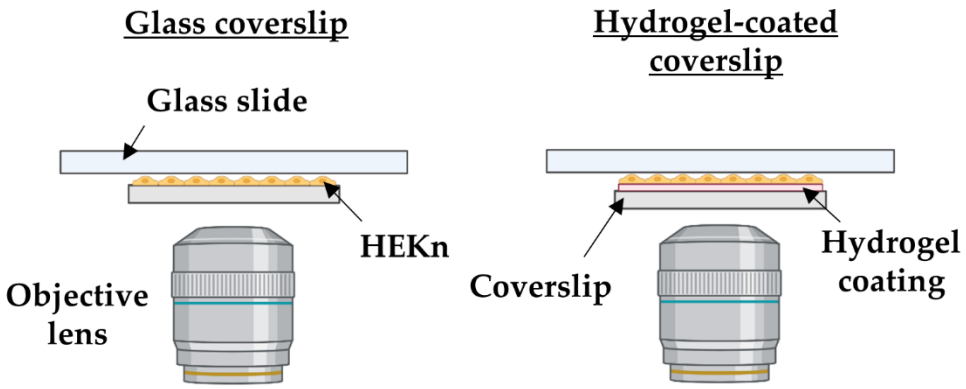

Figure 3.7 Coverslips coated with hydrogel had an increased distance between the microscope objective and cells. *Schematic demonstrating how the addition of a hydrogel layer increased the depth of BM coverslips compared to standard glass coverslips. This increased the distance between the objective and the cells attached to the coverslip.*

The Zeiss LSM 880 is inverted, and when trying to locate the cells on the BM coverslips, the objective had to be raised to such an extent that it began to lift the slide off the stage, resulting in unfocused images (Figure 3.8). This would still be a problem for an upright microscope and would likely result in damage to both the slide and the objective, so it was necessary to acquire a solution that bypassed the issue of the extra coverslip thickness provided by the hydrogel layer.

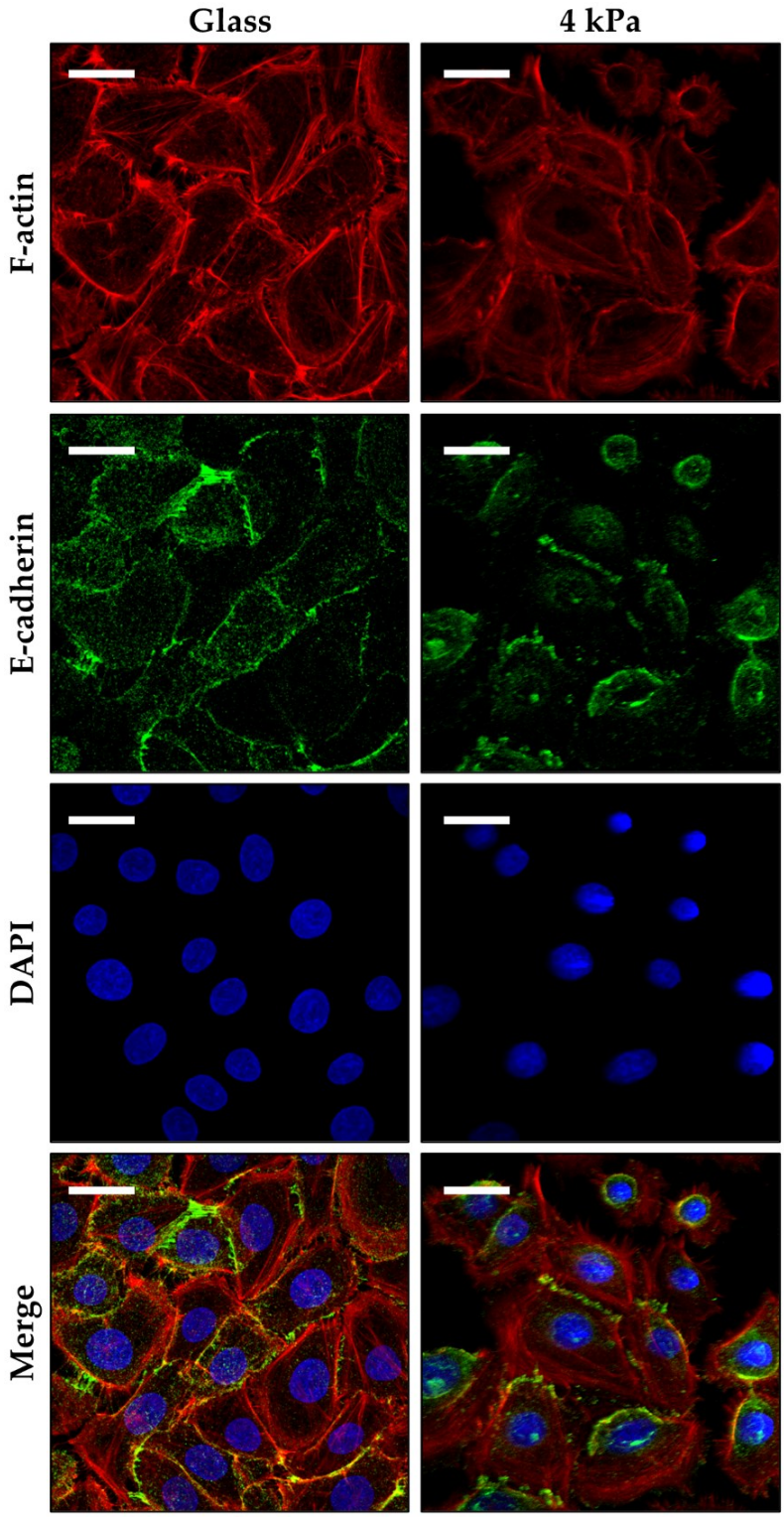

Figure 3.8 Confocal images taken of HEKn on BM coverslips were unfocused. *HEKn were cultured on glass and 4 kPa hydrogel-coated coverslips and immunostained for proteins of interest. Confocal microscopy images display how the extra depth provided by the hydrogel-coating on the BM coverslips resulted in poor quality unfocused images in contrast to those of cells on standard glass coverslips. Scale bars = 25 μm.*

The initial solution was to find a way to image the coverslips by reducing the distance between the objective and the cells. To this end, it was decided to mount coverslips on glass bottom dishes rather than slides, thus enabling the cells to be viewed through the single layer of the glass dish rather than the double layer of the coverslip and hydrogel (Figure 3.9A). Whilst this did solve the issue of poor image quality (Figure 3.9B), it was deemed impractical for largescale immunofluorescence analysis, not only because glass bottom dishes are less cost-effective than slides, but because they cannot be easily stored in large numbers.

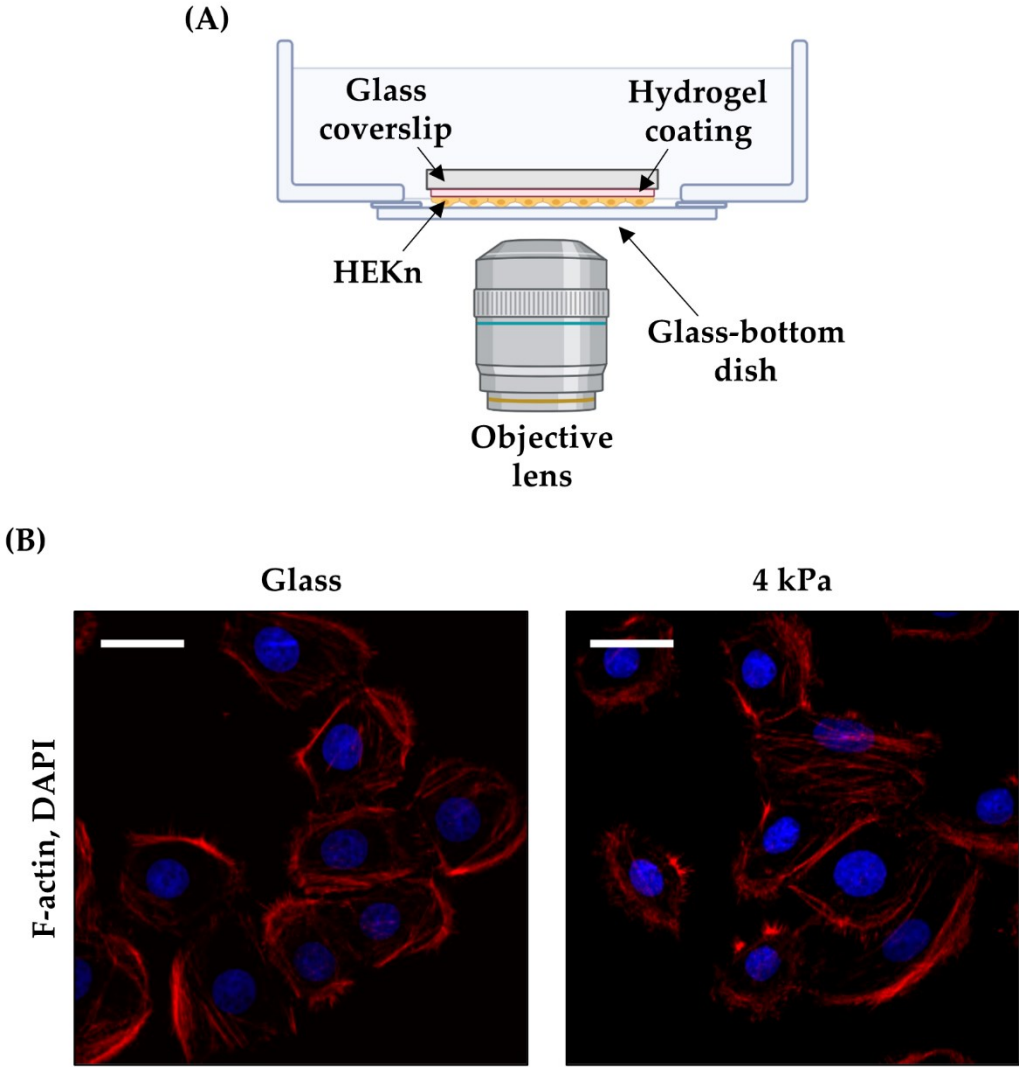

Figure 3.9 Mounting BM coverslips on glass bottom dishes improved confocal image quality. (A) *HEKn cultured on 4 kPa hydrogel-coated coverslips were immunostained and mounted onto glass bottom dishes which reduced the distance between the cells and the objective lens.* **(B)** *Confocal microscopy images display that 4 kPa hydrogel-coated coverslips mounted in this way produced images of quality relative to that of standard glass coverslips. Scale bars = 25 μm.*

Following discussion with the team in the advanced light microscopy facility (Durham University), it was determined that an alternative solution would be to use an objective with a greater free working distance. The free working distance of the Plan-Apochromat 63x/1.4 Oil DIC M27 previously used was 0.19 mm, enabling the imaging of cells mounted on coverslips with a maximum thickness of 0.17 mm. This was replaced with a Plan-Apochromat 63x/1.2 Imm Corr DIC M27 objective with a free working distance of 0.49 mm and allowing a maximum coverslip thickness of 0.19 mm. This objective was suitable for glycerine or oil immersion, and so both were tested to see which provided the best image quality. Whilst the image quality of both immersion techniques were greatly improved in comparison to those taken using the original objective (Figure 3.10), it was determined that oil immersion produced a cleaner image. Consequently, all subsequent confocal imaging was carried out using the Plan-Apochromat 63x/1.2 Imm Corr DIC M27 objective with oil immersion.

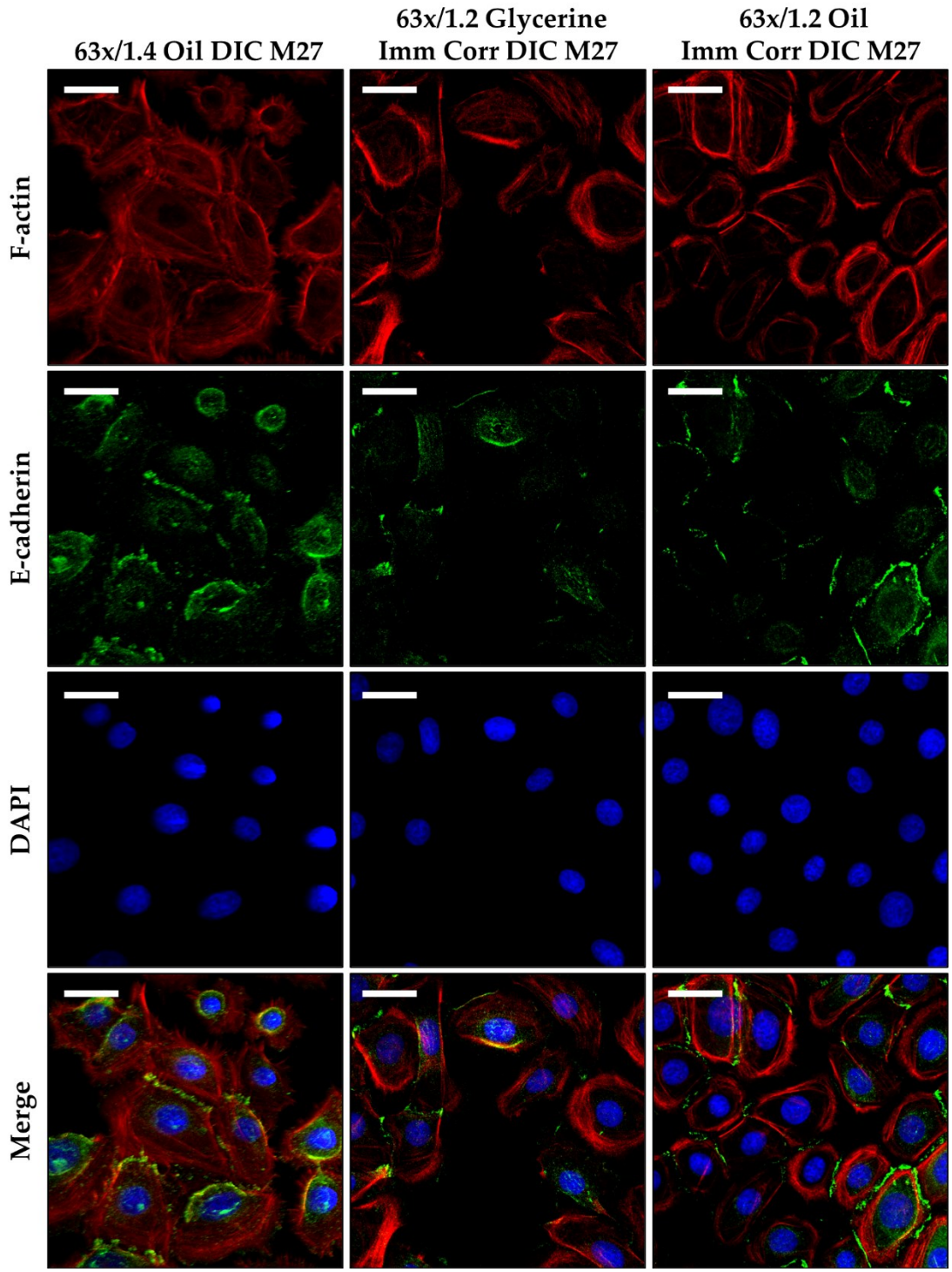

Figure 3.10 Using an objective with a greater free working distance improved confocal image quality for BM coverslips. *HEKn were cultured on 4 kPa hydrogel-coated coverslips, immunostained, and mounted onto glass slides. Confocal microscopy images display coverslips viewed using the standard x63 objective with a 0.19 mm free working distance (left), and a x63 objective with a 0.49 mm free working distance (middle and right). For the longer-range objective images were taken using both glycerine and oil immersion. Scale bars = 25 μm.*

3.4.1.3 HEKn protein yield for lysates was initially poor

The final technical challenge faced was procuring a high enough protein yield from HEKn to perform western blot analysis. Lysates were harvested from HEKn cultured for 4 days on their respective dishes, with cells being lysed in RIPA buffer and then immediately removed from the dish using a cell scraper. Full details of the subsequent steps can be found in 2.8.1. However, staining of gels with InstantBlue™ revealed very faint bands signifying a poor protein yield (Figure 3.11A). Though cells cultured on TCP were also observed to produce a poor yield, suggesting this was not

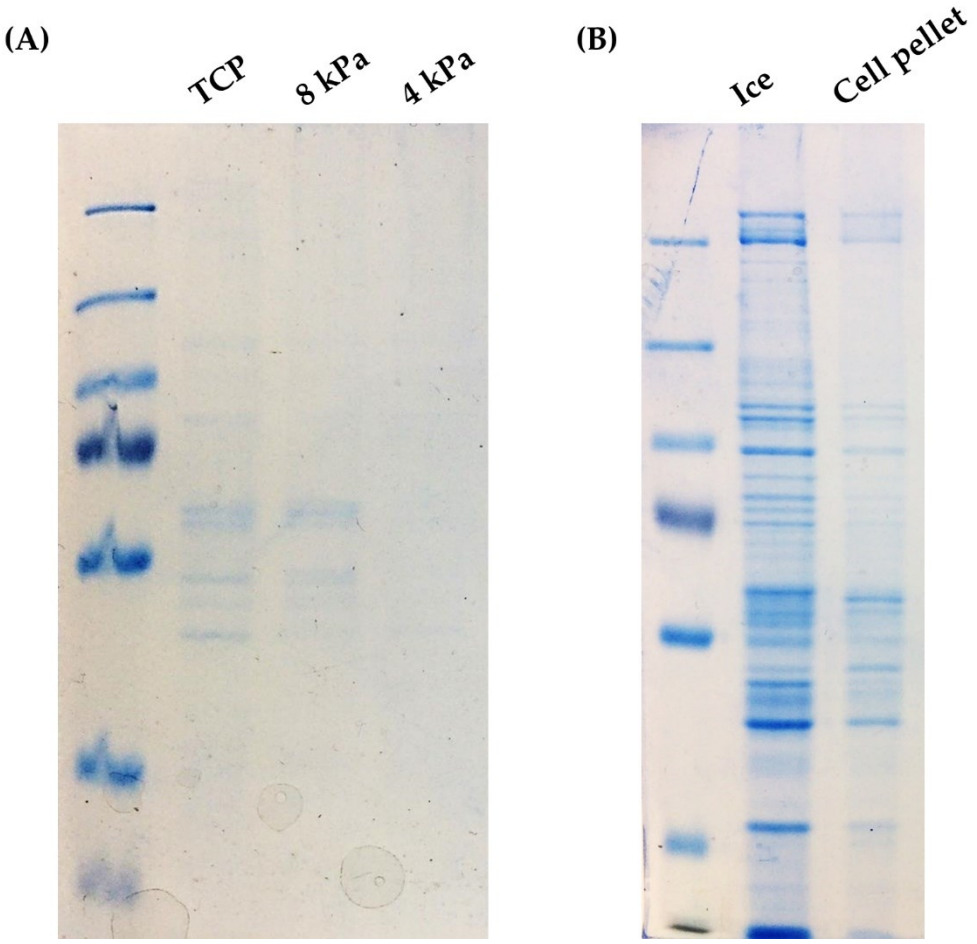

Figure 3.11 HEKn lysates had a better protein yield when cells were incubated with lysis buffer on ice. (A) *HEKn were cultured on TCP, 8 kPa, and 4 kPa dishes and protein lysates were harvested. An InstantBlue™ stained gel displays that protein yield was poor, particularly in the 4 kPa cultured cells.* **(B)** *HEKn were incubated for 30 mins on ice on a rocker in lysis buffer or were dissociated from the dish and the cell pellet was resuspended in lysis buffer. An InstantBlue™ stained gel displays that lysates from HEKn incubated on ice produced a better protein yield than those prepared from a cell pellet.*

an issue caused by the hydrogels, the softer substrates did seem to exacerbate the problem, as evidenced by the complete lack of bands in the 4 kPa lane (Figure 3.11A). Given how delicate the hydrogels are, it is not possible to firmly scrape the surface when harvesting lysates, as this would lead to tearing of the gel and subsequent contamination of the sample. Consequently, it was difficult to ensure that the cells are thoroughly lysed on the BM dishes.

In order to improve the HEKn protein yield, two alternative methods were tested. Firstly, the lysis buffer was added to the dishes as before, but they were then placed on ice on a rocker for 30 mins to allow longer exposure to the buffer. After this time, the lysates were collected using a cell scraper and subsequently treated as normal. Alternatively, HEKn were dissociated from their dish using TrypLE and centrifuged before the resulting cell pellet was resupended in lysis buffer. An InstantBlue™ stain of these two techniques clearly revealed that HEKn placed on ice on a rocker produced a much better protein yield than those made from a cell pellet (Figure 3.11B). All further protein lysates were therefore harvested using this method.

3.4.2 Keratinocytes cultured on softer substrates exhibited increased cell density

3.4.2.1 HaCaT cells had a more 3D appearance on BM hydrogels

As mentioned previously, the BM hydrogels were initially investigated using HaCaT cells in order to ascertain whether there were any significant changes in cell appearance and behaviour. HaCaTs were seeded onto TCP and 8 kPa and 4 kPa BM dishes and cultured for 4 days; a period deemed appropriate to allow the cells time to acclimatise to the substrate stiffness, whilst ensuring they did not become too confluent. The earliest observation was that HaCaTs cultured on 8 kPa and 4 kPa hydrogels seemed to form more densely packed colonies than those on TCP, and the presence of shadowing on the 4 kPa dishes (Figure 3.12A – white arrows) implied that colonies on softer substrates were more 3D. The edges of colonies were distinct, as though raised above the culture dish (Figure 3.12A – red arrows), whereas HaCaTs cultured on TCP did not exhibit defined colony edges and appeared to blend in more

with the underlying substrate. To assess whether the colony density did in fact change on the BM hydrogels, the number of cells per 10,000 μm² was calculated (Figure 3.12B). It was observed that HaCaTs cultured on BM hydrogels were significantly denser than those on TCP, and even between 8 kPa and 4 kPa substrates there was a significant increase in cell density in response to the decrease in stiffness. These observations confirmed that culturing HaCaTs on BM hydrogels led to changes in cell appearance and behaviour. Consequently, it was deemed appropriate to introduce primary HEKn to the experimental plan in preparation for 3D model development.

Figure 3.12 (overleaf) HaCaTs cultured on BM hydrogels exhibited increased cell density within colonies. *HEKn were cultured on TCP and 8 and 4 kPa hydrogels for 4 days.* **(A)** *Phase contrast microscopy images display that when HaCaTs were cultured on 8 and 4 kPa dishes colony edges were more distinct and appeared raised from the underlying substrate (red arrows). Shadowing (white arrows) observed on the 4 kPa dishes suggested a more 3D colony structure. Scale bars = 250 μm* **(B)** *Quantification of the number of cells per 10,000 μm². Data represent mean ±SEM, n = 3 (3x 20 squares), statistical significance was assessed using one-way ANOVA with Tukey's post hoc test, *** p ≤ 0.0001.*

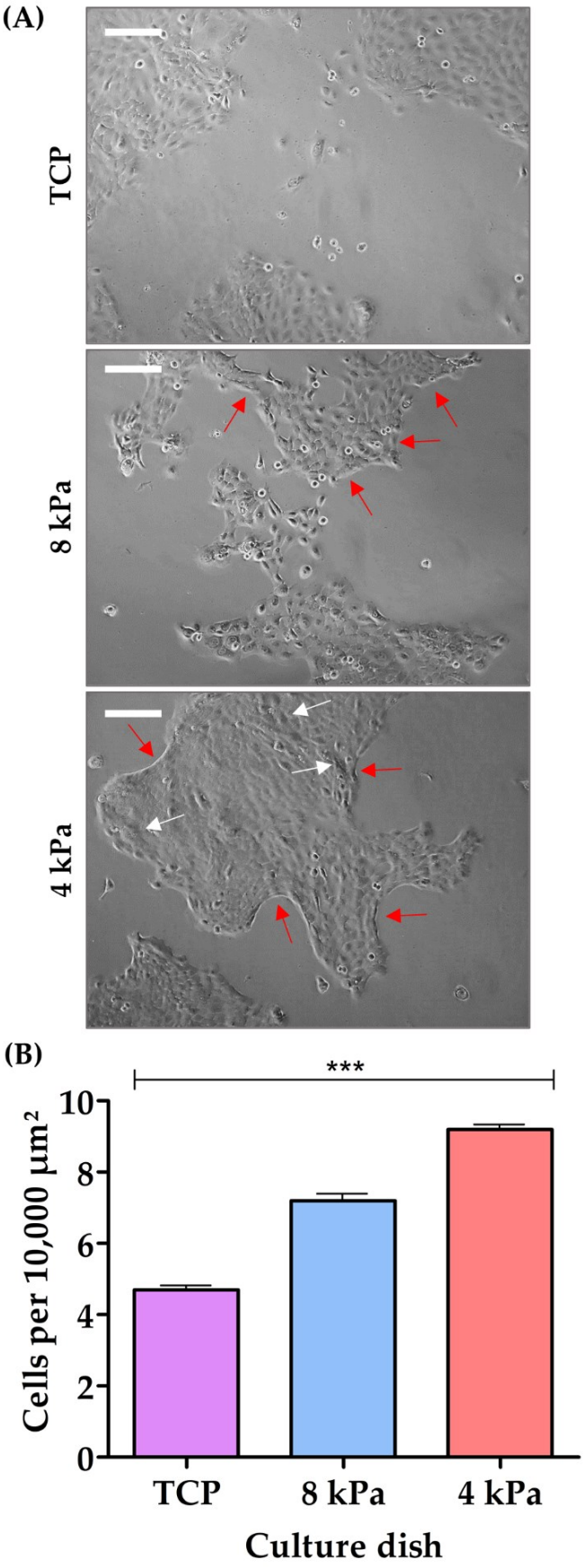
(A)
TCP
8 kPa
4 kPa
(B)
***
Cells per 10,000 μm²
0
2
4
6
8
10
TCP
8 kPa
4 kPa
Culture dish

3.4.2.2 HEKn cultured on BM hydrogels exhibited greater cell density and cobblestone morphology

Following on from the initial investigation using HaCaT cells, primary HEKn were cultured on TCP and BM dishes for 4 days to enable acclimatisation to the substrate stiffness. In addition to the 8 kPa and 4 kPa hydrogels, HEKn were also cultured on 50 kPa substrates due to the significance of this stiffness in relation to epidermal model development (see chapter 5 for further discussion). As with the HaCaT cells, HEKn appeared more densely packed on the BM hydrogel substrates, and they exhibited a regular cobblestone morphology in comparison to those on TCP which appeared more heterogenous (Figure 3.13A). Analysis of the number of cells per 10,000 μm^2 revealed that HEKn cultured on BM hydrogels were significantly denser than those on TCP, and cells on 4 kPa substrates were significantly denser than those on 50 kPa and 8 kPa (Figure 3.13B). Given the significance of the epidermal calcium gradient in keratinocyte differentiation and epidermal assembly, the assessment of cell density was repeated under high calcium conditions. At the day 4 culture time point, the medium was replaced with high calcium medium containing 1.5 mM $CaCl_2$, and the cells were cultured for a further 24 hours. Phase contrast images after this period revealed that HEKn on TCP appeared to increase in density and developed the cobblestone morphology (Figure 3.14A) observed in HEKn on BM dishes under low calcium conditions (Figure 3.13A). The HEKn on BM hydrogels maintained their appearance, though cells on 4 kPa substrates appeared the least heterogenous., Analysis of cell density confirmed that HEKn on BM dishes continued to have a greater cell density than those cultured on TCP (Figure 3.14B). It was therefore apparent that culturing HEKn on BM hydrogels influenced changes to cell density and induced a cobblestone morphology that was only seen under high calcium conditions on TCP.

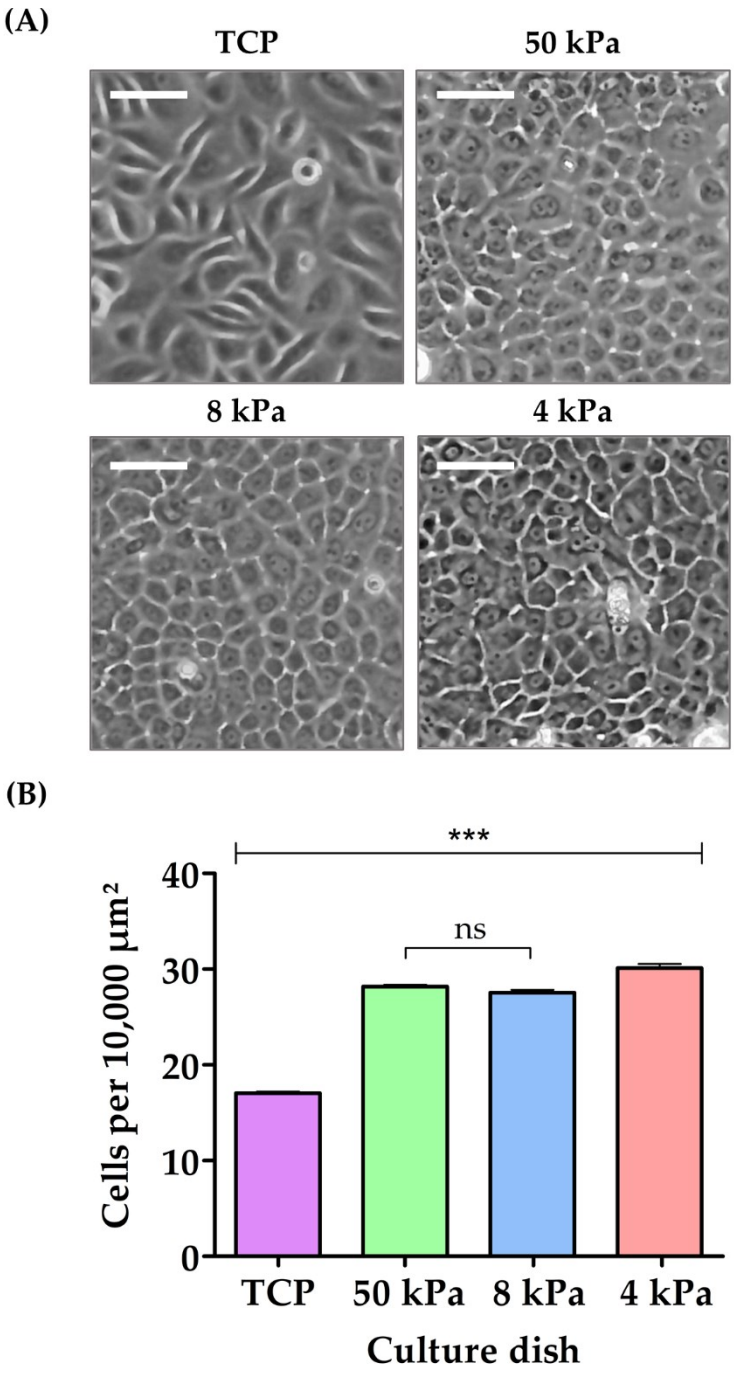

Figure 3.13 HEKn cultured on BM hydrogels had a greater cell density. (A) *HEKn were cultured on TCP and 50, 8 and 4 kPa dishes for 4 days. Phase contrast images display the changes in colony appearance exhibited on the hydrogels, with HEKn adopting a more regular, cobblestone morphology. Scale bars = 50 µm.* **(B)** *Quantification of the number of cells per 10,000 µm². Data represent mean ±SEM, n = 3 (3x 20 squares), statistical significance was assessed using one-way ANOVA with Tukey's post hoc test, *** $p \leq 0.0001$, ns = non-significant.*

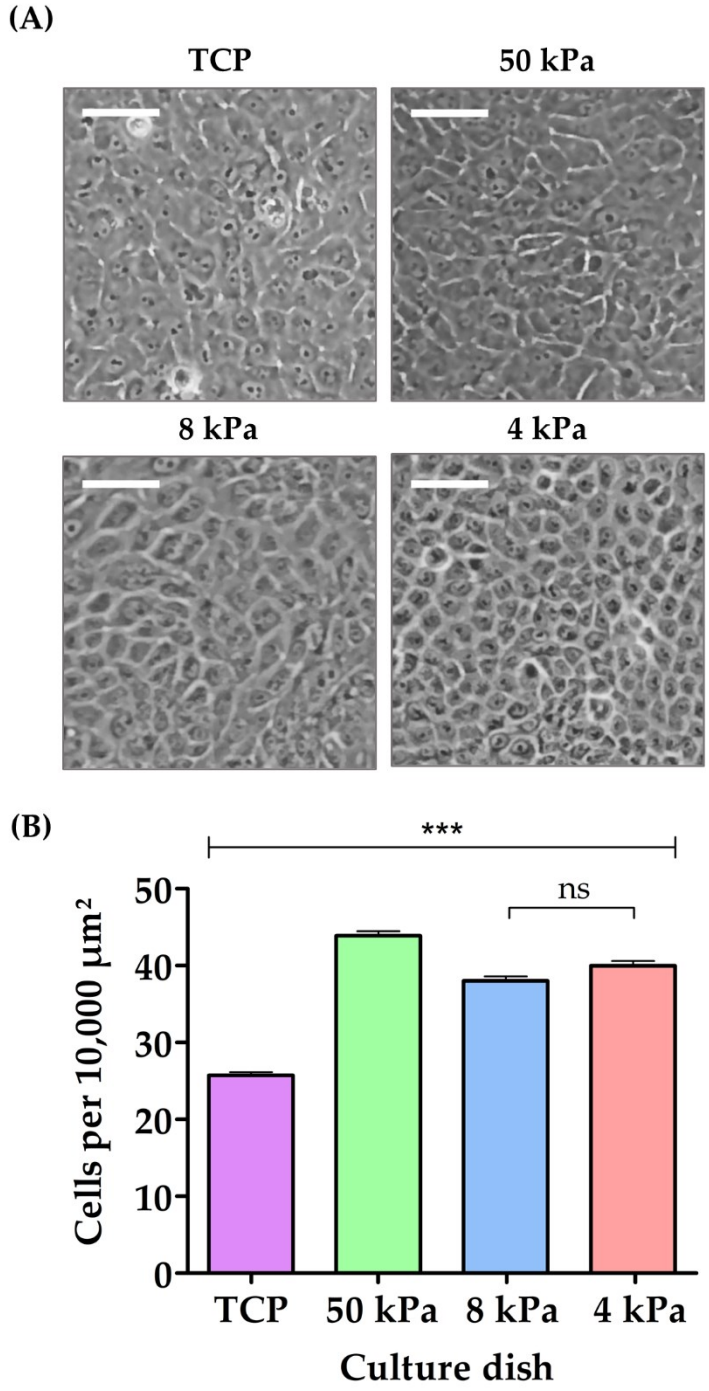

Figure 3.14 HEKn cultured on BM dishes under high calcium conditions still exhibited greater cell density. (A) *High calcium medium was added to HEKn that had been cultured on TCP and 50, 8 and 4 kPa dishes. After 24 hours phase contrast images were taken and display that all HEKn exhibited a regular cobblestone morphology. Scale bars = 50 µm.* **(B)** *Quantification of the number of cells per 10,000 µm². Data represent mean ±SEM, n = 3 (3x 20 squares), statistical significance was assessed using one-way ANOVA with Tukey's post hoc test, *** p ≤ 0.0001, ns = non-significant.*

3.4.3 Culturing keratinocytes on softer substrates led to decreased proliferation and a shift towards differentiation

3.4.3.1 HaCaTs cultured on BM hydrogels exhibited decreased proliferative activity

The next observation when culturing HaCaT cells on BM dishes, was that they appeared to proliferate more slowly than those on TCP, with the dishes appearing less confluent at the end of the 4 day culture period. Though this apparent lower confluency was likely due in part to the increased cell density (Figure 3.12B), an EdU assay was carried out to assess the proliferative activity of the HaCaTs on the different substrates. It was observed that HaCaTs cultured on BM hydrogels had fewer EdU positive cells than those cultured on glass coverslips (Figure 3.15), indicating a reduced level of proliferation.

Figure 3.15 (overleaf) HaCaTs cultured on BM hydrogels exhibited decreased proliferative activity. (A) *HaCaTs were cultured on glass and 8 and 4 kPa coverslips for 4 days, then an EdU assay was completed. Confocal microscopy images display EdU positive nuclei in HaCaTs across the different culture substrates. Scale bars = 25 μm.* **(B)** *Quantification of the percentage of EdU positive cells observed on glass and BM coverslips. Data represent mean ±SEM, n = 3 (3x 100 cells), statistical significance was assessed using one-way ANOVA with Tukey's post hoc test, *** $p \leq 0.0001$, ns = non-significant.*

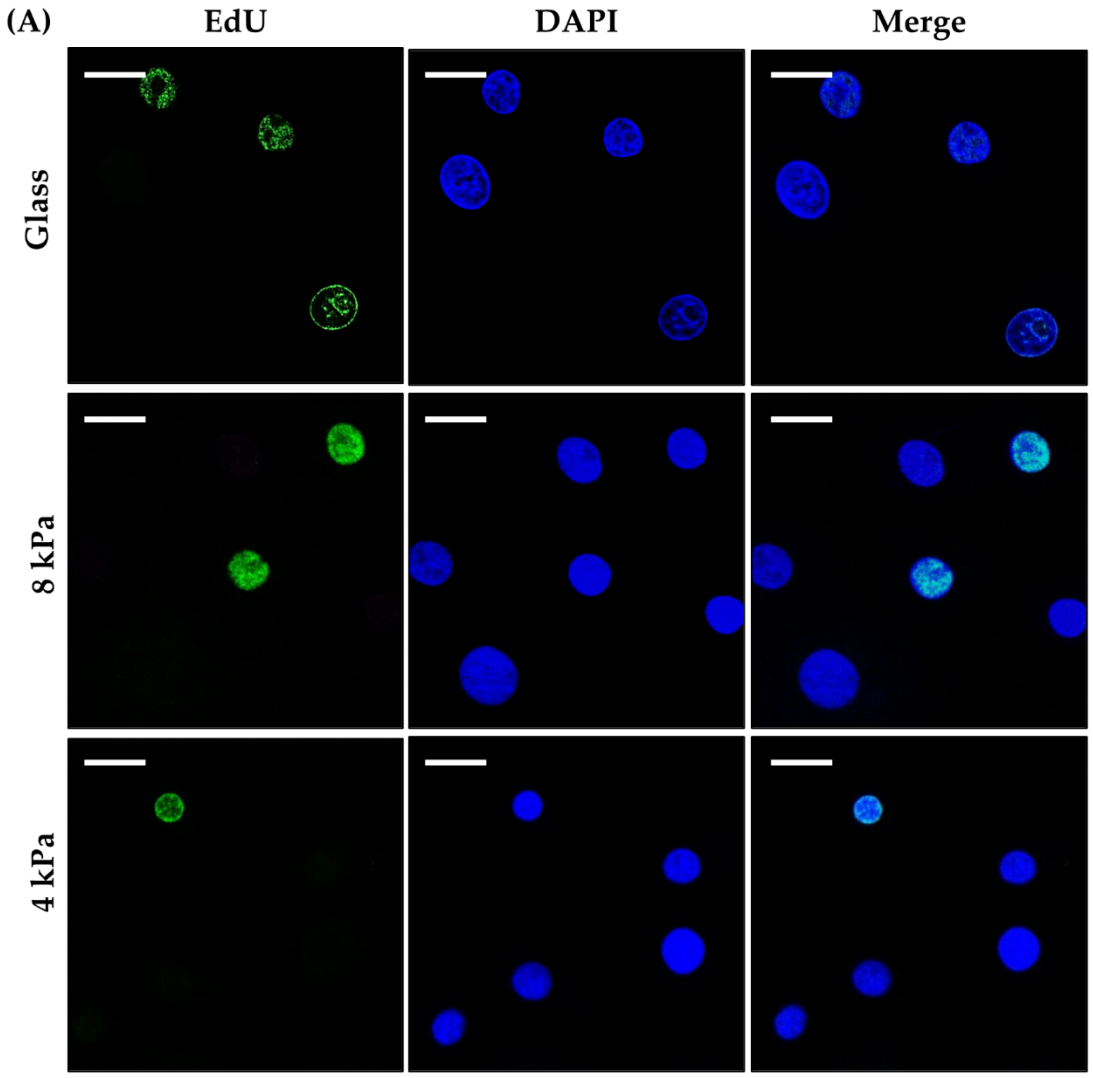
(A)
EdU
DAPI
Merge
Glass
8 kPa
4 kPa

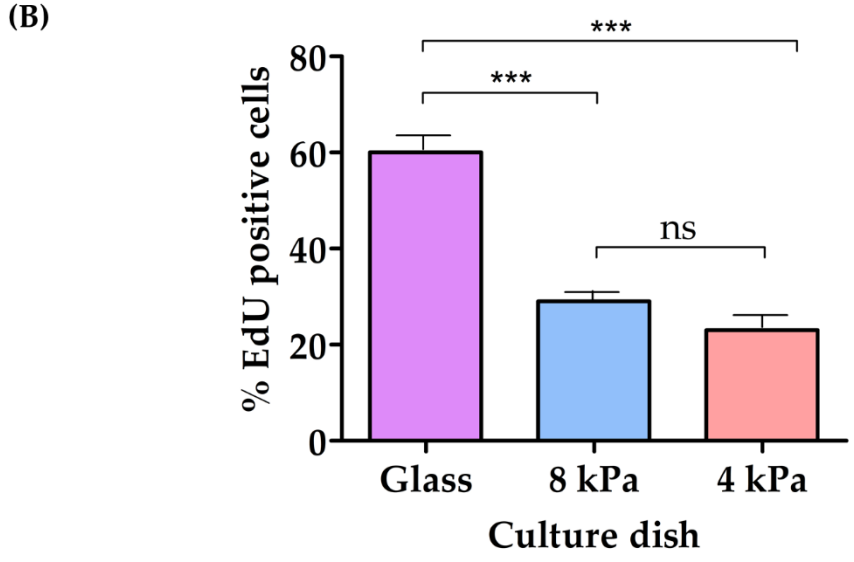
(B)
***
***
ns
80
60
40
20
0
% EdU positive cells
Glass
8 kPa
4 kPa
Culture dish

3.4.3.2 HEKn cultured on BM hydrogels exhibited signs of decreased proliferation as a direct result of substrate stiffness

As was observed with the HaCaT cells, HEKn cultured on BM hydrogels were found to proliferate more slowly than those on TCP, and another EdU assay was carried out to assess the proliferative activity of the HEKn on the different substrates. It was observed that HEKn cultured on BM hydrogels had fewer EdU positive cells than those cultured on glass coverslips (Figure 3.16), indicating a reduced level of proliferation. Moreover, there was a statistically significant reduction between HEKn cultured on 4 kPa dishes compared to those on 50 kPa, despite the relatively small change in substrate stiffness (Figure 3.16B).

Following on from this result, it was necessary to confirm that the decrease in proliferation on BM hydrogels was a direct result of the substrate stiffness. One of the key mechanosensitive pathways involved in epidermal homeostasis is the Hippo signalling pathway (Rognoni and Walko, 2019). In order to assess the activity of the Hippo signalling pathway, HEKn were cultured on TCP and 4 kPa coverslips for 4 days, then immunostained for the transcription factor YAP1; the localisation of which is indicative of whether HEKn are being driven towards a proliferative or differentiated phenotype (Figure 3.17A). Integrated density of the staining in the nuclear and cytoplasmic compartments was analysed, and it was observed that HEKn on TCP had a greater integrated density of YAP1 staining overall, though this was not stastically significant in the nucleus when analysed using One-way ANOVA with a Tukey post hoc test (Figure 3.17B). The integrated density of staining in the cytoplasm was significantly greater for HEKn on TCP, than those on the 4 kPa hydrogel. On a soft ECM, the Hippo pathway is known to be activated, and YAP1 is

Figure 3.16 (overleaf) HEKn cultured on BM substrates exhibited decreased proliferative activity. (A) *HEKn were cultured on glass and 50, 8 and 4 kPa coverslips for 4 days, then an EdU assay was completed. Confocal microscopy images display EdU positive nuclei in HEKn across the different culture substrates. Scale bars = 25 μm.* **(B)** *Quantification of the percentage of EdU positive cells observed on glass and BM coverslips. Data represent mean ±SEM, n = 3 (3x 100 cells), statistical significance was assessed using one-way ANOVA with Tukey's post hoc test, * $p \leq 0.05$, *** $p \leq 0.0001$.*

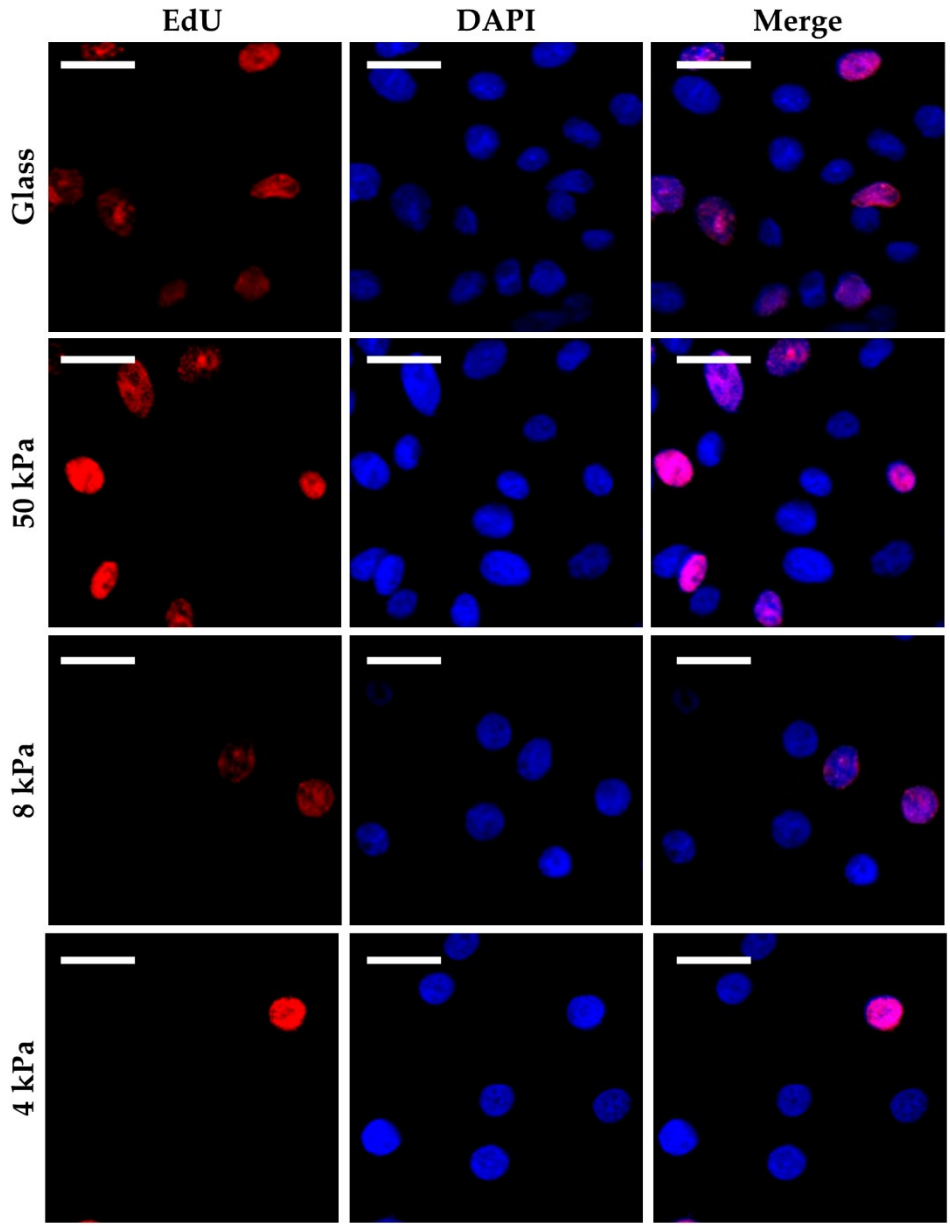
EdU
DAPI
Merge
Glass
50 kPa
8 kPa
4 kPa

(B)

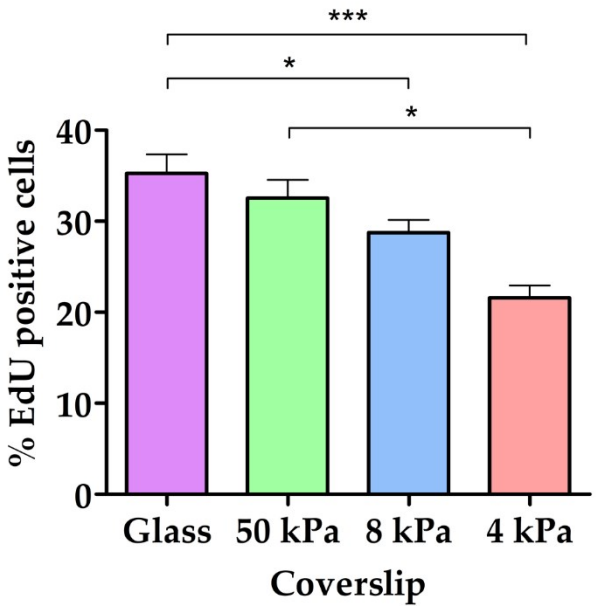
***
*
*
% EdU positive cells
40
30
20
10
0
Glass
50 kPa
8 kPa
4 kPa
Coverslip

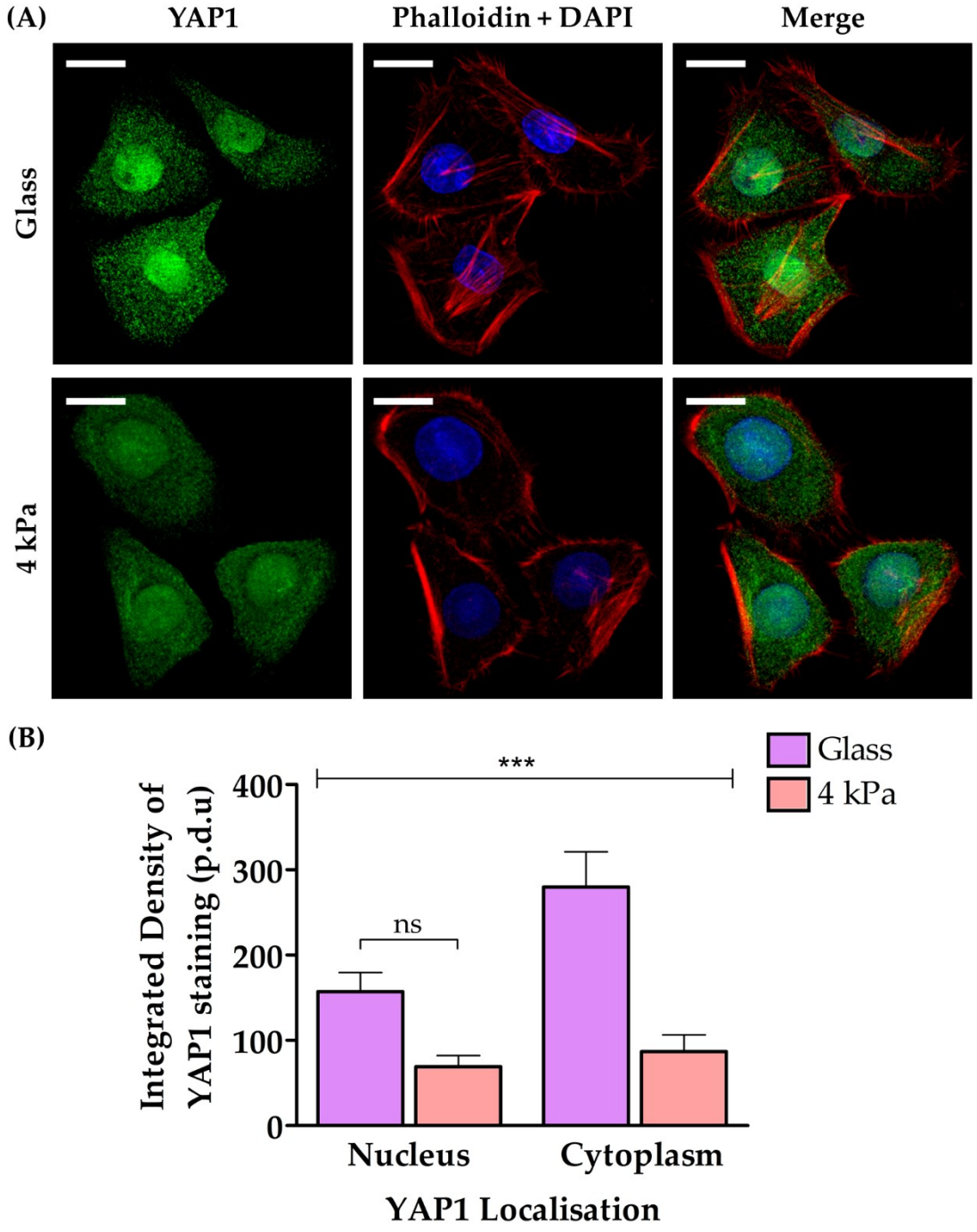

Figure 3.17 HEKn cultured on glass coverslips showed a greater Integrated Density of YAP1 staining. (A) *HEKn were cultured on glass and 4 kPa coverslips for 4 days then immunostained for YAP1. Confocal microscopy images display the localisation of YAP1 in response to the different substrates. The F-actin co-stain highlights the parameters of the cytoplasmic compartment. Scale bars = 25 µm.* **(B)** *Quantification of Integrated Density of YAP1 in the nuclear and cytoplasmic compartments of HEK on glass and 4 kPa BMH coverslips. Data represent mean ±SEM, n = 3 (3x 100 cells), statistical significance was assessed using one-way ANOVA with Tukey's post hoc test, *** $p \leq 0.0001$, ns = non-significant.*

sequestered in the cytoplasm and degraded which reduces proliferation and drives cells towards differentiation (Dupont et al., 2011). Given the reduced intensity of YAP1 staining in the HEKn cultured on 4 kPa coverslips, it was concluded that the Hippo pathway was likely active in cells on the hydrogels which resulted in YAP1 degradation.

In order to further confirm Hippo pathway activation in response to a softer culture substrate, RNA analysis was carried to assess the expression level of multiple regulators of the Hippo signalling pathway. HEKn were cultured on TCP and 50, 8, and 4 kPa cultureware for up to 4 days, with RNA samples being taken 1, 2, 3 and 4 days after seeding in order to monitor gene expression changes as the cells adapted to their environment. Samples were sent to P&G and analysed using WaferGen. The resulting data revealed that culturing HEKn on BM hydrogels did have an effect on the expression of key components of the Hippo signalling pathway (Figure 3.18). The upstream regulator *NF2* was observed to be significantly downregulated for the first 3 days of culture, before seemingly returning to a similar level of expression to TCP (Figure 3.18A). The fellow upstream regulator *WWC1* encoding the kibra protein was significantly upregulated in HEKn on 8 and 4 kPa hydrogels on day 4 (Figure 3.18C). At its core, the Hippo pathway is a kinase cascade, and the kinases MST1 and LATS1 did not show any significant changes in gene expression (Figure 3.18B and D), though *MST1* appeared to trend towards upregulation on day 1 followed by a gradual return to near TCP levels, whilst *LATS1* appeared to trend towards downregulation across all 4 days. *LATS2* appeared to be downregulated across the 4 days, with significant changes observed for 50 kPa and 8 kPa (Figure 3.18). The transcription factor gene *YAP1* was observed to trend towards downregulation by day 3 and 4, with significant changes observed in 8 kPa on day 3 and 50 kPa on day 4 (Figure 3.18F), whilst *TAZ* did not show any significant changes, but appeared to trend towards downregulation on the first 3 days then upregulation on the 4th (Figure 3.18G). Together these data

suggest that culturing HEKn on BM hydrogels induced significant changes in the regulation of the Hippo pathway and the expression of the transcription factor YAP1.

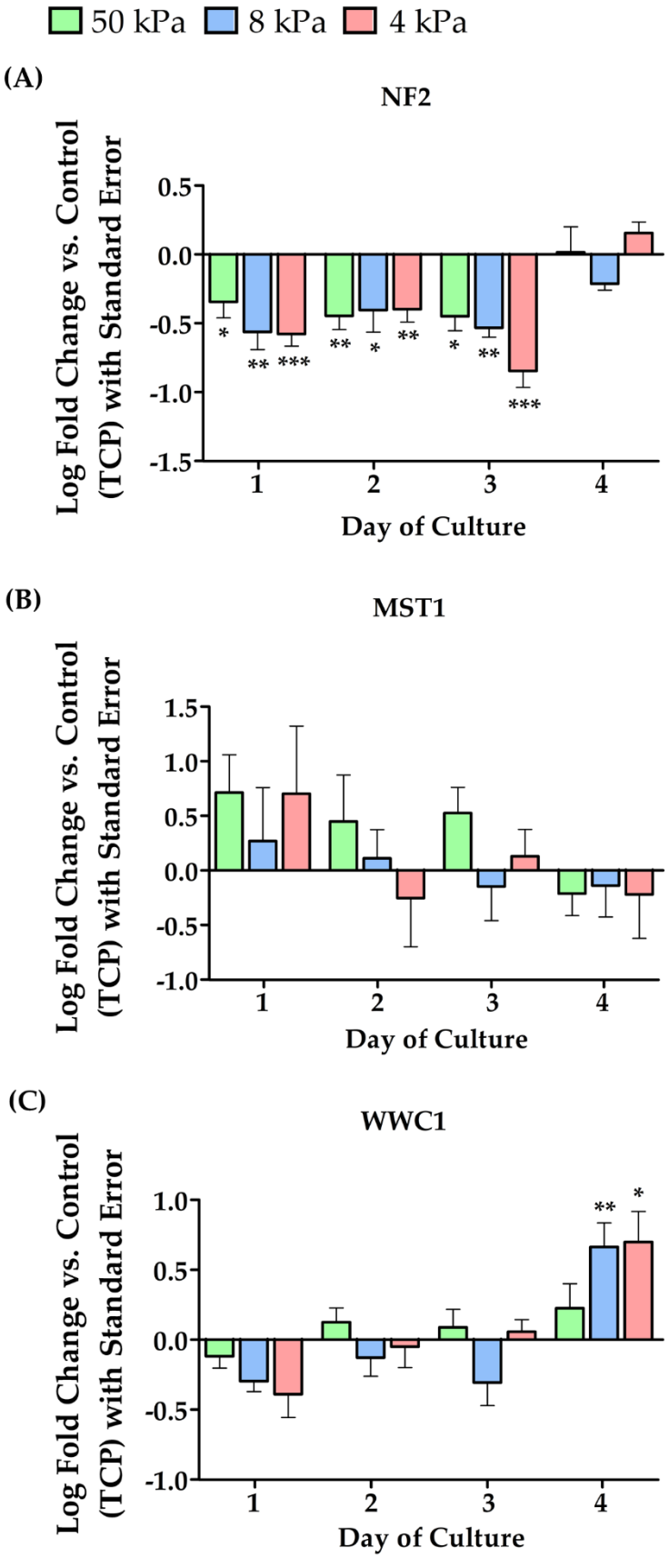

(D)

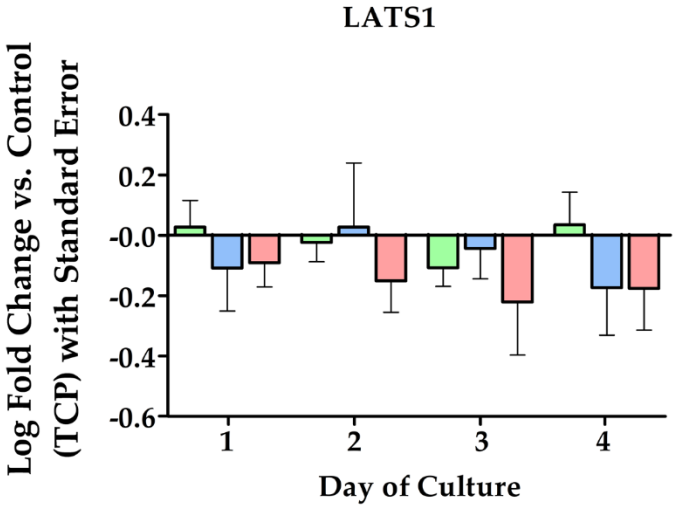
LATS1
Log Fold Change vs. Control (TCP) with Standard Error
0.4
0.2
-0.0
-0.2
-0.4
-0.6
1
2
3
4
Day of Culture

(E)

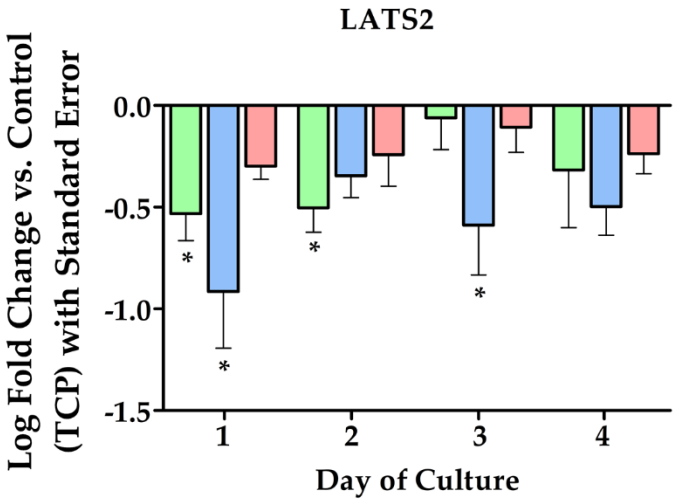
LATS2
Log Fold Change vs. Control (TCP) with Standard Error
0.0
-0.5
-1.0
-1.5
*
*
*
*
1
2
3
4
Day of Culture

(F)

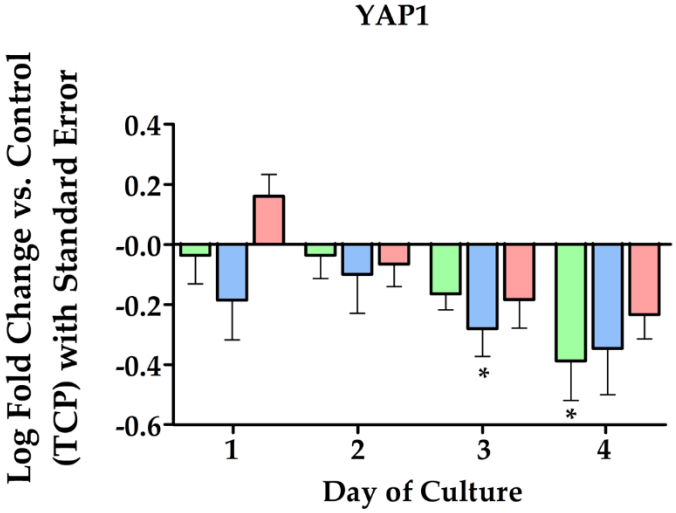
YAP1
Log Fold Change vs. Control (TCP) with Standard Error
0.4
0.2
-0.0
-0.2
-0.4
-0.6
*
*
1
2
3
4
Day of Culture

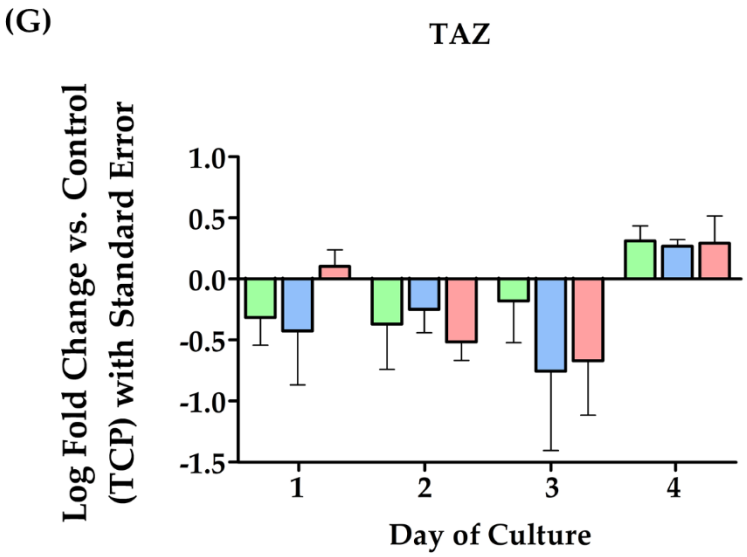

Figure 3.18 RNA analysis of the Hippo signalling pathway revealed changes in expression when HEKn were cultured on BM hydrogels. *HEKn were cultured on TCP and 50, 8 and 4 kPa cultureware and RNA samples were harvested 1,2,3 and 4 days after seeding and analysed using WafeGen.* **(A-G)** *Quantification of Log fold change in Hippo signalling pathway component expression in HEKn on 50, 8 and 4 kPa hydrogels in comparison to the TCP control. Data represent mean ±SEM, n = 6, statistical significance was assessed using two-way ANOVA, no asterisk = non-significant, * p ≤ 0.05, ** p ≤ 0.01 *** p ≤ 0.001.*

3.4.3.3 HEKn cultured on very soft hydrogels exhibited increased expression of epidermal differentiation markers

Epidermal assembly relies on the balance between proliferation and differentiation, and mechanical cues are known to play a significant role in driving keratinocytes towards terminal differentiation as they move through the epidermis (Biggs et al., 2020). Given the observations that HEKn cultured on soft hydrogels have lower proliferative activity, downregulation of YAP1, and reduced staining intensity, it was hypothesised that the BM substrates could be driving HEKn towards a more differentiated phenotype. In order to investigate this, HEKn were assessed for proliferation and differentiation markers. Perhaps the most significant of these in terms of the epidermis are cytokeratin 10 (CK10) and cytokeratin 14 (CK14). CK14 is expressed in mitotically active basal cells, whilst CK10 is expressed in differentiating keratinocytes (Alam et al., 2011).

HEKn were cultured on TCP and 4 kPa cultureware for 4 days and then protein lysates were taken using the method described earlier in the chapter (3.4.1.3). Given the importance of high calcium levels in promoting epidermal differentiation, further lysates were harvested from HEKn that had been exposed to high calcium medium for 24 hours following the 4 days of culture. Lysates were separated using SDS-PAGE and then analysed via western blot to assess the protein levels of CK10 and CK14. The results of the western blot revealed that HEKn on TCP did not express CK10 under low calcium conditions but did begin to express it following 24 hours in high calcium medium (Figure 3.19A). In contrast, HEKn cultured on 4 kPa hydrogels appeared to express a small amount of CK10 even under low calcium conditions and this increased dramatically following 24 hours in high calcium medium (Figure 3.19A). The levels of CK14 did not appear to differ by a significant amount across the different conditions.

The expression of CK10 and CK14 in HEKn on TCP versus BM substrates was further assessed using WaferGen analysis. As described previously, RNA lysates were harvested 1, 2, 3, and 4 days after seeding and samples were analysed by P&G. The results for *KRT10* expression were striking, revealing that expression was significantly upregulated in HEKn on BM substrates from across all timepoints (Figure 3.19B). Moreover, the upregulation in expression appeared to directly correlate with substrate stiffness for days 3 and 4. In contrast, the results for *KRT14* expression were less definitive, with expression seeming to increase in the first 3 days

Figure 3.19 (overleaf) HEKn cultured on 4 kPa hydrogels showed increased expression of the differentiation marker cytokeratin 10. (A) *Protein lysates were taken from HEKn cultured on TCP and 4 kPa dishes in low and high calcium medium. Western blot analysis displays that the differentiation marker CK10 was higher in cells cultured on 4 kPa hydrogels, particularly when the calcium content was high.* **(B)** *Quantification of Log fold change of the CK10 gene KRT10 in HEKn on 50, 8 and 4 kPa hydrogels in comparison to the TCP control. Data represent mean, n = 6, statistical significance was assessed using two-way ANOVA, no asterisk = non-significant, * $p \leq 0.05$, ** $p \leq 0.01$ *** $p \leq 0.001$.* **(C)** *Quantification of Log fold change of the CK14 gene KRT14 in HEKn on 50, 8 and 4 kPa hydrogels in comparison to the TCP control. Data represent mean ±SEM, n = 6, statistical significance was assessed using two-way ANOVA, no asterisk = non-significant, * $p \leq 0.05$, *** $p \leq 0.001$.*

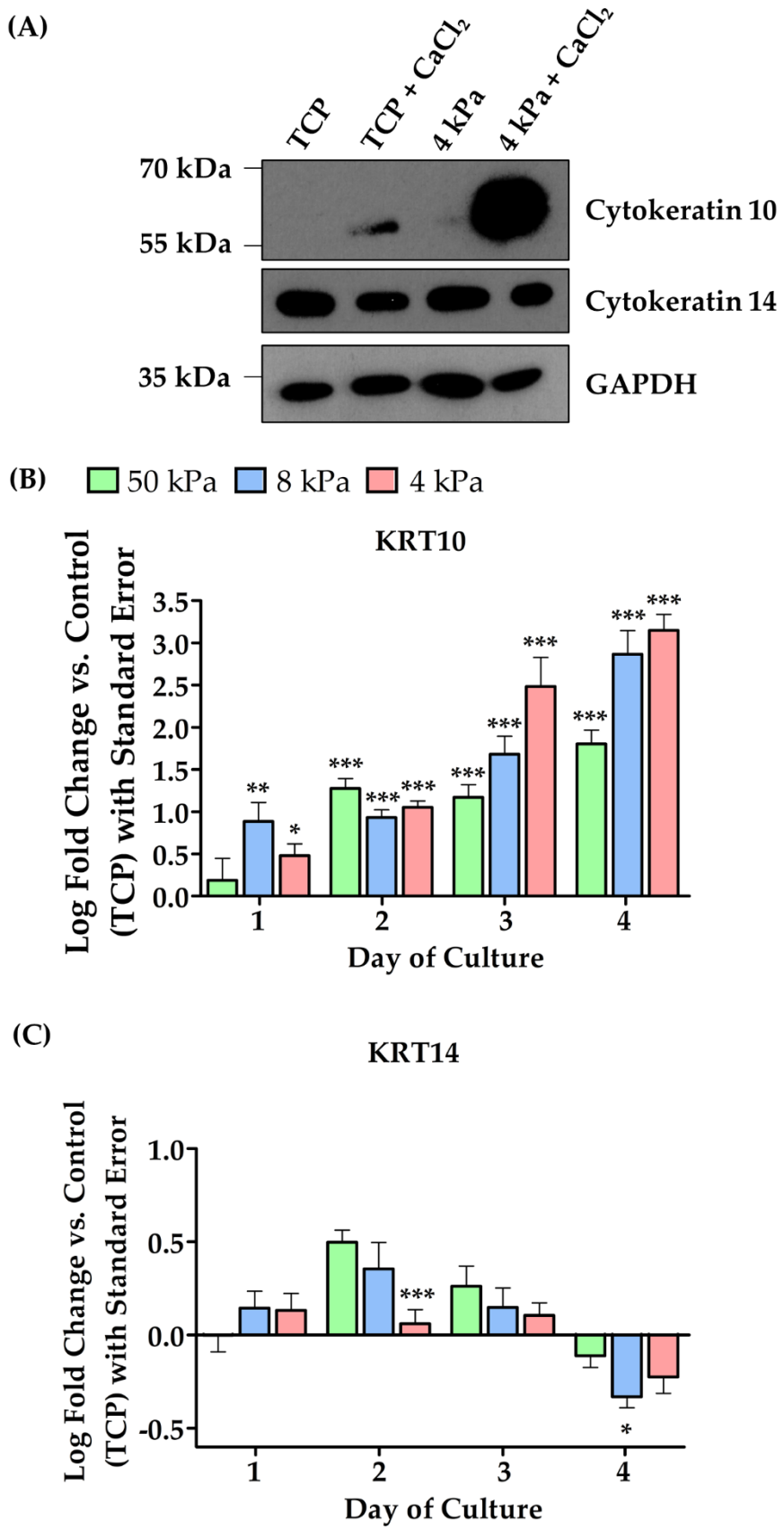
(A)
TCP
TCP + CaCl2
4 kPa
4 kPa + CaCl2
70 kDa
55 kDa
35 kDa
Cytokeratin 10
Cytokeratin 14
GAPDH
(B)
50 kPa
8 kPa
4 kPa
KRT10
Log Fold Change vs. Control (TCP) with Standard Error
Day of Culture
(C)
KRT14
Log Fold Change vs. Control (TCP) with Standard Error
Day of Culture

before being downregulated on the 4th day, though this latter result was only statistically significant for HEKn on the 8 kPa hydrogel (Figure 3.19C).

The CK10 protein and gene expression analysis provided clear evidence that BM hydrogels encourage a more differentiated phenotype in HEKn. Further to these observations, other proliferation and differentiation markers were investigated through WaferGen analysis. The transcription factor p63 is a proliferation marker that is considered to have a master regulatory role in epidermal development (Soares and Zhou, 2017), with knockout mouse models exhibiting a complete lack of epidermis (Mills et al., 1999; Yang et al., 1998; Yang et al., 1999). WaferGen analysis of HEKn on BM substrates suggested an initial spike in p63 expression on day 1, though this was not statistically significant, then a downregulation of the gene compared to TCP which was significant for all three stiffnesses at day 4 (Figure 3.20). This further supports a shift away from a highly proliferative phenotype when HEKn are cultured on softer substrates.

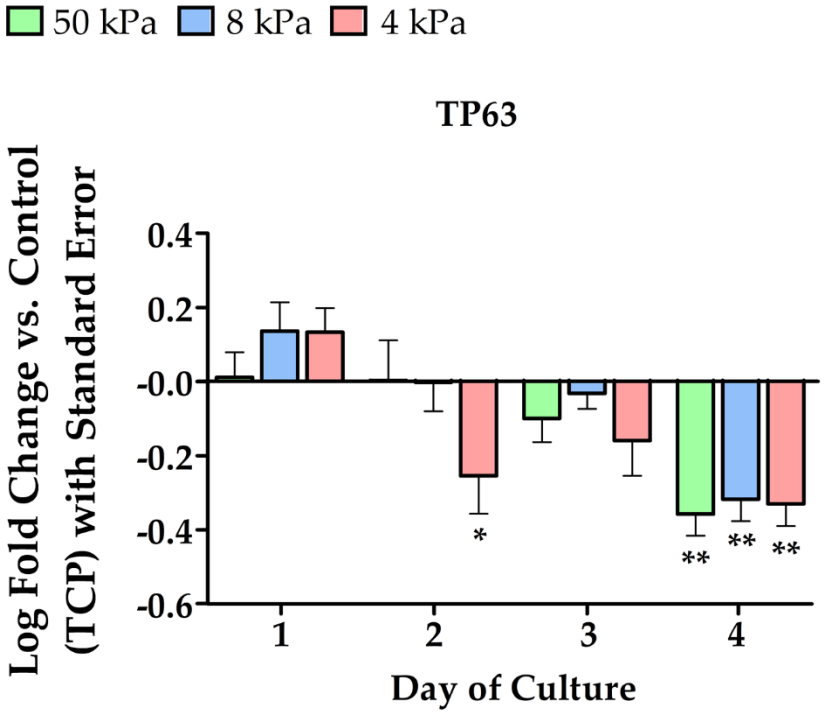

Figure 3.20 HEKn cultured on BM hydrogels exhibited a downregulation of *TP63* after 4 days of culture. *Quantification of Log fold change of the p63 gene TP63 in HEKn on 50, 8 and 4 kPa hydrogels in comparison to the TCP control. Data represent mean ±SEM, n = 6, statistical significance was assessed using two-way ANOVA, no asterisk = non-significant, * p ≤ 0.05, ** p ≤ 0.01.*

As discussed in the introduction to this chapter. The proliferative keratinocytes reside in the basal layer of the epidermis where they sit on the stiff basement membrane. It was therefore hypothesised that basal cell markers responsible for binding keratinocytes to the basement membrane and surrounding matrix would likely be downregulated in HEKn cultured on BM hydrogels. Integrin α6 is a component of α6β4 which forms hemidesmosomes that anchor basal cells to the basement membrane via laminin 332 (Kenny and Connelly, 2015) and is elevated in epidermal stem cells. WaferGen analysis revealed that the *ITGA6* gene appeared to be downregulated in HEKn on all BM stiffnesses, though this was only statistically significant for 8 and 4 kPa on day 2, and 8 kPa on day 3 (Figure 3.21A). Integrin β1 is also upregulated in epidermal stem cells and is a component of α3β1 which forms focal adhesions and directly regulates proliferation and differentiation in the epidermis (Kenny and Connelly, 2015). In HEKn cultured on BM hydrogels, *ITGB1* was found to be downregulated compared to those on TCP, with statistically significant downregulation observed for all three stiffnesses by day 4 of culture (Figure 3.21B).

Figure 3.21 (overleaf) HEKn cultured on BM hydrogels exhibited downregulation of the basal stem cell markers *ITGA6* and *ITGB1*. (A) *Quantification of Log fold change of the integrin α6 gene ITGA6 in HEKn on 50, 8 and 4 kPa hydrogels in comparison to the TCP control. Data represent mean, n = 6, statistical significance was assessed using two-way ANOVA, no asterisk = non-significant, * $p \leq 0.05$.* **(B)** *Quantification of Log fold change of the integrin β1 gene ITGB1 in HEKn on 50, 8 and 4 kPa hydrogels in comparison to the TCP control. Data represent mean ±SEM, n = 6, statistical significance was assessed using two-way ANOVA, no asterisk = non-significant, * $p \leq 0.05$, ** $p \leq 0.01$.*

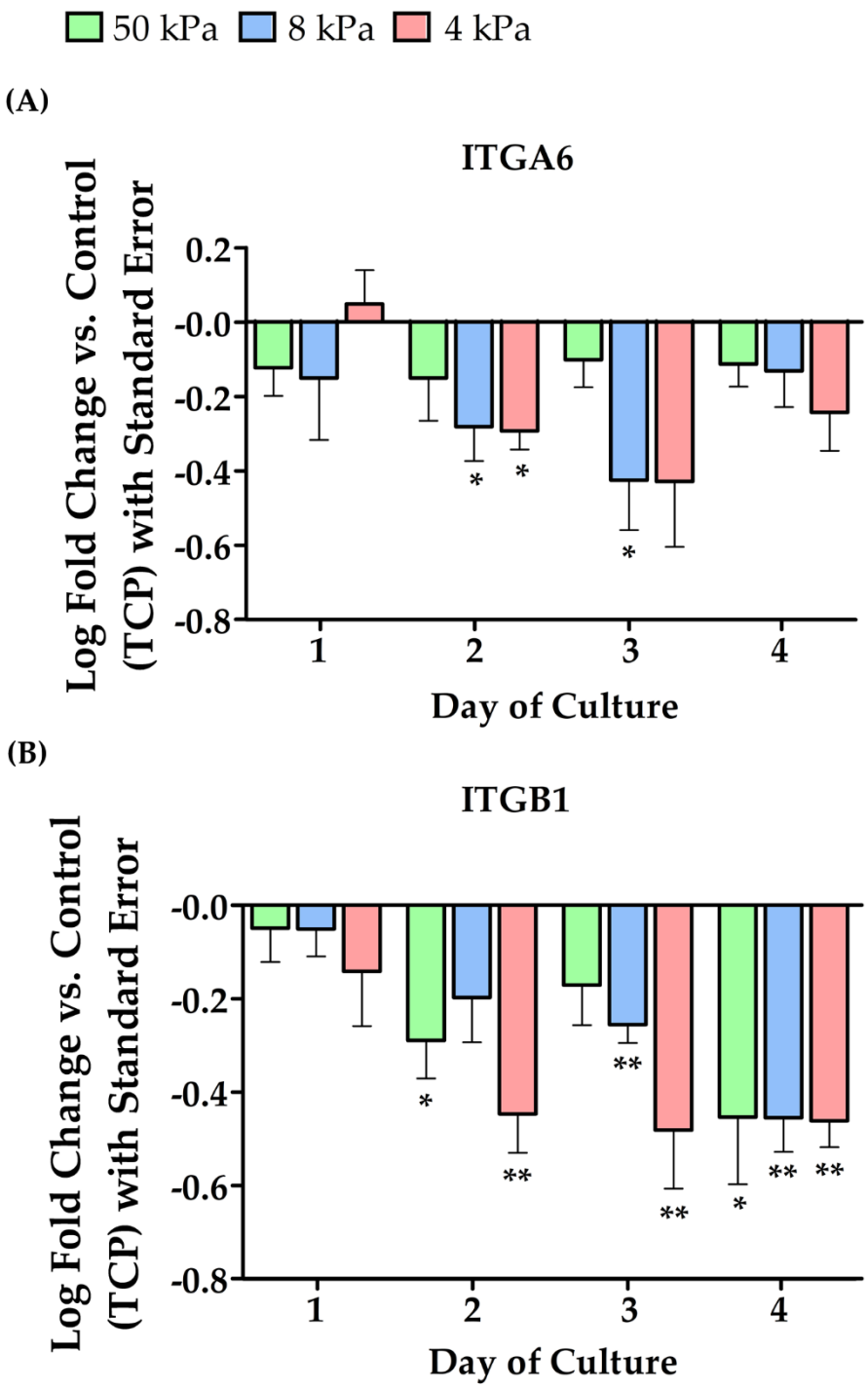

Another group of proteins that play a key role in epidermal differentiation are the Rho-associated kinases ROCK1 and ROCK2 and their upstream regulator small GTPase RhoA. ROCK1 and ROCK2 are involved in regulating cell proliferation, actin cytoskeleton organisation (including stress fibre formation and adhesion), cell motility and apoptosis (Julian and Olson, 2014). ROCK1 promotes a proliferative keratinocyte phenotype by encouraging ECM binding, whilst ROCK2 plays a key role

in keratinocyte terminal differentiation (Lock and Hotchin, 2009). WaferGen analysis of HEKn cultured on BM hydrogels revealed that the upstream regulator *RHOA* trended towards a lower gene expression compared to HEKn cultured on TCP, but the results were not statistically significant (Figure 3.22A). *ROCK1* was also observed to be downregulated, with a statistically significant decrease in expression at day 3, which appeared to directly correlate with substrate softness (Figure 3.22B). Similarly, *ROCK2* expression was also observed to be significantly downregulated in HEKn cultured on softer substrates, particularly on day 3, but with little to no change compared to TCP observed on day 4 (Figure 3.22C).

RhoA is not alone in its role in reorganising the actin cytoskeleton and works in tandem with Rac1. Rac1 coordinates the dynamic organisation of actin and controls membrane protrusion and lamellipodia formation whilst preserving the radial distribution of actin observed in proliferative cells (Nanba et al., 2013). Inhibition of Rac1 has been shown to induce a change in actin organisation that replicates that observed in paraclones: human epidermal keratinocyte stem cells that have lost the ability to proliferate (Nanba et al., 2013). Rac1 is regulated by Akt which binds to Rac1 and prevents its phosphorylation, thus inducing differentiation by preventing the maintenance of a radial actin formation (Nanba et al., 2013). WaferGen analysis of *RAC1* and *AKT1* expression in HEKn cultured on BM hydrogels revealed that *RAC1* was downregulated on 50 kPa and 8 kPa dishes on the first day after seeding, but then did not seem to significantly vary from expression in HEKn cultured on TCP

Figure 3.22 (overleaf) HEKn cultured on BM hydrogels exhibited downregulation of *ROCK1* and *ROCK2*. (A) *Quantification of Log fold change of the RHOA gene in HEKn on 50, 8 and 4 kPa hydrogels in comparison to the TCP control. Data represent mean, n = 6, statistical significance was assessed using two-way ANOVA, no asterisk = non-significant.* **(B)** *Quantification of Log fold change of the ROCK1 gene in HEKn on 50, 8 and 4 kPa hydrogels in comparison to the TCP control. Data represent mean ±SEM, n = 6, statistical significance was assessed using two-way ANOVA, no asterisk = non-significant, * $p \leq 0.05$, ** $p \leq 0.01$, *** $p \leq 0.001$.* **(C)** *Quantification of Log fold change of the ROCK2 gene in HEKn on 50, 8 and 4 kPa hydrogels in comparison to the TCP control. Data represent mean ±SEM, n = 6, statistical significance was assessed using two-way ANOVA, no asterisk = non-significant, * $p \leq 0.05$, *** $p \leq 0.001$.*

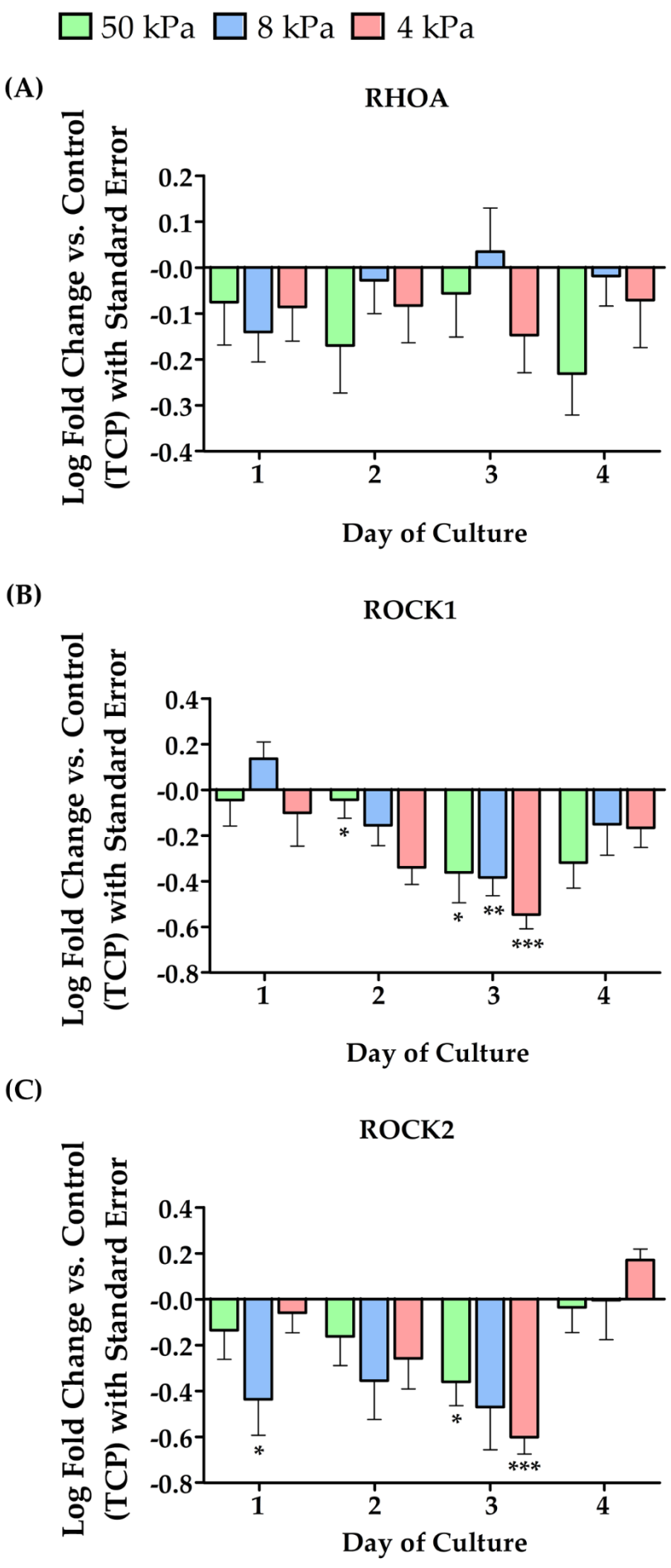
50 kPa
8 kPa
4 kPa
(A)
RHOA
Log Fold Change vs. Control (TCP) with Standard Error
0.2
0.1
-0.0
-0.1
-0.2
-0.3
-0.4
1
2
3
4
Day of Culture
(B)
ROCK1
Log Fold Change vs. Control (TCP) with Standard Error
0.4
0.2
-0.0
-0.2
-0.4
-0.6
-0.8
*
*
**
***
1
2
3
4
Day of Culture
(C)
ROCK2
Log Fold Change vs. Control (TCP) with Standard Error
0.4
0.2
-0.0
-0.2
-0.4
-0.6
-0.8
*
*
***
1
2
3
4
Day of Culture

(Figure 3.23A). In contrast, *AKT1* expression appeared to be significantly downregulated in response to a softer substrate for the first 3 days of culture and continued to trend towards downregulation on the 4th day, though this was not statistically significant (Figure 3.23B).

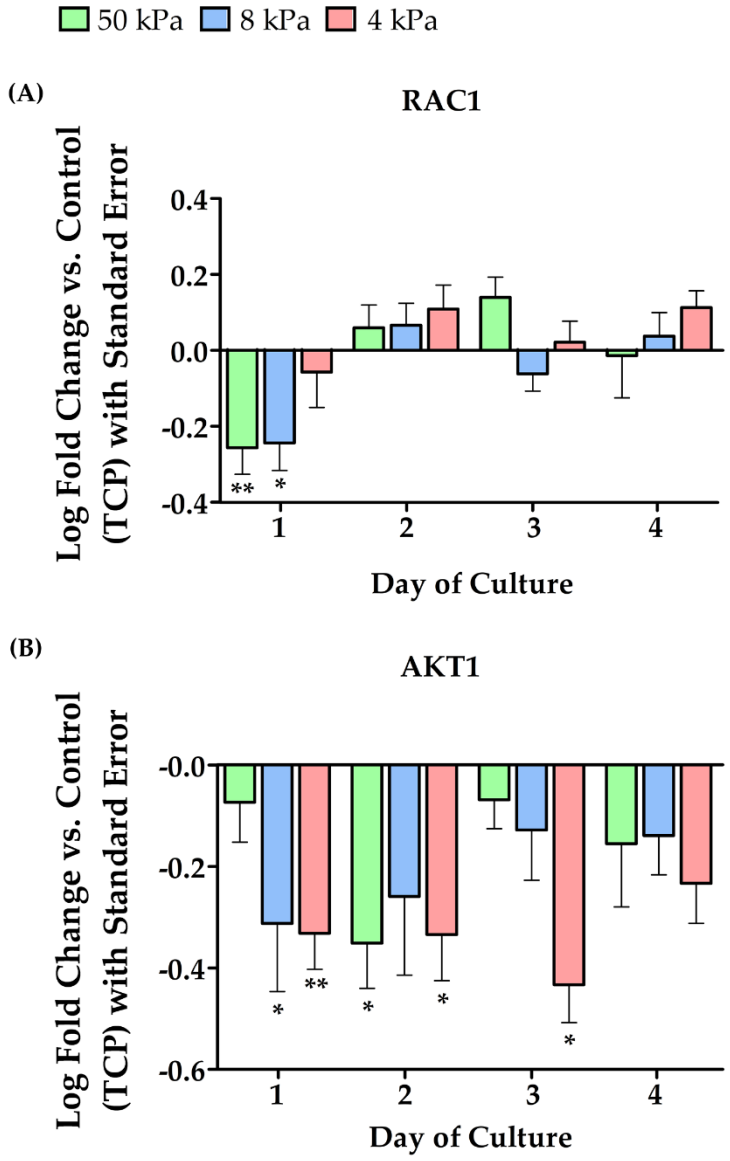

Figure 3.23 HEKn cultured on BM hydrogels exhibited a downregulation in *AKT1* expression. (A) *Quantification of Log fold change of the RAC1 gene in HEKn on 50, 8 and 4 kPa hydrogels in comparison to the TCP control. Data represent mean, n = 6, statistical significance was assessed using two-way ANOVA, no asterisk = non-significant, * p ≤ 0.05, ** p ≤ 0.01.* **(B)** *Quantification of Log fold change of the AKT1 gene in HEKn on 50, 8 and 4 kPa hydrogels in comparison to the TCP control. Data represent mean ±SEM, n = 6, statistical significance was assessed using two-way ANOVA, no asterisk = non-significant, * p ≤ 0.05, ** p ≤ 0.01.*

Another important pathway involved in orchestrating proliferation and differentiation in the epidermis is the Notch signalling pathway. Inhibition of the Notch signalling pathway promotes cell stemness, whilst its activation leads to epidermal differentiation; the activity of the Notch pathway has been linked to YAP/TAZ activity, with mechano-activation of YAP/TAZ by high mechanical tension acting to inhibit Notch signalling and vice versa (Totaro et al., 2017). *HES1* and *HEY1* are target genes of the Notch pathway that influence the timing and balance of epidermal differentiation. WaferGen analysis of these genes in HEKn cultured on BM hydrogels revealed that for the first 3 days of culture there was little pattern in *HES1* or *HEY1* expression, but on the 4th day *HES1* was significantly upregulated on all 3 stiffnesses (Figure 3.24A) whilst *HEY1* trended towards downregulation, though this was not statistically significant (Figure 3.24B).

The final pathway investigated for this section of the project was the Sonic Hedgehog (SHH) signalling pathway. The SHH pathway plays a critical role in epidermal development and homeostasis, as well as contributing to hair follicle development and the maintenance of follicle stem cells (Abe and Tanaka, 2017). GLI is a transcriptional activator in the SHH pathway and Patched 1 is a transmembrane SHH receptor involved in inducing cell proliferation. WaferGen analysis of *GLI1* and *PTCH1* expression in HEKn cultured on BM substrates provided inconclusive information with variable, non-significant changes in expression compared to HEKn cultured on TCP (Figure 3.25). Nonetheless, *GLI1* appeared to show a trend towards downregulation by day 4 of culture (Figure 3.25A), whilst *PTCH1* was significantly downregulated in HEKn cultured on 4 kPa dishes and trended towards downregulation for 50 and 8 kPa hydrogels also (Figure 3.25B).

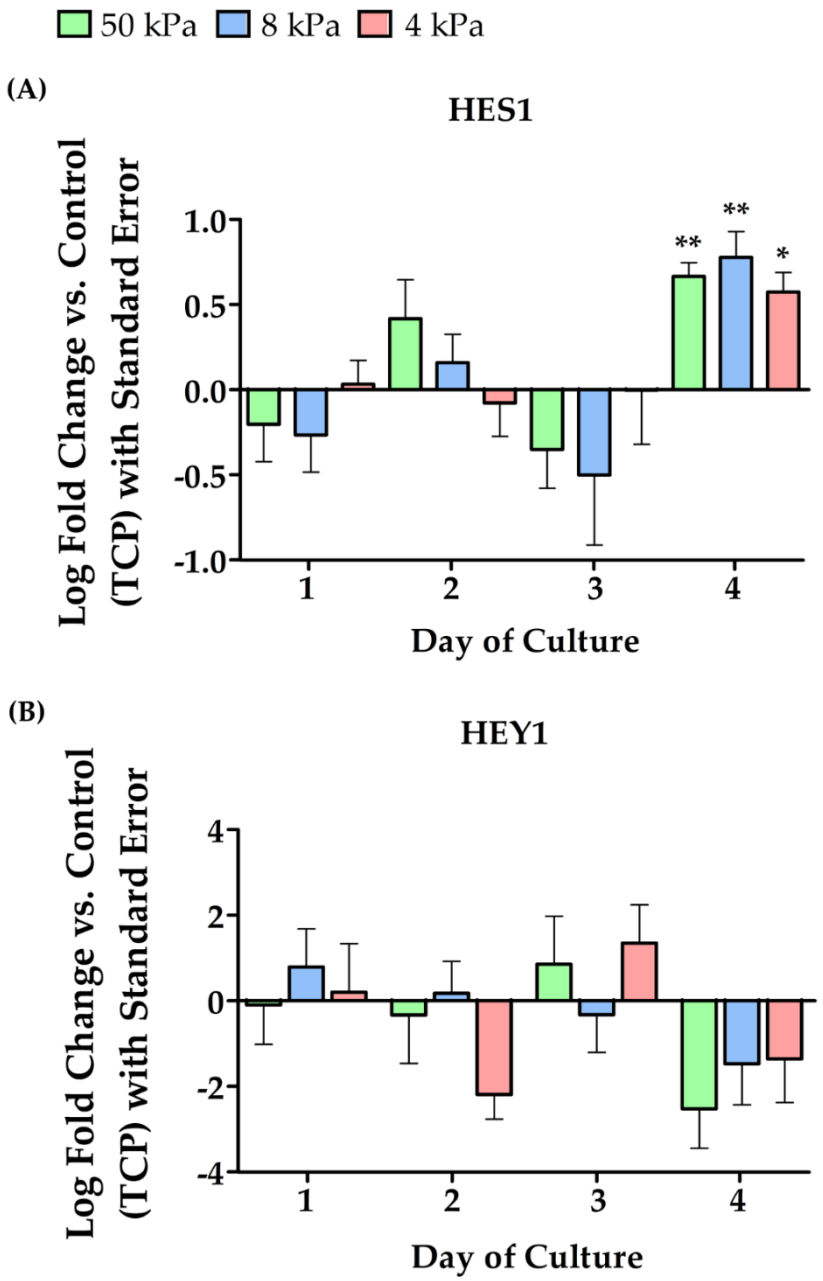

Figure 3.24 HEKn cutured on BM hydrogels exhibited upregulated expression of *HES1*. (A) *Quantification of Log fold change of the HES1 gene in HEKn on 50, 8 and 4 kPa hydrogels in comparison to the TCP control. Data represent mean, n = 6, statistical significance was assessed using two-way ANOVA, no asterisk = non-significant, * $p \leq 0.05$, ** $p \leq 0.01$.* **(B)** *Quantification of Log fold change of the HEY1 gene in HEKn on 50, 8 and 4 kPa hydrogels in comparison to the TCP control. Data represent mean ±SEM, n = 6, statistical significance was assessed using two-way ANOVA, no asterisk = non-significant.*

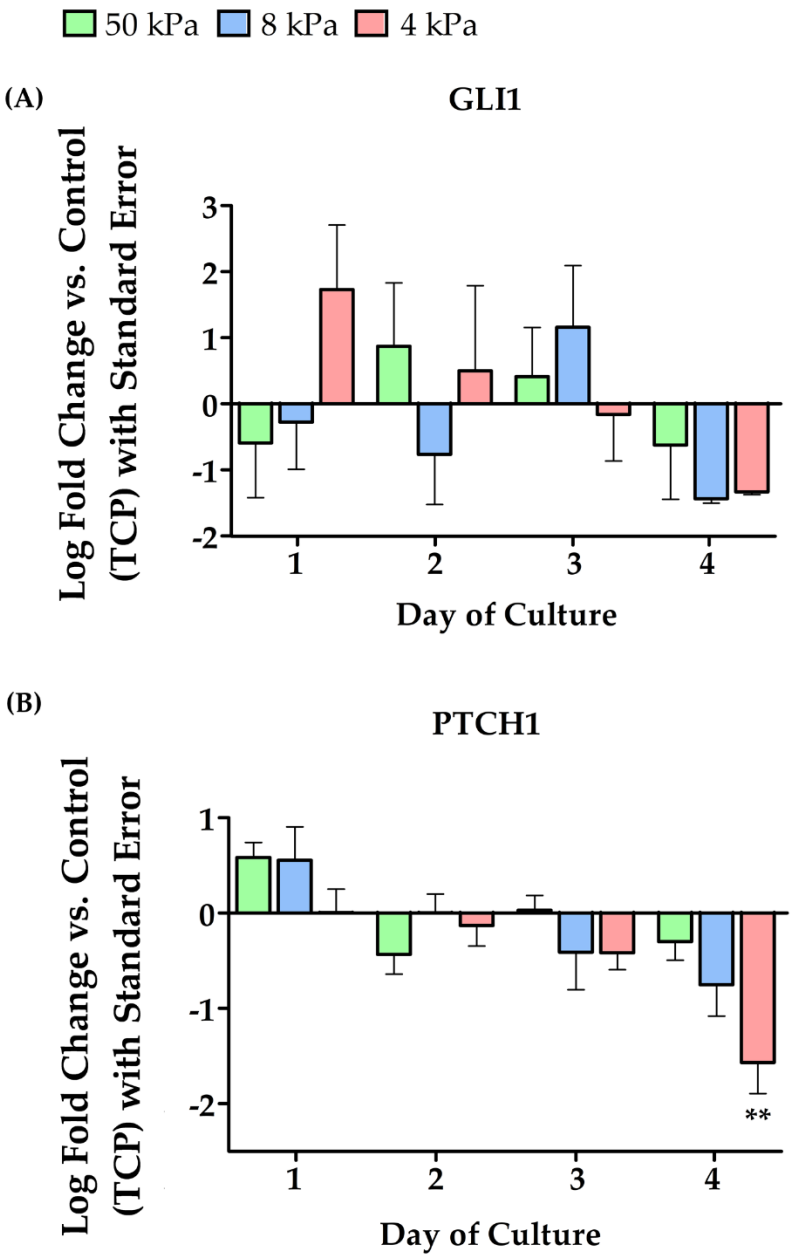

Figure 3.25 HEKn cultured on BM hydrogels exhibited downregulation of *PTCH1*. **(A)** *Quantification of Log fold change of the GLI1 gene in HEKn on 50, 8 and 4 kPa hydrogels in comparison to the TCP control. Data represent mean, n = 6, statistical significance was assessed using two-way ANOVA, no asterisk = non-significant.* **(B)** *Quantification of Log fold change of the PTCH1 gene in HEKn on 50, 8 and 4 kPa hydrogels in comparison to the TCP control. Data represent mean ±SEM, n = 6, statistical significance was assessed using two-way ANOVA, no asterisk = non-significant, ** $p \leq 0.01$.*

3.5 Discussion

The objectives of this chapter were two-fold. Firstly, it was necessary to ascertain whether culturing HEKn on BM hydrogel-coated cultureware facilitated the same ease of use that makes standard 2D cell culture using TCP so appealing. Hydrogels are a good BM alternative to TCP given that they can be used to coat pre-existing cultureware which allows cell culture to be carried out in the traditional format (Kazi, Yamanaka and Osamu, 2019). Secondly, the behaviour of HEKn in response to culture on different hydrogel stiffnesses needed to be observed, and the data obtained used to decide which stiffness best represented the mechanical environment of the various epidermal layers. Mechanical cues play a significant role in maintaining epidermal homeostasis through the balance of proliferation and differentiation in keratinocytes (Wong, Longaker and Gurtner, 2012), and therefore the *in vitro* mechanical environment should be a primary focus when culturing keratinocytes. This discussion will establish whether the BM hydrogels used in this study are a viable alternative to standard TCP and explore the effects that different substrate stiffnesses have on the delicate balance between proliferative activity and terminal differentiation in keratinocytes.

3.5.1 HaCaTs on biomimetic hydrogels required an alternative dissociating factor for cell passaging

As highlighted at various points throughout this chapter, one of the most appealing aspects of 2D cell culture is the ease with which it facilitates the rapid propagation of cells *in vitro*. It is relatively simple, inexpensive, and reproducible and has long been a foundation of biological research. However, one of the main caveats with 2D culture is that the standard materials used, either glass or TCP, are up to 1 million times stiffer than the *in vivo* environment, with TCP known to have a Young's Modulus of around 3 GPa (Landry, Rattan and Dixon, 2019). The development of 3D culturing systems has gone some way towards replicating the mechanical environment of a tissue, but these more realistic culturing conditions often come at the cost of high-throughput, reproducible experiments (Edmondson et al., 2014). Moreover, cells still need to be

grown on 2D cultureware before being used in a 3D model in order to propagate the cell line. In theory, hydrogel-coated cultureware offer a middle-ground scenario in which cells can be grown using the standard 2D culture methods but without the caveat of supraphysiological mechanical signals. The initial objective of this chapter was to therefore ascertain whether culturing keratinocytes, both HaCaT cells and primary HEKn, on BM hydrogel-coated cultureware offered the same ease of use as standard TCP.

At its most basic, expansion of cells in an *in vitro* setting requires cells to be seeded into a dish or flask, maintained until the appropriate confluency, and then dissociated and passaged to produce subcultures. It was immediately observed that HaCaTs seeded onto hydrogel-coated dishes were able to adhere and proliferate on the substrate, but they could not be dissociated following the designated 4-day culture period by using trypsin EDTA (Figure 3.1). It was noted that following removal of the medium the hydrogels retained a red tinge (Figure 3.2A), suggesting that they had absorbed medium. Repeated washes with DPBS did not appear to remove this stain, and it was hypothesised that the retention of medium was inhibiting the trypsin EDTA due to the FBS present in the medium. This theory was strengthened following the preparation of protein lysates from the dishes. An InstantBlue™ stain of these lysates revealed a very strong band below the 70 kDa protein ladder marker which was only observed in lysates taken from the 8 kPa and 4 kPa hydrogel-coated dishes (Figure 3.2B). BSA is a major component of FBS and has a molecular weight of approximately 66 kDa (Sigma-Aldrich, 2021) which correlates with the strong band observed in the hydrogel dish lysates. It was therefore concluded that an alternative to trypsin EDTA would need to be used in order to dissociate HaCaTs from the BM dishes.

It was decided that TrypLE Express Enzyme could be an appropriate substitute for trypsin EDTA as it has been demonstrated to be an effective cell dissociate under serum-supplemented conditions (TrypLE Express User Guide, 2020). It was observed that HaCaTs cultured on TCP and 4 kPa hydrogel-coated dishes were both successfully dissociated after 7 min, following treatment with TrypLE Express

Enzyme (Figure 3.3) and thus it was used for all subsequent passaging of both HaCaTs and HEKn. As previously discussed, one of the initial objectives of this chapter was to determine whether cells could be cultured and propagated as easily on hydrogel-coated dishes as on standard TCP. Whilst the failure to dissociate HaCaTs with trypsin EDTA was initially frustrating, TrypLE Express Enzyme was a viable alternative that did not require any alterations to the standard passaging protocol. Moreover, long exposure to trypsin has been shown to affect human primary keratinocyte growth rate, and use of TrypLE as an alternative was linked to a significant increase in growth rate compared to trypsin (Ścieżyńska et al., 2018). Consequently, using TrypLE Express Enzyme to dissociate keratinocytes did not affect the ease with which cells could be passaged, and in fact was likely to have less of an impact on the growth of HEKn than prolonged exposure to trypsin EDTA.

3.5.2 Hydrogel-coated dishes did not always promote the growth of primary HEKn

Following on from the previous section of this discussion, the primary appeal of 2D cell culture is that it enables the rapid expansion of cells through passaging to produce subcultures. However, it was observed that, whilst HEKn on TCP and 50 kPa hydrogel-coated dishes could be passaged onto a second dish of the same substrate, HEKn cultured on 4 kPa could not be grown beyond one passage (Figure 3.4). Rather than the cells dying following passaging, it appeared that HEKn removed from 4 kPa hydrogels were unable to adhere to a second dish of the same stiffness; an observation supported by the fact that HEKn removed from 4 kPa hydrogels were able to re-adhere when seeded onto a TCP dish following passaging (Figure 3.5).

Whilst the exact reason for this unknown, it was hypothesised that once dissociated using TrypLE, HEKn that had been grown on 4 kPa substrates were unable to reform the cell-substrate interactions that initially allowed the cells to adhere to the hydrogel. Further investigation into protein and gene expression in HEKn cultured on 4 kPa hydrogels revealed that the soft substrate appeared to push HEKn towards a terminally differentiated phenotype. Western blotting revealed that HEKn cultured on 4 kPa possessed a small amount of the differentiation marker CK10 even in low

calcium conditions, and the amount of protein was drastically increased following 24 hours in high calcium medium (Figure 3.19A). Moreover, expression of the *KRT10* gene was upregulated from as early as 1 day after seeding onto 4 kPa hydrogels, and this increased exponentially the longer that cells were exposed to the substrate (Figure 3.19B). Furthermore, WaferGen analysis of *ITGB1* which encodes the cell membrane receptor subunit integrin β1, revealed that *ITGB1* was significantly downregulated in HEKn cultured on 4 kPa hydrogels from as early as 2 days after seeding onto the substrate (Figure 3.21B). Integrin β1 is considered a proliferation marker and is usually confined to the basal layer of the epidermis where it plays a role in cell attachment to the basement membrane (Kenny and Connelly, 2015; Levy et al., 2000).

These results strongly suggest that culturing HEKn on 4 kPa substrates pushes HEKn towards terminal differentiation, and as such it was concluded that cleaving of the cell-substrate attachments during dissociation prevents the cells from reattaching when exposed to further 4 kPa hydrogels as this perpetuates the downregulation of the adhesion molecules required for adherence to the substrate. In contrast, it was hypothesised that seeding the cells back onto TCP provides the required mechanical cues to re-establish the expression of basal cell markers. This latter hypothesis is frustratingly unanswered by subsequent analyses and seems to contradict the concept of terminal differentiation. However, in a recent study currently in pre-print, Wood et al. observed that primary murine mammary epithelial cells and EpH4 (non-transformed murine luminal epithelial cell line) cells embedded in a stiffer ECM environment exhibited downregulation of differentiation markers, suggesting that increased ECM stiffness disrupts normal terminal differentiation (Wood et al., 2020). In order to truly understand what is happening to HEKn on 4 kPa hydrogels versus TCP during this second passage, it would be necessary to repeat the 4 day WaferGen analysis time course and observe gene expression following seeding back onto TCP to assess whether HEKn are in fact recovering their basal cell phenotype.

Given that keratinocyte differentiation was ascertained to be a result of exposure to a soft substrate, the inability to subculture HEKn on 4 kPa dishes, whilst a caveat, was

not considered evidence that hydrogel-coated dishes were more difficult to use than TCP. In fact, the patent changes in gene expression associated with culturing HEKn on hydrogels were considered clear evidence that culturing cells on plastic drastically alters their gene expression profile compared to the *in vivo* environment. Moreover, given that 50 kPa hydrogels did not appear to impact the ability to subculture HEKn, and the fact that not all cell types undergo terminal differentiation, these observations merely served to highlight the importance of selecting an appropriate stiffness range to optimise the mechanical environment for 2D cell culture.

In addition to problems subculturing HEKn on soft BM dishes, issues were also faced with "defective" batches of the dishes purchased from Cell Guidance Systems. On a number of occasions, cells were seeded onto hydrogel-coated dishes only for cells to die during the 4 day culture period (Figure 3.6). This occurred with dishes of all stiffness ranges and invariably every dish within the same batch would produce the same result, suggesting an issue with the manufacture of certain lots rather than an association with a particular rigidity. Whilst this was extremely frustrating at the time, it was not deemed reflective of an inherent issue with the use of hydrogels in culture and it is likely that this may have been avoided had the BM dishes either been purchased elsewhere or made in house. Consequently, despite these batch related issues, everyday growth of keratinocytes on hydrogel-coated dishes was not deemed significantly different from culturing cells on standard TCP cultureware.

3.5.3 Hydrogel-coated coverslips posed problems for microscopy imaging

When culturing keratinocytes on BM dishes no problems were encountered with regards to taking phase contrast microscopy images. However, for immunofluorescence confocal microscopy imaging there were immediate technical issues. In order to ensure high quality, detailed images, the majority of confocal microscopy images for this project were taken using an objective with x63 magnification which requires oil immersion and therefore for the objective to be extremely close to the coverslip. With standard glass coverslips, this ensures that the objective is close to the cells, with only the thin coverslip providing a barrier between the two. However, for the BM coverslips, the distance between the cells and the

objective was increased due to the added thickness of the hydrogel layer (Figure 3.7). For phase microscopy, the extra thickness of the hydrogel did not cause any problems as the cells were imaged at low magnifications, meaning there was plenty of room to manoeuvre the objectives into the appropriate position from the stage to compensate. However, given the requirement for oil immersion with the x63 objective, it was not possible to compensate for the added distance provided by the hydrogel, as the objective could not be moved closer without disrupting the slide from the stage. Without moving the objective closer to the coverslip it was not possible to detect the immunofluorescence stain, and the overall result was poor quality images that lacked the clarity of cells imaged on standard glass coverslips (Figure 3.8).

In order to solve this issue, the coverslips were instead mounted onto glass-bottomed dishes instead of slides meaning that the cells could be imaged directly through the dish, thus negating the effects of the extra distance created by the hydrogel (Figure 3.9A). However, whilst this did improve image quality to match that of glass coverslips (Figure 3.9B), glass bottomed dishes are significantly more expensive than slides, and are more cumbersome meaning that they would be difficult to store in large numbers. Consequently, this was deemed an impractical solution that did not support the desired ease of use considered important for hydrogel-coated cultureware. Following a troubleshooting discussion with the department's microscopy team it was decided that the best solution would be to use an alternative objective with a greater free working distance. The objective used for confocal microscopy up until this stage was the Objective Plan-Apochromat 63x/1.4 Oil DIC M27 (ZEISS) which had a free working distance of 0.19 mm. This was replaced by the Objective LD LCI Plan-Apochromat 63x/1.2 Imm Corr DIC M27 (ZEISS) which had a much greater free working distance of 0.49 mm, and it was hoped that this would be enough to allow imaging through both a coverslip and a hydrogel-coating. This objective could be used for both glycerine and oil immersion, and both conditions were tested to assess optimum image quality. It was observed that there was a marked improvement in image quality using the Objective LD LCI Plan-Apochromat 63x/1.2 Imm Corr DIC M27 compared to the original Objective Plan-Apochromat 63x/1.4 Oil DIC M27, though oil immersion produced better clarity (Figure 3.10).

Consequently, all further confocal microscopy images were taken using the Objective LD LCI Plan-Apochromat 63x/1.2 Imm Corr DIC M27.

The issues faced with confocal microscopy imaging were the first to call into question how well hydrogel-coated cultureware simulate the ease of use experienced with standard glass or TCP products. Though the solution of using an alternative objective did ultimately make the physical process of imaging BM coverslips as simple as it would normally be, it required the use of alternate equipment that many laboratories would be unlikely to possess. Consequently, this solution is not simple or cost-effective, and the inability to image hydrogel-coated coverslips with standard immersion objectives should be considered a significant caveat.

Nevertheless, it should not be concluded that there are no other viable solutions to the issue of imaging immunostained BM cultured cells. In 2010, a study made the profound observation that culturing muscle stem cells on a substrate with mechanical physiological relevance, greatly improved the success of *in vivo* engraftment of the cells (Gilbert et al., 2010). This introduced the concept of "mechanical memory" which was further explored by Yang et al., who observed that the activation of YAP/TAZ in human mesenchymal stem cells cultured on 2 kPa hydrogels was dependent on how long they had previously been cultured on TCP (Yang et al., 2014). In control experiments, cells cultured consistently on TCP exhibited nuclear YAP, whilst cells grown only on 2 kPa hydrogels presented with cytoplasmic YAP. If cells were cultured on TCP for 1 day and then transferred to 2 kPa hydrogels, YAP was observed to deactivate and move to the cytoplasm after 3 days on the softer substrate. However, if cells were cultured on TCP for 7 days before being moved to the 2 kPa hydrogels, YAP remained active indefinitely, suggesting that stem cells not only retain the mechanical memory of previous environments, but are also subject to changes depending on the mechanical "dose" they receive (Yang et al., 2014). In a more recent study involving primary human keratinocytes, it was observed that culturing cells beyond a certain threshold period of time on soft substrates produced evidence of "mechanical memory" that impacted the rate of wound healing during scratch wound assays (Mogha et al., 2019). Consequently, these studies suggest that

mechanosensing is a complex process that potentially has long-lasting impacts on cell behaviour even after they are moved into a new mechanical environment. As a result, it is likely that it would be possible to "prime" cells on BM hydrogels then transfer them to standard glass coverslips for the immunostaining protocol and still be able to observe the changes induced during the time exposed to a softer substrate. This would therefore bypass the issues discussed when using hydrogel-coated coverslips and is an idea that would benefit from further exploration.

3.5.4 Harvesting of protein lysates for HEKn was adapted to improve protein yield

The final technical problem experienced when culturing HEKn on hydrogel-coated cultureware arose when harvesting protein lysates. The standard protocol of adding lysis buffer to the dish and using a cell scraper to remove the lysate produced a very poor protein yield in cells on all substrates, though the BM dishes appeared to exacerbate the problem (Figure 3.11A). Adding in the additional step of incubating the dishes with lysis buffer on ice for 30 min before scraping greatly improved the protein yield (Figure 3.11B). The fact that the protein yield was very poor in HEKn obtained from TCP dishes suggested that this issue was not directly related to the hydrogels. However, one issue noted when taking lysates from the BM dishes was that the hydrogels were extremely delicate and easily torn by the cell scraper which led to contamination of the lysate with gel that was difficult to remove. A benefit of incubating the dishes on ice for 30 min was that it seemed to stiffen the gel slightly, making it easier to scrape the surface of the hydrogel without damaging it. Consequently, though the poor HEKn protein yield was not directly linked to the hydrogel-coated dishes, the additional step of incubating on ice did make the harvesting of protein lysates from BM dishes easier. As this was not a particularly labour intensive or time-consuming addition to the lysate protocol, it was not considered evidence that hydrogel-coated cultureware was more difficult to use than standard TCP.

3.5.5 Keratinocytes cultured on BM hydrogels exhibited increased cell density and reduced proliferation

One of the first observations made when culturing HaCaTs on hydrogel coated dishes was that the colonies appeared more densely packed, particularly on the 4 kPa substrate. Moreover, colonies on the BM dishes appeared more "3D", with distinct colony edges, and shadowing across the top of the colony that suggested the cells were not flat against the surface of the underlying dish (Figure 3.12A). Quantification confirmed that the HaCaTs were in fact denser on the 8 and 4 kPa hydrogels, with a statistically significant difference observed even between the two hydrogels, despite the small change in stiffness (Figure 3.12B). Given the previously mentioned caveats regarding the use of HaCaT cells for keratinocyte assessment (3.1.5), it was necessary to repeat the cultures using HEKn to ensure that the changes in appearance and cell density were a direct effect of the softer substrates. Under low calcium conditions, HEKn cultured on TCP appeared heterogenous in shape, whilst those on 50, 8 and 4 kPa dishes exhibited a regular, cobblestone morphology and appeared denser (Figure 3.13A). Quantification of the cell density confirmed that it was significantly greater in HEKn cultured on BM hydrogels (Figure 3.13B). This cobblestone morphology is well established in the literature as the typical appearance of primary keratinocytes (Hennings et al., 1980; Wong et al., 2019). Heterogenous cell morphology has been noted in primary human keratinocytes cultured on TCP and even collagen I coated dishes, whilst keratinocytes cultured on a fibroblast-derived matrix mimicking the dermal ECM are observed to have the cobblestone morphology witnessed in this study (Wong et al., 2019). Consequently, this suggests that the BM hydrogels used in this study were providing HEKn with a physiologically relevant mechanical environment that promoted an *in vivo*-like cell morphology.

The next stage of this investigation into cell appearance on the hydrogel-coated dishes was to repeat the HEKn culture under high calcium conditions, given the importance of a calcium gradient in the regulating proliferation and differentiation in the epidermis (Cornelissen et al., 2007; Elias et al., 2002). In medium containing 1.5 mM $CaCl_2$, HEKn cultured on TCP began to take on a more homogenous appearance

similar to the cobblestone morphology previously observed only in the BM cultured cells (Figure 3.14A). Moreover, cell density was increased compared to the low calcium conditions, but HEKn cultured on hydrogel-coated dishes remained significantly denser than those on TCP (Figure 3.14B). One of the core functions of the epidermis is to act as a barrier, primarily to prevent the loss of water from the body (Madison, 2003). In order to achieve this barrier, keratinocytes form multicellular sheet structures that are tightly bound together to permit only the passage of small molecules and ions (Simpson, Patel and Green, 2011). These tightly bound epithelial sheets are primarily a feature of the more differentiated epidermal layers, and it was hypothesised that the softer hydrogel-coated dishes could be steering HEKn away from the unnaturally proliferative state promoted by TCP, and towards a more differentiated phenotype. The fact that high calcium conditions triggered increased cell density and a more cobblestone morphology in the HEKn on TCP seemed to support this theory given the role of high calcium in keratinocyte differentiation. Moreover, previous studies have shown that even under low calcium conditions, culturing keratinocytes on softer substrates can induce differentiation (Trappmann et al., 2012; Ya et al., 2019).

This hypothesis was further supported by the observation that both HaCaTs and HEKn appeared to proliferate more slowly on the BM hydrogel-coated dishes. In order to confirm this, EdU assays were carried out for both cell types and it was found that both HaCaTs (Figure 3.15) and HEKn (Figure 3.16) had significantly fewer proliferative cells when cultured on BM hydrogels versus those on TCP. Perhaps most striking was that even between HEKn cultured on 50 kPa and 4 kPa there was a statistically significant decrease in proliferation in correlation with decreased substrate stiffness. The fact that a relatively small difference in stiffness could have a substantial effect on cell behaviour is an observation that will be revisited throughout this thesis and it serves to highlight the importance of controlling *in vitro* mechanics in order to obtain reliable and physiologically relevant results.

3.5.6 HEKn cultured on soft hydrogels showed greater Hippo pathway activation

As mentioned in the introduction to this chapter, the Hippo signalling pathway plays a critical role in epidermal homeostasis and relies on mechanical cues to steer keratinocytes towards either a proliferative or differentiated phenotype (Rognoni and Walko, 2019). As a result of the decreased proliferative activity and increased cell density observed in HEKn cultured on hydrogel-coated dishes, the next logical step was to investigate the activity of the Hippo pathway in cells on the different stiffnesses. As HEKn on 4 kPa exhibited the greatest changes in density and proliferation compared to those on TCP, it was decided to focus only on these two extremes for the immunofluorescence analysis of YAP1 localisation. An initial assessment of the confocal microscopy images suggested that nuclear YAP1 staining was brighter in HEKn on glass coverslips (Figure 3.17A). However, quantification of this revealed that there was no statistical difference in the integrated density of nuclear staining between HEKn on glass and 4 kPa coverslips. Nonetheless, there was a significant decrease in the cytoplasmic staining of YAP1 in cells on the 4 kPa coverslips and the overall intensity of staining in the cell as a whole appeared lower (Figure 3.17B). This coincides with what we know about the Hippo signalling pathway, with soft substrates offering limited mechanical cues which in turn activates the Hippo pathway to sequester YAP1 in the cytoplasm where it is degraded (Dupont et al., 2011; Piccolo, Dupont and Cordenonsi, 2014). Whilst the results of the immunofluorescence analysis seemed to support that YAP1 degradation was taking place in HEKn on 4 kPa, this result would have been strengthened by the addition of western blot analysis to provide more quantifiable data regarding YAP1 protein levels in HEKn on TCP versus 4 kPa cultureware. However, difficulties with finding a reliable YAP1 antibody for western blot meant that it was not possible to carry out this extra analysis.

In order to further explore the effects of substrate stiffness on the Hippo signalling pathway, WaferGen analysis was carried out to assess changes in the gene expression of key pathway components in HEKn cultured on 50, 8 and 4 kPa compared to TCP

(Figure 3.18). The expression patterns of upstream components of the pathway were found to be somewhat contradictory both with each other and with the other data discussed previously (Figure 3.18A-E). NF2 was observed to be significantly downregulated on all hydrogel stiffnesses for the first 3 days of culture, then showed little change compared to TCP on the 4th day. Given that NF2 is an upstream regulator involved in activating the Hippo pathway, it was predicted that gene expression would increase rather than decrease, if there was in fact any change at all. In contrast, the fellow upstream regulator kibra, encoded by *WWC1*, was observed to show no significant change in expression over the first 3 days of culture, and was significantly upregulated on day 4. The kinases MST1 and LATS1 showed variable, non-significant expression changes, whilst LATS2 was found to be downregulated across the 4 days, again seemingly contradicting the Hippo pathway activity suggested by the immunofluorescence (Figure 3.17). Nonetheless, gene expression for YAP1 was observed to be downregulated by the third and fourth days of culture, and TAZ appeared to be downregulated for the first 3 days, though this was not statistically significant.

In order to discuss the WaferGen data, it is important to highlight that the main caveat of studying RNA expression is that it is a notoriously poor representation of what is happening within the cell at a protein level (Maier, Güell and Serrano, 2009). Post-translational modifications, protein-abundance differences, and time-dependent expression patterns are all information that transcriptomics cannot access (Wilhelm et al., 2014), and it is therefore necessary to bear this in bind when considering whether the data obtained supports what is believed to be happening within the cell. Moreover, a lot of the expression changes were not statistically significant, which raises the question of whether they can be trusted. The traditional view would be that they cannot be relied upon, but there are some scientists that have long argued that there is a difference between statistical significance and biological relevance, and that a *P*-value does not reflect the latter (Martínez-Abraín, 2008; Parks and Beiko, 2010). At its core, statistical hypothesis testing is a test of what is presumed to be true: i.e., it is assumed that the null hypothesis of an experiment is correct, and a small *P*-value is taken as strong evidence that the null hypothesis is in fact false (Johnson, 1999). In

reality, it has been shown that there is disparity between the *P*-value and the actual probability that a null hypothesis is true, and this disparity increases as the sample size becomes larger (Berger and Sellke, 1987). Ultimately *P* is a function of the difference between the null hypothesis and reality, and the size of the sample; if it is assumed that the null hypothesis is actually false, which is most likely the case in any given situation, then the *P*-value can be made as small as one wants it to be by increasing the sample size (Johnson, 1999). Essentially, this results in the value of *P* being arbitrary, which is further emphasised when we consider the cut-off value of statistical significance. In a situation where $P = 0.049$ for one experiment, and $P = 0.051$ for another, such a small difference in value, especially when the assumptions of the test producing the values are only partially met, are unlikely to reflect the true biological relevance of the observed change (Preece, 1990).

As a result, the results of the WaferGen analysis of the Hippo signalling pathway must be viewed with these two concepts in mind. Where the gene expression changes do not correlate with other changes observed in the cells, it should not be assumed that this reflects the protein levels. An ideal supporting experiment for this section of the chapter had there been time, would have been to run parallel western blot or proteomics analysis which may have provided further insight into the activity of the pathway. Moreover, for genes where there was no statistical significance, but the bars suggested an overall trend in gene expression in response to culturing HEKn on the hydrogels, it must not be assumed that these changes did not have a biological relevance to the behaviour of the cell. To conclude, the WaferGen analysis of Hippo signalling pathway components confirms that culturing HEKn on BM hydrogels has an effect on Hippo pathway activity that results in changes in the genes encoding those components. However, in order to fully understand the full implications of these changes, further work would need to be done in the future to explore the effects on protein levels and protein localisation within the cell.

3.5.7 HEKn cultured on softer substrates exhibited a more differentiated genotype

As previously discussed (3.5.2), significant increases in both the protein level and gene expression of the differentiation marker CK10 (Figure 3.19) suggested that HEKn cultured on softer hydrogels were drawn away from a proliferative phenotype and steered more towards terminal differentiation. Moreover, the basal cell integrin subunits integrin α6 and β1 were observed to be downregulated on BM hydrogels (Figure 3.21). The subsequent confirmation that proliferation decreased (Figure 3.16), and that YAP1 was both downregulated, and present in lower amounts in cells on BM hydrogels (Figure 3.17) further supported this hypothesis. However, in order to truly assess the effects of culturing HEKn on hydrogels, WaferGen analysis was carried out to analyse the expression levels of various known epidermal proliferation and differentiation markers.

Dubbed as a "master regulator" of epidermal development, tumour protein 63 (p63) plays a critical role in determining keratinocyte fate and commitment to the epidermal lineage (Koster, 2010). High expression of p63 is associated with proliferative cells and epidermal stem cells (Pellegrini et al., 2001), and knock-down of p63 in primary keratinocytes has been observed to result in hypoproliferation and cell cycle arrest (Truong et al., 2006). However, it should be noted that Pellegrini et al. reported p63 expression in the form of western blot data (Pellegrini et al., 2001), meaning that it is not directly comparable to the WaferGen data presented here given that western blotting reflects protein level rather than actual gene activity, and is not accurately quantifiable. Nonetheless, WaferGen analysis of HEKn cultured on BM hydrogels revealed that *TP63* was significantly downregulated on all hydrogel stiffnesses by the 4th day of culture (Figure 3.20). This initially seemed promising as it was hypothesised that if high expression was associated with proliferation, decreased expression would result in differentiation. However, it has also been shown that downregulation of p63 *in vitro* actually prevents primary keratinocytes from undergoing differentiation (Truong et al., 2006), suggesting that the role of p63 in epidermal homeostasis is less clear cut than it is for other epidermal markers.

Knock-down of p63 has been linked to downregulation of MYC which directly results in decreased proliferation in keratinocytes (Wu et al., 2012), and it is well established that p63 affects proliferation and differentiation independently through the manipulation of different pathways. Consequently, it was concluded that culturing HEKn cultured on hydrogel-coated dishes induced a downregulation of p63, which in turn resulted in decreased proliferation as evidenced by the results of the EdU assay (Figure 3.16). However, this result did not necessarily support the hypothesis that HEKn on BM hydrogels are more differentiated than those on TCP.

As mentioned in the introduction to this chapter, reorganisation of the actin cytoskeleton plays a key role in the transition towards terminal differentiation at keratinocytes travel through the epidermal layers (Laly et al., 2021). A more detailed exploration of the effects of hydrogel culture on actin organisation in HEKn will be discussed in the next chapter. However, WaferGen analysis was carried out to investigate changes in the gene expression of proteins known to regulate this actin reorganisation. RhoA is an upstream regulator of ROCK1 and ROCK2 which play a role in promoting keratinocyte proliferation and differentiation respectively. RhoA has been linked to promoting epidermal stem cell proliferation (Wang et al., 2017), and was found to be generally downregulated in HEKn cultured on BM hydrogels (Figure 3.22A). Though these changes were not statistically significant, the previous discussion on the arguments regarding the appropriateness of statistical significance when considering biological relevance highlights that these data should not necessarily be ruled out as unimportant to the behaviour of the cells. In contrast, ROCK1 and ROCK2 were both found to be significantly downregulated in HEKn cultured on hydrogel-coated dishes (Figure 3.22B-C). Whilst the downregulation of ROCK1 supports previous evidence that proliferation is decreased in response to softer substrates, the downregulation of ROCK2 seems to contradict the high levels of CK10 that suggested a strong shift towards a differentiated phenotype. As discussed previously, WaferGen data rarely provides an accurate insight into what is happening at a protein level within a cell (Maier, Güell and Serrano, 2009). If ROCK2 protein levels were already high in the cell, it is possible that the downregulation of

ROCK2 was tied into the downregulation of RhoA to ensure that there was not a deficit between the amount of ROCK2 and its upstream regulator.

In addition to the RhoA/ROCK proteins, Rac1 and Akt1 are also associated with actin reorganisation in relation to keratinocyte proliferation or differentiation. Rac1 is known to preserve the radial distribution of actin observed in proliferative cells, whilst Akt1 promotes terminal differentiation through involvement in the reorganisation of actin fibres into a circumferential network, amongst other roles (Naeem et al., 2015; Nanba et al., 2013). Aside from an initial downregulation of *RAC1* on the first day after seeding, HEKn cultured on BM hydrogels exhibited no clear changes in the expression of this gene (Figure 3.23A). In contrast, *AKT1* expression was downregulated across the four days (Figure 3.23B), which once again did not seem to necessarily support the theory that culturing HEKn on soft hydrogels promoted differentiation. Given the literature's heavy emphasis on the importance of Akt1 in keratinocyte differentiation, not only for actin organisation, but also filaggrin processing, and nuclear degradation (Naeem et al., 2015; Rogerson and O'Shaughnessy, 2018; Rogerson et al., 2021), it is difficult to explain why the WaferGen data revealed such a clear downregulation of *AKT1*. The upregulation in both gene expression and protein level of CK10 observed in HEKn cultured on hydrogels (Figure 3.19) makes it clear that there is some shift towards differentiation signalling in response to softer substrates. In order to fully understand the seemingly contradictory expression changes of *AKT1* and *ROCK2*, further investigation would need to be carried out with emphasis on protein levels across the different stiffnesses. Moreover, given that the biggest increase in the CK10 protein level was found to occur under high calcium conditions (Figure 3.19A), it would be interesting to repeat the WaferGen analysis on HEKn cultured in high calcium medium to observe what effect this may have on the expression of genes linked to differentiation.

The final genes assessed for this section of the project were related to two other key signalling pathways in the epidermis; the Notch pathway and the SHH pathway. The Notch signalling pathway plays a critical role in translating mechanical cues into cell fate decisions (Lloyd-Lewis, Mourikis and Fre, 2019), which in the epidermis

translates into triggering keratinocytes to undergo terminal differentiation (Nguyen, 2006). *HES1* and *HEY1* are Notch target genes, with HES1 considered to be an epidermal differentiation marker (Dainichi et al., 2016; Ezratty et al., 2011). WaferGen analysis of *HES1* revealed that there was little change in expression across the first 3 days of culture, but on the 4th day it was significantly upregulated in HEKn cultured on all hydrogel stiffnesses (Figure 3.24A). This supports the previous observations regarding CK10 expression (Figure 3.19), suggesting that culturing HEKn on BM hydrogels promotes keratinocyte differentiation. In contrast, *HEY1* expression was observed to be variable across the first 3 days of culture, and was downregulated on the 4th day, though this was not significant (Figure 3.24B). As with previous genes, this result paints a more complicated picture of the HEKn response to soft hydrogels than was initially anticipated, and the lack of significance observed for some of the gene expression changes does not necessarily mean that there was not an effect on the cells at a biological level.

In contrast to the Notch signalling pathway, the activity of the SHH pathway is associated with keratinocyte proliferation, with both GLI1 and PTCH1 playing critical roles (Chari et al., 2013). WaferGen analysis of these genes revealed that *GLI1* was variably expressed in the first 3 days of culture, and non-significantly downregulated on the 4th (Figure 3.25A), whilst *PTCH1* again showed variable expression until a signiciant downregulation on the 4th day in HEKn cultured on 4 kPa hydrogels (Figure 3.25B). These data support previous results that showed reduced proliferation in HEKn cultured on hydrogel-coated dishes, and thus back the argument that softer substrates do at least move away from a highly proliferative state.

To conclude, whilst the decreased proliferation, changes to YAP1, and increased CK10 expression discussed earlier in this chapter support the hypothesis that softer substrates trigger HEKn differentiation, the WaferGen analysis was not as conclusive. The significant downregulation of p63, the integrin subunits α6 and β1, and ROCK1 and PTCH1 all support the observation that culturing HEKn on soft hydrogels reduces the proliferative activity of cells compared to those on cultured on TCP.

However, whether this translates to a shift towards terminal differentiation was less clear, with contradictory downregulations of genes such as *ROCK2* and *AKT1* making the picture more complex. As previously highlighted, RNA expression is never a truly accurate representation of protein activity within a cell, and therefore in order to fully understand the effects of soft substrates on keratinocyte differentiation, it would be necessary to perform proteomics analysis. Moreover, it is possible that, whilst cells respond rapidly to mechanical cues when it comes to proliferation, differentiation might be a slower process that takes longer to commit to than the 4 days in which cells were cultured on the substrates. In terms of epidermal biology, this hypothesis has some merit, specifically in relation to wound healing where tissue injury causes immediate changes to the chemical composition and stiffness of the ECM which initiates the process of wound repair (Rosińczuk et al., 2016). Wounding triggers the activation of keratinocytes, and in order for reepithelialisation to take place, keratinocytes migrate into the wounded area where they undergo immediate proliferation; indicating that this is a rapid response following changes to the mechanical integrity of the epidermis (Pastar et al., 2014). Following this initial proliferative response, keratinocytes are deactivated and resume their normal differentiation pathway in order to repair the compromised epidermal barrier (Pastar et al., 2014). Whilst this does not necessarily explain the HEKn response to soft hydrogels, it emphasises that epidermal homeostasis is a complicated process, and this avenue of investigation would benefit from further investigation with longer cell exposure to the different dishes.

3.6 Conclusions

This chapter aimed to determine whether culturing keratinocytes on hydrogel-coated dishes mimicking *in vivo* mechanics would both offer a viable alternative to standard TCP/glass cultureware, and whether the softer substrates would induce changes related to epidermal homeostasis. We hypothesised that by using normal cultureware coated with a thin hydrogel, it would be possible to both maintain the ease of standard 2D culture, whilst examining the effects of substrate stiffness on biomechanics; thus bridging the current gap between 2D and 3D *in vitro*

investigations. Moreover, we hypothesised that keratinocytes would respond to softer substrates by reverting to more a realistic behaviour and phenotype that replicated that found in the epidermis.

Culturing both HaCaTs and HEKn on hydrogel-coated cultureware did raise some initial problems regarding standard 2D culture practices such as passaging cells, harvesting lysates, and imaging mounted coverslips. However, each of these hurdles was successfully troubleshooted, and despite the requirement for some adaptations away from the standard 2D culture procedures, the hydrogel-coated cultureware remained relatively simple and quick to use, and ultimately supported 2D *in vitro* cell culture.

Both HaCaT cells and HEKn were observed to exhibit rapid increases in colony density and decreases in proliferative activity in response to culture on soft hydrogels compared to TCP. Moreover, HEKn exhibited changes in YAP1 expression and localisation that suggested the observed proliferation decrease was directly related to the cells reacting to their new mechanical environment. It was hypothesised at this stage that soft substrates, particularly 4 kPa, promoted a shift from a proliferative phenotype towards terminal differentiation. Whilst a striking increase in CK10 expression in HEKn cultured on BM hydrogels seemed to support this, analysis of other genes associated with epidermal homeostasis was less conclusive. Whilst it was apparent that softer substrates had a clear impact on proliferative activity, it could not be definitively concluded that cells were undergoing terminal differentiation. Given the poor connectivity between RNA levels and protein levels within cells, and the relatively short time in which HEKn were exposed to the hydrogel-coated dishes, further research would need to be carried out in order to fully understand the effects of BM substrates on the keratinocyte proliferation-differentiation balance. However, it is evident that culturing keratinocytes on TCP has a significant impact on colony morphology and induces aberrant proliferation which could contribute to the proliferative decline of HEKn *in vitro*.

4 Investigating the effects of substrate stiffness on cytoskeletal organisation and nuclear mechanics in keratinocytes

4.1 Introduction

In the previous chapter, it was demonstrated that culturing keratinocytes on soft hydrogel-coated dishes induced changes in colony morphology and cell behaviour that were directly linked to the altered mechanical environment following evidence of Hippo signalling pathway activation. The mechanisms via which cells detect their mechanical environment are many and varied, and likely span a much broader spectrum than is currently discussed in the literature.

To recap the concepts introduced in chapter 3, mechanosensing begins at the plasma membrane which marks the interface between the cell and both ECM components and adjacent cells. Integrins provide the method of mechanical attachment to the ECM and are anchored to the actin cytoskeleton via vinculin and talin, whilst E-cadherin is a core cell-cell adhesion molecule and is bound to the actin cytoskeleton via α- and β-catenins. By contracting these adhesion molecules cells are able to calculate the rigidity of their binding partner based on the amount of force needed to induce displacement (Ghassemi et al., 2012; Moore, Roca-Cusachs and Sheetz, 2010; Yang et al., 2018). E-cadherin contraction has been shown to be essential for epidermal assembly and barrier formation (Yang et al., 2018). Due to the attachment of both integrins and E-cadherin to actin, external mechanical information is transmitted directly to the cytoskeleton, and relatively small stiffness changes *in vitro* have been demonstrated to alter actin organisation in epithelial cells (Collins et al., 2017). As discussed in chapter 3, actin reorganisation is a core element of the transition towards terminal differentiation in keratinocytes (Nanba et al., 2013). Actin and other cytoskeletal components are connected to the nuclear Lamina via the LINC complex, which enables the communication of external mechanical cues directly to the nuclear interior (Hieda, 2019). Engagement of integrins at the epidermal basement

membrane relays high tension to the LINC complex, which has been demonstrated to suppress differentiation and promote a basal cell phenotype (Carley et al., 2020). Consequently, it is apparent that the cytoskeleton and LINC complex have a significant role to play in the detection of external mechanical cues in keratinocytes, and thus it was necessary to investigate how culture on BM hydrogels affected these proteins.

4.1.1 The role of the cytoskeleton in mechanotransduction

As mentioned previously, mechanotransduction begins at the cell membrane where cell adhesion molecules bound to adjacent cells and the ECM use small contractions to relay information about external tension to their internal binding partners. Actin is the cytoskeletal component most associated with mechanosensing, and filaments are anchored to integrins by vinculin and talin, and to E-cadherin by α- and β-catenin. In a similar mechanism to sarcomere shortening in skeletal muscle, cells use myosin IIB to contract adhesion molecules along the actin filaments and use the amount of force required to displace the adjacent cell or ECM to infer the stiffness of their surroundings (Moore, Roca-Cusachs and Sheetz, 2010; Yang et al., 2018). Whilst the exact mechanism behind this is not fully understood, the formation of epithelial layers is thought to be very reliant on E-cadherin contraction due to its role in controlling monolayer formation (Yang et al., 2018). It has been demonstrated that changes to the stiffness of *in vitro* polyacrylamide gel substrates can result in alterations in E-cadherin-dependent epithelial cell adhesion which in turn leads to changes in cell spreading and actin organisation (Collins et al., 2017).

Multiple studies on multiple cell types have presented the link between substrate stiffness and actin organisation. An experiment using rat embryonic fibroblast cells revealed that actin cytoskeleton fluidity was dependent on ECM stiffness, and actin organisation was dependent on ECM stiffness and cell shape (Gupta et al., 2019). Cells were imaged live on substrates mimicking soft, intermediately stiff, and very stiff ECMs. It was observed that fibroblasts grown on a soft substrate had no thick actin bundles and the filaments present were in an orthoradial arrangement, whilst those on intermediately stiff substrates had localised, well-ordered stress fibres, and

those on stiff substrates exhibited actin stress fibres across the bulk of the cell (Gupta et al., 2019).

In contrast, the relationship between mechanotransduction and microtubules is less defined but recent studies have evidenced a role in tuning cytoskeletal stiffness in response to external tension. Microtubules are three orders of magnitude stiffer than actin (Gittes et al., 1993), anisotropic in nature, and are able to maintain a given direction across the entirety of a cell, thus are well placed to detect cell-scale tension (Hamant et al., 2019). The contradictory nature of the literature currently available suggests that the mechanism by which microtubules facilitate mechanotransduction may differ between cell types. Studies into skeletal and cardiac muscle propose that detyronised tubulin regulates mechanotransduction by altering the mechanical properties of the cytoskeleton and therefore the level of mechanical resistance a cell provides (Kerr et al., 2015; Robison et al., 2016). However, an investigation into mechanotransduction in astrocytes revealed that detyronisation was not affected by changes to substrate stiffness, and instead a mechanism of crosstalk between actin and microtubules was proposed, with microtubule acetylation as a core regulator (Seetharaman et al., 2020). Finally, a very recent study into cardiomyocytes and skeletal muscle proposed that both detyronisation and acetylation of α-tubulin may be responsible for regulating cytoskeletal stiffness and viscoelastic resistance, implying a more complicated relationship between different microtubule post-translational modifications (Coleman et al., 2021). Consequently, there is still clearly a long way to go before the full role of microtubules in cell mechanosensing is understood.

The final cytoskeletal component is intermediate filaments, which play an important role in regulating cell shape and mechanical integrity due to their unique assembly-disassembly dynamics. One of the most prevalent types of cytoplasmic intermediate filaments are keratins, which have already been highlighted as important in regulating epidermal homeostasis. Crosstalk between keratins and the actin cytoskeleton is a staple part of mechanotransduction; external mechanical strain triggers keratins to activate the ROCK signalling pathway which promotes actin

stress fibre formation and increased cell stiffness (Bordeleau et al., 2012). Additionally, shear stress has been shown to increase peripheral cytoplasmic keratin stiffness following rapid reorganisation of the keratin filament network, suggesting a role in spatial redistribution of tension to ensure the structural integrity of a cell is maintained (Sivaramakrishnan et al., 2008). In the epidermis, keratinocytes with plectin deficiency have been shown disrupt the keratin network and lead to increased nuclear deformability (Almeida et al., 2015). Moreover, a recent study confirmed the close association between focal adhesion and hemidesmosome components and the intermediate filament network and demonstrated that hemidesmosome-intermediate filament interactions counteract cellular tension by reducing cytoskeletal tension, focal adhesion assembly, and YAP signalling (Wang et al., 2020).

4.1.2 Cytoskeletal reorganisation through the epidermal layers

As already touched upon in chapter 3, the epidermis contains a variety of mechanical niches due to the multiple cell layers created as keratinocytes differentiate and migrate to the surface of the tissue. One of the key features of keratinocyte differentiation is reorganisation of the cytoskeleton which helps to facilitate the transition from proliferative basal cells to the terminally differentiated corneocytes found at the stratum corneum.

As keratinocytes differentiate the composition of keratins changes (Biggs et al., 2020), contributing to shifts in cell stiffness and thus the level of resistance that neighbouring cells encounter when contracting their adhesion molecules to assess the mechanics of their external environment. In the basal layer, keratin 5 and keratin 14 are the major keratin types and are bundled as tonafilaments bound to desmosomes and hemidesmosomes which provides the epidermis with its structural integrity (Moll, Divo and Langbein, 2008); dominant-negative mutations in keratin 5 or 14 genes have been shown to cause the hereditary skin blistering disease epidermolysis bullosa simplex (Omary, Coulombe and McLean, 2004). Both keratin 5 and keratin 14 can be observed in the suprabasal layers, but this is due to their remaining integrated into the keratin cytoskeleton rather than due to continued expression, as mRNA for these proteins is notably absent (Moll, Divo and Langbein, 2008). In contrast, keratin

15 is found strictly in the basal layer of the epidermis and is a marker of epidermal stem cells (Bose et al., 2013).

Keratin 1 and keratin 10 are major keratins of keratinocyte differentiation and a switch is made to express these during the keratinocyte migration to the suprabasal spinous cell layers (Fuchs and Green, 1980). Keratins 1 and 10 form particularly dense bundles contributing to the stability of both the individual cell and the epidermis as a whole, and keratin 10 is known to have a role in suppressing proliferation (Moll, Divo and Langbein, 2008). As keratinocytes move into the upper layers of the epidermis, the stratum spinosum and stratum granulosum, they undergo another keratin shift, expressing keratin 2, mutations in which have been associated with skin blistering and cytolysis in the superficial epidermis. In "soft skin" (e.g., nipple, penile shaft, axilla) expression of keratin 2 is minor, leading to the proposition that keratin contributes towards terminal cornification (Collin et al., 1992).

Similarly, actin filaments also undergo a shift in organisation as keratinocytes differentiate and move up through the epidermal layers. Human keratinocyte stem cells cultured *in vitro* exhibit short actin bundles located radially, whilst keratinocytes that have stopped proliferating present with a well-developed circumferential actin network (Nanba et al., 2013). In chapter 3 we touched upon the role that actin regulators (specifically RhoA, ROCK1, ROCK2, Rac1, and Akt1) have in driving the balance between proliferation and differentiation in the epidermis (3.4.3.2). ROCK1 and ROCK2 are downstream mediators of RhoA, and whilst both are present in the epidermis, ROCK2 is the more prevalent; pharmacological inhibition of ROCK2 results in increased keratinocyte proliferation (McMullan et al., 2003). A recent study has also highlighted a significant role for Akt1 in the transition from keratinocyte to corneocyte in terminal differentiation. During the cornification process, a keratinocyte must lose all of its organelles including the nucleus, the latter of which requires the degradation of Lamin A/C, a protein essential for maintaining nuclear integrity. Dispersal of Akt1-dependent phosphorylated Lamin A/C to different parts of the cytoplasm is necessary for the breakdown of the nucleus during differentiation (Rogerson et al., 2021). Immunoprecipitation revealed that Lamin A/C dispersal relies

on a number of Akt1 target proteins such as actin, Arp3 (required for actin nucleation), and Myh9 (a myosin IIA component). Disruption of either actin polymerisation, nucleation or the activity of myosin IIA have all been shown to prevent dispersal of Lamin A/C cytoplasmic structures which inhibited nuclear volume reduction and therefore the terminal differentiation of keratinocytes (Rogerson et al., 2021).

Given the extensive crosstalk existing between all cytoskeletal components, it is no surprise that microtubules are also observed to reorganise in response to keratinocyte differentiation. Basal layer keratinocytes exhibit a microtubule network that emanates from an apical centrosome, whilst in suprabasal keratinocytes the centrosome is still able to nucleate microtubules, but anchoring is transferred to desmosomes (Lechler and Fuchs, 2007). As differentiation progresses, microtubules are observed to become increasingly localised to the cell cortex which is believed to promote stronger cell adhesion and thus epidermal integrity and barrier function (Lechler and Fuchs, 2007; Sumigray, Foote and Lechler, 2012). A study by Hsu et al. induced barrier defects, such as reduced thickness of the cornified layer and lower filaggrin expression, in reconstructed human epidermis through Th2 cytokine treatment. In order to assess whether microtubule stabilisation could promote epidermal barrier repair, they used the microtubule-stabilising compounds paclitaxel and epothilone to demonstrate that stabilising microtubules led to the reparation of induced barrier defects . It was hypothesised that this was due to the potential role that microtubules and microtubule motor dynein play in the assembly of adherens junctions and tight junctions (Hsu et al., 2018). This suggested that not only does microtubule stabilisation promote epidermal barrier formation, but it may also have a role in supporting the healing process in damaged skin (Hsu et al., 2018).

4.1.3 Nuclear mechanics and mechanosensing through the LINC complex

In order for cells to translate external mechanical cues into reactionary changes, the information must be referred to the nucleus. The engagement of adhesion molecules at the cell membrane relays tension to the nucleus through the cytoskeleton which is bound to the LINC complex. The LINC complex is made up of two protein domains;

SUN domain and the C-terminal KASH domain (expressed in nesprin proteins), and collectively they span the nuclear envelope (Bouzid et al., 2019). Nesprins are part of the spectrin protein family and the C-terminal KASH domain binds with the C-terminal half of SUN proteins in the NE lumen, whilst the N-terminal binds to components of the cytoskeleton. The N-termini of SUN domain proteins are bound to the nuclear Lamina which in turn organises chromatin, thus providing the final link between external mechanical stimuli and the nuclear interior (Cartwright and Karakesisoglou, 2014; Chambliss et al., 2013; Hieda, 2019; Padmakumar et al., 2005). This cell-spanning protein network is able to control cell adhesion, nuclear positioning, actin dynamics and directed cell migration in response to the external mechanical environment (Chang et al., 2015; Stewart et al., 2015; Thakar et al., 2017).

4.1.4 The LINC complex in the epidermis

It is well established that the mechanical environment of the epidermis changes as keratinocytes migrate away from the basement membrane, and it is therefore unsurprising that the LINC complex plays differential roles throughout the layers. At the stiff basement membrane, engagement of integrins relays high tension to the nucleus through the LINC complex. A study performed on mouse keratinocytes observed that differentiation was repressed following integrin engagement, but that disruption of the LINC complex led to precocious differentiation both *in vitro* and *in vivo* (Carley et al., 2020). *In vitro* culture of keratinocytes on micro-patterned substrates of different stiffnesses has shown that there is a direct correlation between integrin-mediated adhesion and the level of differentiation. Low adhesive area correlates to terminal differentiation, whilst high expression of integrin $\alpha 6$ and $\beta 1$ subunits is associated with epidermal stem cells (J. Connelly, 2019; Kenny and Connelly, 2014).

This clear shift towards a differentiated phenotype following integrin engagement has been linked to tension applied to the nuclear Lamina, specifically Lamin A. At the basement membrane the stiffness of the ECM relays high tension to Lamin A, and this tension relaxes as keratinocytes migrate up through the epidermis and lose their focal adhesions (Carley et al., 2020). A 2014 study reported that a mouse model with

a skin-specific triple Lamin knockout (Lmna−/− Lmnb1Δ/Δ Lmnb2Δ/Δ) exhibited hyperkeratosis and a thickened epidermal layer which was evidence of precocious epidermal differentiation (Jung et al., 2014). This therefore further supports the role that the nuclear lamina plays in controlling the shift from a proliferative to a differentiated phenotype in the epidermis.

The high expression level of nesprin-2 in the epidermis compared to the dermis, and the significant nuclear deformation observed in keratinocytes where nesprin-2 has been compromised suggests that it plays a core role in maintaining NE architecture in the epidermal compartment (Luke et al., 2008). However, knockout of nesprin-2 is not linked to changes in differentiation or in fact skin morphology, despite a slight thickening of the epidermis believed to be associated with larger nuclei (Luke et al., 2008).

4.2 Hypotheses and Aims

This chapter aims to investigate the molecular changes keratinocytes undergo when cultured on BM hydrogels in order to provide an explanation for the observed changes in cell behaviour discussed in chapter 3. Additionally, this chapter seeks to ascertain the impact that a softer substrate might have on the physical mechanics of a cell, in this instance by measuring the Young's Modulus of HEKn nuclear and cytoplasmic compartments. The cytoskeleton and LINC complex comprise the core mechanosensing machinery of a cell, and it was hypothesised that there would be changes to cytoskeletal and LINC proteins that could drive the behavioural responses HEKn had to being cultured on softer substrates.

Following observed changes in proliferation and differentiation (chapter 3), it was hypothesised that HEKn would exhibit altered cytoskeletal organisation when cultured on softer hydrogels; in particular, the actin cytoskeleton was anticipated to be reorganised to reflect a more differentiated keratinocyte phenotype. Additionally, the increased colony density observed in HEKn cultured on softer dishes (chapter 3) led to the hypothesis that E-cadherin molecules would be arranged to better promote epithelial sheet formation on 4 kPa hydrogels. The expectations for LINC complex

proteins largely revolved around the hypothesis that HEKn cultured on softer substrates would adapt their nuclear stiffness to reflect their environment; it was thus hypothesised that HEKn on BM hydrogels would exhibit a softer nucleus, assisted through the downregulation of LINC protein components.

To summarise, the key hypothesis behind this chapter was that there would be alterations to the cytoskeleton that correlated with the changes in cell density and proliferation reported in Chapter 3. With this in mind, this chapter aims to answer the following questions:

- Does culturing keratinocytes on softer hydrogels induce changes to the cytoskeleton that explain the observed alterations to cell behaviour?
- Do keratinocytes cultured on hydrogels adapt their own Young's Modulus in response to reduced external tension?
- Do keratinocytes cultured on softer substrates alter their expression of LINC protein components?

4.3 Objectives

- Determine whether culturing keratinocytes on hydrogels leads to changes in cytoskeletal and cytoskeletal-associated proteins.
- Determine how the LINC complex responds when keratinocytes are cultured on softer substrates.
- Calculate the Young's Modulus of keratinocytes cultured on TCP and BM hydrogels to determine whether adaptation occurs.

4.4 Results

As discussed in the previous chapter, both HaCaTs and HEKn exhibited changes in behaviour and morphology in response to being cultured on a softer substrate. Exploration of the Hippo pathway confirmed that HEKn were responsive to changes in substrate stiffness (Figure 3.17). This chapter therefore explores how known mechanosensitive proteins such as cytoskeletal and LINC components respond to different substrate stiffnesses.

4.4.1 HaCaTs cultured on softer substrates exhibited changes in cytoskeletal and LINC protein expression

4.4.1.1 HaCaT cells exhibited some changes in core cytoskeletal components when cultured on soft substrates

Following the changes in colony morphology observed in HaCaTs cultured on soft BM hydrogels and discussed in Chapter 3 (i.e., increased colony density and more "3D" appearance), the next step was to investigate what was happening at a molecular level to result in these changes. HaCaTs were cultured on TCP, 8 kPa, and 4 kPa hydrogels for 4 days before protein lysates were harvested and assessed through western blotting. As cell morphology is largely dictated by the cytoskeleton, the initial focus was on actin, microtubules and intermediate filaments (namely keratins given their high prevalence and important role in keratinocytes). It was observed that, though β-actin levels appeared to decrease in HaCaTs cultured on softer hydrogels (Figure 4.1A), it was not a statistically significant result according to densitometry analysis (Figure 4.1B). Similarly, tubulin appeared to decrease slightly on softer hydrogels (Figure 4.1A) but densitometry analysis revealed that this trend was not statistically significant (Figure 4.1C). A pankeratin antibody was used to assess the protein levels of multiple keratin types and the bands were matched to their potential keratins based on the molecular weights. Western blotting revealed that all keratin types appeared to decrease in response to culture on 8 and 4 kPa BM hydrogels (Figure 4.1A). Densitometry analysis further confirmed these changes, with a general trend of lower protein expression on softer hydrogels (Figures 4.1D-G) which was statistically significant for CK10, CK13/14 and CK15.

Figure 4.1 (overleaf) HaCaTs cultured on BM hydrogels exhibited changes in cytoskeletal protein levels. (A) *Protein lysates were taken from HaCaTs cultured on TCP, 8 kPa, and 4 kPa dishes. Western blot analysis displays that β-actin, tubulin and pankeratin all seemed to decrease on hydrogel substrates.* **(B-G)** *Quantification of the relative expression of proteins when normalised to TCP using densitometry. Data represent mean, n = 3, statistical significance was assessed using one-way ANOVA with Tukey's post-hoc test, ns = non-significant, * p ≤ 0.05.*

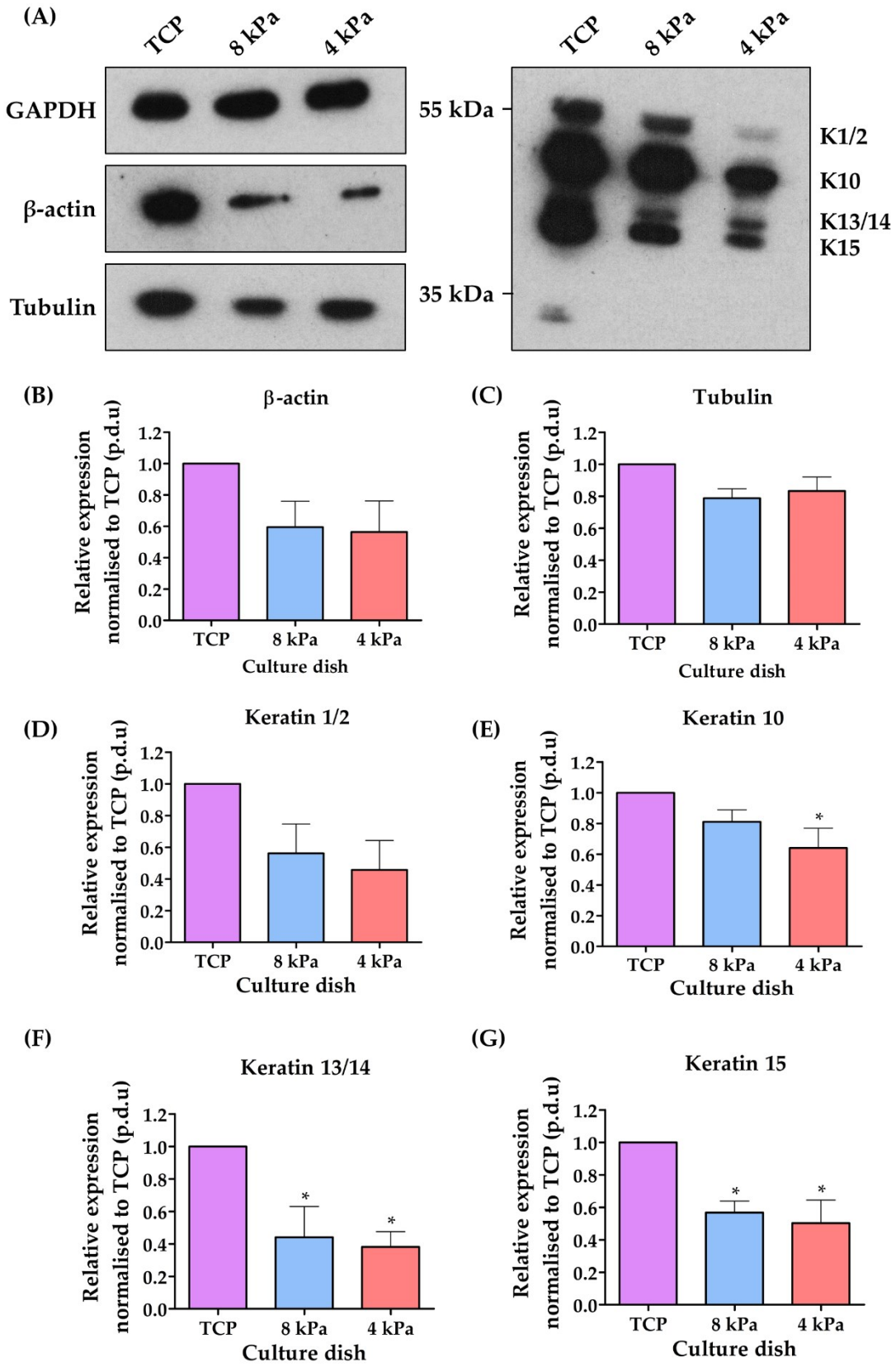
(A)
TCP
8 kPa
4 kPa
GAPDH
β-actin
Tubulin
55 kDa
35 kDa
K1/2
K10
K13/14
K15
(B)
β-actin
Relative expression normalised to TCP (p.d.u)
Culture dish
(C)
Tubulin
(D)
Keratin 1/2
(E)
Keratin 10
(F)
Keratin 13/14
(G)
Keratin 15

4.4.1.2 HaCaT cells exhibited decreased levels of LINC complex proteins when cultured on softer substrates

The next proteins targeted for western blot analysis were components of the LINC complex due to their key role in cellular mechanosensation. Once again HaCaTs were cultured on TCP, 8 kPa, and 4 kPa dishes for 4 days before protein lysates were harvested. Emerin is a nuclear envelope (NE) protein that has associations with both microtubules at the outer nuclear membrane, and chromatin at the inner nuclear membrane. Western blotting revealed that protein levels of emerin decreased in cells cultured on soft hydrogels (Figure 4.2A) and densitometry analysis showed that this decrease was statistically significant between TCP and 4 kPa dishes (Figure 4.2B). SUN1 and SUN2, core LINC components that anchor nesprins to the nuclear Lamina, were both observed to decrease in HaCaTs cultured on hydrogels (Figure 4.2A), and densitometry analysis confirmed a statistically significant decrease in band intensity for HaCaTs cultured on 8 kPa and 4 kPa dishes compared to those on TCP (Figure 4.2C-D). Finally, Lamin A/C and Lamin B1 were assessed via western blot. Lamin A/C was observed to decrease to a striking degree in cells on softer substrates (Figure 4.2A), and Lamin B1 was also observed to decrease to a statistically significant degree on 4 kPa hydrogels compared to TCP (Figure 4.2E).

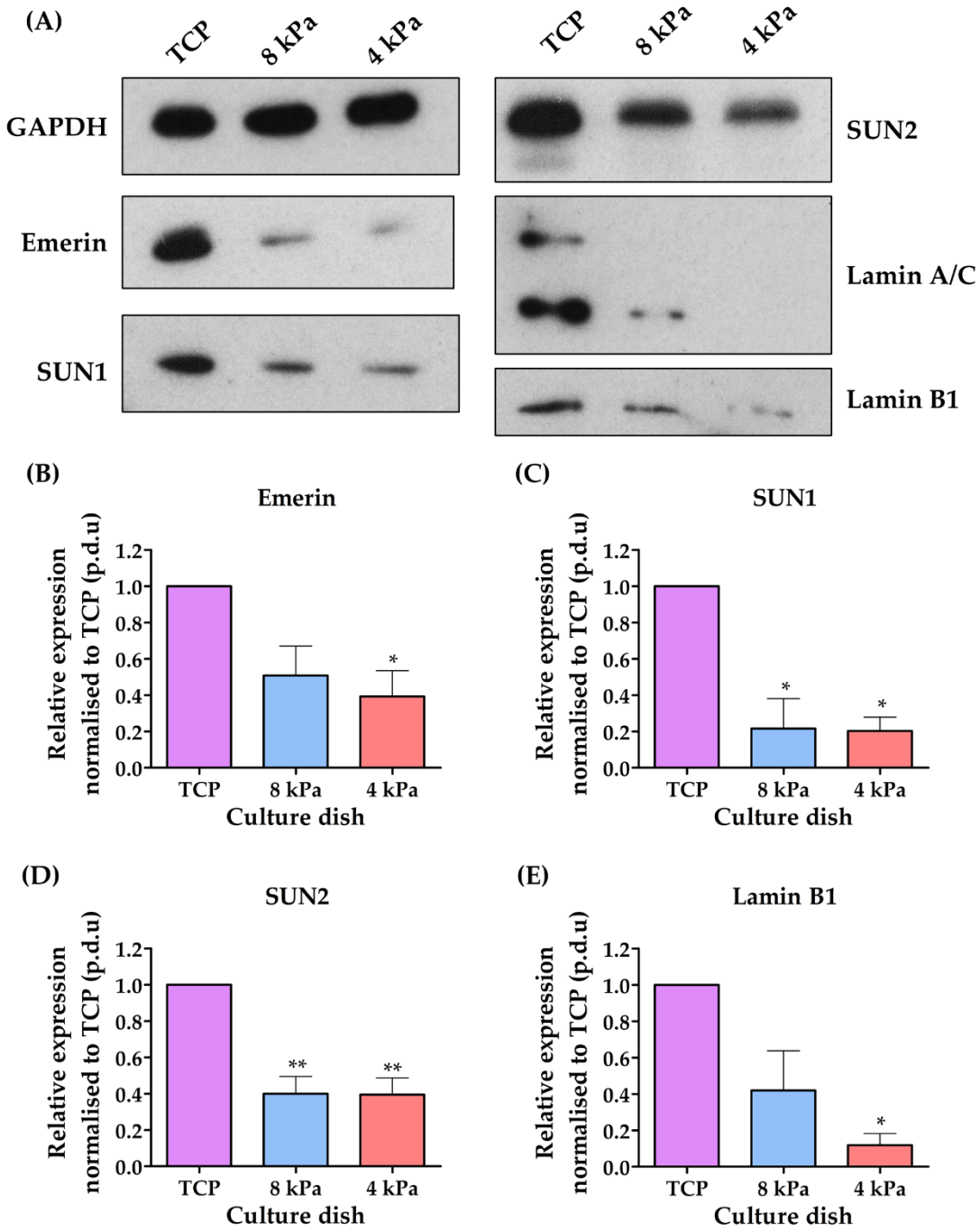

Figure 4.2 HaCaTs cultured on BM hydrogels exhibited changes in LINC protein levels. (A) *Protein lysates were taken from HaCaTs cultured on TCP, 8 kPa, and 4 kPa dishes. Western blot analysis displays that emerin, SUN1 and SUN2, and Lamin A/C and Lamin B1, all seemed to decrease on hydrogel substrates.* **(B-G)** *Quantification of the relative expression of proteins when normalised to TCP using densitometry. Data represent mean, n = 3, statistical significance was assessed using one-way ANOVA with Tukey's post-hoc test, ns = non-significant, * p ≤ 0.05, ** p≤0.01.*

4.4.2 Deeper investigation into Hippo pathway components could not be easily carried out in keratinocytes

Following the striking changes observed in LINC complex protein levels when HaCaTs were cultured on BM hydrogels, the next proteins of interest were components of the Hippo signalling pathway which plays a key role in regulating epidermal homeostasis in response to mechanical cues (Rognoni and Walko, 2019). In particular, the transcription factor YAP1, and the upstream regulator KIBRA were selected as key target proteins; YAP1 due to its role as an effector of the Hippo pathway, and KIBRA as a result of previous data obtained within the laboratory group that suggests an interaction between KIBRA and the KASH-domain of nesprin-2 that could perhaps link the Hippo pathway and LINC complex together (Karakesisoglou et al., unpublished). However, both proteins presented consistent problems when it came to analysing through western blotting. YAP1 has an expected molecular weight of 55 kDa, but analysis of YAP1 levels in HaCaTS resulted in a persistent strong band between 70 and 100 kDa, and a fainter one just above 100 kDa (Figure 4.3).

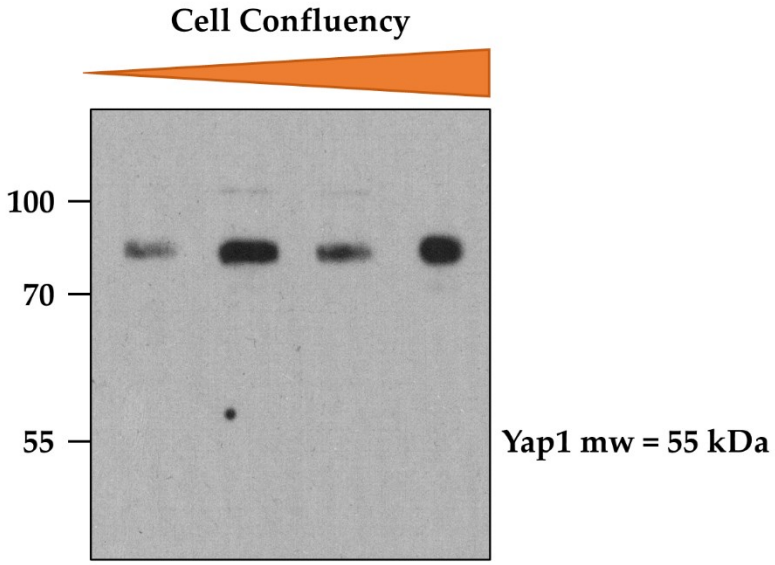

Figure 4.3 HaCaTs assessed for YAP1 levels through western blotting presented with bands of the incorrect molecular weight. *Protein lysates were taken from HaCaTs cultured to different confluencies (25 – 100%). Western blot analysis displays that the YAP1 antibody produced bands of the incorrect molecular weight (mw).*

Similar issues were experienced when assessing KIBRA, with Abcam (ab107637) and Sigma-Aldrich (HPA038016) anti-KIBRA antibodies producing no bands at all, and Santa Cruz (SC-133374) consistently producing bands of the incorrect molecular weight. KIBRA is highly expressed in the brain, thus in order to check that the SC-133374 antibody used was suitable for western blotting, HaCaT lysates were run alongside a CD1 mouse brain lysate, and the mouse neuronal cell lines CAD (undifferentiated and differentiated), and NSC-34 (undifferentiated and differentiated) in order to provide controls. Full-length KIBRA has a predicted molecular weight of approximately 125 kDa, and the differentiated CAD and NSC-34 lysates were observed to express a faint band of a similar weight (Figure 4.4 – white arrows). Moreover, it was observed that CD1 and all four neuronal lysates produced bands that were associated with alternate isoforms of KIBRA (Figure 4.4); assessment of the antibody epitope confirmed that it is present in all known KIBRA isoforms. HaCaTs at 100% confluency were observed to express a band that matched the molecular weight of isoform 5, in addition to a lighter band that was also found in 25% confluent HaCaTs (Figure 4.4). This lower band was consistently observed in all blots performed using the SC-133374 KIBRA antibody and did not appear to correlate with any known KIBRA isoforms.

Figure 4.4 (overleaf) Mouse brain and neuronal lysates confirmed that the Santa Cruz anti-KIBRA antibody SC-133374 showed specificity for multiple known KIBRA isoforms. *Protein lysates were taken from CD1 mouse brain, undifferentiated and differentiated CAD and NSC-34 cells, and 100% and 25% confluent HaCaTs (control brain and neuronal lysates were prepared by a previous student in the group). Western blot analysis displays that the Santa Cruz KIBRA antibody is specific for multiple known isoforms of KIBRA including the full-length protein (white arrows). HaCaTs expressed an unknown lighter band. MAP2 was used to confirm tissue validity of brain and neuronal control lysates. β-actin was used as a loading control.*

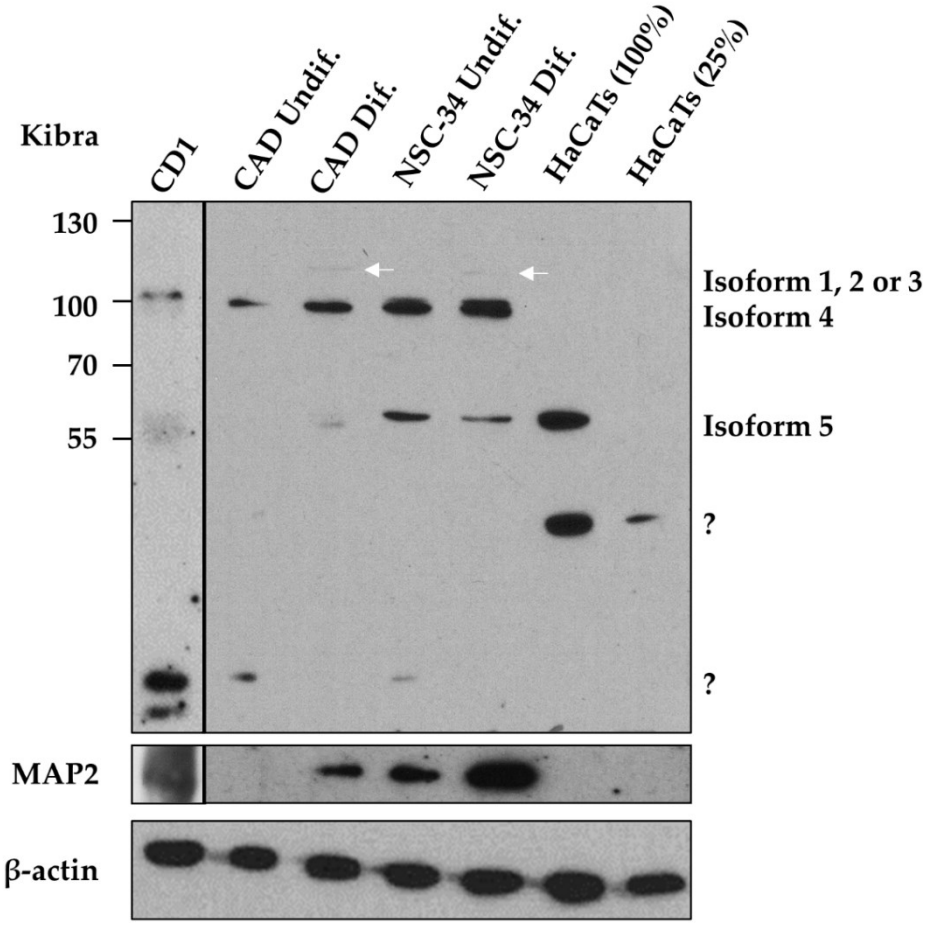

In order to explore what was happening in terms of KIBRA localisation within the cells, further assessment was carried out through immunofluorescence staining. COS-7 cells were transfected with Myc-KIBRA (kindly provided by Kremerskothen group, University of Münster) and immunostained with all three antibodies to assess staining specificity prior to using the antibodies on keratinocytes. The ab107637 and SC-133374 antibodies were found to be non-specific when used for immunofluorescence (not shown), whilst HPA038016 anti-KIBRA staining correlated with anti-myc (Figure 4.5A). As referenced previously, unpublished data from the laboratory group suggests that KIBRA binds to the KASH domain of nesprin-2, and therefore it was predicted that KIBRA would be observed to localise at the NE. However, contrary to this, KIBRA staining in HEKn was observed to be highly specific to the Golgi apparatus as confirmed through co-staining with the Golgi marker GM130 (Figure 4.5B). Given the increasingly apparent complexity of KIBRA

expression and localisation in keratinocytes, this avenue of investigation was not pursued further during this project.

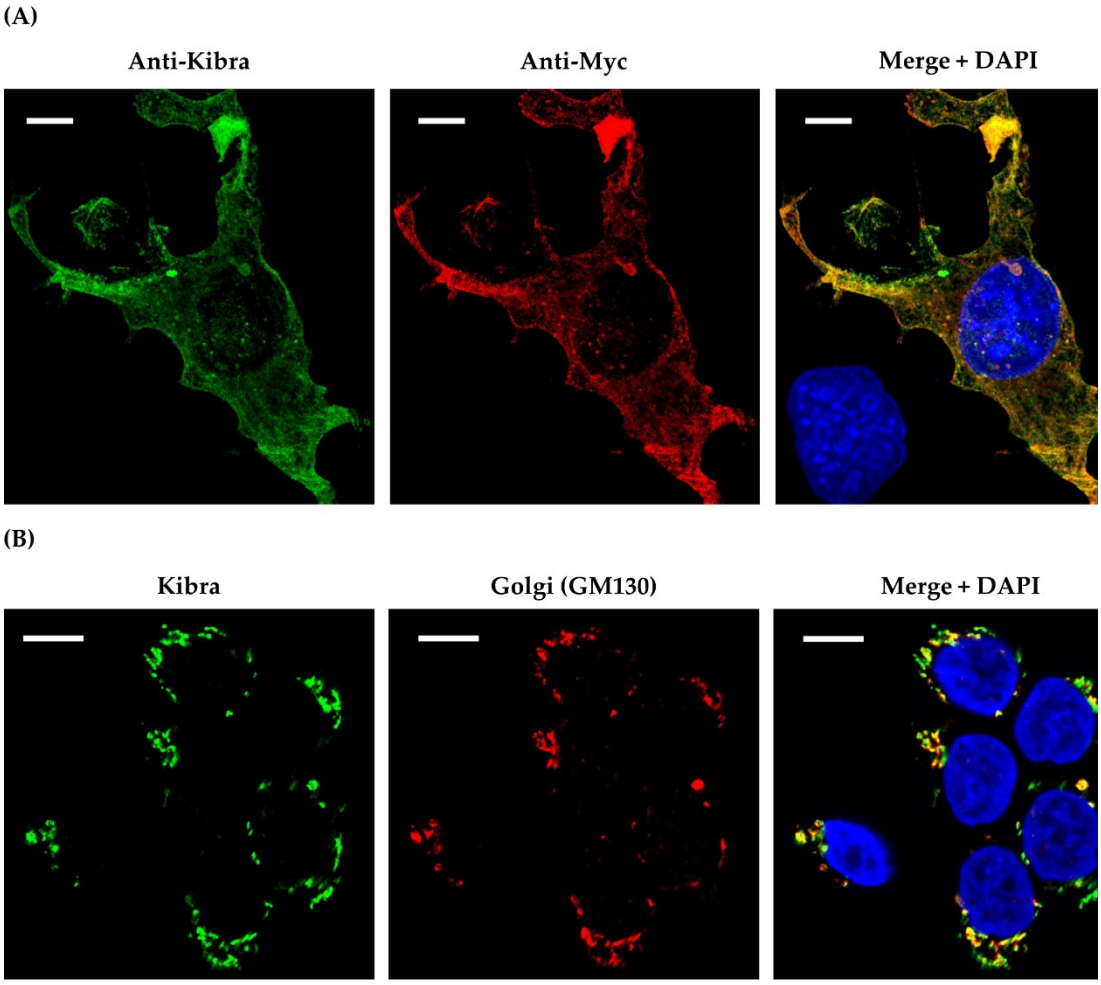

Figure 4.5 KIBRA was observed to localise at the Golgi apparatus in HEKn. **(A)** *COS-7 cells were transfected with a Myc-KIBRA construct (Kremerskothen group) and immunostained for myc and KIBRA. Confocal microscopy images display that myc and KIBRA antibodies were observed to produce co-localised staining. Scale bars = 10 μm.* **(B)** *HEKn were immunostained for KIBRA and the Golgi marker GM130. Confocal microscopy images display that KIBRA and GM130 were co-localised. Scale bars = 10 μm.*

4.4.3 Cytoskeletal and cell junctional proteins were altered in HEKn cultured on BM hydrogels

Following on from the striking changes observed in HEKn proliferation, differentiation and Hippo pathway activity when cultured on BM hydrogels, the next step of the investigation was to repeat the analysis of cytoskeletal components that

had been carried out on the HaCaTs. However, here the assessment was more thorough, compiling western blot, immunostaining and WaferGen data, and exploring both core cytoskeletal components and proteins involved in the cell junctions so important for epidermal barrier function.

4.4.3.1 HEKn cultured on BM hydrogels exhibited changes in cytoskeleton and cell junction protein levels and localisation

HEKn were cultured on TCP, 50 kPa, 8 kPa and 4 kPa dishes for 4 days then protein lysates were harvested and assessed through western blotting. β-actin levels were observed to decrease slightly in response to a softer culture substrate (Figure 4.6A) and this was confirmed through densitometry analysis which showed statistical significance in the downregulation on 4 kPa (Figure 4.6B). In contrast, levels of tubulin and E-cadherin did not appear to change in response to the stiffness of the culture substrate (Figure 4.6A) and this was again confirmed by densitometry analysis which revealed no significant differences across the dishes (Figure 4.6C-D).

Figure 4.6 (overleaf) HEKn cultured on soft hydrogels had lower β-actin levels. (A) *Protein lysates were taken from HEKn cultured on TCP, 50 kPa, 8 kPa and 4 kPa dishes. Western blot analysis displays that β-actin decreased on softer substrates, whilst tubulin and E-cadherin showed little change.* **(B-D)** *Quantification of the relative expression of proteins when normalised to TCP using densitometry. Data represent mean, n = 3, statistical significance was assessed using one-way ANOVA, ns = non-significant, * $p \leq 0.05$.*

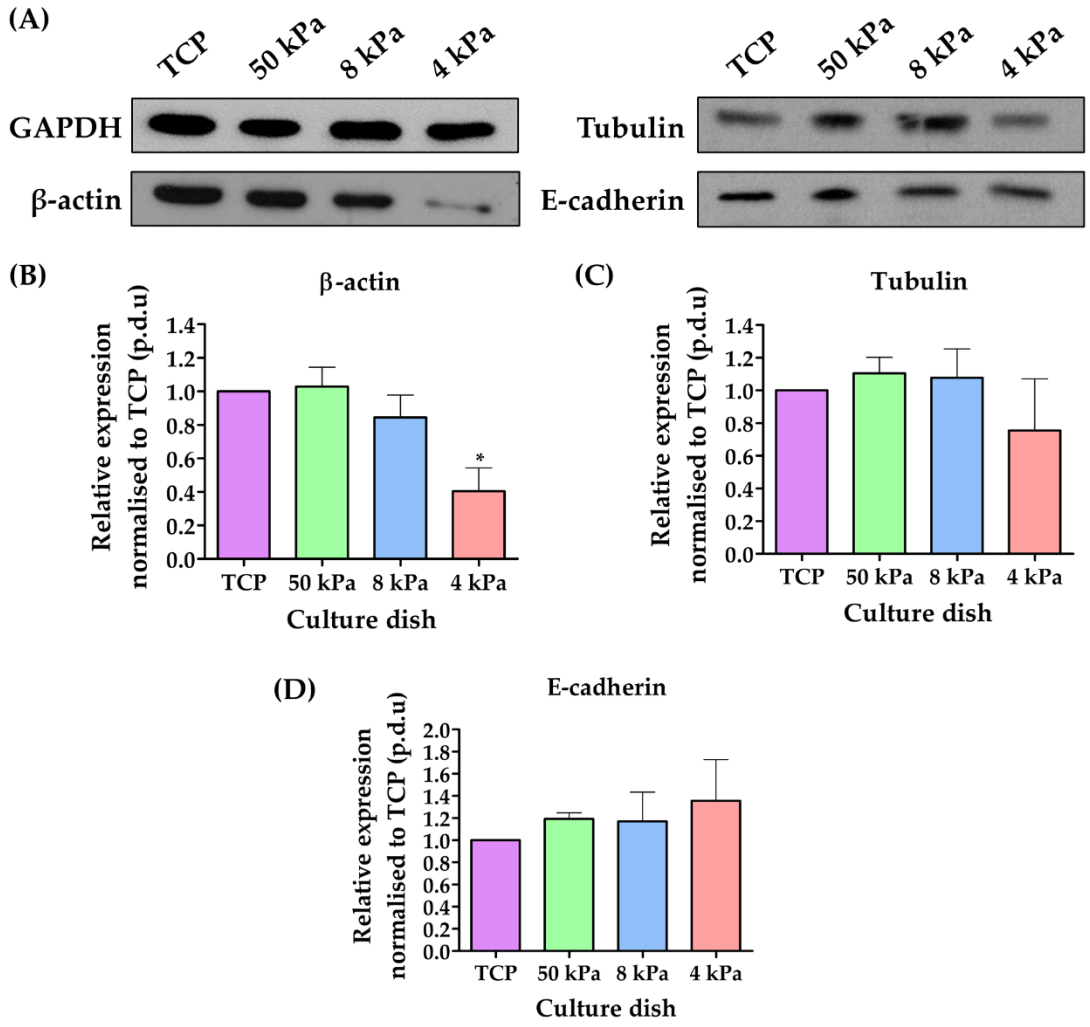

The next analysis aimed to assess cytoskeletal and cell junction components through immunostaining to look for any changes in localisation in response to the BM dishes. HEKn were cultured on glass or 4 kPa coverslips for 4 days before being fixed and stained for F-actin. It was observed that HEKn cultured on glass coverslips exhibited high numbers of basal actin fibres that were notably absent in the majority of cells cultured on 4 kPa coverslips (Figure 4.7A). Quantification of these basal fibres revealed that HEKn on glass coverslips had a statistically higher number than those on the soft hydrogel coverslips (Figure 4.7B).

In contrast to F-actin, staining of HEKn cultured on glass and 4 kPa coverslips with a tubulin antibody did not reveal any significant changes to microtubule organisation (Figure 4.8). Plectin is a large protein involved in the connection of intermediate filaments to microtubules, and the anchoring of intermediate filaments to

hemidesmosomes and desmosomes which is essential for firm basal layer attachment (Castañón et al., 2013). HEKn cultured on 4 kPa coverslips were observed to have strong perinuclear plectin staining and clear localisation in the cytoplasm around the nucleus that was much less apparent in HEKn on glass coverslips (Figure 4.9A). Quantification of this perinuclear localisation confirmed that the phenotype occurred in significantly more cells on the 4 kPa coverslips than on glass (Figure 4.9B).

Another protein that plays a vital role in epidermal barrier function is E-cadherin which is involved in regulating tight junctions, gap junctions, and desmosomes (Tunggal et al., 2005). HEKn were again cultured on glass or 4 kPa coverslips for 4 days and were then fixed and immunostained for E-cadherin. The localisation difference of E-cadherin between the two coverslips was striking, with HEKn on glass exhibiting punctate staining that highlighted where adherens junctions were in the process of being formed, whilst HEKn on 4 kPa coverslips had linear staining along the membranes of adjoining cells (Figure 4.10A). Quantification of these different phenotypes revealed that HEKn glass had more cells with punctate staining than linear, whilst those on 4 kPa coverslips had a significantly greater number of cells with linear staining (Figure 4.10B), suggestive of a more developed connection between adjoining cells.

In addition to the punctate and linear staining, it was also observed that in HEKn on glass coverslips, there was diffuse E-cadherin staining throughout the cytoplasm, whilst in HEKn on 4 kPa coverslips this appeared more concentrated to the perinuclear region (Figure 4.11A). Quantification of this observation revealed that there was a striking difference between the two substrate stiffnesses, with 78.1% of HEKn on 4 kPa exhibiting perinuclear E-cadherin versus 1.2% of HEKn on glass (Figure 4.11B).

Figure 4.7 (overleaf) HEKn cultured on glass coverslips showed a greater number of basal actin fibres. (A) *HEKn were cultured on glass and 4 kPa coverslips for 4 days then immunostained for F-actin. Confocal microscopy images display the localisation of actin fibres, and the presence of more basal actin structures in HEKn on glass coverslips (white arrows). Scale bars = 25 μm.* **(B)** *Quantification of basal actin fibres in HEK on cultured on glass and 4 kPa BM coverslips. Data represent mean ±SEM, n = 3 (3x 100 cells), statistical significance was assessed using a two-tailed unpaired t-test, *** $p \leq 0.001$.*

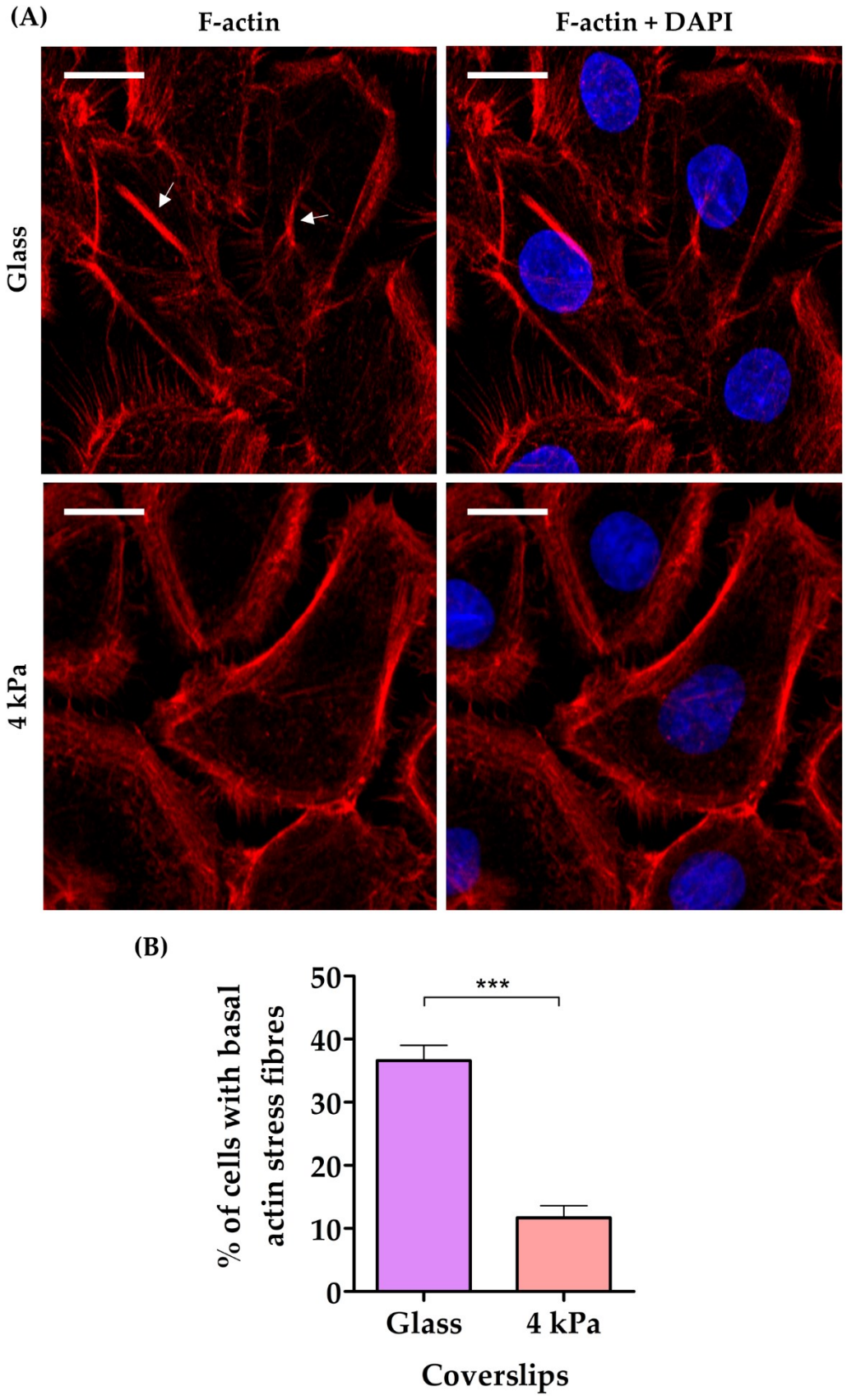
(A)
F-actin
F-actin + DAPI
Glass
4 kPa
(B)
% of cells with basal actin stress fibres
50
40
30
20
10
0
***
Glass
4 kPa
Coverslips

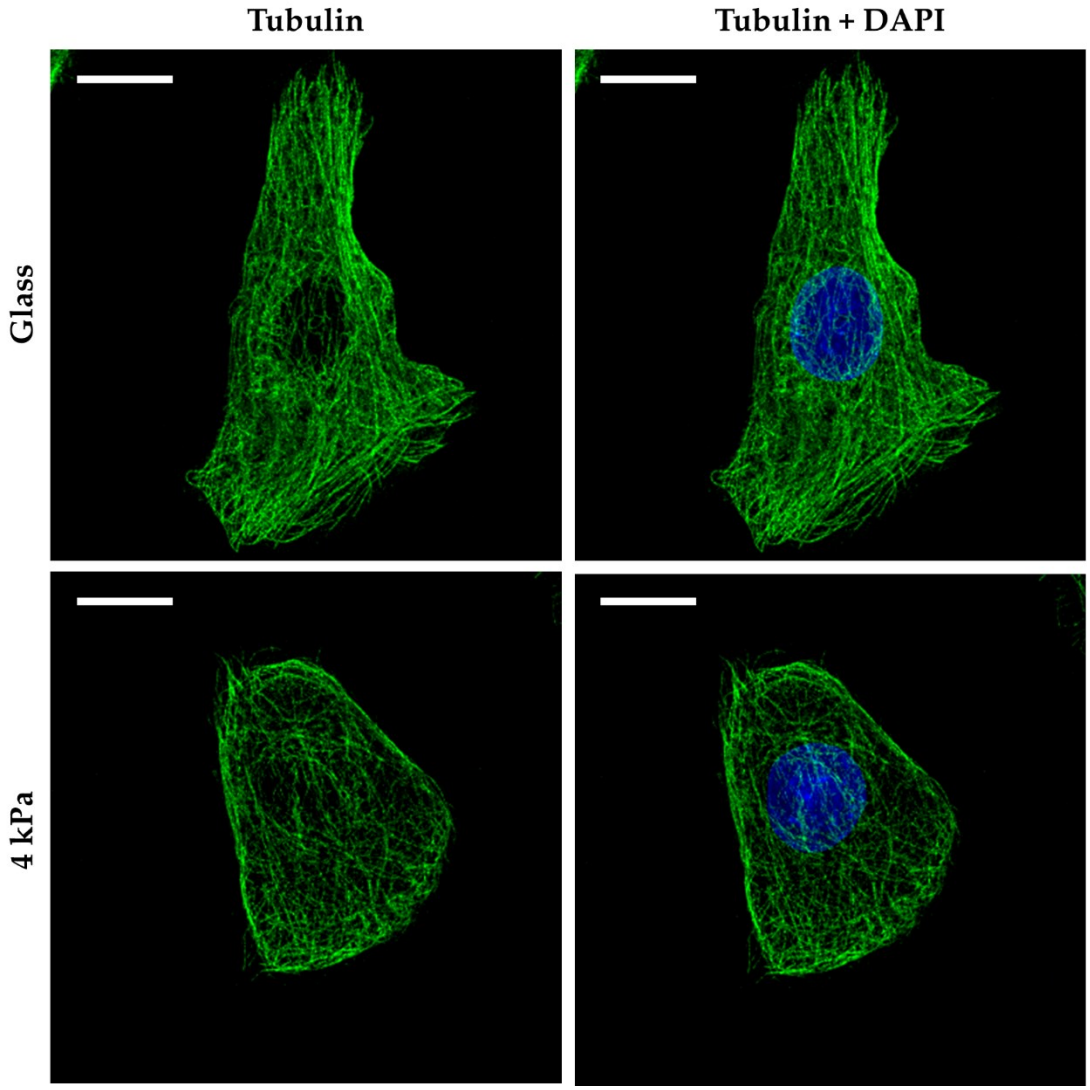

Figure 4.8 No change in microtubule organisation was observed between HEKn cultured on glass and 4 kPa coverslips. *HEKn were cultured on glass and 4 kPa coverslips for 4 days then immunostained for tubulin. Confocal microscopy images display the localisation and organisation of microtubules in response to substrate stiffness. Scale bars = 25 μm.*

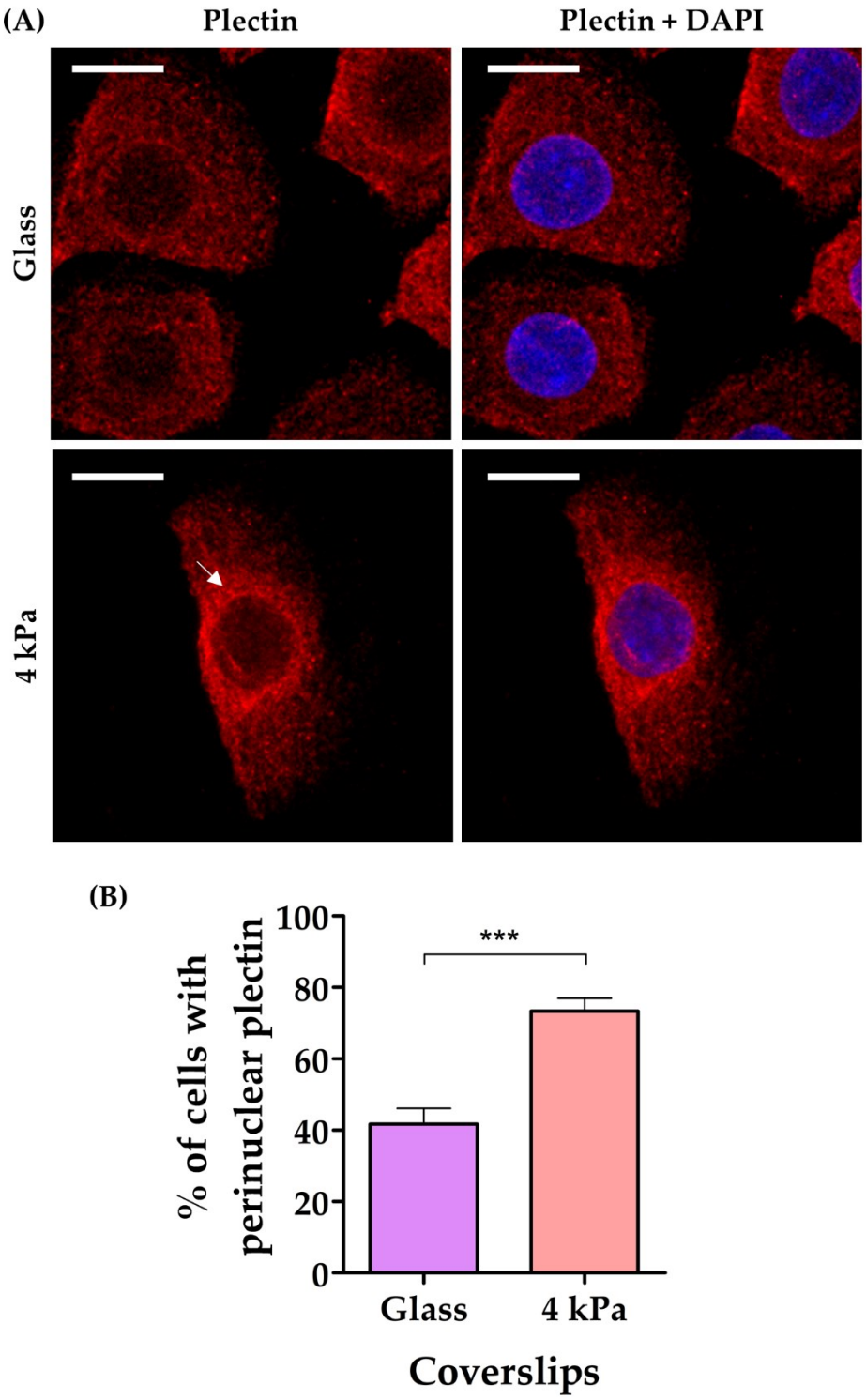

Figure 4.9 HEKn cultured on 4 kPa coverslips exhibited perinuclear plectin staining. (A) *HEKn were cultured on glass and 4 kPa coverslips for 4 days then immunostained for plectin. Confocal microscopy images display the localisation of plectin, and the presence of strong perinuclear staining in HEKn on 4 kPa coverslips (white arrow). Scale bars = 25 μm.* **(B)** *Quantification of perinuclear plectin in HEKn on cultured on glass and 4 kPa BM coverslips. Data represent mean ±SEM, n = 3 (3x 100 cells), statistical significance was assessed using a two-tailed unpaired t-test, *** $p \leq 0.0001$.*

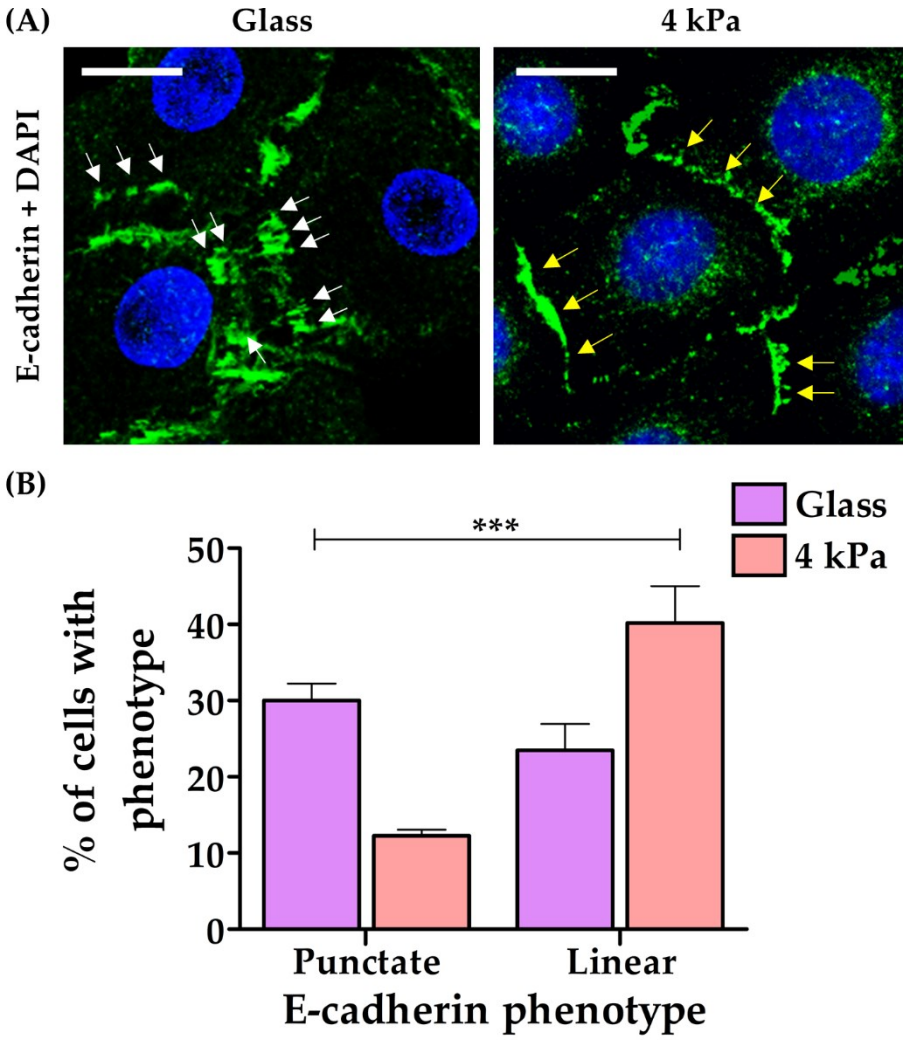

Figure 4.10 HEKn cultured on 4 kPa coverslips exhibited linear E-cadherin staining rather than punctate. (A) *HEKn were cultured on glass and 4 kPa coverslips for 4 days then immunostained for E-cadherin. Confocal microscopy images display the localisation of E-cadherin, and the presence of punctate staining in HEKn on glass coverslips (white arrows) versus linear on 4 kPa coverslips (yellow arrows). Scale bars = 25 μm.* **(B)** *Quantification of punctate and linear E-cadherin in HEKn on cultured on glass and 4 kPa BM coverslips. Data represent mean ±SEM, n = 3 (3x 100 cells), statistical significance was assessed using a two-tailed unpaired t-test, *** $p \leq 0.001$.*

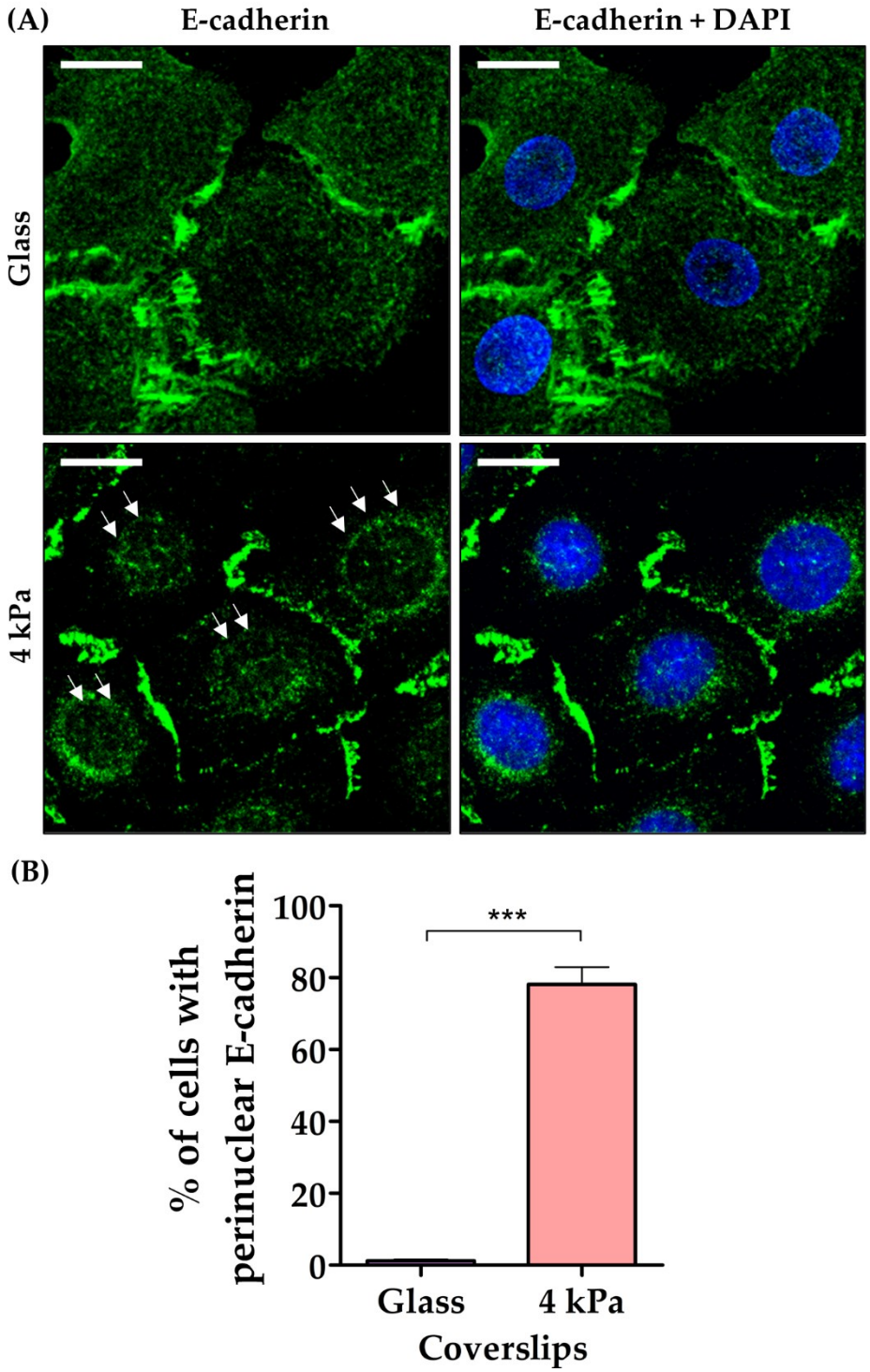

Figure 4.11 HEKn cultured on 4 kPa coverslips exhibited perinuclear E-cadherin staining. (A) *HEKn were cultured on glass and 4 kPa coverslips for 4 days then immunostained for E-cadherin. Confocal microscopy images display the localisation of E-cadherin, and the presence of strong perinuclear staining in HEKn on 4 kPa coverslips (white arrows). Scale bars = 25 μm.* **(B)** *Quantification of perinuclear E-cadherin in HEKn on cultured on glass and 4 kPa BM coverslips. Data represent mean ±SEM, n = 3 (3x 100 cells), statistical significance was assessed using a two-tailed unpaired t-test, *** $p \leq 0.001$.*

4.4.3.2 HEKn cultured on BM hydrogels exhibited changes in the gene expression of cytoskeletal and cell junction components

In order to gain a deeper insight into how the stiffness of a culture substrate affects the expression of cytoskeletal and cell junctional proteins, RNA analysis was performed using WaferGen. HEKn were cultured on TCP, 50 kPa, 8 kPa and 4 kPa plates for 4 days and RNA lysates were taken at 1, 2, 3 and 4 days after seeding. This time course made it possible to track gene expression changes over time and see how quickly cells adapted in response to new mechanical stimuli. As with the previous section, the first protein investigated was actin which binds to mechanosensitive focal adhesions and so is known to play a significant role in mechanotransduction (Martino et al., 2018). WaferGen analysis of β-actin revealed a downregulation of *ACTB* across all hydrogel stiffnesses from as early as day 1 after seeding, and this trend continued across the 4 days with several statistically significant reductions in expression (Figure 4.12A). *VCL* encodes the protein vinculin, which plays a role in anchoring actin filaments to the cell membrane via cell adhesion molecules such as integrins and E-cadherin (Martino et al., 2018). *VCL* was observed to start becoming significantly downregulated from 2 days after seeding onto hydrogels, and this trend increased with each day of culture on a soft substrate (Figure 4.12). *CDC42* encodes the protein Cdc42 which is a key regulator of actin dynamics and is rapidly activated during cell adhesion and required for cell spreading due to its role in filopodia formation (Kühn et al., 2015). WaferGen analysis revealed inconclusive changes in *CDC42* expression, with a fluctuating trend between upregulation and downregulation across the 4-day culture period compared to HEKn on TCP (Figure 4.12C).

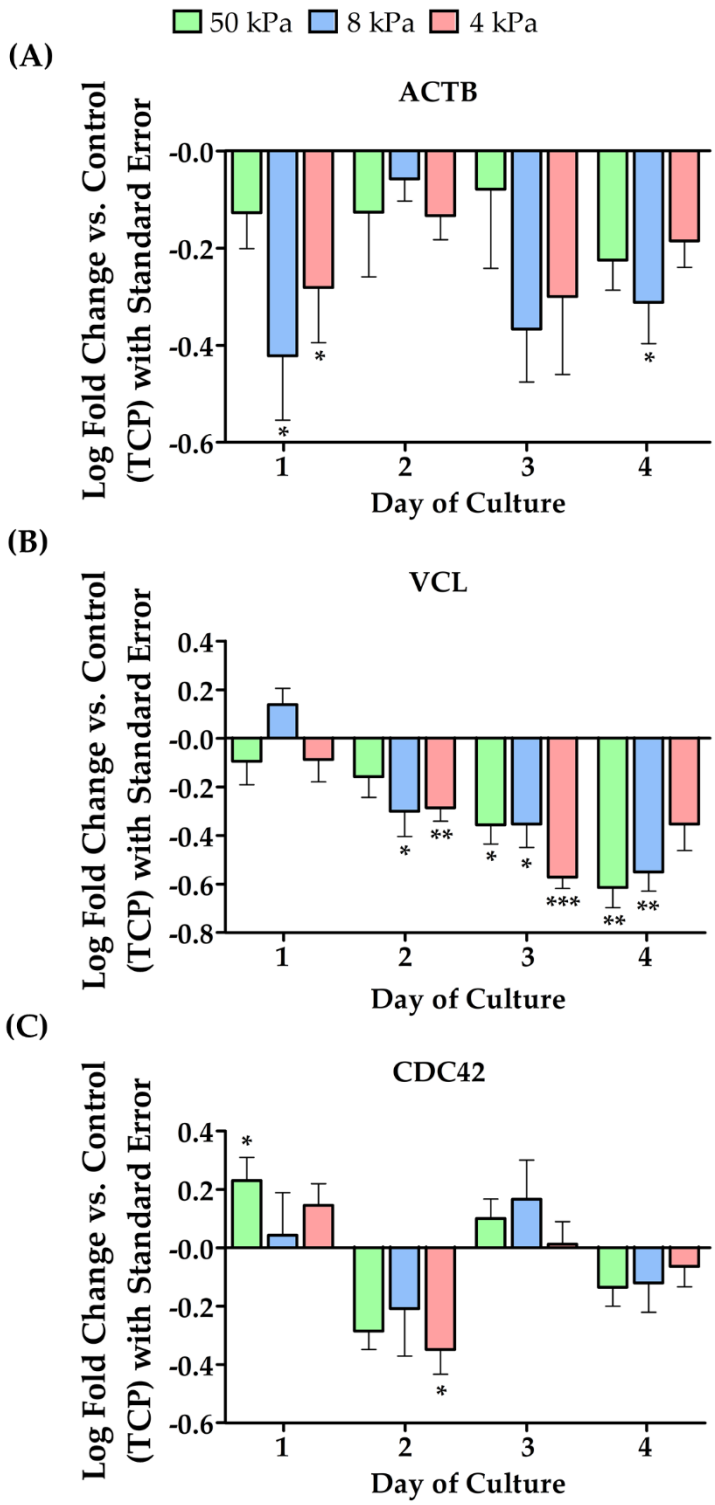

Figure 4.12 RNA analysis revealed significant downregulation of actin and vinculin when HEKn were cultured on BM hydrogels. *HEKn were cultured on TCP and 50, 8 and 4 kPa cultureware and RNA samples were harvested 1,2,3 and 4 days after seeding and analysed using WaferGen.* **(A-C)** *Quantification of Log fold change in gene expression in HEKn on 50, 8 and 4 kPa hydrogels in comparison to the TCP control. Data represent mean ±SEM, n = 6, statistical significance was assessed using two-way ANOVA, no asterisk = non-significant, * $p \leq 0.05$, ** $p \leq 0.01$, *** $p \leq 0.001$.*

At a protein level, tubulin was not observed to change in response to softer substrates in terms of amount of protein or localisation (Figures 4.6C and 4.8). However, WaferGen analysis of the *TUBB* gene revealed statistically significant downregulations in tubulin expression across all 4 days of the time course, particularly in HEKn cultured on 8 and 4 kPa hydrogels (Figure 4.13A). Analysis of *PLEC*, the gene encoding plectin, revealed a general trend towards downregulation, with a slight upregulation on day 4, though none of these results were statistically significant (Figure 4.13B). *KIF5B* encodes kinesin-1 heavy chain which connects nesprin-2 to microtubules and is important for nuclear migration and polarity (Zhu, Antoku and Gundersen, 2017). RNA analysis showed a trend towards downregulation across all substrate stiffnesses for the first 3 days after seeding, though this was not significant, then a trend towards upregulation on day 4 that was statistically significant in HEKn on 4 kPa hydrogels (Figure 4.13C).

The final genes examined for this section of the chapter were *CDH1*, *CTNNA1*, and *PTK2* which all play a role in cell adhesion. *CDH1* encodes E-cadherin which has already been highlighted as an important protein involved in the maintenance of skin barrier function and was observed to have distinct differences in localisation in HEKn cultured on glass versus 4 kPa coverslips (Figure 4.10 and 4.11). WaferGen analysis revealed that E-cadherin trended towards downregulation across the time course, with the change being most apparent day 1 after seeding, though the results were only statistically significant for HEKn on 4 kPa hydrogels, 1 and 2 days after seeding (Figure 4.14A). *CTNNA1* encodes α-catenin which binds to β-catenin and E-cadherin to form a complex connecting adherens junctions to actin (Kobielak and Fuchs, 2004). Additionally, α-catenin also plays a role during Hippo pathway activation, binding YAP1 to the cell membrane in order to prevent its translocation into the nucleus (Schlegelmilch et al., 2011). RNA analysis revealed that *CTNNA1* trended towards downregulation on softer hydrogels, particularly on days 3 and 4 after seeding where it was statistically significant for some hydrogel stiffnesses. *PTK2* encodes focal adhesion kinase, a tyrosine kinase concentrated at focal adhesions that transmits signals into downstream pathways and has been shown to mediate cell response to

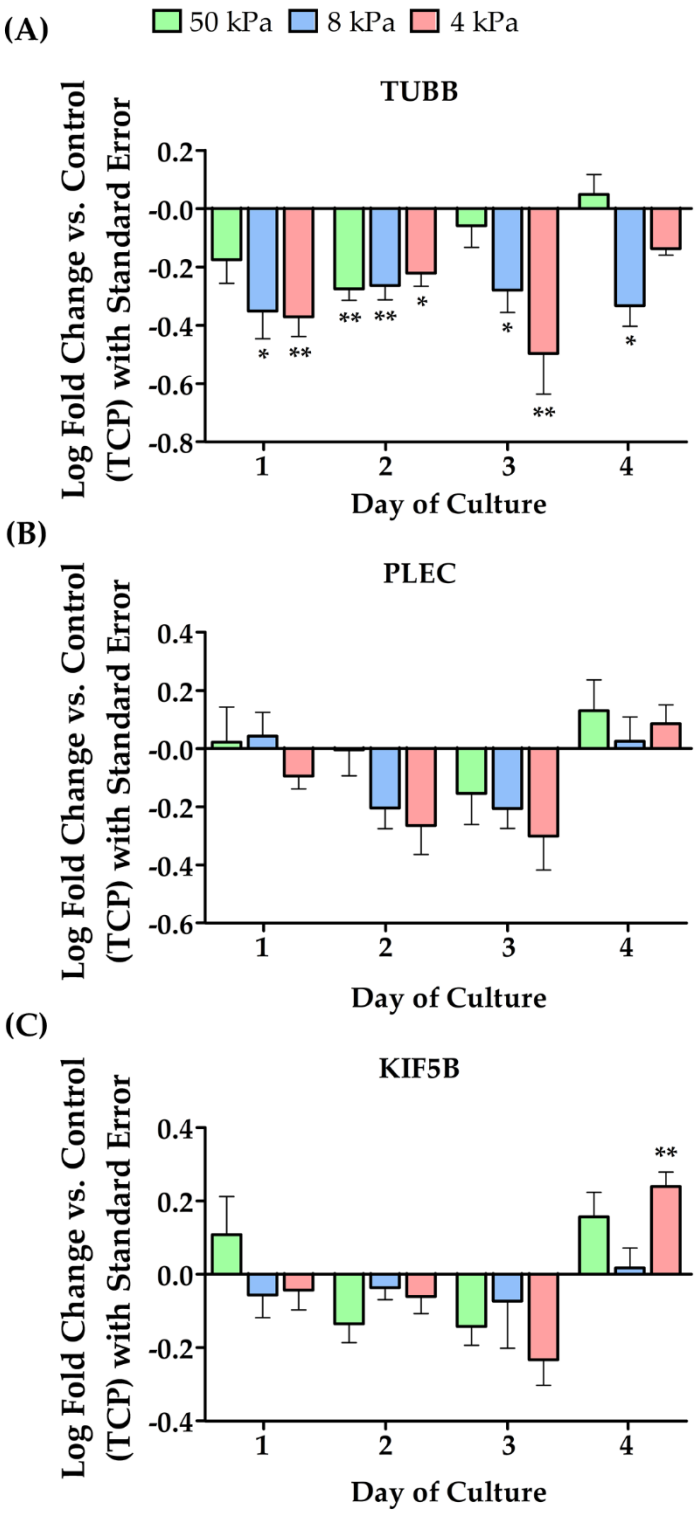

Figure 4.13 RNA analysis revealed significant downregulation of tubulin when HEKn were cultured on BM hydrogels. *HEKn were cultured on TCP and 50, 8 and 4 kPa cultureware and RNA samples were harvested 1,2,3 and 4 days after seeding and analysed using WaferGen.* **(A-C)** *Quantification of Log fold change in gene expression in HEKn on 50, 8 and 4 kPa hydrogels in comparison to the TCP control. Data represent mean ±SEM, n = 6, statistical significance was assessed using two-way ANOVA, no asterisk = non-significant, * $p \leq 0.05$, ** $p \leq 0.01$.*

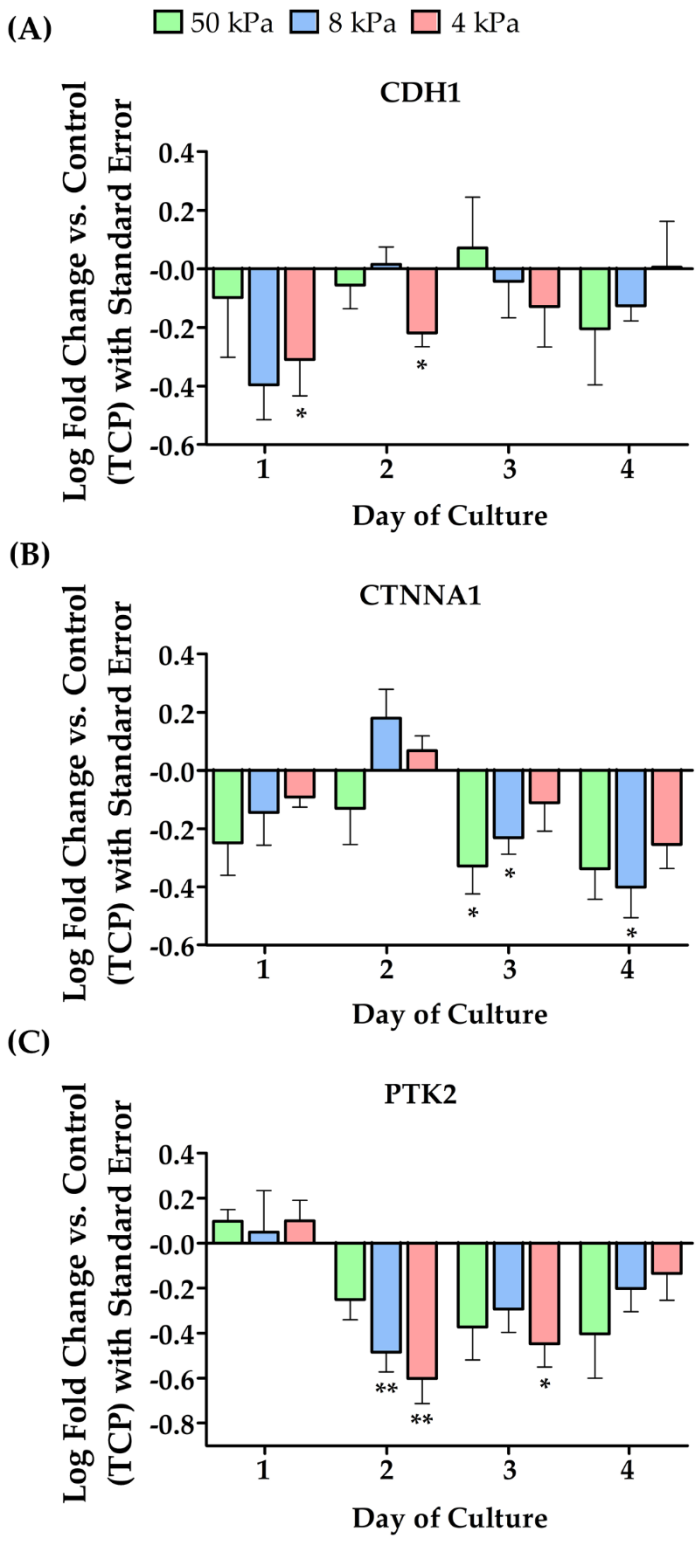

Figure 4.14 RNA analysis revealed some downregulation of adhesion proteins when HEKn were cultured on BM hydrogels. *HEKn were cultured on TCP and 50, 8 and 4 kPa cultureware and RNA samples were harvested 1,2,3 and 4 days after seeding and analysed using WaferGen.* **(A-C)** *Quantification of the Log fold change gene expression in HEKn on 50, 8 and 4 kPa hydrogels in comparison to the TCP control. Data represent mean ±SEM, n = 6, statistical significance was assessed using two-way ANOVA, no asterisk = non-significant, * $p \leq 0.05$, ** $p \leq 0.01$.*

subject rigidity by modulating YAP1 activation (Lachowski et al., 2018). RNA analysis revealed a trend towards downregulation in expression that was statistically significant in HEKn on 8 and 4 kPa substrates on day 2, and on 4 kPa on day 3 after seeding (Figure 4.14C).

4.4.4 HEKn cultured on BM hydrogels exhibited changes in LINC complex protein levels and gene expression

4.4.4.1 Western blot analysis revealed reduced levels of core LINC proteins in HEKn on softer substrates

The LINC complex is one of the core mechanosensory systems within a cell, and it is via this collection of proteins that external mechanical stimuli are transmitted to the nucleus and translated into changes in gene expression and protein regulation (Hieda, 2019). The initial investigation into LINC regulation in HaCaTs in response to substrate stiffness revealed a general downregulation of critical proteins in the complex (4.4.1.2). Consequently, the next step in the project was to see whether these changes were also observed in primary HEKn which are more reflective of the *in vivo* situation. HEKn were cultured on TCP, 50 kPa, 8 kPa and 4 kPa dishes for 4 days before protein lysates were harvested and analysed via western blotting. When looking at the blots alone, Lamin A/C, Lamin B1, emerin, and SUN1 all appeared to decrease in response to the softer culture substrates, whilst SUN2 did not appear to change (Figure 4.15A). However, densitometry analysis revealed that, whilst Lamin A/C and Lamin B1 did significantly decrease on softer hydrogels (Figure 4.15B-D), there was no significant change in protein level for emerin, SUN1 or SUN2 (Figure 4.15E-G).

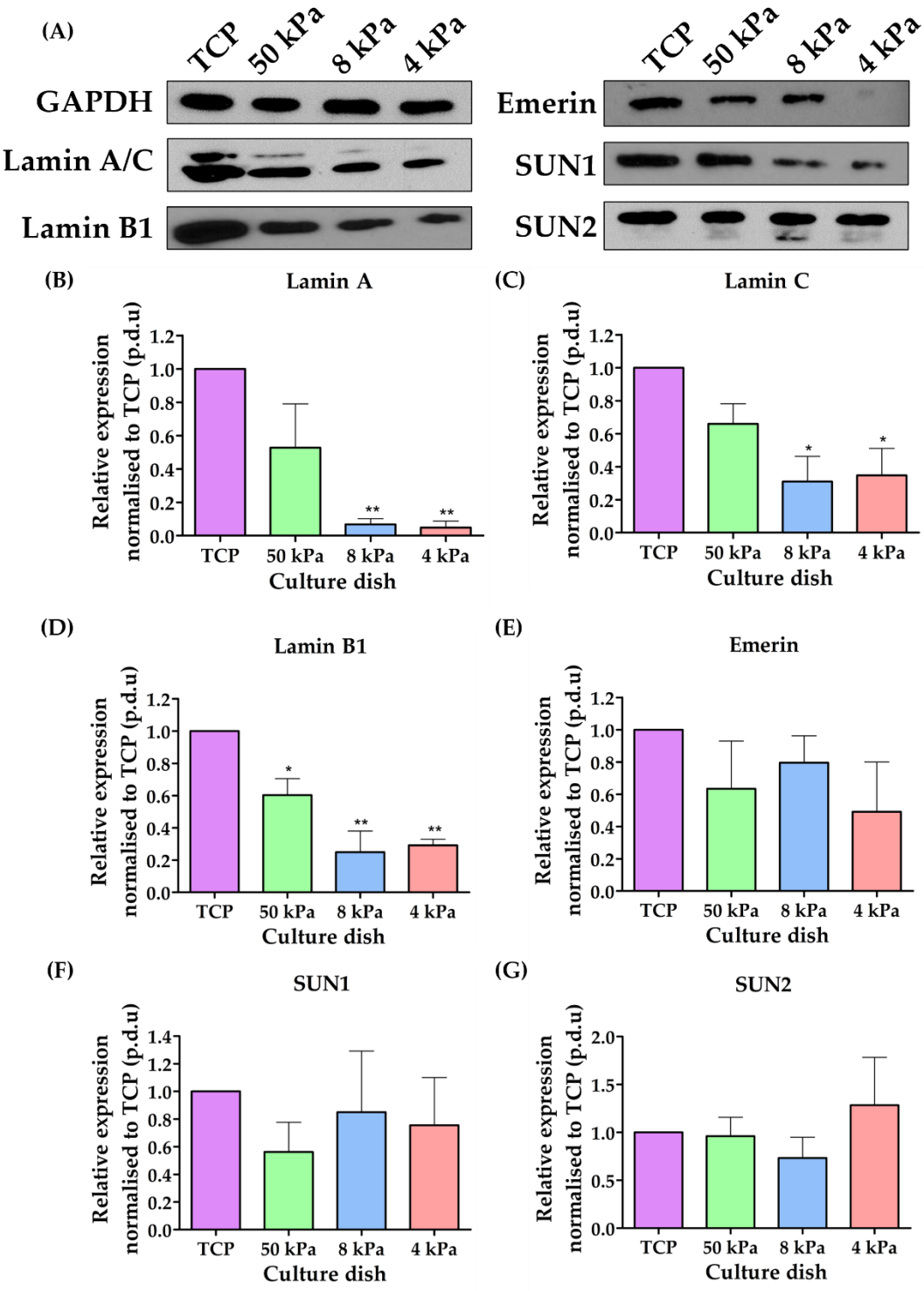

Figure 4.15 HEKn cultured on BM hydrogels exhibited decreased Lamin levels. (A) *Protein lysates were taken from HEKn cultured on TCP, 50 kPa, 8 kPa and 4 kPa dishes. western blot analysis displays the effect that substrate stiffness had on the levels of Lamin A/C, Lamin B1, emerin, SUN1 and SUN2 proteins.* **(B-G)** *Quantification of the relative expression of proteins when normalised to TCP using densitometry. Data represent mean, n = 3, statistical significance was assessed using one-way ANOVA with Tukey's post-hoc test, ns = non-significant, * $p \leq 0.05$, ** $p \leq 0.01$.*

Nesprin-1 binds SUN1 and SUN2 and anchors actin filaments (directly) and microtubules (via kinesin) to the NE (Stroud, 2018). There are multiple isoforms of nesprin-1 that each have different roles in the cell and the antibody used for western blot analysis detects multiple of these. It was observed that the levels of most of the isoforms decreased as the culture dish became softer (Figure 4.16A). Densitometry analysis was performed on four of the prominent bands and revealed that this downregulation in protein level was statistically significant for all of them (Figure 4.16B-E).

Nesprin-2 is another core LINC complex component and also binds actin filaments and microtubules to the NE via SUN1 and SUN2. Again nesprin-2 has multiple isoforms of which the antibody used detected many. Western blot analysis revealed that some isoform levels were unchanged across the culture dishes, but a number of isoforms decreased in response to a softer substrate, including nesprin-2 giant which is denoted by an asterisk (Figure 4.17A). Densitometry analysis was performed on six of the more prominent bands and revealed that, though there was a trend in downregulation, most of the changes observed were not statistically significant (Figure 4.17B-G). Nesprin-3 is a tissue specific protein that has been shown to not be expressed in keratinocytes and so it was not part of these analyses (Ketema et al., 2013).

Figure 4.16 (overleaf) HEKn cultured on BM hydrogels exhibited decreased levels of multiple nesprin-1 isoforms. (A) *Protein lysates were taken from HEKn cultured on TCP, 50 kPa, 8 kPa and 4 kPa dishes. Western blot analysis displays the effect that substrate stiffness had on the levels of nesprin-1 isoforms, * denotes nesprin-1 giant, numbers correlate with graphs for bands quantified through densitometry* **(B-E)** *Quantification of the relative expression of proteins when normalised to TCP using densitometry. Data represent mean, n = 3, statistical significance was assessed using one-way ANOVA with Tukey's post-hoc test, ** $p \leq 0.01$, *** $p \leq 0.001$.*

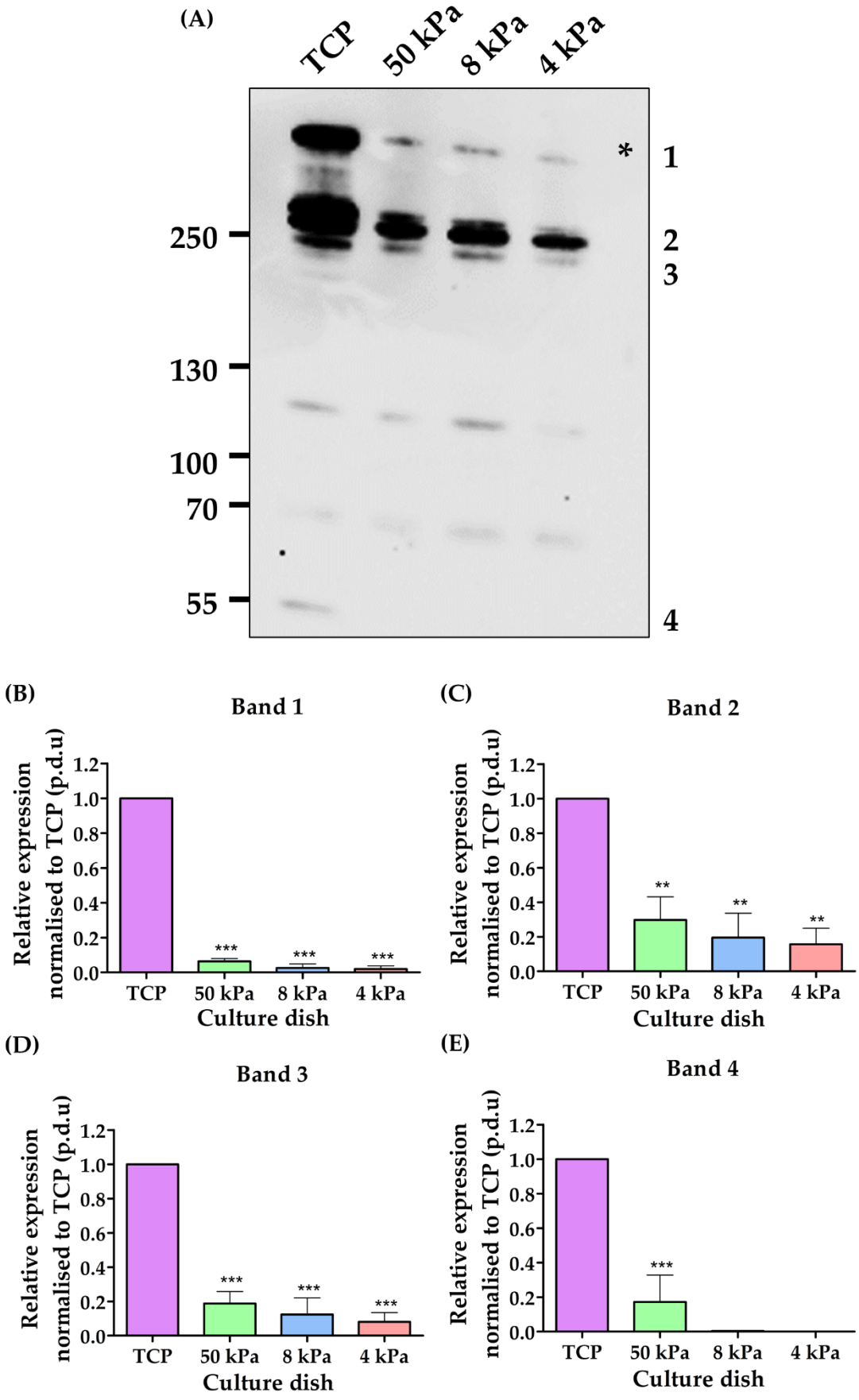
(A)
TCP
50 kPa
8 kPa
4 kPa
250
130
100
70
55
*
1
2
3
4
(B)
Band 1
Relative expression normalised to TCP (p.d.u)
1.2
1.0
0.8
0.6
0.4
0.2
0.0
***
***
***
TCP
50 kPa
8 kPa
4 kPa
Culture dish
(C)
Band 2
Relative expression normalised to TCP (p.d.u)
1.2
1.0
0.8
0.6
0.4
0.2
0.0
**
**
**
TCP
50 kPa
8 kPa
4 kPa
Culture dish
(D)
Band 3
Relative expression normalised to TCP (p.d.u)
1.2
1.0
0.8
0.6
0.4
0.2
0.0
***
***
***
TCP
50 kPa
8 kPa
4 kPa
Culture dish
(E)
Band 4
Relative expression normalised to TCP (p.d.u)
1.2
1.0
0.8
0.6
0.4
0.2
0.0
***
TCP
50 kPa
8 kPa
4 kPa
Culture dish

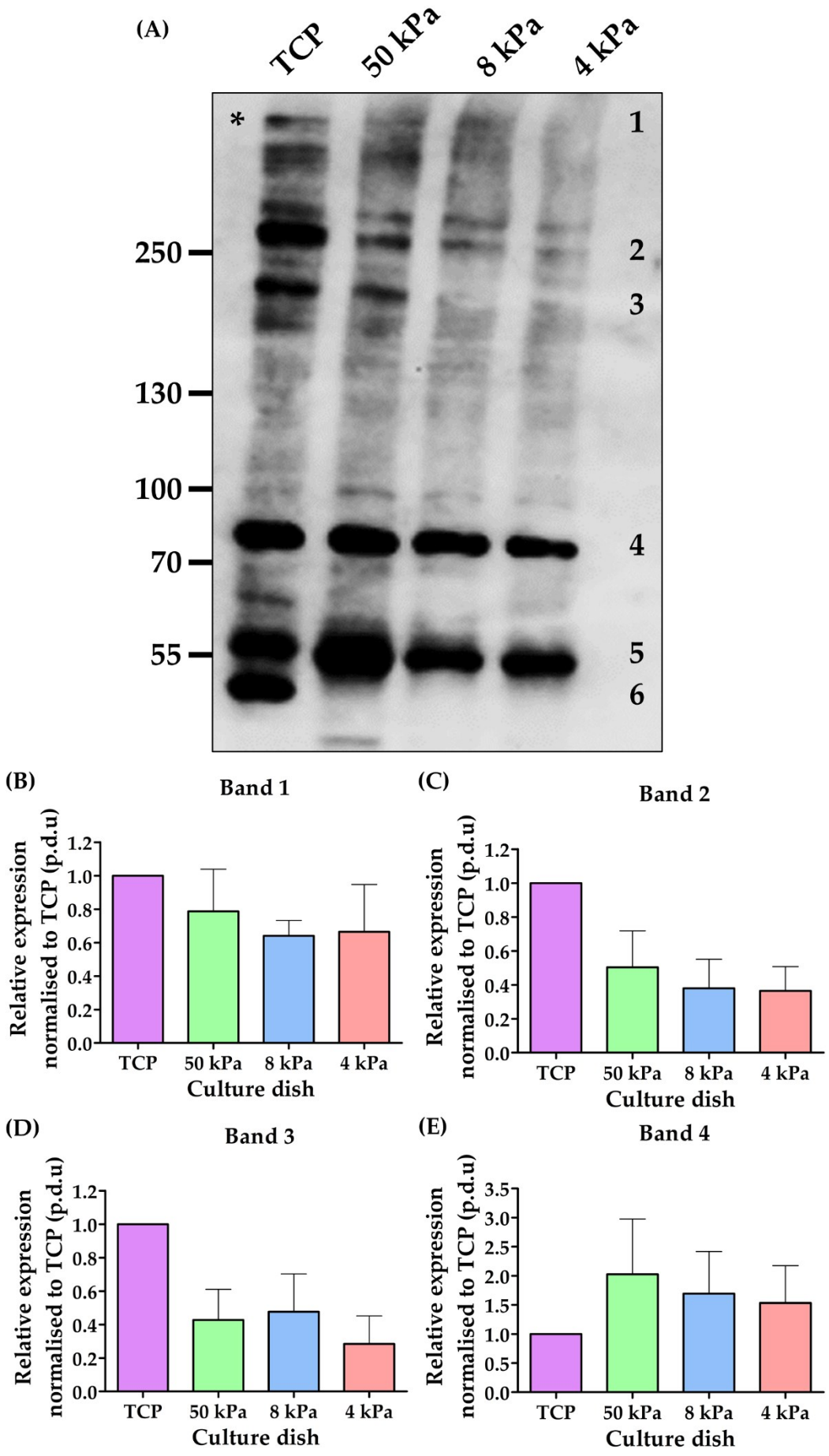
(A)
TCP
50 kPa
8 kPa
4 kPa
*
1
2
3
4
5
6
250
130
100
70
55
(B)
Band 1
Relative expression normalised to TCP (p.d.u)
1.2
1.0
0.8
0.6
0.4
0.2
0.0
TCP
50 kPa
8 kPa
4 kPa
Culture dish
(C)
Band 2
Relative expression normalised to TCP (p.d.u)
1.2
1.0
0.8
0.6
0.4
0.2
0.0
TCP
50 kPa
8 kPa
4 kPa
Culture dish
(D)
Band 3
Relative expression normalised to TCP (p.d.u)
1.2
1.0
0.8
0.6
0.4
0.2
0.0
TCP
50 kPa
8 kPa
4 kPa
Culture dish
(E)
Band 4
Relative expression normalised to TCP (p.d.u)
3.5
3.0
2.5
2.0
1.5
1.0
0.5
0.0
TCP
50 kPa
8 kPa
4 kPa
Culture dish

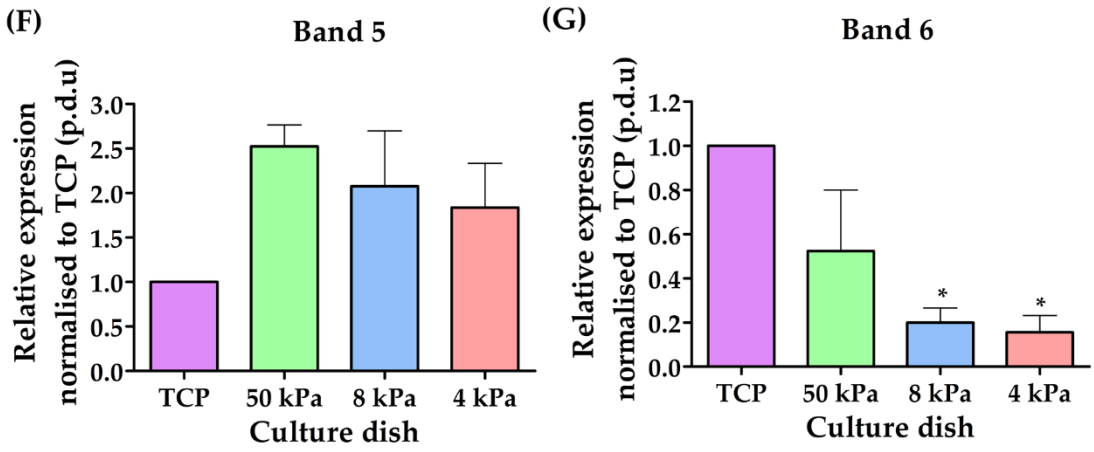

Figure 4.17 HEKn cultured on BM hydrogels showed some reduction in nesprin-2 levels. (A) *Protein lysates were taken from HEKn cultured on TCP, 50 kPa, 8 kPa and 4 kPa dishes. western blot analysis displays the effect that substrate stiffness had on the levels of nesprin-2 isoforms, * denotes nesprin-2 giant, numbers correlate with graphs for bands quantified through densitometry* **(B-G)** *Quantification of the relative expression of proteins when normalised to TCP using densitometry. Data represent mean, n = 3, statistical significance was assessed using one-way ANOVA with Tukey's post-hoc test, ns = non-significant, * $p \leq 0.05$.*

4.4.4.2 Gene expression of LINC complex and Nuclear Pore Complex proteins changed in response to culturing HEKn on BM dishes

In order to gain a more detailed picture of how softer culture substrates influence the LINC complex RNA analysis was performed using WaferGen. It was observed that emerin, encoded by the *EMD* gene, showed a general trend towards downregulation in HEKn cultured on BM hydrogels compared to TCP, but this was not statistically significant (Figure 4.18).

In contrast to emerin, Lamin A/C, encoded by *LMNA*, showed a general trend towards upregulation on day 1 after cells were seeded onto their respective dishes, but then a shift towards downregulation that was statistically significant in HEKn cultured on 4 kPa dishes (Figure 4.19A). *LMNB1*, encoding Lamin B1, was observed to show a striking level of downregulation across all days within the time course and for each BM dish stiffness (Figure 4.19B). However, *SUN1* and *SUN2* were observed show no statistical difference in expression in response to a softer substrate, though

SUN2 did seem to trend towards downregulation on days 3 and 4 after seeding (Figure 4.20).

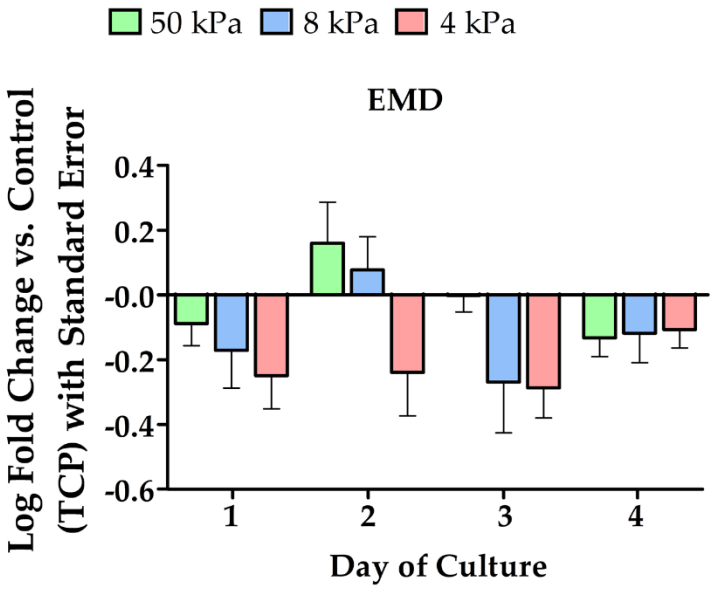

Figure 4.18 RNA analysis revealed no statistically significant change in emerin expression in HEKn cultured on BM hydrogels. *HEKn were cultured on TCP and 50, 8 and 4 kPa cultureware and RNA samples were harvested 1,2,3 and 4 days after seeding and analysed using WaferGen. Quantification of the Log fold change in emerin gene expression in HEKn on 50, 8 and 4 kPa hydrogels in comparison to the TCP control. Data represent mean ±SEM, n = 6, statistical significance was assessed using two-way ANOVA, no asterisk = non-significant.*

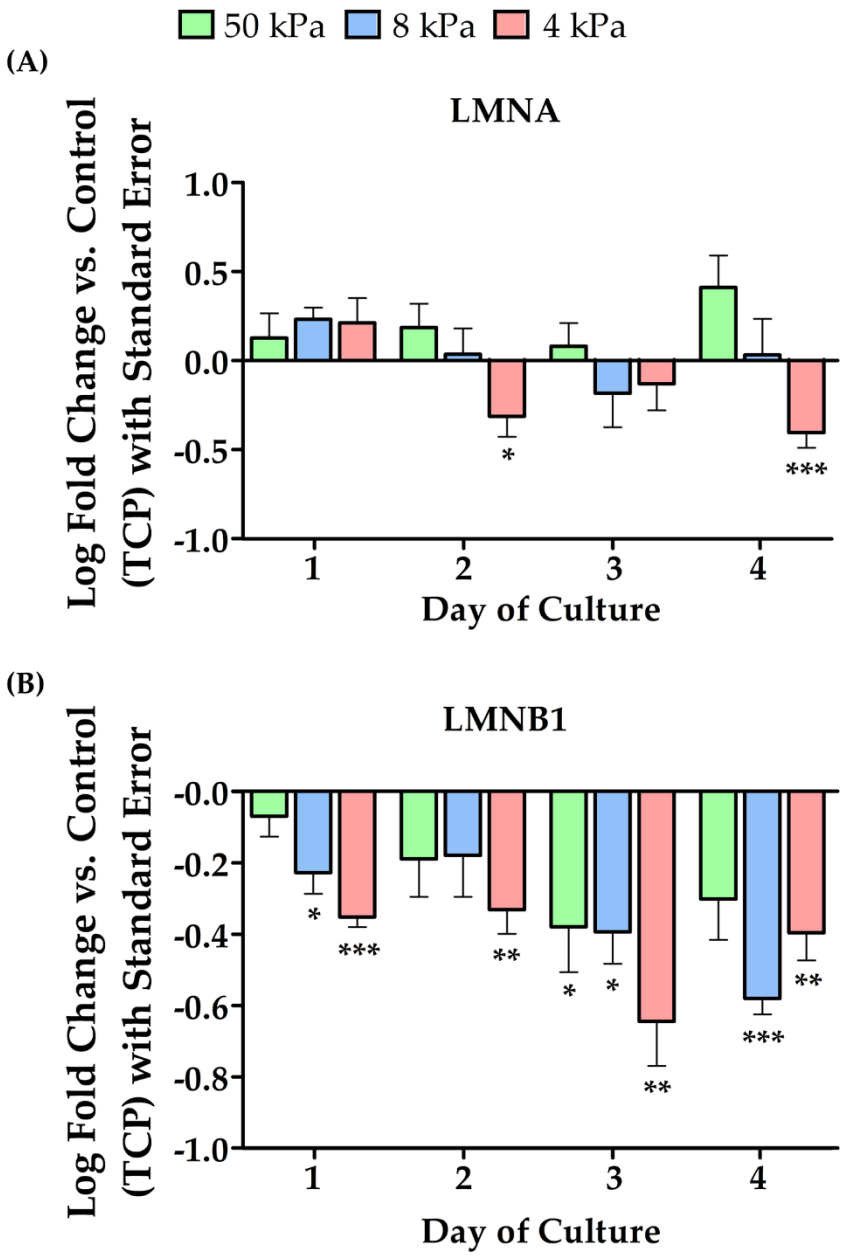

Figure 4.19 RNA analysis revealed significant downregulation of Lamins in HEKn cultured on BM hydrogels. *HEKn were cultured on TCP and 50, 8 and 4 kPa cultureware and RNA samples were harvested 1,2,3 and 4 days after seeding and analysed using WaferGen.* **(A-B)** *Quantification of the Log fold change in Lamin A/C and Lamin B1 gene expression in HEKn on 50, 8 and 4 kPa hydrogels in comparison to the TCP control. Data represent mean ±SEM, n = 6, statistical significance was assessed using two-way ANOVA, no asterisk = non-significant, * $p \leq 0.05$, ** $p \leq 0.01$, *** $p \leq 0.001$.*

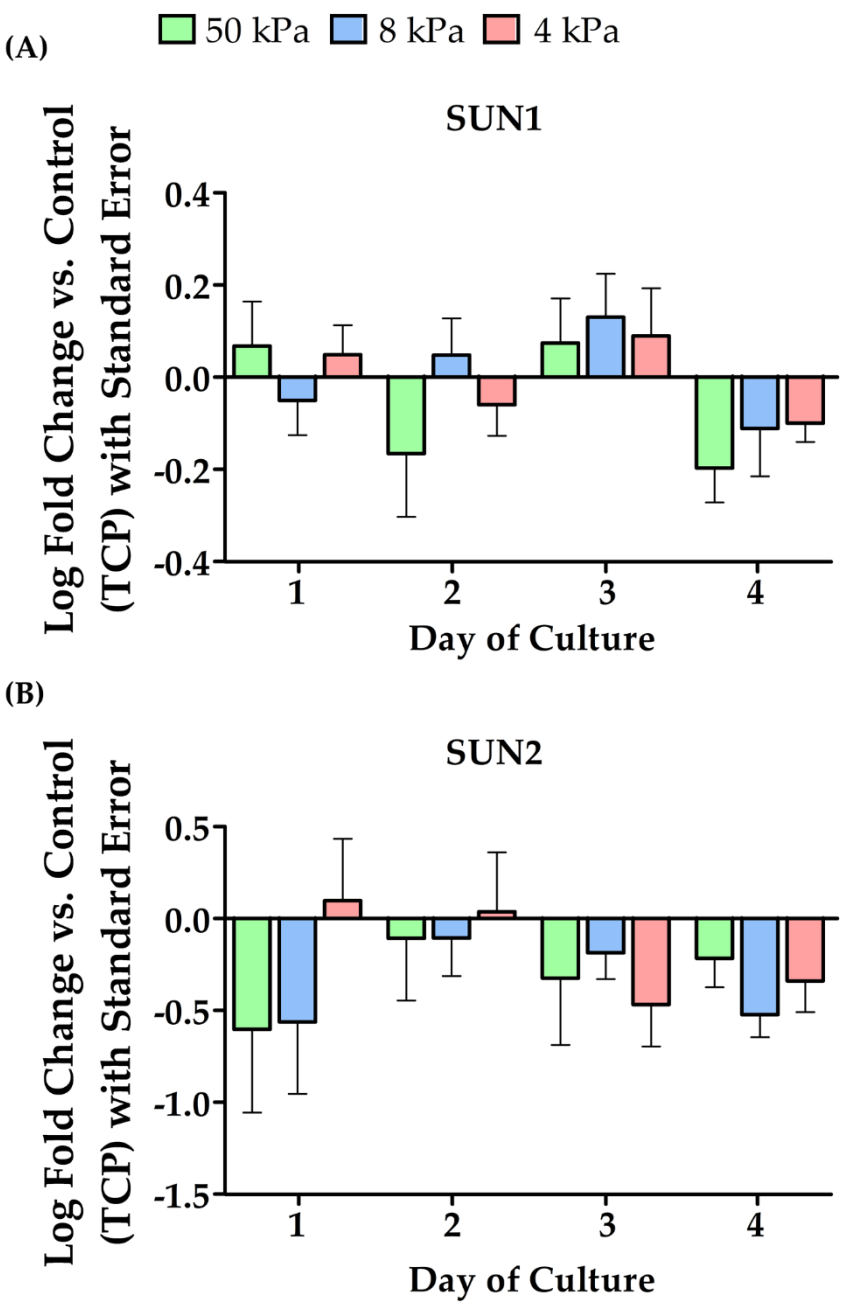

Figure 4.20 RNA analysis revealed no statistically significant changes in SUN1 and SUN2 expression in HEKn cultured on BM hydrogels. *HEKn were cultured on TCP and 50, 8 and 4 kPa cultureware and RNA samples were harvested 1,2,3 and 4 days after seeding and analysed using WaferGen.* **(A-B)** *Quantification of the Log fold change in SUN1 and SUN2 gene expression in HEKn on 50, 8 and 4 kPa hydrogels in comparison to the TCP control. Data represent mean ±SEM, n = 6, statistical significance was assessed using two-way ANOVA, no asterisk = non-significant.*

The next set of proteins examined through RNA analysis were nesprins, encoded by *SYNE* genes. *SYNE1* was observed to be significantly downregulated on BM dishes compared to TCP on days 3 and 4 after seeding (Figure 4.21A), whilst *SYNE2* showed a significant downregulation on day 1, and a significant upregulation on day 4 (Figure 4.21B). Nesprin-3 was included in the WaferGen analysis and *SYNE3* was observed to be significantly downregulated on soft substrates compared to TCP (Figure 4.21C).

The final RNA analysis carried out for this section of the project targeted nuclear pore complex (NPC) genes in order to both assess whether those associated with LINC components were affected, and to investigate whether NE proteins not traditionally associated with mechanosensation were impacted by a change in substrate stiffness. *NUP62* plays a role in mitotic cell cycle progression by regulating centrosome segregation, centriole maturation and spindle orientation (Hashizume et al., 2013), and was observed to be increasingly downregulated the softer the BM hydrogel HEKn were cultured on (Figure 4.22A). *NUP107* is a core NPC component and plays a role in NPC assembly and mRNA export (Shi et al., 2020), and was observed to be significantly downregulated compared to TCP on days 1 and 3 after seeding (Figure 4.22B). *NUP153* is an NPC component that binds SUN proteins (Donnaloja et al., 2019), and it too was observed to be downregulated in response to culturing HEKn on BM hydrogels (Figure 4.22C). Finally, *RANBP2* encodes nucleoporin 358 which is a critical component of NPC involved in the shuttling of proteins between the nucleus and cytoplasm (Wälde et al., 2011), whilst *NDC1* plays a key role in the de novo

Figure 4.21 (overleaf) RNA analysis revealed significant changes in nesprin expression in HEKn cultured on BM hydrogels. *HEKn were cultured on TCP and 50, 8 and 4 kPa cultureware and RNA samples were harvested 1,2,3 and 4 days after seeding and analysed using WaferGen.* **(A-C)** *Quantification of the Log fold change in SYNE1, SYNE2 and SYNE3 gene expression in HEKn on 50, 8 and 4 kPa hydrogels in comparison to the TCP control. Data represent mean ±SEM, n = 6, statistical significance was assessed using two-way ANOVA, no asterisk = non-significant, * $p \leq 0.05$, ** $p \leq 0.01$, *** $p \leq 0.001$.*

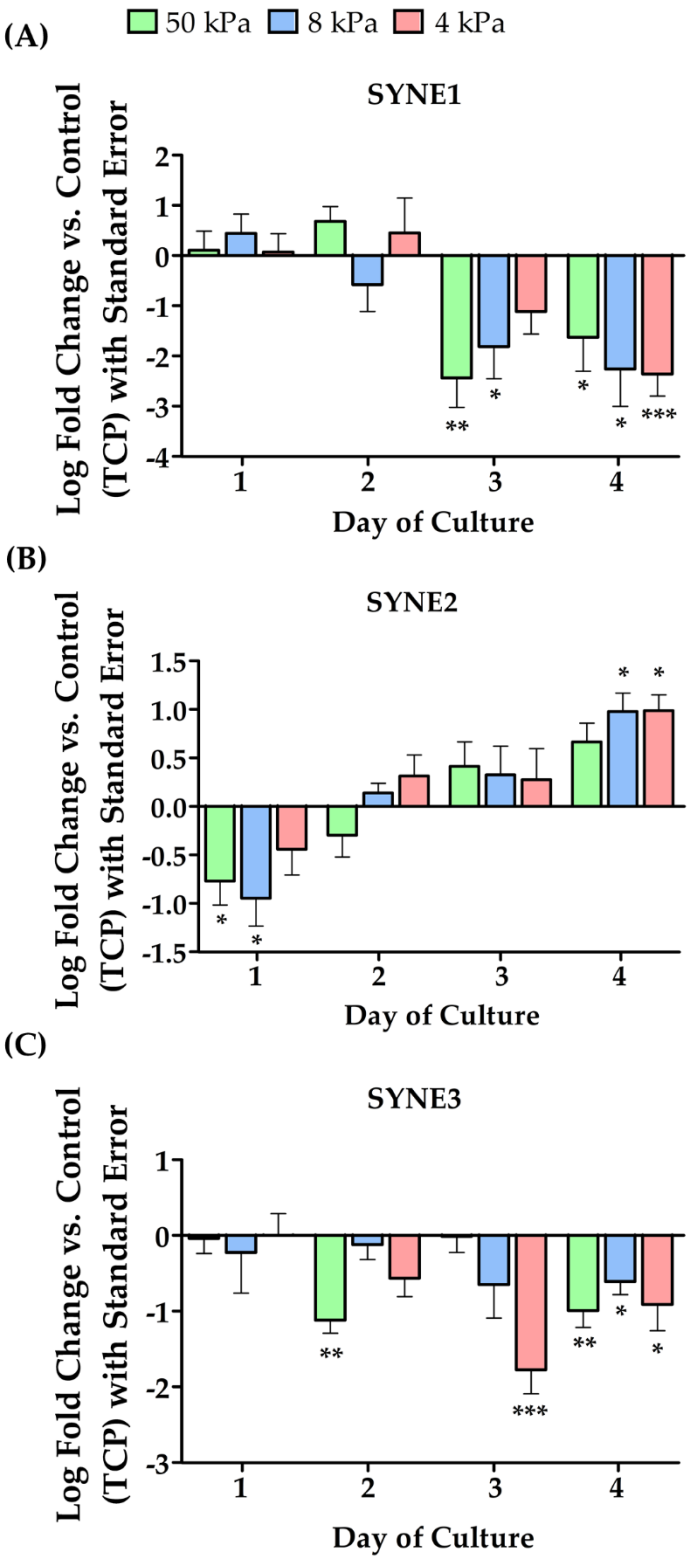

assembly of NPCs and their insertion into the NE (Mansfeld et al., 2006). Both proteins showed less distinct changes in gene expression in response to substrate stiffness, though *RANBP2* was significantly upregulated on day

1 on 50 kPa dishes, and on day 4 on 4 kPa dishes (Figure 4.22D). Moreover, *NDC1* generally trended towards downregulation across the 4-day time course, with a significant downregulation on 4 kPa dishes on day 2, and 50 kPa dishes on day 3 (Figure 4.22E).

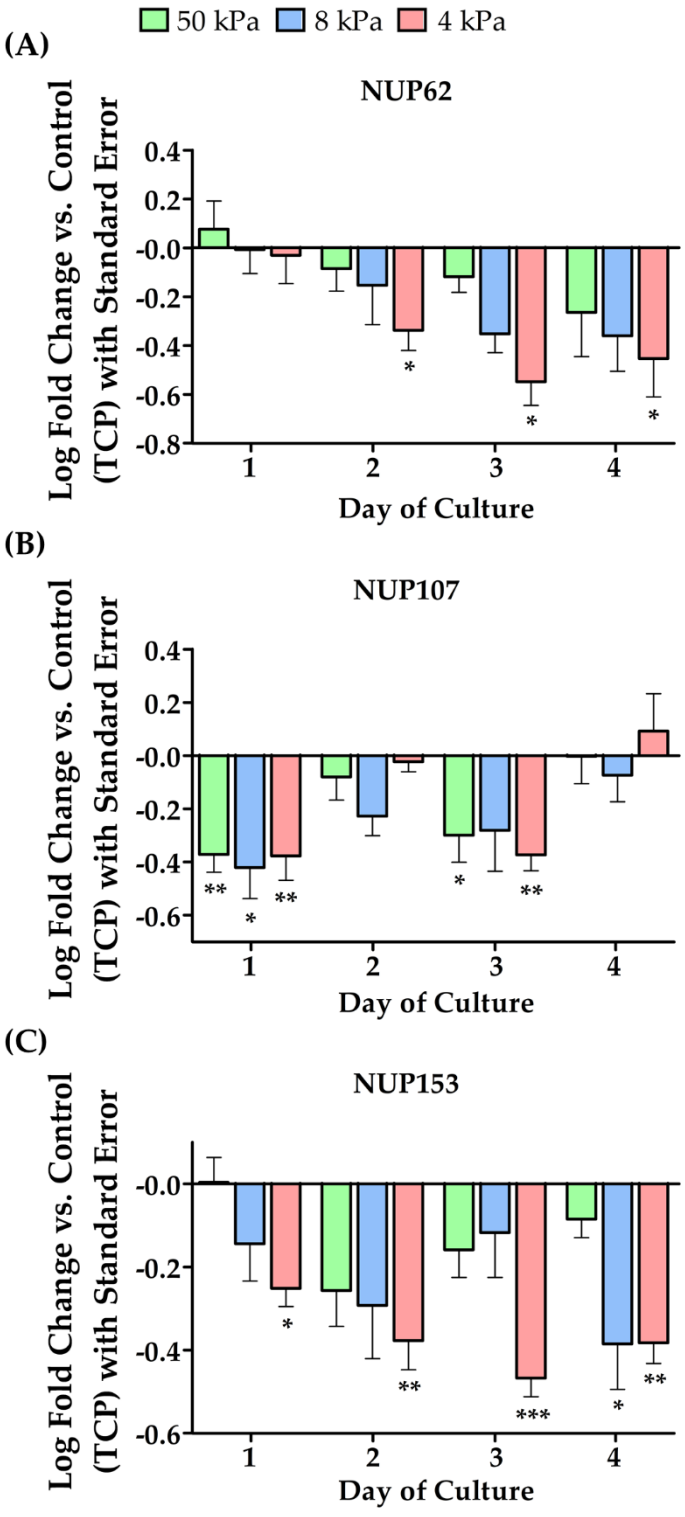

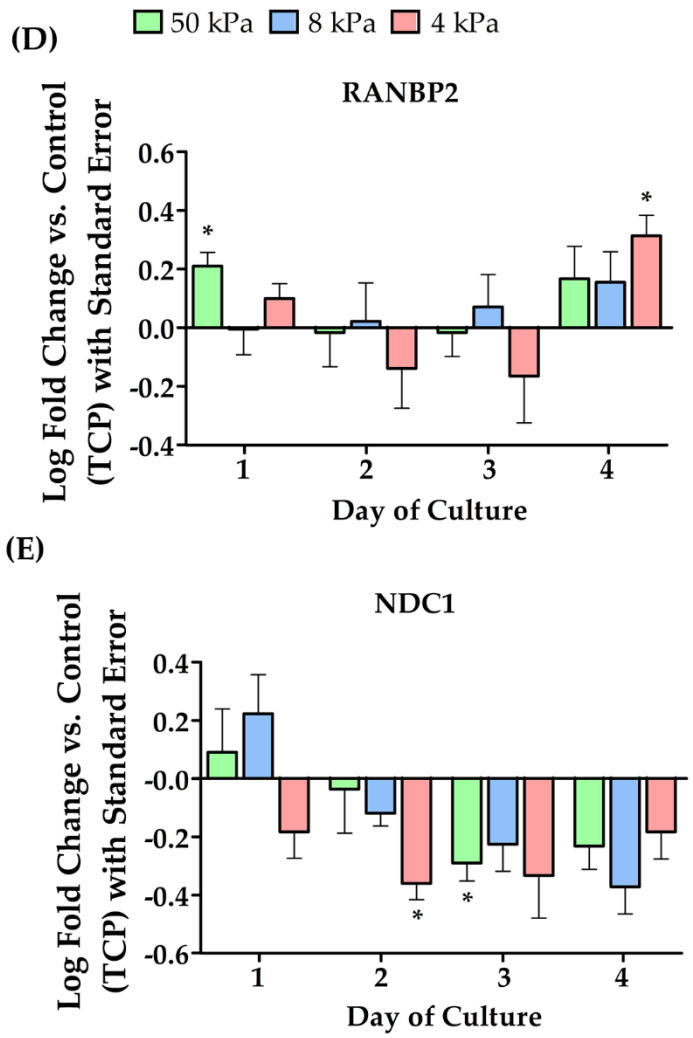

Figure 4.22 RNA analysis revealed significant changes in the expression of NPC components in HEKn cultured on BM hydrogels. *HEKn were cultured on TCP and 50, 8 and 4 kPa cultureware and RNA samples were harvested 1,2,3 and 4 days after seeding and analysed using WaferGen.* **(A-E)** *Quantification of the Log fold change in NPC protein gene expression in HEKn on 50, 8 and 4 kPa hydrogels in comparison to the TCP control. Data represent mean ±SEM, n = 6, statistical significance was assessed using two-way ANOVA, no asterisk = non-significant, * $p \leq 0.05$, ** $p \leq 0.01$, *** $p \leq 0.001$.*

4.4.5 HEKn cultured on BM hydrogels were observed to be softer

4.4.5.1 HEKn on BM hydrogels exhibited greater nuclear deformation in response to osmotic shock

Following on from the analysis of cytoskeletal and LINC complex proteins in HEKn cultured on TCP versus BM hydrogel-coated dishes, it was hypothesised that cells on

softer substrates might have softer nuclei as a result of the decreased levels of Lamin proteins and redistribution of actin filaments. The initial experiment performed to assess this was an osmotic shock assay, in which HEKn were cultured on TCP and 4 kPa dishes for 4 days then transferred to glass coverslips and exposed to a high concentration sucrose solution before being fixed and stained for a NE marker (Lamin B1). The prediction was that HEKn cultured on 4 kPa BM dishes would have softer nuclei and therefore exhibit greater nuclear deformation in response to osmotic shock. This was quantified by counting the number of cells with visible nuclear abnormalities following osmotic shock, and the results confirmed that HEKn primed on the BM hydrogel dishes had a higher incidence of nuclear deformation than those on TCP (Figure 4.23), suggesting a softer nucleus.

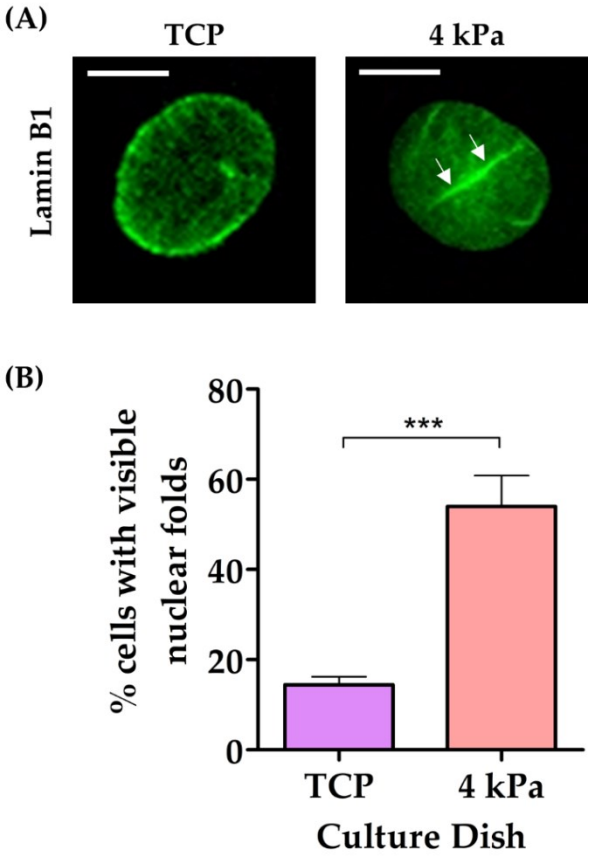

Figure 4.23 HEKn cultured on 4 kPa dishes exhibited more nuclear deformation following osmotic shock. (A) *HEKn were cultured on TCP or 4 kPa dishes then exposed to high concentrations of sucrose to induce osmotic shock and stained for the NE marker Lamin B1. Confocal microscopy images display the NE staining and visible abnormalities (white arrows).* **(B)** *Quantification of the number of cells with visible nuclear abnormalities. Data represent mean, n = 3 (3x 100 cells), statistical significance was assessed using a two-tailed unpaired t-test, *** $p \leq 0.001$.*

4.4.5.2 AFM analysis revealed HEKn cultured on 4 kPa hydrogels had softer nuclei and cytoplasm

Given that the results of the osmotic shock assay suggested that HEKn cultured on 4 kPa dishes had softer nuclei than those on TCP, the next step was to better quantify the stiffness of cells on each substrate. HEKn were cultured on TCP or 4 kPa dishes for 4 days then assessed through the use of an AFM to measure the Young's Modulus of cells primed on each substrate. The results of this experiment revealed that both the nucleus and the cytoplasm of HEKn cultured on 4 kPa for 4 days were softer than those on TCP (Figure 4.24).

Figure 4.24 (overleaf) HEKn cultured on 4 kPa hydrogels had a lower Young's Modulus than those on TCP. (A) *HEKn primed on TCP and 4 kPa were analysed using an AFM to measure the Young's Modulus of the entire cell. Heat maps display the different Young's Modulus values measured across a single keratinocyte primed on each substrate stiffness.* **(B)** *Quantification of Young's Modulus of the cytoplasm and nucleus. Data represent mean, n = 6 (6 cells, 10 Young's Modulus readings per cell compartment), statistical significance was assessed using one-way ANOVA, *** $p \leq 0.001$.*

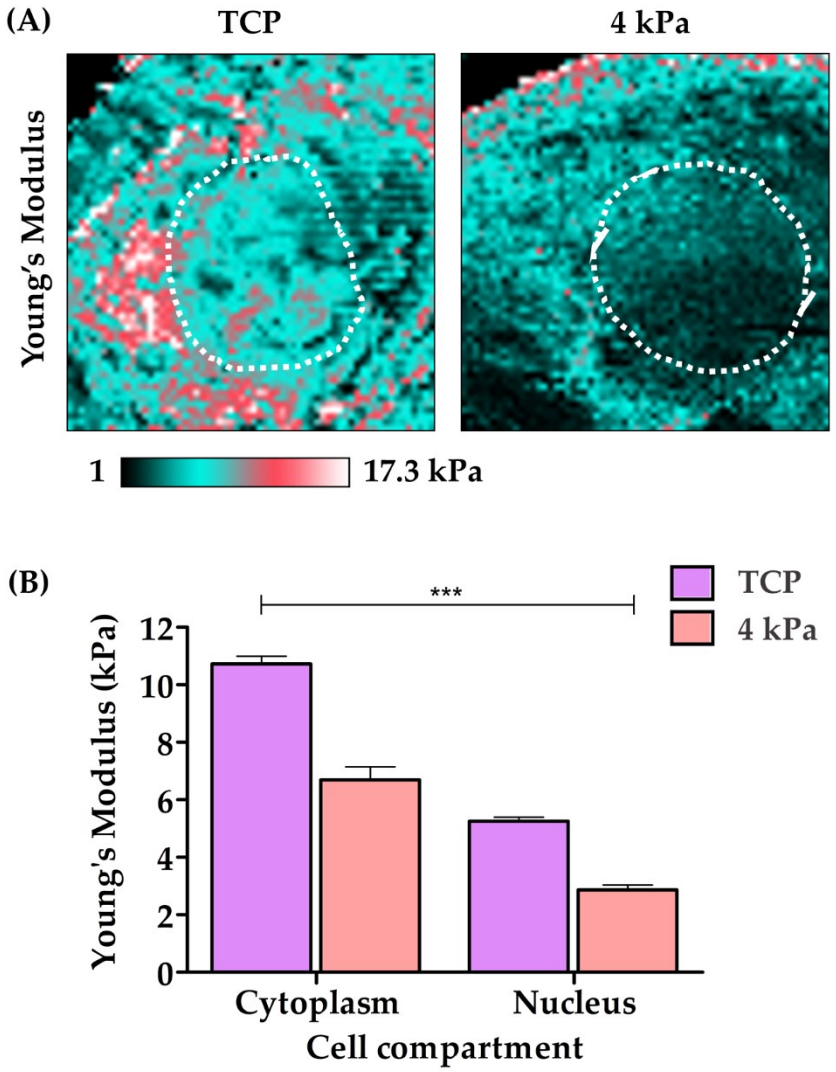

4.4.5.3 Keratinocyte differentiation induces changes in some LINC complex proteins

Chapter 3 largely explored the hypothesis that culturing HEKn on softer substrates pushes cells towards a more differentiated phenotype. Given the changes observed in LINC complex proteins in response to softer culture dishes, the final section of this chapter explores whether differentiation could account for these observations. HEKn were cultured under low and high calcium conditions to provide a sample of proliferative and differentiated cells and protein lysates were harvested before being assessed for changes in LINC complex protein levels through western blotting. CK10 was observed to be upregulated under high calcium conditions, confirming that cells were more differentiated (Figure 4.25). Emerin, Lamin A/C, Lamin B1, and SUN1 and SUN2 levels were all assessed, and it was observed that the most striking changes in

expression came from emerin which was upregulated following differentiation, and Lamin B1 which was downregulated (Figure 4.25). Lamin A/C and SUN1 did not appear to change between low and high calcium conditions, but SUN2 appeared to decrease slightly in response to differentiation (Figure 4.25).

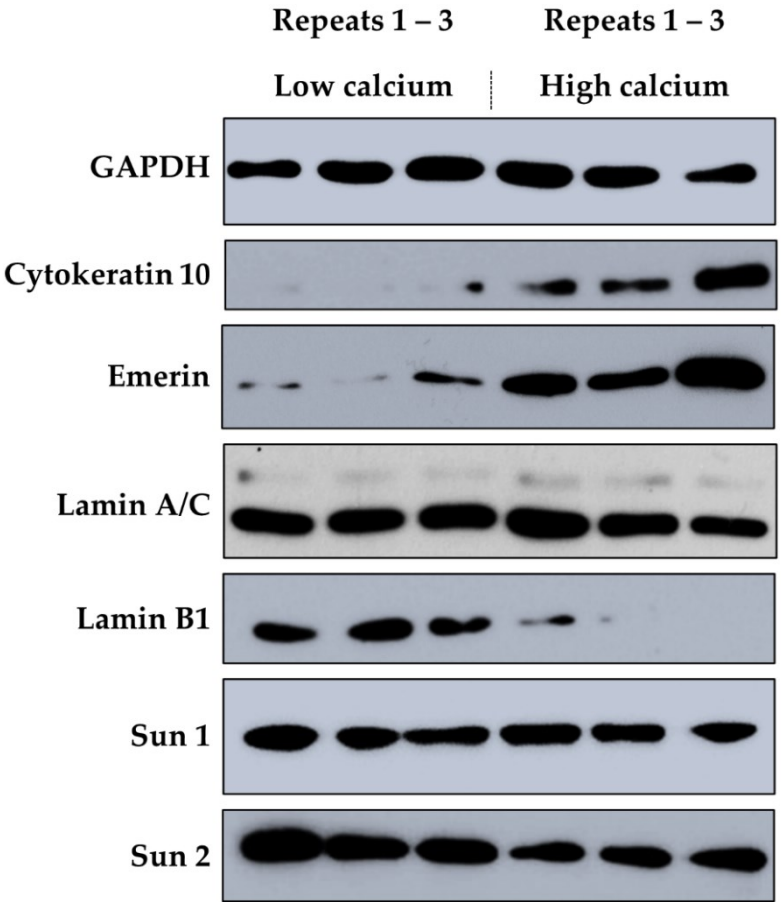

Figure 4.25 Differentiated HEKn exhibited changes in emerin and Lamin B1 levels. *Protein lysates were taken from HEKn cultured under low and high calcium conditions and protein levels were assessed through western blotting. CK10 was used as a control to confirm keratinocyte differentiation. Emerin was observed to be upregulated under high calcium conditions and Lamin B1 was downregulated. n = 3 representing 3 independent lysates and all repeats are presented.*

4.5 Discussion

In this chapter the objective was to delve deeper into the mechanism behind the responses observed in keratinocytes when cultured on TCP versus BM hydrogel-coated dishes. Given the role that cytoskeletal proteins play in mechanosensation, the first objective was to investigate whether keratinocytes cultured on hydrogels

exhibited changes in the expression and/or localisation of cytoskeletal and cytoskeletal-associated proteins (e.g., E-cadherin and plectin). Additionally, the LINC complex is known to play a significant role in mechanosensation and thus this chapter also aimed to explore how components of the LINC complex were affected in keratinocytes following exposure to softer culture dishes. With this assumption that keratinocytes were physically changing their internal mechanics in response to surface stiffness came the final objective to ascertain whether the Young's Modulus of the cells was altered in response to culture dish stiffness.

4.5.1 HaCaTs exhibited some changes in cytoskeletal protein levels in response to softer culture dishes

The first experiment carried out for this chapter was a western blot analysis of cytoskeletal components in HaCaTs. The cytoskeleton plays a significant role in mechanotransduction given the cell-spanning nature of the proteins that provide a direct link between the cell membrane and the nucleus. Cells use actin filaments and the associated myosin IIB protein to make small contractions at adhesion molecules that enable them to determine the level of resistance provided by binding partners (Moore, Roca-Cusachs and Sheetz, 2010; Yang et al., 2018). The role of microtubules in mechanosensing is less defined but evidence suggests that they facilitate the detection of cell-scale tension (Hamant et al., 2019) and regulate cytoskeletal stiffness and viscoelastic resistance (Coleman et al., 2021). The most prevalent intermediate filament type in keratinocytes are keratins, and keratin composition changes throughout the epidermal layers as the cells differentiate (Biggs et al., 2020). Crosstalk between keratins and the actin cytoskeleton plays a key part in mechanotransduction, with keratins reacting to mechanical strain by triggering the ROCK signalling pathway which prompts changes in actin organisation (Bordeleau et al., 2012).

Western blot analysis showed that levels of tubulin did not appear to change in response to culture on BM hydrogels (Figure 4.1A). Though the western blot appeared to suggest a reduced amount of β-actin when cultured on softer substrates, densitometry analysis revealed that there was no statistically significant difference across the dishes (Figure 4.1). Similarly, the western blot of pankeratin seemed to

show a reduced intensity for all bands in HaCaTs on BM hydrogels, but this was not fully reflected in the densitometry analysis where some bands did not show a significant change (Figure 4.1). In chapter 3 we explored the debate regarding whether statistical significance is always reflective of biological relevance. This largely centres around the fact that it has been shown that the *P*-value and the actual probability of a null hypothesis being true are often not aligned with one another and this disparity only increases as the sample size becomes larger (Berger and Sellke, 1987). Moreover, some would argue that the *P*-value is essentially an arbitrary value given that it can be made as small as one wants it to be by simply assuming the null hypothesis is actually false (the most likely scenario) and increasing the sample size (Johnson, 1999). This argument is further supported by the weight placed on the *P*-value being equal to or less than 0.05; in a situation where an experiment produces a *P*-value of 0.06 then the result would be written off as insignificant, but in the world of biology there is no evidence that this result does not still have biological relevance.

With this concept fresh in mind, it seems reckless to entirely disregard the apparent downregulation of β-actin and the highest keratin band (keratin 1/2) (Figure 4.1) given that the western blot shows a clear change in band intensity, and the densitometry graph shows distinct trends towards a lower level of protein in HaCaTs cultured on 8 and 4 kPa hydrogels. An additional consideration is that densitometry is not always an accurate measure of protein quantification. The western blots carried out on the HaCaT samples were copied onto film and scanned using a standard office scanner, which introduces the first potential pitfall; office scanners not only have a limited dynamic range, but they are programmed to achieve a factory set range of optical density outputs and therefore use an automatic gain control to alter the illumination and contrast of an image which could have implications on the band intensity that impacts the final analysis measurement (Gassmann et al., 2009). A 2019 study into whether quantification of western blotting can be misleading observed that it cannot be assumed that optical density data directly correlates to protein abundance and linear proportionality should not be assumed (Butler et al., 2019). Additionally, using high abundance proteins such as GAPDH as a loading control can cause problems as even at very low sample loading the signal intensity may show

saturation which can compromise calculations when normalising target protein optical density data to the housekeeping protein (Butler et al., 2019; Murphy and Lamb, 2013). Consequently, the western blot analyses discussed here should be viewed with a small measure of scepticism and used as a guide to recognise potential changes in protein level. However, to more accurately ascertain whether there is a linear change in protein level in response to culture on BM hydrogels, further work would need to be carried out using a more accurate experimental method such as mass spectrometry.

The final point to discuss regarding the analysis seen in Figure 4.1 is the apparently statistically significant reduction in some of the pankeratin bands following culture of HaCaTs on 8 and 4 kPa hydrogels. The main problem with using a pankeratin antibody for this analysis was that it was not possible to definitively confirm which keratins were observed in the western blot, and thus bands were labelled based on which keratins are known to have a molecular weight similar to the bands observed. The band labelled as keratin 10 was observed to decrease slightly in HaCaTs cultured on 4 kPa hydrogels (Figure 4.1E) which contradicts observations made in HEKn (chapter 3) which suggested that softer culture substrates led to increased differentiation marker expression. However, given the lack of proof that this band is indeed keratin 10, this result does not cause too much concern. Moreover, the column and error bar on the graph is comparable to that of the keratin 1/2 column that was deemed not significant following densitometry analysis (Figure 4.1D), and thus we must reacknowledge the potential unreliability of densitometry quantification. For the final two bands, labelled keratin 13/14 (Figure 4.1F) and keratin 15 (Figure 4.1G), the difference between the TCP column and the BM hydrogel columns is more striking, and again these proteins were observed to decrease on softer culture dishes. Keratin 14 is a major keratin in the epidermal basal layer and is a key protein contributing towards the structural integrity of the epidermis (Moll, Divo and Langbein, 2008), whilst keratin 15 is a marker of epidermal stem cells and is found exclusively in the basal layer (Bose et al., 2013).

If we assume that these bands were in fact keratin 14 and keratin 15, this result supports the previous evidence that softer substrates induce a shift away from a proliferative to a more differentiated phenotype. However, given that we cannot confirm which keratins are being captured in these analyses, we must conclude that, whilst the data show that culturing HaCaTs on softer substrates does have an impact on keratin levels, further analysis using specific keratin antibodies would need to be carried out in order to obtain the full picture.

4.5.2 HaCaTs cultured on hydrogel-coated dishes exhibited reduced protein levels of core LINC complex components

The next proteins investigated through western blotting in HaCaT samples were components of the LINC complex and associated proteins. The LINC complex is responsible for relaying mechanical information from the cytoskeleton to the nuclear Lamina, thus helping to regulate chromatin organisation in response to external mechanical cues (Cartwright and Karakesisoglou, 2014). In the epidermis, the LINC complex has been shown to play a role in controlling the shift towards terminal differentiation by relaying variable tension to the nuclear Lamina throughout the layers, and disruption of the LINC complex has been shown to result in precocious differentiation (Carley et al., 2020).

Emerin is a NE protein that anchors microtubules and the nuclear Lamina to the outer and inner nuclear membrane respectively. The western blot showed that the bands for emerin decreased dramatically in intensity in HaCaTs cultured on BM dishes (Figure 4.2A), and densitometry analysis confirmed that this was statistically significant for cells cultured on 4 kPa dishes compared to TCP (Figure 4.2B). In response to force, emerin becomes tyrosine phosphorylated and regulates nuclear rigidity following increased tension incurred through adhesion (Guilluy et al., 2014). Given that external tension is lower for cells cultured on hydrogel-coated dishes, we could hypothesise that emerin levels were downregulated as a result of a reduced need for emerin's role in regulating nuclear mechanics. However, the same study observed that a depletion in emerin actually increased nuclear rigidity (Guilluy et al., 2014); the AFM analysis of HEKn cultured on 4 kPa BM will be discussed in depth

later (4.5.8), but it was observed that culturing cells on hydrogel-coated dishes reduced nuclear stiffness in comparison to those on TCP (Figure 4.24). Consequently, whilst it is known that emerin has a significant role to play in regulating nuclear mechanics in response to external tension, further investigation would need to be carried out in order to explain why protein levels may be reduced in HaCaTs cultured on softer dishes. Moreover, the problems raised in 4.5.1 regarding the reliability and accuracy of densitometry analysis can also be applied here, and thus a more comprehensive quantitative analysis of emerin protein levels would be desirable for future investigation.

SUN1 and SUN2 make up one of the two protein domains that comprise the LINC complex, and bind nesprin proteins within the NE lumen, and the nuclear Lamina within the nucleus (Bouzid et al., 2019; Padmakumar et al., 2005). Western blot analysis of SUN1 and SUN2 in HaCaTs revealed that cells on softer dishes had reduced protein levels (Figure 4.2A) and this was found to be statistically significant following densitometry analysis (Figure 4.2C-D). Similarly, Lamin A/C and Lamin B1 were also observed to decrease in HaCaTs on 8 and 4 kPa dishes (Figure 4.2A), and densitometry analysis revealed that this was statistically significant for cells on 4 kPa hydrogels compared to TCP (Figure 4.2E).

The nuclear Lamina has been linked to the regulation of differentiation in the epidermis; at the basement membrane, engagement of integrins relays high tension to the nuclear Lamina, particularly Lamin A, and this in turn is associated with a more proliferative keratinocyte phenotype (Carley et al., 2020). A triple Lamin knockout mouse model (Lmna−/− Lmnb1Δ/Δ Lmnb2Δ/Δ) has been found to result in precocious epidermal differentiation (Jung et al., 2014). Moreover, in a 2013 study published by Swift et al. it was observed that Lamin A protein levels increased 30-fold from soft to stiff tissues, with Lamin B1 also increasing though to a much lesser extent (Swift et al., 2013). Consequently, the reduction in Lamin A/C and Lamin B1 protein levels observed in HaCaTs cultured on BM hydrogels can likely be attributed to the reduction in substrate stiffness which would relay less tension to the nuclear Lamina. In chapter 3 we explored whether culturing keratinocytes on soft hydrogels

promoted a shift from proliferation to differentiation, and though results were inconclusive, there was strong evidence to suggest that proliferative activity is reduced on softer substrates. The downregulation of nuclear Lamins witnessed in Figure 4.2 could potentially play a role in facilitating a shift towards a more differentiated phenotype as found in the epidermis.

However, the downregulation of SUN1 and SUN2 proteins is less readily explained by the literature. Swift et al. reported that overexpressing SUN2 led to rounding of the nucleus and decreased Lamin A levels (Swift et al., 2013) which would correlate with the decrease in Lamin A and softening of the nucleus observed in this study but contradicts the reduction in SUN2 exhibited in Figure 4.2. However, in a separate study by Rapisarda et al., specific analysis of epidermal keratinocytes revealed that the transcription factor p63 regulates NE-associated gene expression (Rapisarda et al., 2017). It was reported that in p63-/- mice, the log fold change between the knockout and wildtype following microarray analysis was 0.44 for SUN1 and 0.24 for SUN2 (Rapisarda et al., 2017). In chapter 3 it was observed that expression of the p63 gene was significantly downregulated in HEKn that had been cultured on 50, 8 and 4 kPa hydrogels for 4 days in comparison to those on TCP. Consequently, the reduced SUN1 and SUN2 protein levels observed in HaCaTs cultured on BM dishes (Figure 4.2) could be attributed to a potential shift away from a highly proliferative phenotype.

Finally, as a closing remark regarding the HaCaT western blot analysis it is worth reiterating the caveats that stem from working with HaCaTs that were highlighted in section 3.1.5. The primary concern surrounding HaCaT culture is the requirement for additional FBS supplementation in the medium which induces a partially differentiated phenotype, making it difficult to fully explore the concept of epidermal homeostasis when assessing HaCaT data (Wilson, 2013). Moreover, the gene transcription profile of HaCaTs is well documented to be different to that of primary keratinocytes (Seo et al., 2012). Consequently, whilst the western blot data discussed here and in section 4.5.1 serve to highlight that BM hydrogels did have an impact on

cytoskeletal and LINC complex proteins, a more in-depth exploration of these proteins was reserved for the primary keratinocyte samples.

4.5.3 Exploration of Hippo pathway protein levels met with complications

As discussed in chapter 3, a key mechanosensitive pathway in the epidermis is the Hippo signalling pathway which relies on mechanical cues to steer keratinocytes towards either proliferation or differentiation (Rognoni and Walko, 2019). In chapter 3 we observed that YAP1 localisation was altered in HEKn cultured on 4 kPa hydrogels (Figure 3.17), and the gene expression of several Hippo pathway components changed in response to a softer substrate (Figure 3.18). In this chapter we aimed to delve a little deeper into the Hippo pathway at a protein level, with the focus being on key effector YAP1 and the upstream regulator KIBRA, which was of additional interest due to its being previously observed to bind to the KASH domain of nesprin-2 (Karakesisoglou et al.). However, a number of technical problems and unexpected results meant that this avenue of investigation was set aside relatively early on in the project.

The first problem encountered was finding YAP1 and KIBRA antibodies that would work for western blotting. Several YAP1 antibodies were tested including the one that provided promising immunofluorescence results in chapter 3, but they consistently provided either no signal or a band that was significantly heavier than the molecular weight of YAP1 (55 kDa). Assessment of YAP1 isoforms in the literature confirmed that none were the weight observed in the western blots produced (Figure 4.3). Similarly, the hypothesis that the band observed might be a protein dimer was ruled out as it was too light. It is well established that western blotting is a technique rife with errors that require troubleshooting, and bands appearing at a higher molecular weight than expected can be due to artifacts such as protein-protein interactions, antibody cross-reactivity, and post-translational modifications such as glycosylation (Bio-rad, 2021). Attempts at troubleshooting the problem did not yield any improvement and ultimately it was decided that the value of the result did not justify the time that would be required to obtain a working western blot, particularly when WaferGen data for the gene was available.

Following this decision, attention was shifted to KIBRA and western blot and immunofluorescence was carried out using a variety of antibodies. KIBRA has a predicted molecular weight of 125 kDa but western blot analysis of HaCaTs presented with no bands at all for the Abcam (ab107637) and Sigma-Aldrich (HPA038016) antibodies tested, and bands that were much too light using the Santa Cruz (SC-133374) antibody. In order to determine whether these bands represented non-specific artifacts or a genuine result, the blot was repeated using positive controls. KIBRA, as per its name, is highly expressed in kidney and brain tissue and so lysates for CD1 mouse brain and undifferentiated and differentiated mouse neuronal cell lines CAD and NSC-34 were run alongside HaCaTs (Figure 4.4). It was observed that in the differentiated cell lines, a band correlating to full length KIBRA was present, whilst further lighter bands correlating to isoform 4 and isoform 5 were also found. Isoform 5 was observed in the 100% confluent HaCaT sample but not the 25% confluent sample. A lower band was witnessed in both HaCaT samples that did not correlate to any known KIBRA isoforms which raised questions regarding the validity of this band. Given that this band had not been observed in any previous KIBRA blots on HaCaT samples, and as it was absent in the positive control samples, it was deemed non-specific and subsequently ignored.

However, the presence of a band correlating with the small KIBRA isoform in HaCaTs was a potentially exciting result. In a study by Kremerskothen et al., a Northern blot was used to assess the mRNA of KIBRA in multiple adult human tissues (not including skin), the results of which suggested that the expression of different KIBRA isoforms may be tissue dependent; heart was observed to possess a band for mRNA half the size of full-length KIBRA mRNA (Kremerskothen et al., 2003). Consequently, this study supports the validity of the smaller KIBRA isoform witnessed in HaCaTs and suggests that potentially KIBRA plays an alternative role in keratinocytes than it does in other tissues.

This hypothesis was further strengthened following immunofluorescence analysis of KIBRA in HEKn. In the same study previously referenced, Kremerskothen et al. used a Myc-KIBRA construct to analyse the expression and subcellular localization of

KIBRA in green monkey kidney cells (Kremerskothen et al., 2003). Professor Kremerskothen kindly donated a sample of this Myc-KIBRA construct to support this project and it was subsequently transfected into COS-7 cells, chosen due to their being derived from African green monkey kidney tissue thus making them an appropriate positive control. Immunofluorescence analysis of these transfected cells revealed that the Abcam and Santa Cruz antibodies were non-specific and therefore unsuitable for further analysis. However, the Sigma-Aldrich antibody (HPA038016) was observed to bind specifically to the Myc-KIBRA construct in COS-7 cells (Figure 4.5A) and this was therefore chosen for subsequent immunofluorescence analysis in HEKn.

Localisation of Myc-KIBRA was observed to be diffuse throughout the cytoplasm in COS-7 cells with some stronger staining at the cell periphery, particularly in the processes extending out from the main cell body (Figure 4.5A). This is somewhat consistent with the literature where KIBRA has been reported to be found in the cytoplasm, more specifically co-localising with actin, tubulin, and at the lamellipodia of a cell's leading edge (Duning et al., 2008). However, in HEKn the antibody was found to bind with high specificity to a localisation that appeared to correlate with the Golgi apparatus. A co-stain of anti-KIBRA and anti-GM130 (a component of the Golgi peripheral membrane) confirmed that in HEKn, KIBRA was found to be located in the Golgi. The literature has little information to explain this observation, with the majority of published studies focusing on brain and kidney tissue, or the role that KIBRA plays in regulating the Hippo pathway in epithelial cells. The combined results regarding KIBRA expression in HaCaTs and HEKn suggested that the role for KIBRA in the epidermis is potentially tissue specific and more complex than initially anticipated. Given the already broad scope of the planned project it was deemed too time consuming to pursue investigation into KIBRA any further. However, the implications of this initial work are exciting and certainly warrant further investigation in the future with a more specific project focus on the role of KIBRA in the epidermis and its potential relationship to nesprin-2 and the LINC complex as a whole.

4.5.4 HEKn cultured on softer substrates exhibited changes in cytoskeletal and cytoskeletal associated protein levels and organisation

Once it had been ascertained that HaCaTs exhibited some changes in mechanosensitive protein levels, the investigation switched focus to HEKn which were the cells of primary interest for this project. As with the HaCaTs, experiments began with western blot analysis of HEKn lysates taken from cells cultured on TCP and BM hydrogel-coated dishes (50, 8 and 4 kPa). Levels of β-actin were observed to decrease slightly on softer substrates, particularly in HEKn cultured on 4 kPa hydrogels (Figure 4.6A) and this was observed to be statistically significant (Figure 4.6B). Additional blots were carried out on tubulin and E-cadherin but neither of these were observed to change levels in response to substrate stiffness (Figure 4.6A, C D). Whilst in HaCaTs the downregulation of β-actin was not observed to be significant (Figure 4.1B), there was a trend towards reduced protein levels on softer substrates that was noticeable in the blot itself. Consequently, both the HaCaT and HEKn results suggested that keratinocytes reduced their actin levels in response to a softer substrate.

Whilst there is little information in the literature regarding actin downregulation in response to ECM stiffness, it is well established that ECM mechanics influence actin organisation. This is largely due to the different adhesion that takes place; on rigid surfaces cells are spread out and possess large focal adhesions that tend to be uniformly orientated, whilst on soft substrates cells are rounder and possess numerous radially orientated adhesions that are much smaller (Prager-Khoutorsky et al., 2011). Given that the actin skeleton is bound to focal adhesion molecules, it is logical that changes in adhesion distribution and size would impact the organisation of the actin cytoskeleton. In a study by Gupta et al., it was observed that rat embryonic fibroblasts cultured on soft substrates (9 nM μm^{-1}) did not form bundles of actin stress fibres and had more fluid like rheological properties. However, on a stiff substrate (85 nM μm^{-1}) well developed stress fibres were observed which increased overall matrix stiffness and altered the rheology of the actin cytoskeleton to a more solid state (Gupta et al., 2015).

In keratinocytes, actin reorganisation is associated with a shift towards terminal differentiation, which in the epidermis also correlates to a migration of cells away from the stiff basement membrane into a less rigid mechanical environment (Biggs et al., 2020). Epidermal stem cells cultured *in vitro* are found to exhibit short actin bundles located radially, whilst keratinocytes that have undergone terminal differentiation present with a well-developed circumferential actin network (Nanba et al., 2013). Immunofluorescence analysis of F-actin in HEKn cultured on glass and 4 kPa coverslips revealed a difference in actin organisation, with those on glass exhibiting noticeably more stress fibre-like bundles in comparison to those on 4 kPa hydrogels (Figure 4.7A). Quantification of this confirmed that significantly more HEKn on glass exhibited basal stress fibre structures which correlated with the available literature (Figure 4.7B). This change in actin organisation could also explain the reduced protein levels observed (Figure 4.6), as HEKn cultured on 4 kPa hydrogel-coated coverslips were not assembling stress fibres and therefore were unlikely to undergo as much actin polymerisation as those on glass.

Whilst tubulin did not appear to change in terms of protein level, immunofluorescence analysis was carried out to assess for changes in localisation in response to substrate stiffness. However, assessment of the cells following tubulin staining did not reveal any significant differences in microtubule morphology (Figure 4.8). As discussed in the introduction to this chapter, microtubules are not viewed as the most significant part of a cell's mechanosensing machinery and the mechanism by which microtubules facilitate mechanotransduction is still not fully understood. Additionally, microtubule reorganisation in the epidermis is strongly linked to keratinocyte differentiation but not necessarily to mechanical changes in the different layers. Whilst chapter 3 explored the idea that HEKn may begin to differentiate following culture on 4 kPa hydrogels, results were far from conclusive and certainly did not suggest terminal differentiation. Therefore, given that we do not fully understand the relationship between substrate stiffness and microtubule organisation it could be that differentiation rather than ECM stiffness is the biggest driver of microtubule reorganisation *in vivo*.

Plectin is a large protein that connects intermediate filaments to microtubules, and anchors intermediate filaments to hemidesmosomes and desmosomes which is essential for firm basal layer attachment (Castañón et al., 2013). Immunofluorescence analysis of plectin in HEKn cultured on glass and 4 kPa coverslips revealed that those on softer coverslips presented with strong perinuclear plectin staining that was much less apparent on glass (Figure 4.9A). Quantification of this observation confirmed that perinuclear plectin was significantly more prevalent in HEKn cultured on 4 kPa coverslips (Figure 4.9B). Plectin has been shown to play a role in regulating nuclear morphology in keratinocytes (Almeida et al., 2015), and protects against nuclear deformation by binding keratin 14 to form a perinuclear network which limits nuclear movement (Bouameur et al., 2014; Castañón et al., 2013).

As will be further discussed later in this chapter, the osmotic shock assay (Figure 4.23) and AFM analysis (Figure 4.24) of HEKn cultured on TCP versus 4 kPa dishes suggested that the nuclei of cells on BM hydrogel-coated dishes were significantly softer and more vulnerable to deformation. HEKn cultured on softer substrates were observed to have greater colony density (Figure 3.11) which suggested tighter cell-cell interactions and better epithelial sheet formation. Whilst there do not appear to be any published studies discussing a direct relationship between colony density in keratinocytes and mechanical pressure on nuclei, there is reported evidence that monolayer polarisation gradients induce mechanical stress within cells during epithelial expansion (Banerjee, Utuje and Marchetti, 2015). As a result, it is possible that the perinuclear plectin observed in HEKn on 4 kPa coverslips may be attributed to increased mechanical stress transmitted through cell-cell adhesion molecules and a resulting need for recruitment of a stable keratin network to protect the nucleus. However, this theory contradicts the lower Young's Modulus readings taken from above the nucleus during the AFM analysis, and thus further investigation into keratin localisation would be required in order to explore this hypothesis. A final consideration here is that the perinuclear plectin may not have been a result of a change in protein localisation at all, but rather reflected the unmasking of an epitope as a result of cytoskeletal reorganisation. Epitope masking as a result of cross-linking between adjacent proteins is a common methodological problem that arises during

the fixation step when formaldehyde is used (Scalia et al., 2016). Given the changes to actin organisation and keratin expression observed in HEKn on soft dishes, it is clear that significant changes were occurring to the cytoskeleton in response to a softer mechanical environment. As such, it is possible that on the glass coverslips keratins may have been crosslinked to perinuclear plectin, thus preventing the plectin antibody from binding to the epitope. However, upon moving to the softer coverslips, changes to keratin expression may have resulted in the epitope being unmasked and thus perinuclear plectin appearing in immunofluorescence images. In order to rule out epitope masking, it would be necessary to repeat the immunofluorescence using alternative fixatives such as methanol or acetone to limit the possibility of protein cross-linking.

The final protein assessed via immunofluorescence for this section was E-cadherin, the adhesion molecule that plays a vital role in epidermal barrier formation. As referenced above, HEKn cultured on softer dishes were observed to have increased colony density (Figure 3.11) which could not be attributed to increased levels of E-cadherin protein (Figure 4.6D) but was hypothesised to be associated with a change in E-cadherin localisation. This was confirmed through immunofluorescence analysis which revealed that HEKn cultured on glass coverslips presented with large amounts of punctate E-cadherin staining, whilst those on 4 kPa coverslips exhibited more linear localisation along the membranes of adjacent cells (Figure 4.10A). Quantification of this staining confirmed that significantly more HEKn on 4 kPa coverslips exhibited linear staining than those on glass (Figure 4.10B). It appeared that HEKn cultured on glass coverslips were beginning to form trans-cadherin interactions, whilst those on 4 kPa coverslips were more closely bound to neighbouring cells, thus explaining the increased colony density on softer substrates. Moreover, E-cadherin-α/β-catenin complexes at adherens junctions are bound to actin filaments (Kobielak and Fuchs, 2004), and thus this increased concentration of E-cadherin at the extreme cell periphery may be associated with the increased cortical localisation of F-actin observed in HEKn on 4 kPa coverslips (Figure 4.7A). Additionally, the tighter cell-cell connections observed on hydrogels further supports

the hypothesis that the perinuclear plectin (Figure 4.9) is a protective mechanism against increased mechanical stress as a result of a more developed cell monolayer.

In addition to more linear staining, the final observation made from the E-cadherin immunofluorescence analysis was that HEKn on 4 kPa coverslips exhibited a large amount of perinuclear localisation that was strikingly almost entirely absent from those on glass (Figure 4.11). There is little information in the literature to explain this observation, with perinuclear or nuclear E-cadherin staining largely being associated with numerous neoplasms (Lobo et al., 2019). However, a recent study into the effects of mechanical strain on epithelial cell monolayers observed a similar E-cadherin staining pattern in Caco2 cells but only in response to 5% strain (Daulagala et al., 2020). This contradicts the results of this project as one would expect the level of strain HEKn experienced on 4 kPa coverslips to be less than they would on glass. A much older study reported perinuclear E-cadherin staining co-localising with Ras-associated protein-1 (Rap1) (Balzac et al., 2005), a small GTPase involved in a number of signalling pathways including those regulating proliferation and cytoskeletal dynamics (Yi-Lei Zhang et al., 2016). The study reported that Rap1 plays a critical role in the formation of integrin-based adhesive structures, with internalisation of E-cadherin by endocytosis triggering Rap1 activation in a process recognised to be necessary for integrin adhesion molecule assembly (Balzac et al., 2005). Whilst these results are interesting, they again contradict the observations made in this project as numerous results suggest that culturing HEKn on softer substrates moves them away from a proliferative basal cell phenotype and thus one would expect integrin expression to be downregulated as was observed in Figure 3.21.

With a deficit of supporting literature, there is clearly no biological answer readily available for the observed perinuclear E-cadherin staining in HEKn on 4 kPa coverslips. This therefore raises the question as to whether it may be the consequence of technical issues with the immunofluorescence technique rather than an actual result. As discussed for plectin, this phenomenon could be linked to epitope masking on glass coverslips which was lost following reorganisation of cytoskeletal components in response to the softer mechanical environment of the BM coverslips.

However, given the unlikelihood of any E-cadherin being localised to the perinuclear region in keratinocytes, shown by the absence of supportive literature, epitope masking also does not seem to explain this observation. Instead, it is possible that the staining is the result of non-specific antibody binding, either to alternative E-cadherin isoforms or degradation products, or to alternative cadherins. The immunogen used to generate the antibody utilised in this study is proprietary to the company meaning it is not possible to cross-check the epitope with all E-cadherin isoforms and other cadherins. In order to rule out non-specific staining, it would be necessary to repeat the immunofluorescence with an alternative E-cadherin antibody, ideally one for which the epitope has been mapped.

4.5.5 HEKn cultured on BM hydrogels exhibited gene expression changes in cytoskeletal and cytoskeletal-associated proteins

Following on from the protein analysis, which made it clear that softer culture substrates had an impact on the cytoskeleton and associated proteins, the next step was to investigate further at a gene expression level. This was done though the WaferGen analysis first discussed in chapter 3 and offered the opportunity for a more in-depth assessment of how HEKn responded to culture on hydrogel-coated dishes. Western blot analysis of β-actin had revealed a decrease in protein levels on softer dishes (Figure 4.6), and immunofluorescence showed that HEKn on 4 kPa dishes had significantly fewer basal stress fibres than those on TCP (Figure 4.7). WaferGen analysis revealed a clear trend towards downregulation of *ACTB* across all 4 days after cells were seeded on a softer dish, with some statistically significant changes noted on days 1 and 4 (Figure 4.12A). Additionally, the *VCL* gene which encodes vinculin, which helps to anchor actin filaments to the cell membrane via cell adhesion molecules (Martino et al., 2018), was observed to be significantly downregulated on softer dishes from 2 days after seeding (Figure 4.12B). *CDC42* which encodes the key actin regulator Cdc42 showed less conclusive expression changes, appearing to fluctuate between upregulation and downregulation across the days following seeding (Figure 4.12C).

This trend towards downregulation in β-actin expression fits with the observed changes in protein levels and could be due to the fact that HEKn cultured on softer substrates do not have such a high demand for actin polymerisation due to reduced stress fibre formation. Additionally, the striking amount of vinculin downregulation observed could be linked to the fact that HEKn cultured on BM dishes move away from a basal cell phenotype and exhibit a downregulation in integrin expression (Figure 3.21). As vinculin anchors actin to both integrins and E-cadherin, this downregulation in focal adhesions would logically reduce the amount of vinculin required by the cell. Moreover, the shift towards cortical actin organisation (Figure 4.7) and more liner E-cadherin staining (Figure 4.10) suggests a reorganisation of adherens junctions that may have an impact on vinculin expression. However, the changes observed in E-cadherin require further investigation, and thus these changes to vinculin would also benefit from a better understanding of how adhesion molecules are changing in HEKn cultured on softer substrates. In addition, the changes in *CDC42* expression provided no clear picture as to how BM dishes affected its expression. However, given its connection to actin dynamics, cell adhesion and filopodia formation (Kühn et al., 2015), it would be interesting to carry out further investigation using HEKn that have been exposed to a softer substrate beyond the 4 days captured in this experiment to see whether a clearer pattern emerged.

The next set of genes investigated were *TUBB* (tubulin), *PLEC* (plectin) and *KIF5B* (kinesin-1 heavy chain). Tubulin did not present with any clear changes at a protein level but was significantly downregulated in HEKn on softer dishes from as early as 1 day after seeding (Figure 4.13A). The role of microtubules in mechanosensation is not fully understood, though evidence suggests that they may control cytoskeletal stiffness in response to external mechanics through a currently unknown mechanism (Kerr et al., 2015; Robison et al., 2016; Coleman et al., 2021). Consequently, this downregulation could be a result of reduced strain on the cells cultured on BM hydrogels and thus a lower requirement for microtubules to provide viscoelastic resistance. Moreover, in chapter 3 it was shown that HEKn on softer dishes have reduced proliferative activity and therefore the reduced tubulin expression could be a result of a lower rate of cell division. Whilst an interesting result, this observation

requires further investigation to better understand what is taking place, in particular whether the downregulation at a gene level is reflected at a protein level in HEKn cultured on BM hydrogels for longer than 4 days.

In contrast to *TUBB*, the *PLEC* and *KIF5B* genes showed less definitive changes in response to softer substrates. Plectin was observed to trend towards downregulation on days 2 and 3 after seeding then increased on day 4 though with no statistical significance throughout (Figure 4.13B). *KIF5B* showed a trend towards downregulation on days 1 to 3, again not significant, then was upregulated on day 4 which was statistically significant for HEKn on 4 kPa hydrogels (Figure 4.13C). We previously discussed the hypothesis that the perinuclear plectin observed in HEKn on 4 kPa dishes could be due to the increased external pressure caused by denser colonies and thus a requirement for greater nuclear protection. Following on from this it could be proposed that the initial downregulation in plectin was due to the early reduction in strain that cells presumably encounter when transitioning from a stiff to a soft substrate. However, by day 4 colonies were well developed and thus the increased mechanical pressure of neighbouring cells may have driven an increase in plectin expression. In order to fully understand the changes to plectin in response to substrate stiffness, significant further investigation would be required. Kinesin-1 heavy chain connects nesprin-2 to microtubules and is important for nuclear migration and polarity (Zhu, Antoku and Gundersen, 2017). The trend towards downregulation in gene expression may be linked to the significant downregulation of tubulin, however it is difficult to hypothesise from such small non-significant changes in gene expression. Additionally, this result could be better supported with the addition of some cell migration analysis, and thus future work would benefit from exploring this aspect of cell behaviour in response to softer substrates.

The final batch of proteins assessed through WaferGen for this section of the project were *CDH1* (E-cadherin), *CTNNA1* (*α*-catenin), and *PTK2* (focal adhesion kinase) which all play a critical role in cell adhesion. All three genes were observed to show a general trend towards downregulation on softer dishes with some statistically significant changes (Figure 4.14). Whilst the downregulation of E-cadherin seemed to

contradict the denser colonies observed in HEKn on BM hydrogels and is not reflected at a protein level (Figure 4.7), it could potentially be explained by the transition from punctate to linear staining seen on 4 kPa substrates (Figure 4.10). When cells are forming a colony, it makes sense for them to upregulate expression of adhesion molecules in order to increase the chance of connecting with adjacent cells. However, in HEKn on 4 kPa coverslips, it was observed that adjacent cells had formed clear linear connections that spanned their neighbouring cell membrane regions (Figure 4.10). Consequently, the need to form new adherens junctions would be reduced compared to cells on glass coverslips which were actively searching for cell-cell connections. Moreover, this reduction in E-cadherin expression correlates with the downregulation of vinculin also observed on softer substrates (Figure 4.12B). This hypothesis would also explain the reduction in *CTNNA1* expression as α-catenin binds cadherins at adherens junctions.

Focal adhesion kinase is a tyrosine kinase concentrated at focal adhesions that transmits signals regulating focal adhesion and adherens junction formation amongst many other roles (Kleinschmidt and Schlaepfer, 2017). It has already been discussed that HEKn on BM dishes exhibit downregulation of integrins, and assuming the hypothesis regarding the reduced need for adhesion molecule expression in dense colonies is true, it makes sense that *PTK2* is also downregulated once dense colonies have been established. It is well established that FAK has a key mechanosensory role in cells, and it has been shown to mediate cell response to subject rigidity by modulating YAP1 activation (Lachowski et al., 2018). As a result, it is likely that the effects of substrate stiffness on adhesion molecule and FAK expression is much more complicated than discussed here. This avenue of investigation would benefit from further experiments, ideally exploring these molecules at a protein level and over a longer period of substrate exposure.

To conclude, the WaferGen analysis of cytoskeletal and adhesion proteins in HEKn on BM hydrogels provided some exciting initial results that suggested some striking changes to gene expression in response to a softer substrate. As discussed in chapter 3, it is important to view WaferGen data in the context that RNA expression is a

notoriously poor representation of what is happening within the cell at a protein level (Maier, Güell and Serrano, 2009). This is largely due to the limitations in the information that transcriptomics analysis can access, and post-translational modifications, protein-abundance differences, and time-dependent expression patterns are not represented by RNA levels (Wilhelm et al., 2014). Consequently, whilst the data viewed here are promising, they should be viewed as a way of narrowing down key genes of interest for further investigation rather than as a conclusive insight into the molecular response to substrate stiffness.

4.5.6 HEKn exhibited reduced protein levels of core LINC complex and LINC associated proteins in response to softer substrates

Initial western blot analyses using HaCaTs revealed that some core components of the LINC complex were reduced in response to culture on a softer substrate (Figure 4.2). In HEKn this investigation was repeated in greater depth with the inclusion of nesprin proteins. Western blot analysis of HEKn cultured on TCP, 50 kPa, 8 kPa and 4 kPa dishes revealed that there was a significant reduction in Lamin A/C and Lamin B1 protein levels on the BM hydrogel substrates (Figure 4.15A-D). In contrast, whilst emerin and SUN1 appeared to decrease in the blots (Figure 4.15A), densitometry analysis revealed that there was no statistically significant difference in relative expression when normalised to TCP (Figure 4.15E-F). SUN2 was not observed to change in either the blot or the densitometry analysis (Figure 4.15G).

The antibodies used for nesprin-1 and nesprin-2 detected multiple isoforms of the proteins which made assessment of the expression levels slightly more difficult. Densitometry analysis was performed on the most prominent bands or on bands where it was difficult to discern a change in band intensity by eye. Nesprin-1 was observed to exhibit statistically significant reductions in relative expression normalised to TCP for all isoforms assessed using densitometry (Figure 4.16). In contrast, nesprin-2 appeared to show reduced expression in a number of the higher bands in the western blot (Figure 4.17A), but densitometry analysis determined that there were no statistically significant changes for any of the bands except for band 6 (Figure 4.17G).

In section 4.5.2 the potential reasons for reduction in Lamin proteins in HaCaTs on BM hydrogels was discussed, and the results observed in primary keratinocytes further consolidate that Lamin protein levels appear to decrease in response to softer substrates. To briefly reiterate the points made in 4.5.2, reduction in Lamin proteins has been linked to keratinocyte differentiation (Jung et al., 2014) and higher levels of Lamins is associated with a stiffer tissue environment (Swift et al., 2013). Additionally, in the absence of p63, *LMNB1* and *LMNA* genes have been shown to be significantly downregulated (Rapisarda et al., 2017). Rapisarda et al. presented real-time PCR data from *p63−/−* primary mouse keratinocytes normalised to the control; relative expression of *LMNA* in the knockout was approximately 0.60, whilst for *LMNB1* it was approximately 0.40 (Rapisarda et al., 2017). Consequently, the chosen hypothesis for the reduced Lamin levels observed in western blot analysis was that HEKn cultured on softer hydrogels exhibit a downregulation in p63 expression as they move away from a basal cell proliferative phenotype towards a more differentiated phenotype, and this triggers a reduction in Lamin A/C and Lamin B1 expression.

However, unlike HaCaTs, HEKn exhibited no statistical change in emerin, or SUN1 or SUN2 levels when cultured on BM dishes. In section 4.5.2, it was observed that the apparent reduction in emerin levels in HaCaTs seemed to contradict the available literature which suggested that downregulation of emerin is linked to increased nuclear rigidity which was not witnessed in this study (Guilluy et al., 2014). Additionally, whilst downregulation of *SUN1* and *SUN2* is also associated with a lack of p63 (Rapisarda et al., 2017), again it was difficult to fully reconcile a reduction in SUN1 and SUN2 in HaCaTs with the available literature. Nonetheless, further western blot repeats performed by other members of the laboratory group did reveal a statistically significant decrease in SUN1 expression in response to softer substrates (Hunter-Featherstone et al., 2021). Consequently, this analysis would benefit from further investigation by future parties, ideally using fresh lysate samples, to exclude any artifacts caused by personal error or variability in technique.

Whilst nesprin-1 was observed to strikingly decrease in response to softer substrates, nesprin-2 was shown to have no statistically significant decreases in intensity for most bands despite the blot appearing to show otherwise. Moreover, repeats performed by others in the group again revealed that some bands were in fact statistically reduced in the BM hydrogel samples (Hunter-Featherstone et al., 2021). The likely cause of the variability for the nesprin-2 densitometry analysis is that the nesprin-2 antibody used produces a lot of background in each lane caused by the sample passing through the gel. Whilst this is not as obvious following lower development times, developing the blot for a shorter period runs the risk of losing bands that take a little longer to show up. Consequently, if densitometry is performed on blots that have had a long exposure time to capture all of the bands, the background within each lane will interfere with the densitometry analysis, as was likely the case in the analyses presented in Figure 4.17. However, if a low exposure time image is used with minimal background, then the densitometry analysis will likely be more accurately representative of the bands, but this comes with the caveat of completely losing less strongly expressed bands that would have appeared following longer exposure. Consequently, densitometry analysis cannot be relied upon to accurately provide quantification of relative protein expression and should rather be used as a guide to select proteins that would warrant more in-depth analysis using more accurate methods.

With this in mind, we might propose that nesprin-2 may in fact show decreased protein levels for numerous isoforms in HEKn cultured on softer substrates. If this is the case, the downregulation observed in nesprins and SUN1, but lack of change observed in SUN2 and emerin, could be due to the fact that molecular changes in the LINC complex are more pronounced at the outer nuclear membrane following relatively short exposure (i.e., 4 days) to the soft BM hydrogels. The changes in nesprin-1 and nesprin-2 levels varied depending on the isoform, and it was noted that those with actin-binding domains, including the full-length giants, were downregulated. Whether this downregulation was a response to or a facilitator of the actin reorganisation and downregulation observed in HEKn on BM dishes is not known. However, it is well established that nesprins define the perinuclear

cytoskeleton in keratinocytes (Schneider et al., 2010). In order to obtain more detailed mechanistic insights into how the LINC complex and cytoskeleton interplay on different substrate stiffnesses, a systematic and thorough proteome analysis would be required. The most significant question raised by the protein changes observed in HEKn is which molecular adaptations happen first? With so many proteins known to be interconnected and mechanosensory, the analyses discussed here provide only a surface investigation into the complexity of the cellular response to external mechanics.

4.5.7 HEKn cultured on BM hydrogels exhibited gene expression changes in NE proteins

As with the cytoskeletal proteins, once protein levels of LINC and LINC-associated proteins had been investigated the next step was to assess what was happening to the gene expression of these proteins. It was noted that the WaferGen results largely aligned with the western blot data, suggesting that for LINC proteins the transcriptomic information was translated to the protein level. *EMD* (emerin) was observed to fluctuate between downregulation and upregulation with no statistical significance (Figure 4.18) which was similar to the inconclusive change in protein levels. Lamin expression also matched with the western blot data; *LMNA* trended towards upregulation on the first day but was observed to be statistically downregulated in HEKn on 4 kPa BM hydrogels, whilst *LMNB1* was strikingly downregulated with statistical significance across the majority of dishes at each timepoint (Figure 4.19). SUN1 and SUN2 were both observed to show fluctuating trends in expression across the dishes and days, ending on a trend towards downregulation at day 4 that was not statistically significant (Figure 4.20). The nesprin data were a little harder to align to the western blot analyses as they did not show the individual isoform information. However, *SYNE1* was significantly downregulated in response to softer substrates which correlates to the majority of protein bands (Figure 4.21A), and *SYNE2* was significantly downregulated on day 1 but became significantly upregulated by day 4 after seeding (Figure 4.21B). The

WaferGen analysis also included nesprin-3 which was observed to be significantly downregulated on softer substrates (Figure 4.21C).

The fact that both emerin and the SUN-domain proteins did not show significant changes in either protein levels or RNA levels suggests that they did not change in response to substrate stiffness. However, there are caveats to using densitometry analysis as highlighted in 4.5.6 and the trend towards downregulation may still be biologically significant, thus further investigation into these proteins should not be ruled out, particularly over a longer culture period. In contrast, the striking changes observed in both the protein and RNA levels of Lamin A/C and Lamin B1 strongly suggest that softer substrates induce a downregulation in Lamins in keratinocytes (the hypotheses for this are discussed in 4.5.6). As mentioned previously, the WaferGen analysis of nesprins lacks information on which isoforms are being represented by the data as it is not known whether the target sequence is present in all isoforms; these data could represent the entire RNA content transcribed from the gene, or just a small proportion. As a result, these data provide clear evidence that nesprin expression is affected by substrate stiffness, but further study looking at more specific transcriptomic information would be needed to conclude which isoforms are changing and hypothesise how this might fit into the broader picture.

Whilst the main focus of the research for this chapter was on known mechanosensory proteins, it was also considered that investigating additional NE proteins not typically associated with mechanosensation, might provide a broader picture of what was happening at the nuclear membrane. With this in mind, additional WaferGen analysis was carried out focusing on the change in expression of NPC proteins which were chosen because they were considered suitable "controls" of NE protein expression. However, recent studies have highlighted the role of NPCs in mechanotransduction, even going so far as to suggest that they are as important as nuclear lamina and chromatin in translating stimuli transmitted by SUN proteins into cell fate decisions (Donnaloja et al., 2019; Kassianidou, Kalita and Lim, 2019; Maurer and Lammerding, 2019).

NUP62 was observed to be downregulated from day 2 onwards which was statistically significant in 4 kPa samples (Figure 4.22A). NUP62 has a role in mitotic cell cycle progression, regulating centrosome segregation, centriole maturation and spindle orientation (Hashizume et al., 2013), thus it is not surprising it was downregulated given that HEKn cultured on BM hydrogels were observed to exhibit reduced proliferation. NUP107 plays a role in NPC assembly and exporting mRNA from the nucleus (Shi et al., 2020), and was found to be significantly downregulated on days 1 and 3 after seeding before returning to similar levels of expression as TCP on day 4 (Figure 4.22B). NUP153 was an interesting protein to examine as it binds SUN-domain proteins, and the gene was observed to be significantly downregulated across the entire culture period in HEKn on 4 kPa hydrogels (Figure 4.22C). *RANBP2* encodes NUP358 which plays a critical role in the shuttling of proteins between the nucleus and the cytoplasm (Wälde et al., 2011). The majority of samples did not seem to show much change in expression, though there was a trend towards upregulation on day 4 that was statistically significant for the 4 kPa sample (Figure 4.22D). Finally, the WaferGen analysis provided data on the expression of *NDC1* which assists with the de novo assembly of NPCs and their insertion into the NE (Mansfeld et al., 2006). From day 2 onwards, expression of *NDC1* was seen to trend towards downregulation which was significant for a couple of samples (Figure 4.22E).

Whilst there is currently no evidence in the literature that directly connects mechanical stimuli with NPC activation, there have been numerous studies that have shown a link between cell stretch and changes in the shuttling of molecules between the cytoplasm and the nucleus (Donnaloja et al., 2019). Of particular interest is the role that NPCs have been shown to play in facilitating the selective transport of mechanosensitive transcription factors into the nucleus. In chapter 3 we explored the Hippo pathway, focusing particularly on YAP1 which was shown to have a greater nuclear localisation in HEKn cultured on glass coverslips than those on 4 kPa hydrogels (Figure 3.17). It is still debated whether force is the primary effector of YAP nuclear import, but it has been shown that applying direct force to the nucleus via AFM results in YAP translocating to the nucleus within minutes (Elosegui-Artola et al., 2017; Kassianidou, Kalita and Lim, 2019). When nuclei are stretched, for example

when cells are cultured on a 2D TCP surface, NPCs within the NE take on a more open confirmation which actively promotes the nuclear import of YAP. However, this does not appear to be caused by the opening of NPCs alone, as osmotic swelling does not trigger YAP import, thus suggesting that the opening of NPCs to promote mechanosensitive transcription factor transport is mechanically controlled, likely by LINC complex proteins (Elosegui-Artola et al., 2017; Enyedi and Niethammer, 2017).

It is clear that NPCs do have a role to play in mechanotransduction, but there is a long way to go before we are able to fully understand the mechanisms behind cell responses to mechanical cues. Additionally, there is little in the literature related to NPCs and mechanosensing that could explain why the WaferGen analysis performed in this study demonstrated gene expression changes of core NPC components. However, it is well established that different tissues possess different compositions of NPCs, and a 2012 study reported that changes to this composition regulated myogenic and neuronal differentiation (D'Angelo et al., 2012). Terminal differentiation in keratinocytes marks an exit from the cell cycle and ultimately the degradation and loss of the entire nucleus and therefore the nucleus undergoes marked structural changes as cells migrate away from the basement membrane to the cornified layer (Gdula et al., 2013). In chapter 3, evidence was presented that culturing HEKn on softer substrates caused a shift away from proliferation towards a more differentiated phenotype as shown by upregulation of some differentiation markers. Consequently, the changes in expression of the NPC proteins seen here could be due to a compositional change linked to differentiation rather than a direct effect of altered external mechanics. However, given the complexity of nuclear mechanotransduction it would be interesting to investigate this further, perhaps using fibroblasts which are not subject to differentiation and therefore would more directly demonstrate what changes are linked to mechanical cues.

4.5.8 HEKn tuned their nuclear and cytoplasmic stiffness based on the rigidity of their culture dish

In the introduction to this chapter, it was highlighted that microtubules could play a role in tuning cellular mechanics in response to external forces by regulating

cytoskeletal stiffness and viscoelastic resistance (Kerr et al., 2015; Robison et al., 2016; Coleman et al., 2021). Additionally, it is well documented in the literature that AFM analysis of numerous different cell types has shown them to alter their stiffness to match their culture surface when transitioned to a softer environment like the hydrogels used in this study (Liu, Sun and Simmons, 2013; Rianna and Radmacher, 2017; Solon et al., 2007). Consequently, the next step in the investigation for this chapter was to see whether the changes observed in cytoskeletal and nuclear protein expression translated to a change in the physical stiffness of HEKn.

It was decided that an osmotic shock assay was an appropriate first test of nuclear stiffness and would provide guidance on whether the more time-consuming and technical AFM analysis was necessary. HEKn were primed for 4 days on glass and 4 kPa coverslips before osmotic shock was induced using a high sucrose concentration, and cells were stained for Lamin B1 to highlight the NE. The number of folds in the NE were observed to be higher in HEKn cultured on 4 kPa coverslips (Figure 4.23), suggesting that these nuclei were softer than those on glass as they were less able to resist the mechanical stress induced by osmotic shock. As a result, it was concluded that AFM analysis would be appropriate and enable a more quantifiable analysis of any stiffness changes induced by culturing HEKn on softer substrates.

HEKn were again primed for 4 days, this time on TCP and 4 kPa dishes, before being moved to smaller TCP dishes and allowed to adhere overnight. AFM analysis was performed the next day and HEKn primed on 4 kPa dishes were found to exhibit significantly softer nuclear and cytoplasmic compartments than those primed on TCP (Figure 4.24). In 2020, a *Nature Materials* paper reported that cortical cell stiffness is independent of substrate mechanics; the study criticised AFM indentation as way to measure of cell stiffness, showing that the force of the cantilever indentation causes significant deformation of the underlying soft substrate, thus resulting in an underestimation of the cell's elastic Modulus (Rheinlaender et al., 2020). The team subsequently found that once they had corrected for the deformation of the substrate the stiffness of the cell was observed to be independent of substrate mechanics. The AFM data presented in this chapter was obtained prior to the publication of this

study, however, it was anticipated that the hydrogel coating may provide less resistance than TCP and therefore diminish the accuracy of AFM measurements. As previously reported, in order to control for this, HEKn were moved onto new TCP dishes the night before the AFM was performed so that, though the cells had been primed on different substrate stiffnesses, they were both measured on the same substrate. Consequently, it is not possible for the substrate to have interfered with the Young's Modulus values obtained in this study, thus making the data potentially more reliable than many results reported in the literature.

However, this is not to say that there were no limitations associated with the AFM analysis performed here. One of the biggest problems faced was how long the measurements took to take which meant that the TCP cells and 4 kPa cells ended up being measured on different days. However, the conditions and methodology were kept identical to limit how much impact this might have had on the results. Additionally, the time taken to measure each cell meant that in a full day only 8 cells per condition were measured, though each of these cells provided thousands of data points. Given the limited access to the AFM and the requirement for assistance from someone trained to use it, it was not possible to perform any biological repeats, which would have significantly strengthened the data presented here.

Consequently, though the AFM analysis would certainly have been reinforced by additional repeats had there been the luxury of time, the data obtained offers exciting evidence that keratinocytes do in fact adapt their nuclear and cytoplasmic mechanics in response to external stiffness, correlating with the downregulation of actin and the nuclear lamina.

4.5.9 HEKn cultured in high calcium medium exhibited changes in some LINC complex proteins suggesting an association with differentiation

In chapter 3 it was suggested that culturing HEKn on soft BM hydrogel-coated dishes may push cells towards a differentiated phenotype, and this was supported by some of the data. In this chapter we have explored the changes in cytoskeletal proteins, adhesion molecules, and LINC components observed in HEKn cultured on TCP and

BM dishes. This raised the question of whether the softer substrates were inducing differentiation which then led to changes in the cytoskeletal and NE architecture, or whether changes to the cytoskeleton and LINC complex were driving differentiation.

In order to gain a better understanding of how the start of keratinocyte differentiation affects LINC complex protein levels in the absence of variable external mechanics, HEKn were cultured on TCP dishes in low and high calcium medium. Western blot analysis was performed, and early differentiation was confirmed using CK10, which was observed to be greatly increased under high calcium conditions (Figure 4.25). This experiment revealed that Lamin A/c and SUN1 were unaffected by the beginning of keratinocyte differentiation, SUN2 looked to decrease slightly, Lamin B1 was significantly decreased in high calcium medium, and emerin was significantly increased (Figure 4.25). Whilst these results clearly demonstrate that differentiation does result in changes to LINC protein levels, the fact that the protein profile was notably different from that of TCP versus hydrogel samples (Figure 4.15) suggests that the expression changes observed on softer substrates are independent of keratinocyte differentiation.

It is well documented that the cytoskeleton plays a predominant role in regulating cell stiffness and adapting cells to match soft elastic substrates (Solon et al., 2007). Therefore, given the results presented in Figure 4.25, it seems more likely that changes in LINC expression are a direct result of cells adapting to mimic a softer mechanical environment rather than being directly linked to differentiation. It is well documented in the literature that the LINC complex helps regulate the transcriptomic response to external mechanical cues (Alam et al., 2011). Moreover, triple lamin-knockout mice exhibit precocious epidermal differentiation (Jung et al., 2014), which further supports the hypothesis that it is changes to the LINC complex that drives epidermal differentiation rather than the other way around.

4.6 Conclusions

This chapter aimed to determine whether culturing keratinocytes on soft hydrogel-coated dishes led to cytoskeletal and LINC protein changes that could explain the

changes to cell behaviour and colony morphology presented in chapter 3. Moreover, this chapter aimed to ascertain whether HEKn were adapting their own stiffness to replicate their culture substrate as has been documented for other cell types in the literature. We hypothesised that cells would exhibit altered cytoskeletal organisation when cultured on softer hydrogels, particularly the actin skeleton which was anticipated to reflect a more differentiated keratinocyte actin structure. Additionally, we hypothesised that E-cadherin would be arranged in a way that would explain the denser colonies observed on BM dishes which suggested superior epidermal sheet formation. Given the supporting literature, we anticipated that HEKn would be softer after being cultured on the hydrogel-coated dishes, and that this would be facilitated by changes in LINC and LINC-associated protein expression.

HEKn cultured on softer hydrogel-coated dishes exhibited changes in actin and E-cadherin organisation that seemed to correlate with the hypothesis that BM dishes promote a more differentiated phenotype. Actin reorganisation on 4 kPa coverslips was similar to that observed in terminally differentiated keratinocytes, and a more linear E-cadherin localisation along the cell membrane suggested more developed cell-cell interactions that would facilitate better epidermal sheet formation. In addition, HEKn on BM hydrogels exhibited changes in gene expression for proteins associated with cell adhesion such as vinculin, α-catenin, and E-cadherin which suggested that cells were altering their methods of adhesion.

Assessment of the LINC complex revealed that HEKn on softer dishes presented with a striking downregulation of nuclear Lamins, as well as changes in multiple isoforms of nesprin-1 and potentially nesprin-2. Following AFM analysis of HEKn primed on TCP and 4 kPa dishes, it was shown that cell nuclear and cytoskeletal compartments were softer after being cultured on hydrogels. This correlated to the downregulation of Lamins which play a significant role in maintaining nuclear integrity. Moreover, a preliminary assessment into the effects of keratinocyte differentiation on LINC protein levels suggested that the changes observed on soft hydrogels was due to external mechanical changes rather than differentiation, and in fact it was these mechanoproteins that were driving the differentiated phenotype.

Given the vital role that differentiation plays in epidermal assembly, this chapter offers an exciting insight into how cultureware mechanics could be harnessed in order to manipulate epidermal homeostasis to facilitate better model development. However, these data should only be viewed as a preliminary venture into understanding the mechanisms behind the complexity of the keratinocyte response to external mechanical stimuli. Further investigation with fresh samples and a more in-depth exploration of proteomics and transcriptomics is certainly necessary for a complete understanding. Moreover, one of the most striking things to note from the results presented here is that even after a relatively short culture period of 4 days, HEKn were responding to slight changes in stiffness with statistically significant alterations in RNA and protein levels. As a result, it would be interesting to culture cells on BM dishes for a longer period and see whether prolonged exposure might provide more definitive results for those genes and proteins that showed ambiguous or no change in this study.

5 Investigating the effects of 2D substrate stiffness on the development of 3D epidermal models *in vitro*

5.1 Introduction

Despite the clear importance of external mechanical stimuli on the behaviour and gene expression profile of cells, *in vitro* cell culture still relies heavily on the use of plastic and glass which are significantly stiffer than the physiological microenvironment (Gilbert et al., 2010). Whilst there are no exact stiffness values for the human epidermis or epidermal basement membrane in the literature, human skin as a whole has been shown to have a Young's Modulus range of 0.1 to 10 kPa (Achterberg et al., 2014). In stark contrast, TCP possesses a Young's Modulus in the gigapascal range (GPa) which is over one million times stiffer (Landry, Rattan and Dixon, 2019).

To combat the unrealistic environment that TCP and glass cultureware provide, the development of 3D tissue models has found a lot of traction, with recent advancements providing cells with a scaffold into which they can construct their own microenvironment through ECM deposition (Guyot et al., 2014). However, it is still common practice to culture cells on TCP cultureware prior to setting up 3D models, meaning that the transcriptome and proteome of the cells being used do not reflect those of the *in vivo* environment. *In vitro* skin models have been shown to express similar genes to hyperproliferative skin, with marked upregulation of keratin 16 which is found in psoriatic epidermis and at wound sites and is a hallmark of keratinocyte activation (Smiley et al., 2005; Smiley et al., 2006). *In vitro* 3D skin models are therefore not fully representative of *in vivo* tissue, and more needs to be done to bridge to gap between standard 2D cell culture and model development.

5.1.1 *In vitro* 3D skin models and their role in epidermal research

Whilst an inappropriate mechanical environment is a major limitation of 2D culture, another significant flaw is that cells growing in a 2D monolayer lack the heterogeneity of *in vivo* tissue, and do not exhibit the full transcriptomic and proteomic profiles, or the surrounding ECM. For this reason, development of 3D culture and synthetic tissue models has been on the rise. Whilst our knowledge of skin is relatively expansive compared to some other tissues, it is still not fully understood; particularly with relation to wound healing, ageing and diseases such as psoriasis, eczema, and melanoma, which can all be explored through *in vitro* skin models.

Epidermal skin models have been around in one form or another since the late 1990s and were primarily of interest in order to test the corrosive properties of chemicals (Eaglstein and Falanga, 1997; Fentem et al., 1998). More recently, EEs have provided an alternative to animal testing in the cosmetics industry following a ban by the European Union in 2009 (EC, 2010). Commercially available models such as EpiSkin™ and EpiDerm™ are among the most commonly used for skin irritation analysis (Kose et al., 2018), and have both been validated by the European Reference Laboratory On Alternatives To Animal Testing (EURL ECVAM) (EC, 2017a; EC, 2017b). These models use human-derived epidermal keratinocytes cultured at the ALI on either collagen matrices (EpiSkin™) (EpiSkin, 2021) or pre-treated tissue culture inserts containing a polycarbonate (PC) membrane (EpiDerm™) (MatTek Life Sciences, 2021).

Whilst culturing keratinocytes on top of collagen gels or PC membranes are the most frequently used methods for generating an epidermal model, these still provide an underlying substrate that does not necessarily replicate the basement membrane. In order to combat that, alternative models have been produced which first generate a dermal equivalent within a scaffold onto which keratinocytes can then be seeded. Models produced in this way have been shown to develop their own basement membrane (Roger et al., 2019), making this the most realistic *in vitro* environment available for epidermal model generation. A more simplified version of this model is to produce organotypic full skin constructs using the hanging drop culturing method;

this technique has been successfully used to study more complex skin models such as hair follicles (Higgins et al., 2013) and melanoma (Müller and Kulms, 2018).

5.1.2 The limitations of current 3D epidermal models

Whilst the models described above demonstrate the numerous innovative ways in which 3D epidermal tissue can be produced *in vitro*, there are still limitations to existing models. Perhaps some of the biggest hurdles to overcome from a practical standpoint are that *in vitro* tissue models are often time consuming to prepare, lack high throughput, and are difficult to reproduce between laboratories. Some of the main reasons for this include the use of complex in-house media recipes, high serum concentrations, and lack of protocol transparency in the literature (Bertolero et al., 1984; Faller and Bracher, 2002; Ng and Ikeda, 2011). Moreover, epidermal models face the additional drawback that not all primary keratinocytes are able to differentiate and stratify in an *in vitro* setting (Eves et al., 2000; Stark et al., 1999). This makes reproduction of reliable epidermal models difficult, though there are research groups that have tried to standardise a more robust protocol (Roger et al., 2019).

However, alterations to the 3D culture protocol can only go so far towards improving model development, and it is critical that researchers begin to focus their attention on the 2D culture stage. Regardless of the 3D model technique used (i.e., collagen matrix, PC membrane etc), it is still standard practice to first revive and expand the cell population on TCP cultureware prior to model set-up. Having already highlighted the clear differences between HEKn cultured on TCP versus BM dishes in the previous two chapters, it can come as no surprise that cells going into models following TCP culture are not representative of their *in vivo* counterparts. This has been highlighted by comparisons of gene expression between skin models and *in vivo* skin tissue. There are multiple studies that have observed gene expression profiles revealing that *in vitro* epidermal models exhibit a hyperproliferative and activated phenotype more reminiscent of wounded native skin (Simard-Bisson et al., 2018; Smiley et al., 2005; Smiley et al., 2006). Skin models exhibit upregulated keratins 6, 16, and 17 which are all known markers of keratinocyte activation and hyperproliferative epidermis (Smiley et al., 2006). Moreover, tissue engineered

epidermis has been shown to strongly express the lipoxygenase enzyme 15-LOX-1 which is also associated with wound healing and is not observed in normal human skin tissue (Simard-Bisson et al., 2018). Thus, cultured epidermal substitutes are by no means genotypically representative of *in vivo* skin regardless of how they may appear histologically, and likely never will be until the use of TCP cultureware is removed from the equation.

Another potential impact of priming cells on TCP prior to model set-up is that there will likely be a lag period in which cells must adjust to their new environment. It has already been highlighted that laborious protocols are a key limitation of 3D tissue development, with epidermal models requiring at least a fortnight of culture time. In chapters 3 and 4 we observed from WaferGen analysis that gene expression altered over the 4 days following seeding of HEKn onto BM dishes after TCP culture. Consequently, this could contribute towards the long culture time of *in vitro* models and adjusting the mechanical environment of the 2D stage may reduce the time required to develop epidermal models.

5.2 Hypotheses and Aims

This chapter aims to investigate the effects on 3D epidermal assembly *in vitro* when HEKn are pre-cultured on a substrate mimicking the stiffness of the *in vivo* basement membrane. It has already been highlighted that one of the main weaknesses of current 3D models is that cells are still being cultured on TCP at the 2D stage, which may result in a lag period whilst cells adjust to their new mechanical environment. Moreover, it is well established in the literature, and has been demonstrated in chapters 3 and 4, that culturing cells on TCP *in vitro* causes changes in their transcriptome and proteome compared to their *in vivo* counterparts. It was hypothesised, firstly, that culturing keratinocytes on softer substrates replicating the *in vivo* environment would reduce the risk of a lag period and enable cells to undergo quicker epidermal assembly in 3D culture. Additionally, it was hypothesised that if the changes in gene and protein expression presented in chapters 3 and 4 were reflective of *in vivo* keratinocytes, this would translate into superior epidermal models that were more organised and had better barrier function.

Finally, given the evidence that dishes of different stiffnesses may push keratinocytes towards either proliferation or differentiation, it was hypothesised that mixing cells primed on different dishes at different stages of 3D culture may produce an even better epidermal equivalent model.

To summarise, the key hypothesis behind this chapter was that priming keratinocytes in a more physiologically relevant mechanical environment at the 2D stage would promote the development of superior 3D epidermal models with better organisation and function than TCP primed. This chapter therefore aimed to answer the following questions:

- Does culturing keratinocytes on hydrogels prior to setting up 3D culture facilitate superior epidermal assembly?
- Should hydrogel primed keratinocytes exhibit superior epidermal assembly, does this translate into changes in protein expression and barrier function?
- Is it possible to produce an epidermal model more quickly by priming keratinocytes on hydrogel-coated dishes first?

5.3 Objectives

- Determine whether culturing keratinocytes on hydrogel-coated dishes in 2D, improves the appearance of 3D epidermal models.
- Characterise protein expression in epidermal models produced from keratinocytes primed on TCP and hydrogel-coated dishes.
- Assess barrier function of epidermal models produced from keratinocytes primed on TCP and hydrogel-coated dishes.
- Determine whether priming keratinocytes on hydrogel-coated dishes leads to faster epidermal model development.

5.4 Results

As introduced in chapter 3, one of the main aims of this project was to investigate whether making the mechanical environment more *in vivo*-like during 2D keratinocyte culture can improve epidermal assembly in *in vitro* 3D models. This chapter therefore explores the effects that priming HEKn on TCP and BM dishes had

on the development of 3D EEs. Two key methods were used in the development of 3D EEs for this chapter; spheroid models created using the hanging drop method, and models generated using membrane inserts upon which cells were seeded and prompted to undergo epidermal assembly. The type of membrane used in these insert models can vary in terms of material, pore size, and pore density, the effects of which will be explored in the section below. However, Figure 5.1 provides an overview of the key methodologies used to generate the models described in this chapter.

Figure 5.1 (overleaf) Schematic outlining the key methodologies used to generate 3D EEs for this thesis. (A) *Spheroid models* **(i)** *1) HEKn were cultured on TCP/BM dishes before being dissociated and seeded in droplets onto the lid of a dish and suspended over sterile deionised water to ensure humidity; 2) After 3 days of culture, a spheroid of cells was formed.* **(ii)** *1) HDFn were cultured on TCP dishes before being dissociated and seeded in droplets onto the lid of a dish and suspended over sterile deionised water to ensure humidity; 2) After 3 days of culture, a fibroblast spheroid was formed. HEKn were seeded into the same droplet containing the HDFn spheroid; 3) After 3 more days of culture the HEKn had coated the dermal spheroid to form a 3D skin model.* **(B)** *Membrane insert models 1) HEKn were cultured on TCP/BM dishes before being dissociated; 2) Cells were seeded onto the membrane of plate inserts and allowed to adhere; 3) Models were cultured fully submerged in medium for 4 days to promote proliferation; 4) Models were raised to the air-liquid interface to promote differentiation and cultured for a further 12 days.*

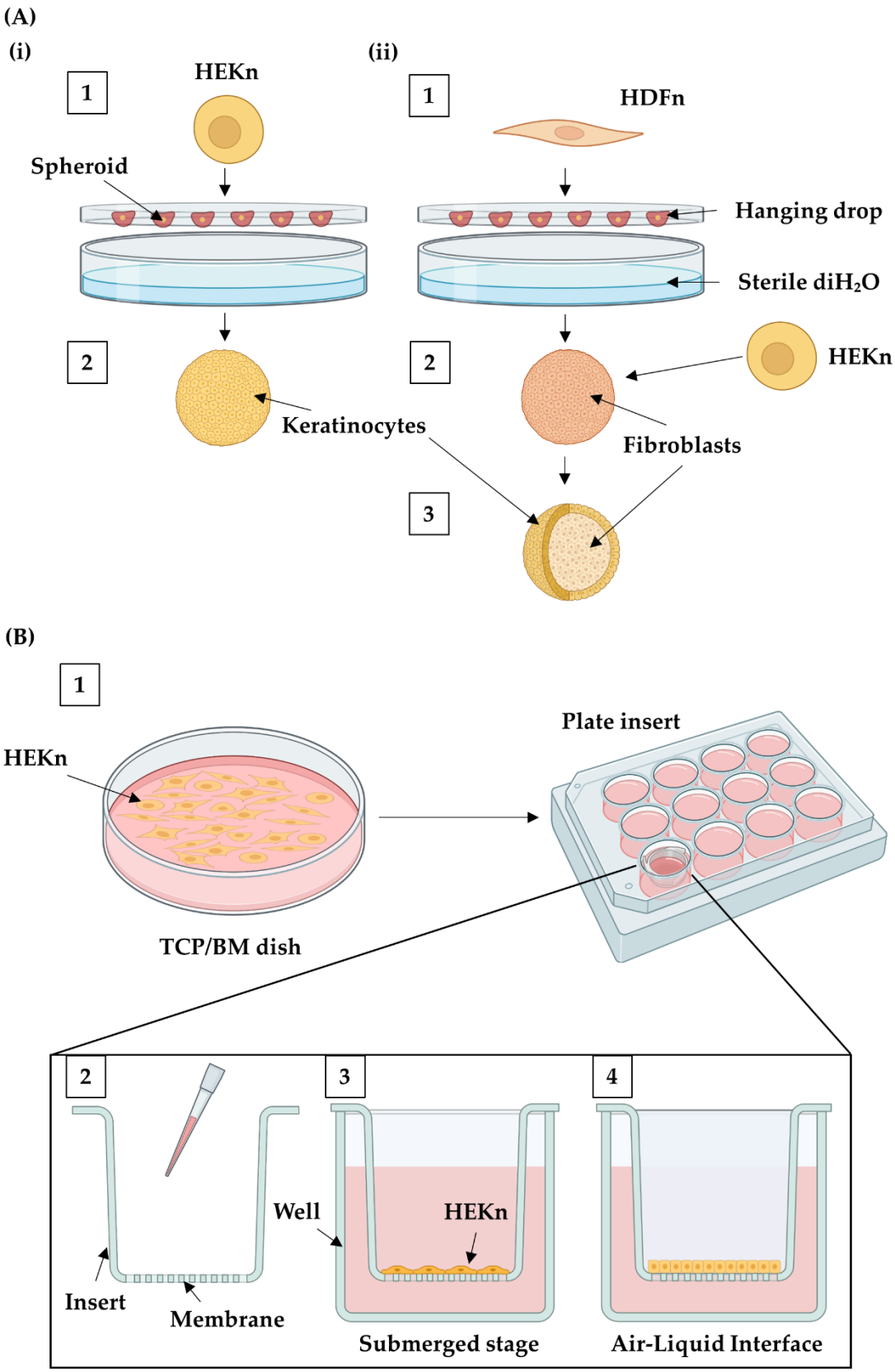
(A)
(i)
1
HEKn
Spheroid
2
Keratinocytes
(ii)
1
HDFn
Hanging drop
Sterile diH₂O
2
HEKn
Fibroblasts
3
(B)
1
HEKn
TCP/BM dish
Plate insert
2
Insert
Membrane
3
Well
HEKn
Submerged stage
4
Air-Liquid Interface

5.4.1 Early EE development encountered many technical problems that affected model quality

One of the first challenges faced when beginning EE development was choosing a protocol and cell batch that produced optimal models. Consequently, 2D substrate stiffness was not considered for initial models and only TCP primed cells were used to minimise variables. Early experiments were carried out using polyester (PET) membrane inserts, chosen for their transparency under the microscope, with 1.0 μm pores to promote greater access to medium when models were at the ALI. Initially EEs were developed using Gibco® HEKn (Cat # C-001-5C) of varying lot numbers to test the ability of the cells to undergo epidermal assembly *in vitro*. Figure 5.2A shows a schematic of this early protocol using lot # 1776789; 200,000 cells were seeded onto each insert and models were kept in submerged culture for 2 days and 7 days at the ALI. However, models were observed to be very thin with poor disorganisation and readily detached from the membrane during processing (Figure 5.2B). Moreover, abnormal differentiation led to extensive parakeratosis, defined as retention of nuclei in the stratum corneum (Figure 5.2C).

The excessive detachment of models from the PET membrane observed in these early experiments was later attributed to the fact that the Gibco® Coating Matrix Kit used had been mistakenly stored at -20°C instead of 5°C upon arrival in the laboratory. It was therefore assumed that the matrix had been compromised and HEKn were unable to readily adhere when seeded. In order to test this theory, HEKn were seeded onto PET membranes that were either not coated or had been coated with new Coating Matrix stored at the correct temperature prior to use. Neutral red staining of

Figure 5.2 (overleaf) Early EE models were poorly developed and showed abnormal differentiation. (A) *Schematic of early EE protocol 1) HEKn were cultured on TCP dishes before being dissociated and spun down; 2) 200,000 cells were seeded onto 24-well PET inserts in 200 μl medium and incubated for 2 hours at 37°C; 3) EEs were cultured at submerged stage for 2 days in 1.8 ml medium; 4) EEs were raised to ALI and cultured for 7 days in 500 μl medium. Medium was replaced every 48 hours.* **(B)** *Many EEs had detached from the PET membrane in large sections of the model. Scale bar = 20 μm.* **(C)** *Models exhibited poor organisation and abnormal differentiation characterised by parakeratosis (red arrows). Scale bar = 20 μm.*

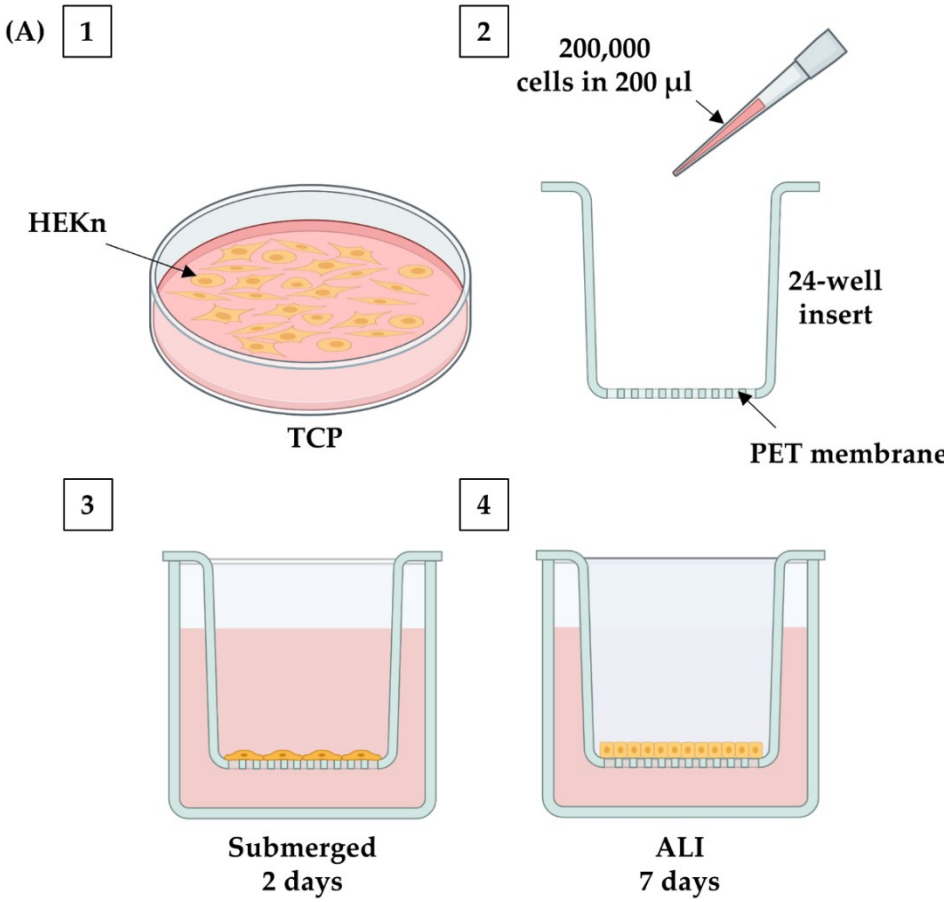

(B)

Detachment from membrane

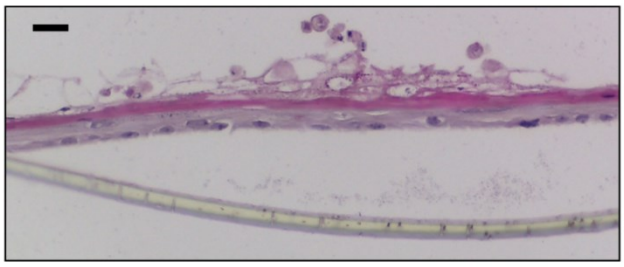

(C)

Parakeratosis

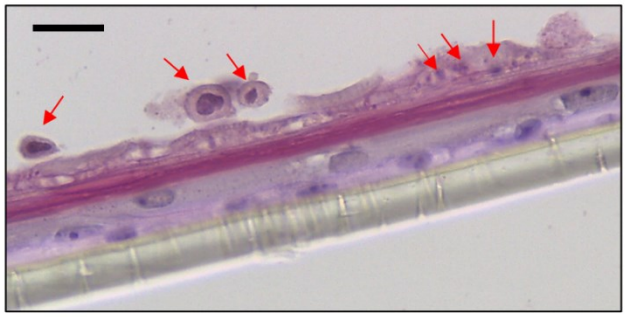

models at the end of the submerged stage was used to assess cell coverage under both conditions. HEKn were observed to adhere readily to PET membranes regardless of whether they had been coated (Figure 5.3), meaning it was unlikely that the detaching models were due to compromised Coating Matrix. However, it was noted in both non-coated and coated that there were patches of white within the neutral red staining that suggested either low cell viability or an absence of cells in these regions. The aim of the submerged stage of culture is to promote proliferation so that there are enough cells available to start epidermal assembly following transfer to the ALI. If cells were not viable or there were gaps in the basal layer, this could explain the thinness of the early EE models (Figure 5.2B-C).

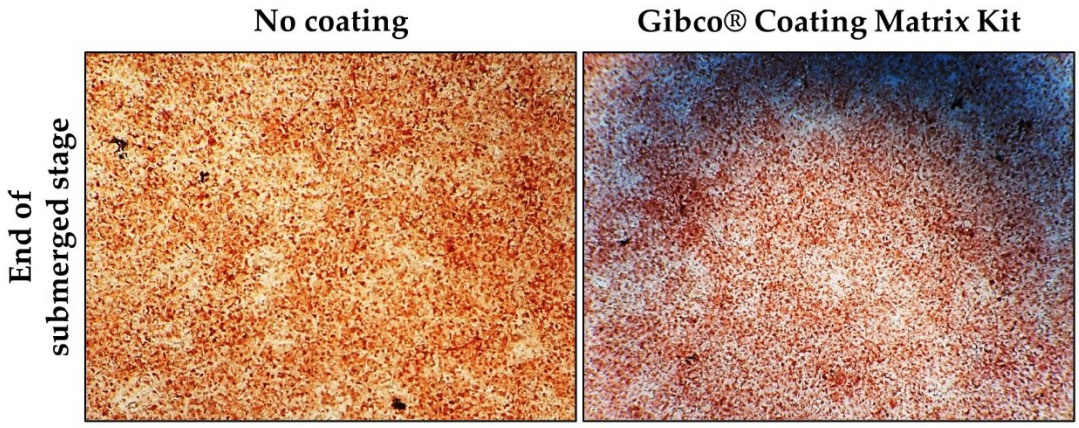

Figure 5.3 Neutral red staining of EEs showed that HEKn adhered to PET membrane regardless of the presence of coating matrix. *HEKn were seeded onto PET membranes and cultured for 2 days submerged before being stained with neutral red dye and imaged. Brightfield dissecting microscope images show strong cell viability and good adherence following submerged culture on both the non-coated and coated PET membranes.*

One feature of the Gibco® HEKn that was noted during culture was that a significant number of them were binucleated, quantification of which showed that around 20% had 2 nuclei (Figure 5.4). Given the white patches observed in the neutral red staining of EEs, this put the viability of the HEKn being used into question. Testing of different Gibco® HEKn lot numbers did not yield better EE results, and therefore the HEKn used for this, and all other aspects of the project, were changed to Lifeline® HEKn # FC-0007 which were recommended and provided by P&G. At around the same time, it was noted that there were a reasonable number of HEKn growing on the bottom of

the wells, leading to the hypothesis that the larger pore size in the PET membranes might be allowing HEKn to escape through them which could also explain the areas of white in the neutral red stained models (Figure 5.3).

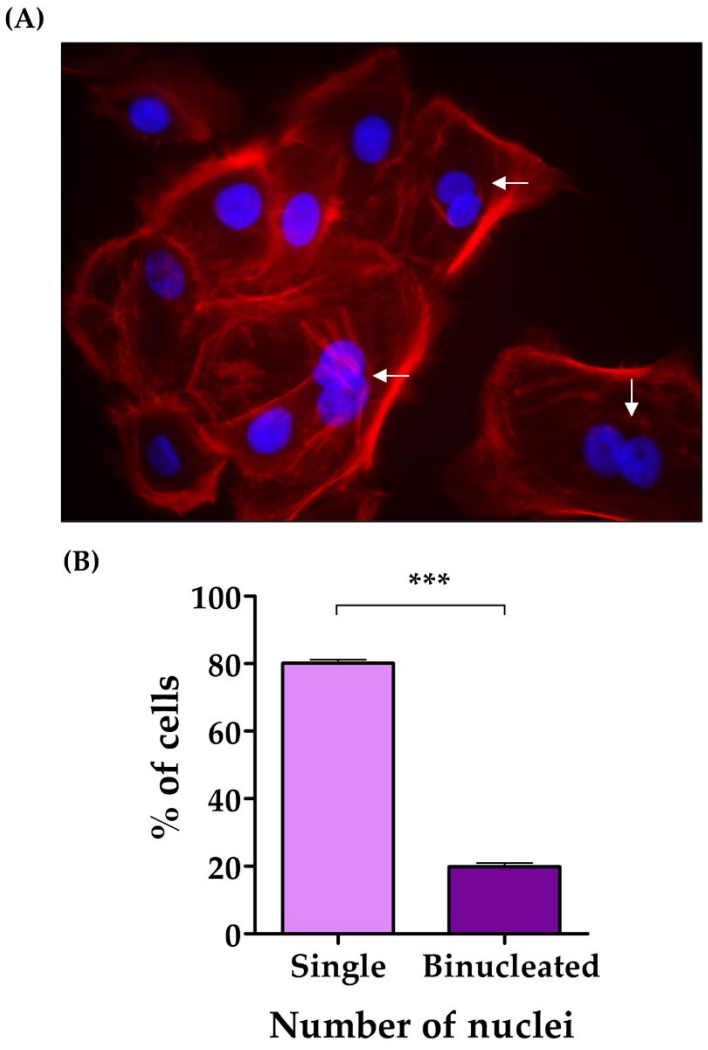

Figure 5.4 A reasonable proportion of HEKn were observed to be binucleated. During 2D culture of Gibco™ HEKn it was observed that many of the cells were binucleated. (A) *Immunofluorescent microscopy image (taken on Ziess Axioskop) shows binucleated HEKn (white arrows).* **(B)** *Quantification of proportion of binucleated HEKn on coverslips. Data represent mean ±SEM, n = 3 (3x 100 cells), statistical significance was assessed using an unpaired, two-tailed t-test, *** $p \leq 0.0001$.*

To combat this, new models were produced using PET membranes with 0.4 μm pores. However, these models were observed to be even more poorly developed than earlier EEs with no evident cell layers and abnormal differentiation and extensive parakeratosis (Figure 5.5A). After trying a number of different inserts, the final insert

design tested was BRAND*plates*™ which are PC membranes with 0.4 μm pores at a much greater density than the PET membrane. Moreover, the inserts contain holes in the sides that enables flow of medium between the interior of the insert and the well. The BRAND*plates*™ plate design also ensures greater availability of medium due to the merging of 4 adjacent wells which allows a greater volume of medium to be added. HEKn cultured using the BRAND*plates*™ system were observed to be better organised with more appropriate differentiation (Figure 5.5B). Given that the change in cells and insert design coincided, it was difficult to determine which alteration yielded the improved EE results observed. However, the combination of Lifeline® HEKn and BRAND*plates*™ produced far superior EEs to all previous attempts and thus these were both used for subsequent models for the rest of the project.

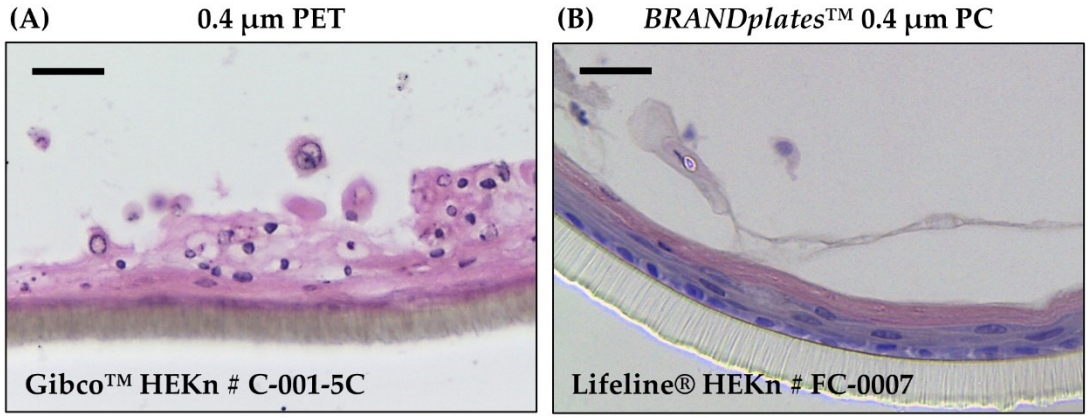

Figure 5.5 HEKn cultured on BRANDplates™ PC inserts produced superior EEs. (A) *Brightfield microscopy image shows a H&E stained section of a Gibco® HEKn model cultured on a PET membrane with 0.4 μm pores. Epidermal assembly is poor with abnormal differentiation and parakeratosis. Scale bar = 20 μm.* **(B)** *Brightfield microscopy image shows a H&E stained section of a Lifeline® HEKn model cultured on a BRANDplates™ PC inserts with 0.4 μm pores. Epidermal assembly was superior to previous models. Scale bar = 20 μm.*

Whilst the new Lifeline® HEKn BRAND*plates*™ model was significantly better in terms of thickness and organisation compared to previous EEs, there was still a lack of defined epidermal layers reflective of the *in vivo* tissue. In order to check the ability of these cells to assemble a realistic epidermal model, EEs were developed with a layer of Matrigel® added in place of the Gibco® Coating Matrix (Figure 5.6A). Matrigel® is an ECM mixture secreted by mouse tumour cells that is protein rich and

contains many factors found in the epidermal basement membrane such as laminin and collagen IV (Corning, 2021). H&E images of these models showed that the layer of Matrigel® added was too thick, meaning that cells had grown inside the gel rather than on top of it. However, by chance the cells appeared to have entered a bubble within the Matrigel®, providing them with the space to develop a full epidermal model with organised layers (Figure 5.6B). This confirmed that the Lifeline® HEKn were capable of fully differentiating *in vitro* and that it was likely the culture conditions of standard models that were hindering optimal EE development.

Figure 5.6 (overleaf) HEKn showed superior epidermal assembly in the presence of Matrigel®. (A) *1) Matrigel® was diluted 1:1 in medium (~4 – 6 μg final protein content), PC membranes were coated with 100 μl, and incubated for 75 min at 37°C; 2) 500,000 HEKn were seeded onto the coated membrane in 200 μl of medium and incubated for 2 hours at 37°C; 3) EEs were cultured at submerged stage for 4 days in 10 ml medium; 4) EEs were raised to ALI and cultured for 12 days in 3.5 ml medium. Medium was replaced every 48 hours.* **(B)** *Brightfield images show H&E stain of a sectioned EE model. HEKn exhibited superior epidermal assembly compared to previous models, demonstrating columnar basal cells (red arrows), flattening of cells in suprabasal layers (yellow arrows), and loss of nuclei in the stratum granulosum region (blue arrows). Scale bars = 20 μm.*

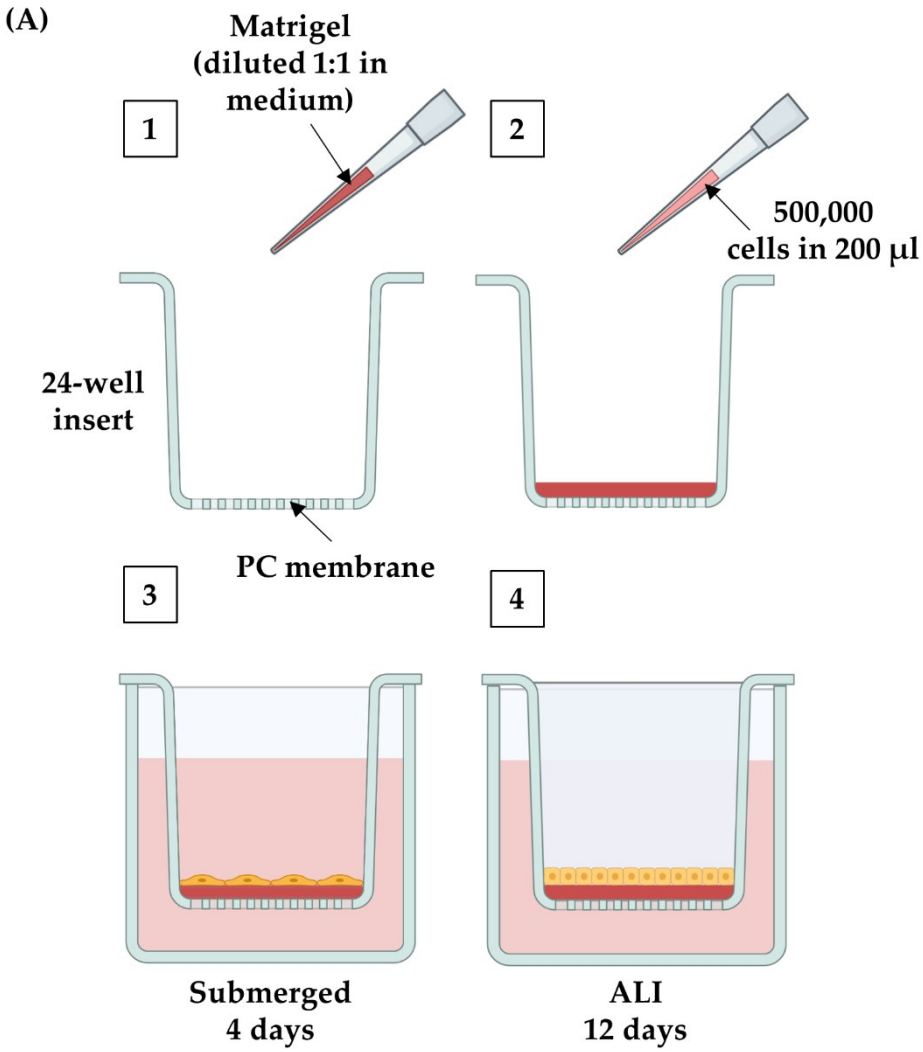
(A)
Matrigel
(diluted 1:1 in
medium)
1
2
500,000
cells in 200 µl
24-well
insert
PC membrane
3
4
Submerged
4 days
ALI
12 days

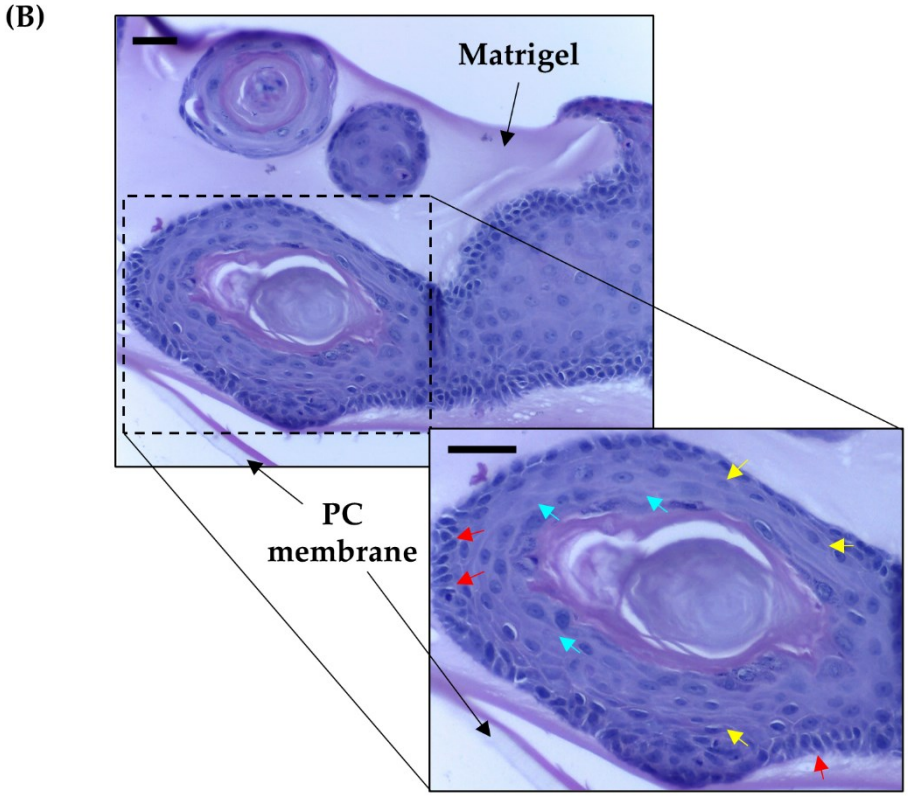
(B)
Matrigel
PC
membrane

5.4.2 Hanging drop spheroid models provided new insight into the effects of substrate stiffness on HEKn behaviour in 3D culture

At around the time that the final EE protocol was being established, it was decided to begin introducing HEKn primed on BM dishes to see what effect this had on model development. Up until this stage in the project only 4 kPa and 8 kPa dishes had been used for 2D culture, and thus 4 kPa was chosen due to its being the softest substrate. However, early attempts at utilising cells primed on 4 kPa dishes yielded thin and poorly developed EEs. Given all of the problems encountered whilst getting the TCP primed models to work, it was decided that the best option would be to temporarily remove the use of inserts altogether and find an alternate method to test the differences between TCP and 4 kPa primed cells in a 3D setting. As such, the hanging droplet technique was introduced with the aim being to develop 3D spheroid models.

For the first round of hanging drop experiments, HEKn were primed on either TCP or 4 kPa dishes for 4 days then seeded onto the lid of a petri dish in 10 μl droplets and imaged every few days using a dissecting microscope. It was observed that cells from neither dish type formed a spheroid, but TCP primed HEKn formed branch-like aggregated structures, whilst 4 kPa aggregation was more clustered towards the centre of the droplet (Figure 5.7). The next set of experiments involved the use of dermal spheroids which acted in place of an insert membrane to provide a foundation for HEKn to build an epidermal model around. Three-day old fibroblast spheroids were kindly donated by Melissa Jackson, who assisted with all elements of spheroid work. HEKn were then seeded into droplets containing a single dermal spheroid and imaged every few days using a dissecting microscope. HEKn primed on TCP were observed to have coated the dermal spheroid at day 3, though the structure of this keratinocyte layer was more fragmented by day 7 (Figure 5.8). However, 4 kPa

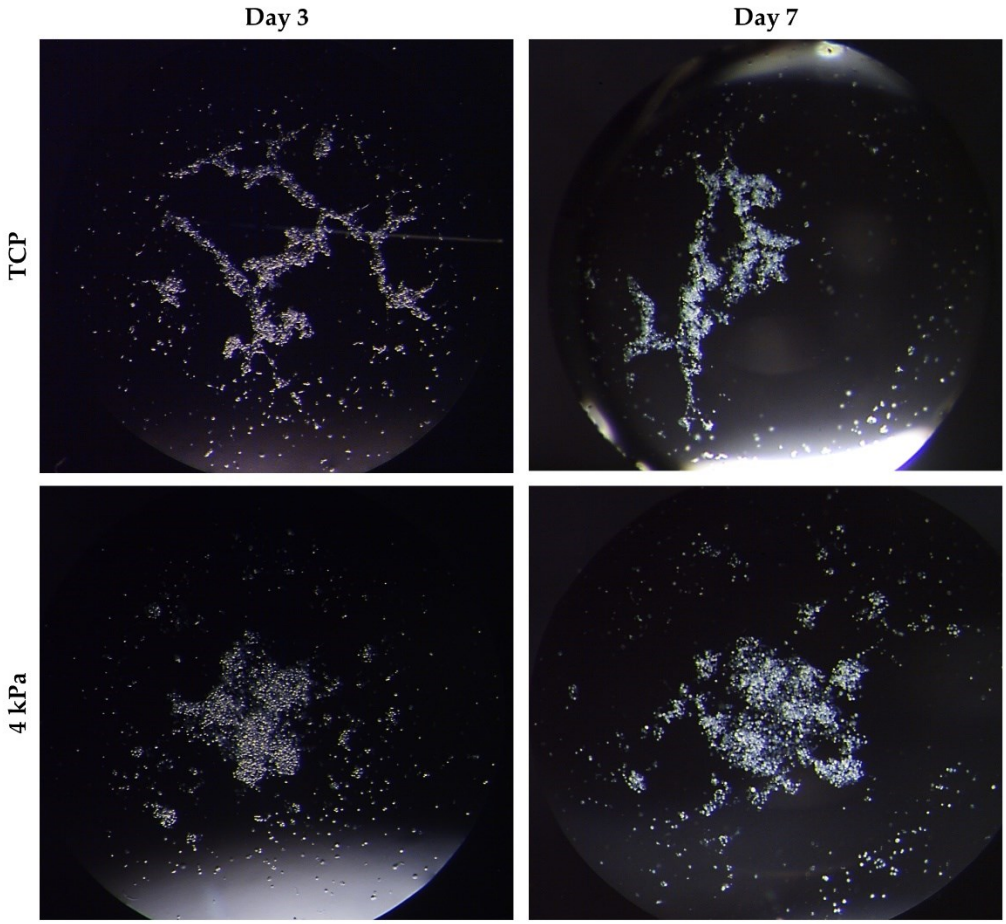

Figure 5.7 HEKn primed on TCP and 4 kPa BM dishes showed different aggregation patters when transferred into hanging droplets. *HEKn were primed on TCP or 4 kPa dishes then transferred into 10 µl hanging droplets. Darkfield dissecting microscope images show hanging droplets containing HEKn primed for 4 days on either TCP or 4 kPa BM dishes. Photos were taken 3 and 8 days after hanging droplets were seeded. Droplets contained 10 µl medium and were approximately 3 mm in diameter.*

primed HEKn did not appear to coat the dermal spheroid at all and were instead observed to localise in the medium surrounding the spheroid (Figure 5.8). This began the early hypothesis that 4 kPa may be too soft a substrate to promote a basal cell phenotype. In order to better visualise the HEKn that had coated the dermal spheroids, and to confirm that there was no attachment by the 4 kPa primed cells, spheroids were harvested and embedded into OCT to be assessed through immunofluorescence. Spheroids were stained for the fibroblast marker vimentin, and F-actin. It was observed that HEKn primed on TCP did coat the fibroblast spheroid, albeit in a thin layer, whilst 4 kPa primed HEKn did not coat the dermal spheroid at all (Figure 5.9).

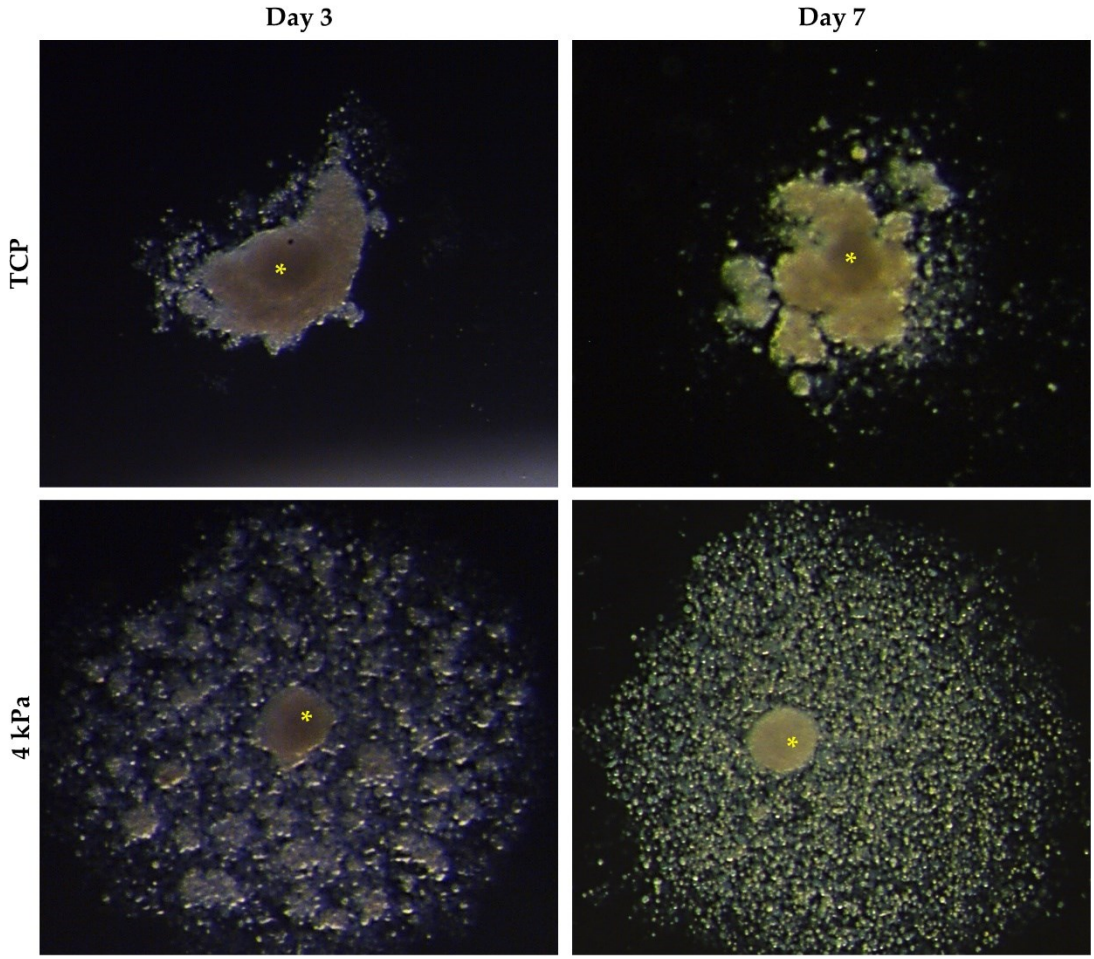

Figure 5.8 HEKn primed on 4 kPa BM dishes were unable to coat a dermal spheroid when transferred into hanging droplets. *HEKn were primed on TCP and 4 kPa dishes before being transferred into hanging droplets containing a dermal spheroid. Darkfield dissecting microscope images show dermal spheroids (yellow asterisk) co-cultured with HEKn primed on either TCP or 4 kPa BM dishes. HEKn primed on TCP dishes were observed to coat the dermal spheroid and form a bilayer, whilst those primed on 4 kPa dishes did not. Photos were taken 3 and 8 days after HEKn were seeded into hanging droplet containing a dermal spheroid. Droplets contained 20 µl medium and were approximately 5 mm in diameter.*

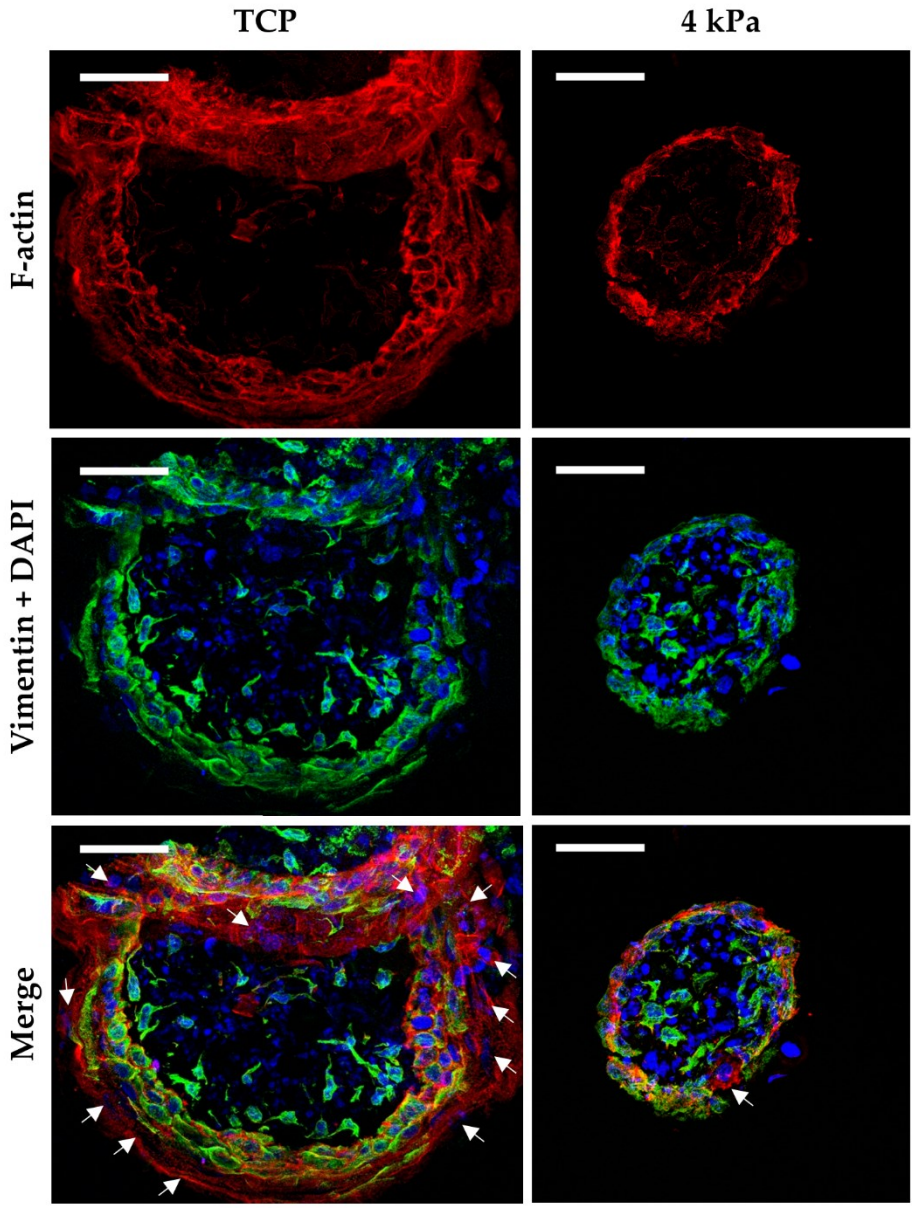

Figure 5.9 Immunofluorescence analysis of hanging droplets confirmed HEKn primed on 4 kPa did not coat dermal spheroids. *Spheroids were harvested from hanging droplets and embedded in OCT and cryosection then stained for F-actin and vimentin (fibroblast marker). Confocal microscopy images show that HEKn primed on TCP coated the dermal spheroid (white arrows), whilst those primed on 4 kPa did not (white arrow shows single keratinocyte cell). Scale bars = 50 μm.*

The next decision regarding the spheroid work was to introduce high calcium medium since calcium plays such a key role in epidermal differentiation, and high calcium conditions were used during the ALI stage of the insert protocol. HEKn were primed on TCP and 4 kPa under low calcium conditions then seeded into hanging droplets containing a single dermal spheroid using medium with either low (60 μM)

or high (1.5 mM) concentrations of $CaCl_2$. An immediate difference in aggregation around the dermal fibroblast was observed, with both TCP and 4 kPa primed HEKn forming a thick spheroid around the existing dermal spheroid (Figure 5.10). However, because the spheroids were so big, harvesting them for immunofluorescence analysis proved difficult, and the structure of the aggregates was found to be relatively fragile which meant too much manipulation caused them to fall apart. As such, a more in-depth analysis of the structure of the spheroids was not possible.

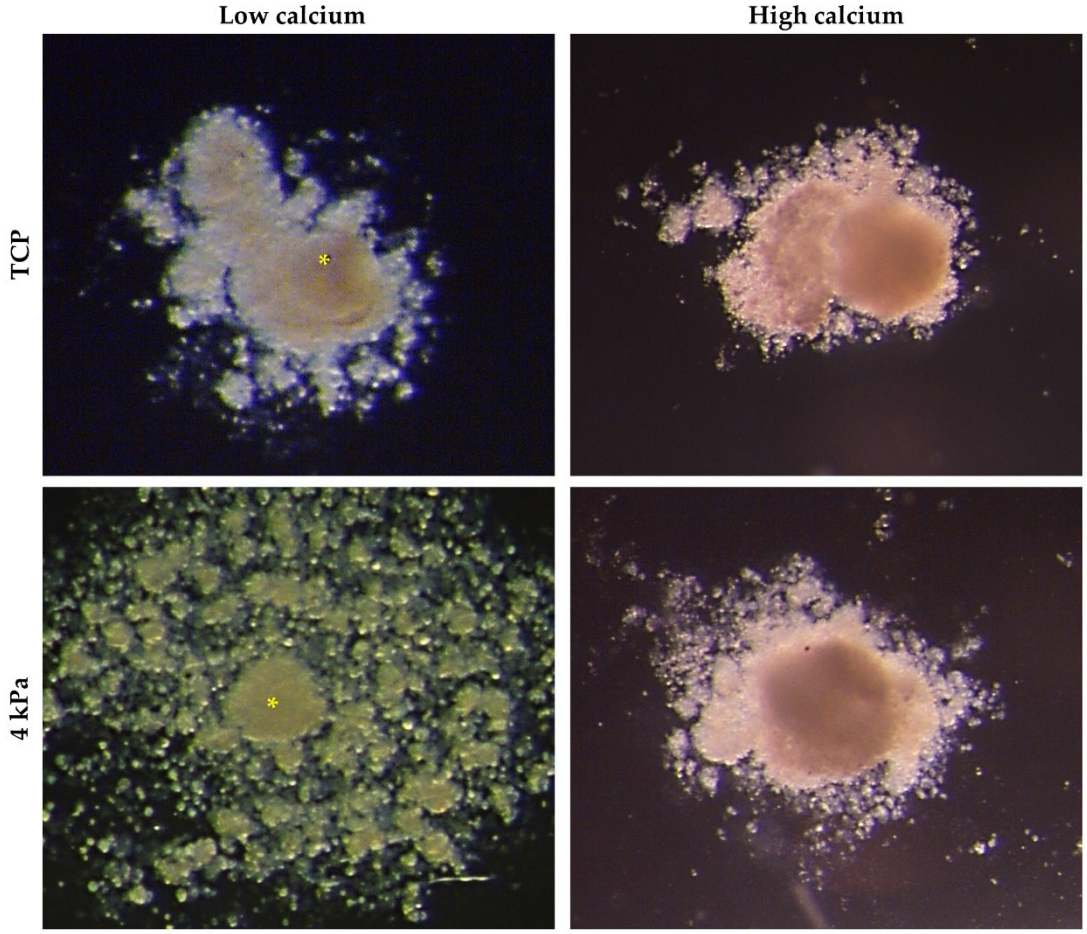

Figure 5.10 HEKn cultured in hanging droplets of high calcium medium were better able to coat a dermal spheroid. *HEKn were primed on TCP and 4 kPa dishes before being transferred into hanging droplets containing a dermal spheroid. Droplets contained either low calcium medium (60 μM $CaCl_2$) or high calcium medium (1.5 mM $CaCl_2$). Darkfield dissecting microscope images show that high calcium medium greatly improved the aggregation of 4 kPa primed HEKn around a dermal spheroid. Droplets contained 20 μl medium and were approximately 5 mm in diameter.*

Given that the epidermal/dermal bilayer spheroids were too difficult to embed, it was decided that the next step should be to try culturing the HEKn alone again, but this time in high calcium medium to see whether this improved aggregation. Moreover, given the intriguing differential aggregation patterns observed when HEKn were primed on TCP versus 4 kPa dishes, it was decided to investigate what would happen if the cells were combined in a droplet. HEKn were primed on TCP and 4 kPa dishes for 4 days, then seeded in 10 μl droplets in high calcium medium either individually or at a 1:1 ratio. Once again, the changes in aggregation were notable compared to low calcium (Figure 5.7), with TCP primed cells forming a single dense aggregate and 4 kPa forming several large dense aggregates across the droplet (Figure 5.11). Interestingly, combining the cells seemed to "rescue" the 4 kPa primed cells so that they once again formed a single dense aggregate. However, rather than forming spheroids, all cell combinations appeared to aggregate in a flat disc shape, and therefore could not be embedded and analysed beyond a visual assessment in culture.

Nonetheless, observing the cells in culture was enough to identify a new feature of the combined cell aggregates that was consistently observed. In aggregates where TCP and 4 kPa primed cells were mixed, a transparent layer was visible around the outer edge (Figure 5.11, black arrows). Following the initial co-culture of HEKn with dermal spheroids (Figure 5.8) it was hypothesised that 4 kPa may potentially be too soft to promote a basal cell phenotype and could instead push cells towards differentiation. As a result, it was further hypothesised that the transparent layer might be a stratum corneum, suggesting that when combined the cells were able to organise themselves and assemble an epidermal structure. Given the inability to embed the aggregates for further investigation, a cell tracker was used to try and identify where the HEKn primed on the 4 kPa dishes were located in the final aggregate. However, problems were encountered with the cell tracker being too bright, and Hoechst staining being too dim to identify the non-tracked HEKn and thus it was not possible to get quality images to analyse. Given the time-constraints of the project and the primary interest of P&G in EEs cultured on inserts, it was not

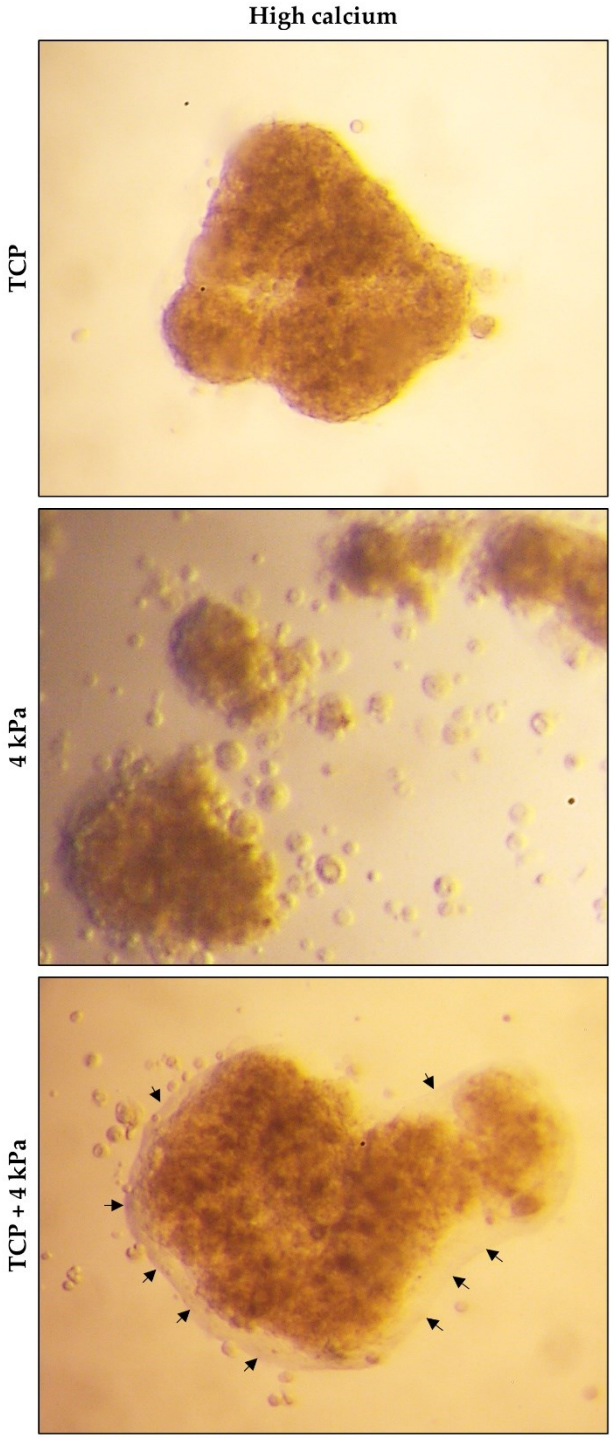

Figure 5.11 Culturing TCP and 4 kPa primed HEKn in the same hanging droplet may lead to organised epidermal assembly under high calcium conditions. *HEKn were primed on TCP or 4 kPa BM dishes then transferred into hanging droplets in high calcium medium (1.5 mM $CaCl_2$). Brightfield dissecting microscope images show that TCP primed HEKn formed a single aggregate, whilst 4 kPa primed HEKn formed multiple smaller aggregates. Mixing HEKn primed on TCP and 4 kPa dishes together resulted in a single aggregate possessing a transparent outer layer (black arrows) which could indicate the presence of a stratum corneum. Droplets contained 10 µl medium and were approximately 3 mm in diameter.*

deemed essential to devote time to troubleshooting this issue, and the spheroid work was not pursued beyond this point.

5.4.3 HEKn primed on 50 kPa BM dishes produced thicker and more organised EEs

Following the work with the hanging droplet spheroid models, it had begun to become clear that 4 kPa primed HEKn were potentially too soft to be reminiscent of basal cell keratinocytes. This hypothesis was further explored and to some extent confirmed by the experiments discussed in chapters 3 and 4. It was at this stage in the project that the 50 kPa BM dishes were introduced to the study, having previously been considered too stiff; 50 kPa has been measured as the elastic Modulus of the Descemet's membrane of the corneal endothelium, which is a significantly harder tissue than the skin (Last et al., 2012). However, a study in 2016 measured the Young's Modulus of the dermal-epidermal interface of dermal explants to be around 48.09 kPa (Kao, Connelly and Barber, 2016). Thus, the 50 kPa dishes were deemed an appropriate addition to the study.

In order to draw a direct comparison between 50 kPa and 4 kPa dishes, HEKn were primed on TCP, 50 kPa and 4 kPa dishes for 4 days then seeded onto BRAND*plates*™ inserts and cultured as described in chapter 2 (2.2.2). H&E staining of the sectioned models revealed that 50 kPa primed HEKn produced a far superior EE in comparison to the TCP and 4 kPa primed. 50 kPa HEKn models appeared thicker and had a much more *in vivo*-like organisation with a defined basal layer and flattening of

Figure 5.12 (overleaf) HEKn primed on 50 kPa BM dishes produced thicker EEs than TCP and 4 kPa dishes. *HEKn were primed on TCP, 50 kPa and 4 kPa dishes then cultured into 3D epidermal models.* **(A)** *Brightfield images of sectioned H&E stained human epidermis and laboratory generated EEs show that HEKn primed on 50 kPa produced more organised epidermal layers that appeared thicker. Scale bars = 20 μm. Epidermis image taken from Masters thesis http://etheses.dur.ac.uk/12341/.* **(B)** *Quantification of the thickness of epidermal equivalents (measured from top of membrane to bottom of stratum corneum). Data represent mean ±SEM, n = 3, statistical significance was assessed using one-way ANOVA with Tukey's post hoc test, *** $p \leq 0.0001$.*

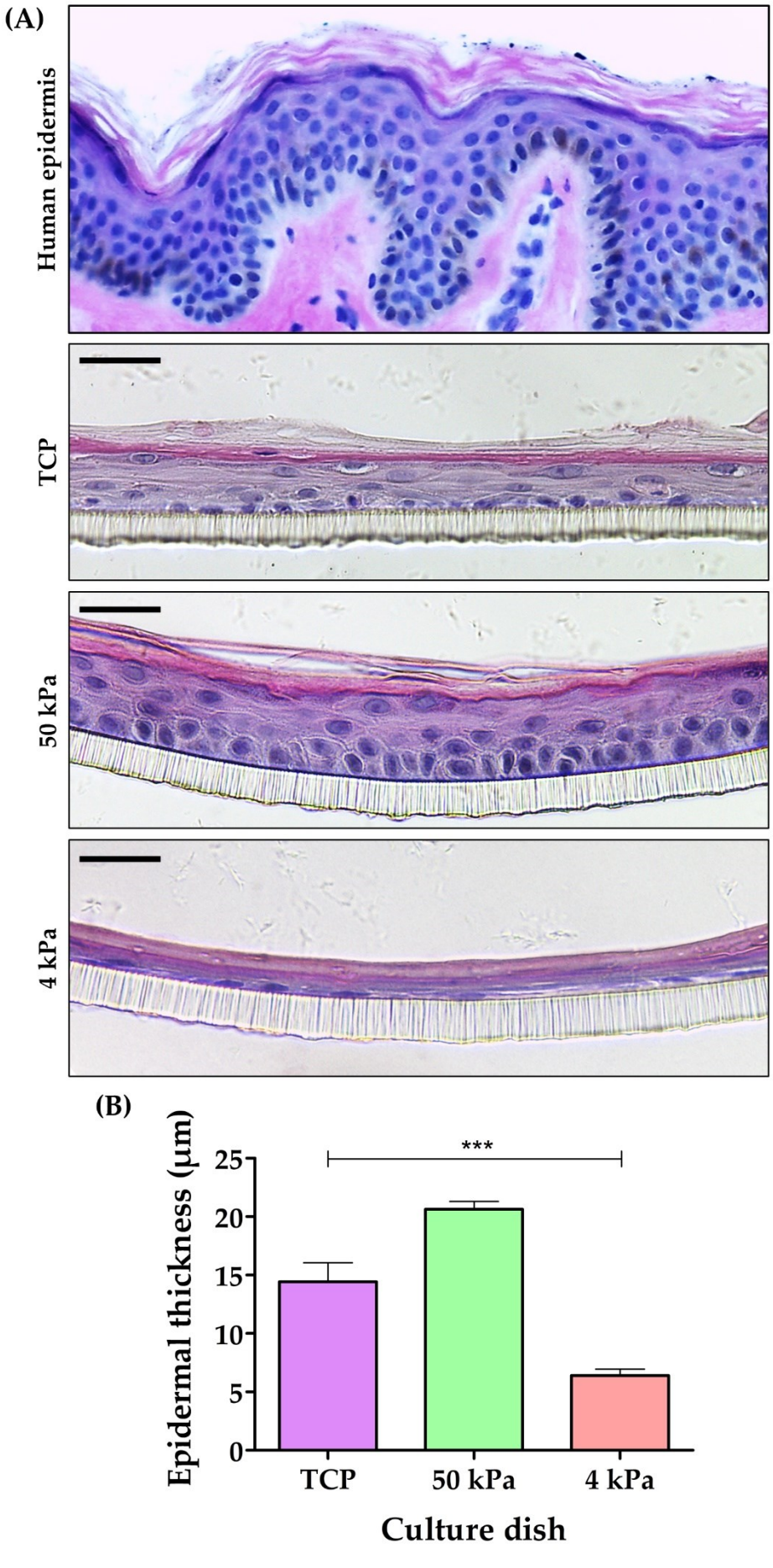
(A)
Human epidermis
TCP
50 kPa
4 kPa
(B)
Epidermal thickness (μm)
25
20
15
10
5
0
***
TCP
50 kPa
4 kPa
Culture dish

keratinocytes as they moved upward in the model, making them far more reflective of human *in vivo* epidermis than the TCP and 4 kPa models (Figure 5.12A). Quantification of the thickness of the models confirmed that 50 kPa primed HEKn produced EEs that were significantly thicker than the other conditions, particularly compared to 4 kPa which produced EEs that were around 70% thinner than 50 kPa (Figure 5.12B).

Immunofluorescence analysis was used to characterise the models further and draw more detailed comparisons between TCP and 50 kPa primed EEs. Models were stained for the proliferation marker CK14 and the differentiation marker CK10. Both TCP and 50 kPa primed EEs had the correct localisation of these proteins, with CK14 confined mainly to the basal layer with staining in the odd suprabasal cell, and CK10 found in all layers except the basal layer (Figure 5.13A). Given the distinct CK14 staining in the basal layer, it was possible to see that the shape of the basal cells was different between the two different models. Basal cells in the TCP primed model appeared quite flat, whilst those in the 50 kPa model were more cuboidal or columnar in shape (Figure 5.13A). Quantification of the number of basal cells per 100 μm revealed that TCP primed models had fewer cells, which supported that cells were flatter and therefore took up more space (Figure 5.13B).

In addition to CK14 and CK10, the EEs were stained for E-cadherin to assess cell-cell connections within the model, and p63 to look at how prevalent proliferative keratinocytes were and where they were located. E-cadherin staining in TCP primed EEs was observed to be unevenly distributed throughout the model, with individual cells being difficult to distinguish. In contrast, 50 kPa primed models showed bright, regular E-cadherin staining throughout all layers, and the outline of individual cells was clear (Figure 5.14). p63 staining was observed in all basal cells and a number of suprabasal cells in both TCP and 50 kPa primed models, with no apparent differences between the two (Figure 5.14).

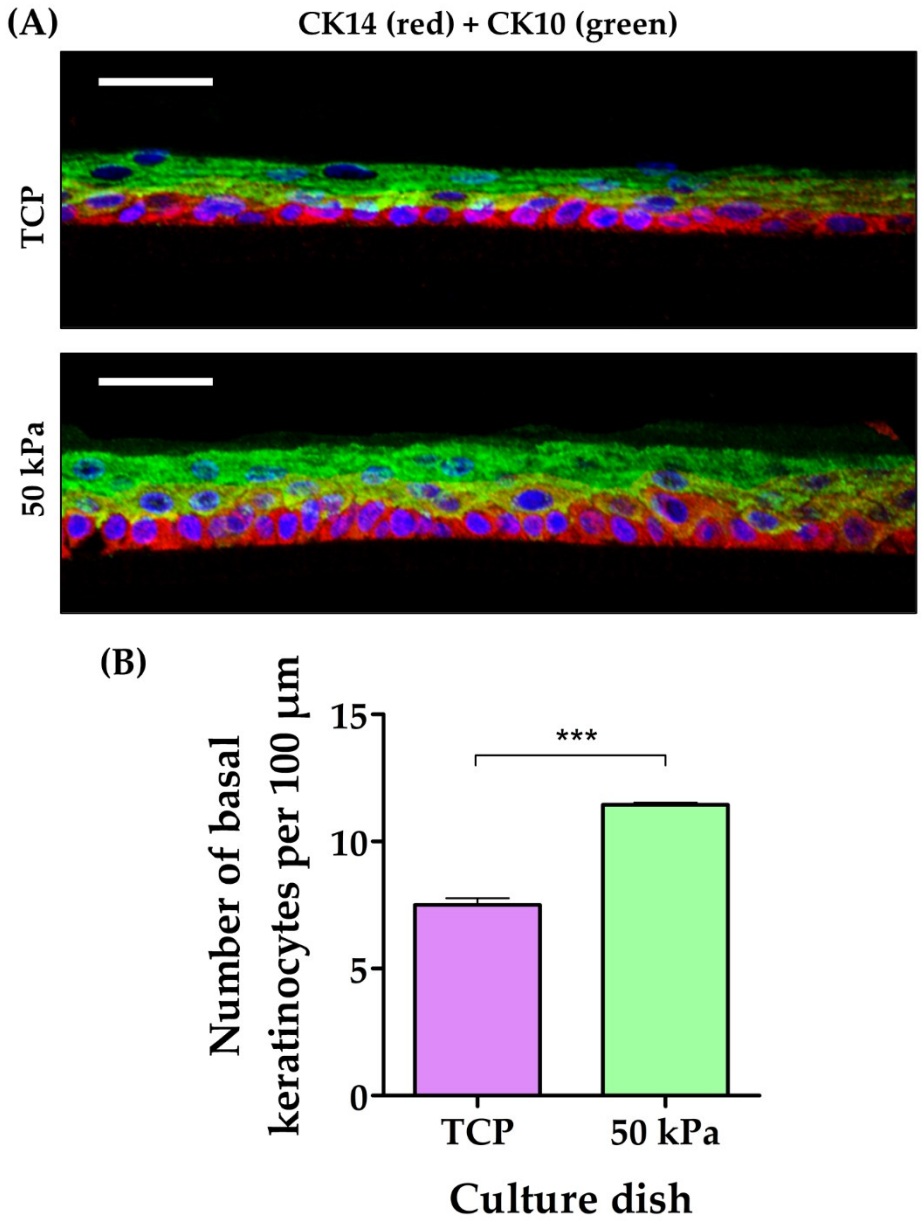

Figure 5.13 HEKn primed on 50 kPa dishes had more columnar basal cells than those on TCP in EEs. *HEKn were primed on TCP and 50 kPa dishes then cultured into 3D epidermal models.* **(A)** *Confocal microscopy images show staining for basal cell marker CK14 (red) and differentiation marker CK10 (green) was localised to the right layers in EEs. The basal cells of EEs formed from 50 kPa HEKn appeared more columnar, whilst those from TCP were flatter and more spread out. Scale bars = 20 µm.* **(B)** *Quantification of the number of basal cells per 100 µm. Data represent mean ±SEM, n = 3, statistical significance was assessed using one-way ANOVA with Tukey's post hoc test, *** $p \leq 0.0001$.*

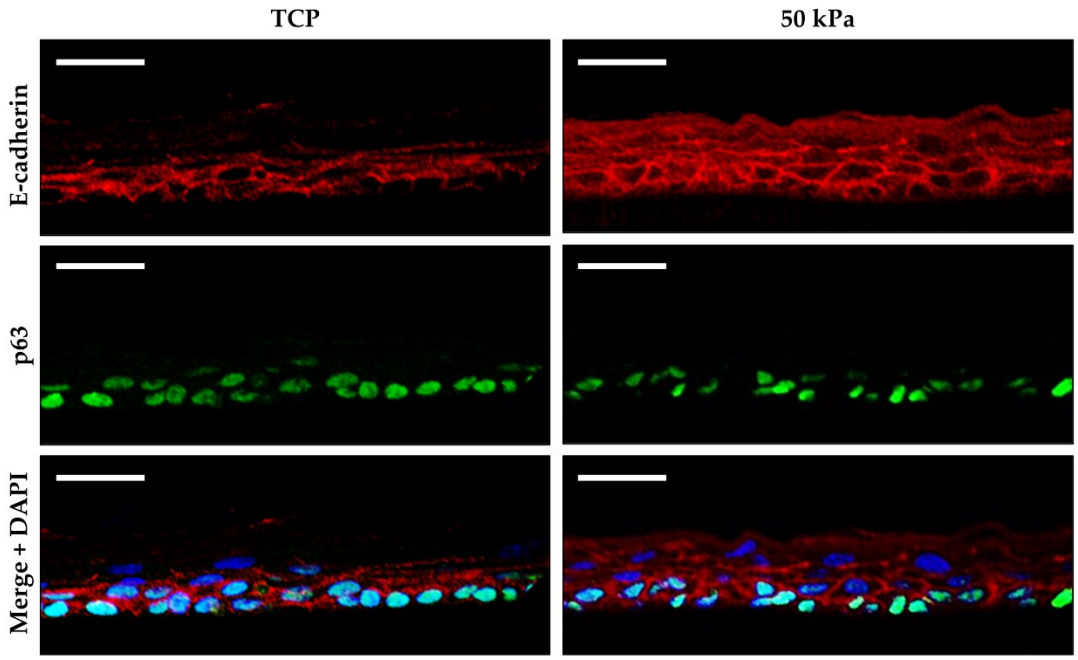

Figure 5.14 HEKn primed on 50 kPa dishes had more defined epidermal layers and clearer E-cadherin staining in EEs. *HEKn were primed on TCP and 50 kPa dishes then cultured into 3D epidermal models. Confocal microscopy images show more regular E-cadherin staining and clearer distinction of epidermal layers in HEKn primed on 50 kPa dishes. Proliferation marker p63 was expressed in basal cell nuclei for both TCP and 50 kPa primed HEKn. Scale bars = 20 μm.*

Whilst the data shown in Figures 5.11 – 5.13 shows exciting evidence that 50 kPa priming can improve *in vitro* EE development, all subsequent experiments on the epidermal models were beset by repeated issues with model quality. Whilst there was still a distinct organisational difference between TCP and 50 kPa primed cells, the 50 kPa models never reached the same level of organisation and thickness as was observed in the models seen in Figures 5.11, 5.12 and 5.13. Whilst this was greatly frustrating, attempts at troubleshooting yielded no improvement and the time constraints of the project meant that it was necessary to work with the models produced regardless of their appearance. Consequently, it is acknowledged that much of the rest of the data presented in this chapter is obtained from suboptimal models and will need to be repeated in the future to obtain more conclusive results and publishable material. However, that is not to say that these experiments did not add value to the overall project and the data obtained were still promising.

5.4.4 Assessing barrier function proved difficult with the BRAND*plates*™ system

The next step in characterising the EEs developed from TCP and 50 kPa primed HEKn was to try and assess barrier function. In the literature one of the most standardised and "user friendly" techniques to assess skin barrier function is to perform a Lucifer Yellow assay (Schmitz et al., 2015). Lucifer Yellow fluorescent dye is applied to the top of the model and can then be viewed under a fluorescent microscope to assess how far the dye has penetrated from the surface. A good epidermal model should have penetration of the dye beyond the stratum corneum.

A Lucifer Yellow assay was therefore performed on TCP and 50 kPa primed models. However, technical problems were immediately encountered as a result of the BRAND*plates*™ insert design. Lucifer Yellow dye was added to the top of models at the end of the ALI stage, and they were incubated for an additional 2 hours at 37°C. However, due to the holes in the sides of the inserts, the dye immediately escaped from the internal insert compartment and contaminated the medium (Figure 5.15A), allowing the dye to enter the model through the pores of the PC membrane and stain the cell layers from the bottom (Figure 5.15B). In order to combat this, the experiment was repeated and parafilm was wrapped around the inserts to try and seal the dye into the insert. This prevented initial leakage but after the 2-hour incubation period the medium was slightly contaminated (Figure 5.15A), which resulted in the staining of a number of basal and suprabasal cells in the model (Figure 5.15B).

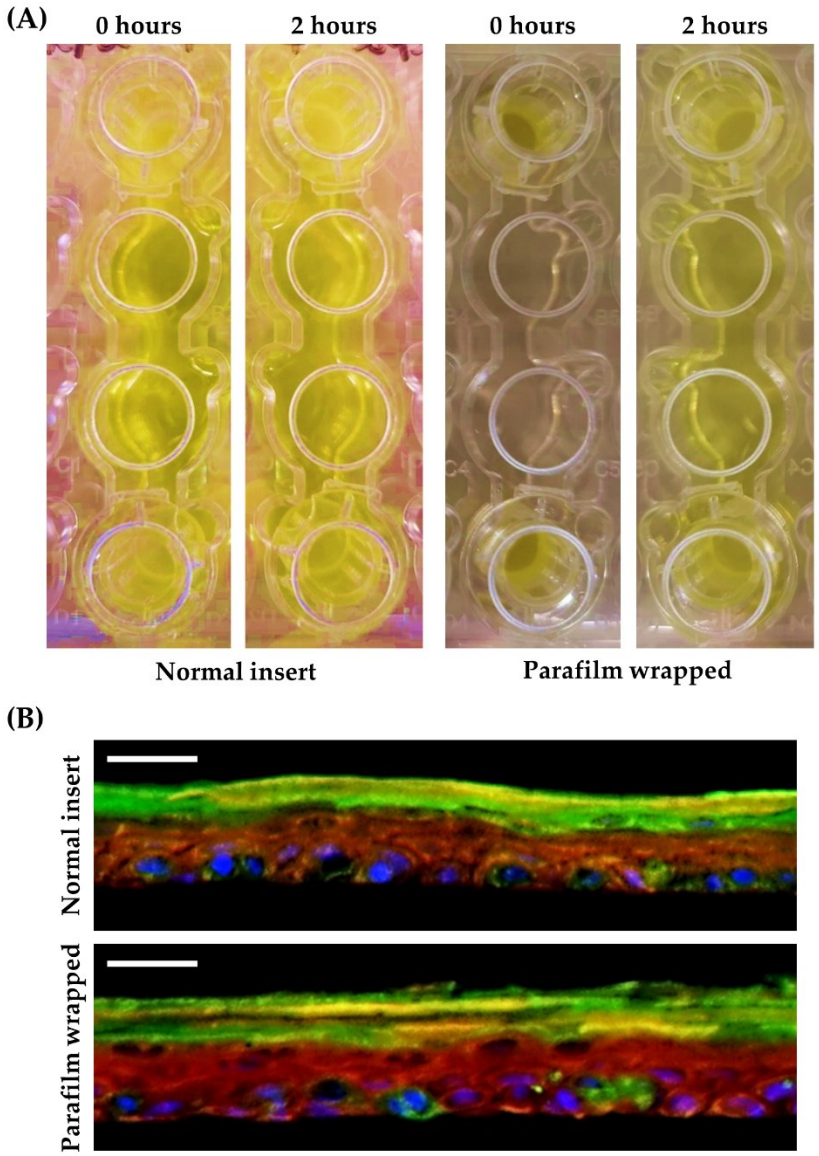

Figure 5.15 Lucifer Yellow barrier function assay was difficult using the BRANDplates™ culture system. *Barrier function of EEs was assessed by adding Lucifer Yellow dye to the surface of the model.* **(A)** *The holes in the BRANDplates™ inserts meant Lucifer Yellow dye immediately leaked into the medium. Wrapping parafilm around the inserts prevented immediate leakage but there was still some contamination to the medium after 2 hours.* **(B)** *Microscopy images (imaged on Zeiss Axioskop) show that Lucifer Yellow penetrated all layers of the model. Scale bars = 20 μm.*

Given the inability to seal off the inserts, it was decided that the only way to fully rule out contamination from below the models was to remove the medium from the wells. Whilst the lack of medium for 2 hours may have an effect on the cells, it was not considered a risk to the barrier function of the model which was the only thing to be assessed with this experiment. As a result, the experiment was repeated without

medium in the wells, and it was observed that both TCP and 50 kPa primed models had good barrier function, with Lucifer Yellow being contained to the stratum corneum and not penetrating the cell layers (Figure 5.16).

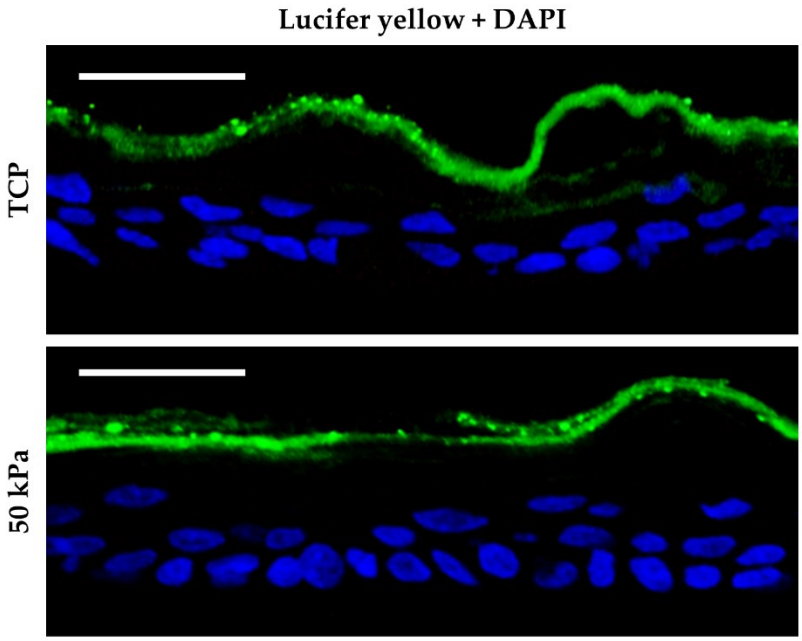

Figure 5.16 HEKn primed on 50 kPa dishes had the same barrier function as TCP. *HEKn were primed on TCP and 50 kPa dishes then cultured into 3D epidermal models. Lucifer Yellow fluorescent dye was applied to the surface of the model to assess barrier function. Confocal microscopy images show that Lucifer Yellow did not penetrate beyond the stratum corneum for either TCP or 50 kPa primed models. Scale bars = 20 μm.*

5.4.5 HEKn primed on 50 kPa dishes were more responsive to extended time at ALI during EE development

One of the most striking differences observed in 50 kPa primed EEs compared to TCP primed was the increased thickness and organisation of the models. This raised the question of whether 50 kPa models would always be superior, or if the models merely developed faster and TCP primed HEKn would be able to reach similar levels of organisation if given more culture time. As such, TCP and 50 kPa primed models were set up and half were cultured for the standard 12 days at ALI whilst the rest were taken up to 18 days at ALI. Comparison of the models revealed that both TCP and 50 kPa primed models were suboptimal at 12 days, but extended culture time still yielded changes in model development. TCP primed EEs showed slight model

thickening and more obvious cell layers after 18 days at ALI compared to 12 days (Figure 5.16). However, 50 kPa primed EEs exhibited a striking change, going from a similar level of thinness and cell flattening at day 12 as the TCP models, to a thicker model with a clearly defined columnar basal cells, and multiple epidermal layers at day 18 (Figure 5.17). This result therefore suggested that priming HEKn on 50 kPa dishes gives them a superior ability to undergo epidermal assembly that TCP primed cells cannot catch up to.

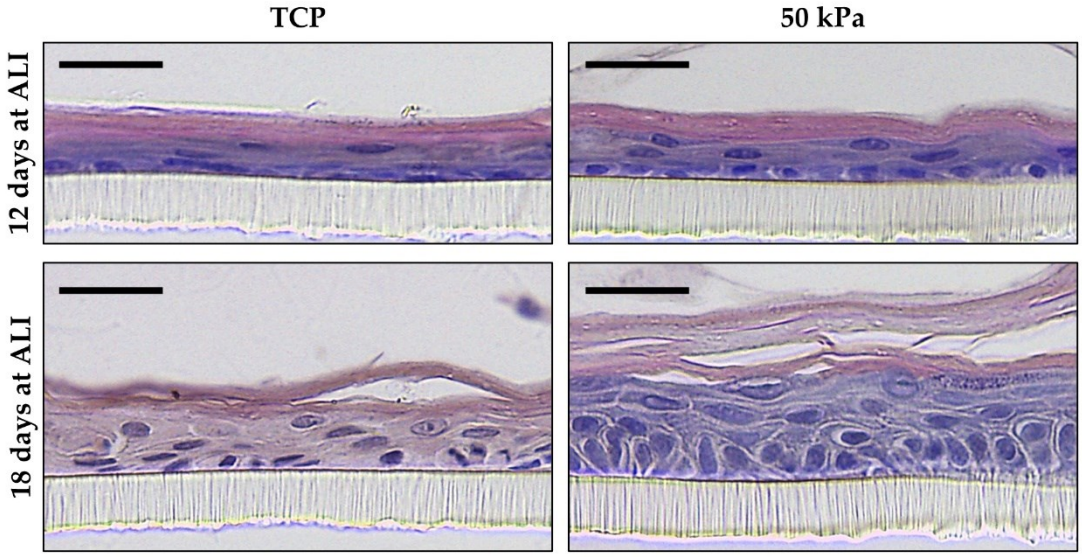

Figure 5.17 HEKn primed on 50 kPa BM dishes showed greater improvement following longer culture time at the ALI. *HEKn were primed on TCP and 50 kPa dishes then cultured into 3D EEs. Brightfield microscopy images of H&E stained EE sections show that models made from 50 kPa primed HEKn responded more readily to a longer culture time at ALI. Scale bars = 20 μm.*

5.4.6 Combining 50 kPa and 4 kPa primed HEKn did not produce optimal EEs

Earlier in this chapter we looked at what happened when TCP and 4 kPa primed HEKn were combined in hanging droplets and considered the hypothesis that the cells were able to organise themselves based to optimise epidermal assembly (Figure 5.11). With this in mind, it was decided to combine 50 kPa and 4 kPa primed cells in BRAND*plates*™ inserts to see whether they could produce a superior model. HEKn primed on 50 kPa dishes were seeded onto inserts and cultured at the submerged stage for 4 days. Cells primed on 4 kPa dishes were then seeded on top and the

models were raised to the ALI. The resulting models were far inferior to 50 kPa alone but did show a marked improvement compared to the 4 kPa only models, with a clear basal layer made up of rounder cells and an additional suprabasal layer (Figure 5.18). It was concluded from this preliminary experiment that the 4 kPa cells had been added too soon, and the 50 kPa primed cells would have benefited from a few days at the ALI to enable them to arrange a better foundation layer of basal and suprabasal cells on which the 4 kPa cells could build from. However, optimisation of this protocol was likely to be time consuming, and due to time constraints and the necessity to finalise other experiments, it was decided that this should be highlighted as a future experiment for anyone following on from this project.

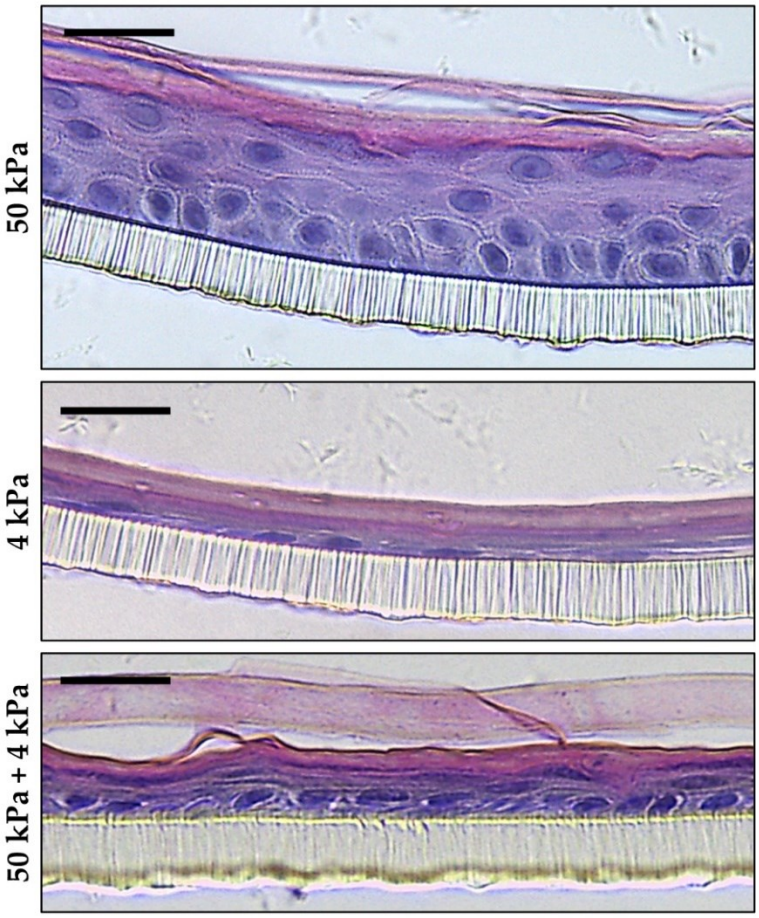

Figure 5.18 Mixing 50 kPa and 4 kPa primed HEKn produced an EE of intermediate quality. *HEKn were primed on 50 kPa and 4 kPa BM dishes then cultured into 3D EEs. Brightfield microscopy images of H&E stained sections show that combining 50 kPa and 4 kPa primed HEKn produced an epidermal model that had a more defined basal layer than 4 kPa alone but was far inferior in thickness and organisation to 50 kPa alone. Scale bars = 20 μm.*

5.5.7 Pre-screening HEKn for basal phenotype cells greatly improved organisation of TCP primed EEs

During model development, one of the things that was considered when facing problems with suboptimal EEs was whether the cells themselves were appropriate for epidermal assembly. It is well established that not all primary keratinocytes produce the same standard of *in vitro* models as a result of donor and skin source variability (Poumay and Coquette, 2007; Smits et al., 2017). One of the potential reasons for this is that primary keratinocytes are isolated from the entire epidermis, and this not all of the cells present in a purchased vial are of a basal phenotype. In 2017, a study explored different methods of isolating keratinocyte stem cells from transitory amplifying cells which arise from keratinocyte stem cell differentiation (Metral et al., 2017). It was therefore decided to incorporate one of these methods into the EE protocol to see whether this had an effect on epidermal assembly. The first experiment carried out was to prime HEKn on TCP and 50 kPa dishes, then pre-screen TCP primed HEKn for basal phenotype cells before seeding them onto a model. To do this, a dish was coated with Gibco™ Coating Matrix and after being dissociated from the TCP, HEKn were seeded onto the coated dish and incubated for 10 min. After 10 min, any cells that had adhered to the dish were dissociated and it was this pool of cells alone that were seeded onto the insert.

The result of this pre-screening process was a model that lay somewhere in the middle of the TCP and 50 kPa primed EEs. TCP pre-screened models were observed to be of a similar thickness to normal TCP models, but the organisation of the basal and suprabasal layers was more reflective of the 50 kPa primed models (Figure 5.19). This was further highlighted through immunofluorescence analysis, which showed that TCP pre-screened models had more cuboidal basal cells compared to normal TCP, and the E-cadherin staining was much more regular across all layers, with defined cell membrane staining for individual cells similar to the 50 kPa models (Figure 5.19).

The results of this initial pre-screening assessment suggested that 50 kPa dishes might already select for basal cell phenotype, or that the rate of terminal differentiation may

be slower as a result of reduced proliferation, which could explain the improved models observed following 50 kPa priming. In order to test the effect that pre-screening had on 50 kPa primed HEKn, the experiment was repeated and TCP and 50 kPa pre-screened cells were directly compared. Frustratingly, both the TCP and 50 kPa models set up using the standard protocol were far from optimal, which made it difficult to determine the full impact that pre-screening had on model development. However, it was still possible to see that pre-screening had a marked improvement on the organisation of TCP primed EEs but had no significant impact on the appearance of the 50 kPa primed models (Figure 5.20). Whilst this experiment definitely warrants repeating due to the poor quality of the controls, it is possible to tentatively conclude that pre-screening for basal keratinocytes had no impact on the appearance of EEs developed from 50 kPa primed HEKn.

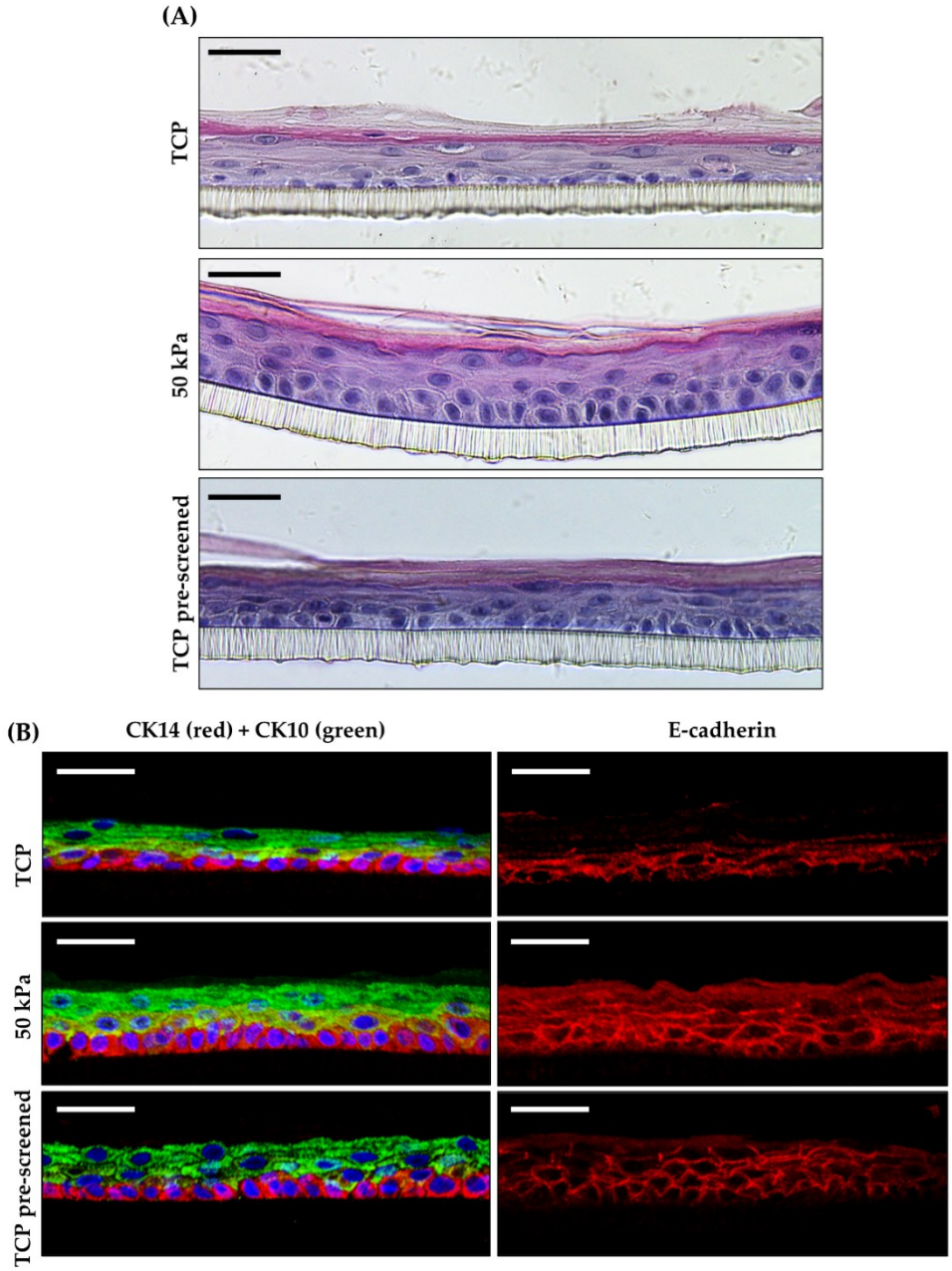

Figure 5.19 EEs produced from TCP primed HEKn pre-screened for basal cell phenotype cells produced more organised models that were reminiscent of 50 kPa primed. *HEKn were primed on TCP and 50 kPa dishes and cultured into 3D EEs. A portion of TCP primed HEKn were pre-screened for basal cell phenotype before being seeded onto models.* **(A)** *Brightfield microscopy images of H&E stained sections show that pre-screened TCP cells had better cell layer organisation than non-screened and were more similar to 50 kPa EEs. Scale bars = 20 μm.* **(B)** *Confocal microscopy images show that TCP pre-screened models had a less flattened basal layer, more defined layers, and more consistent E-cadherin staining throughout compared to non-screened TCP. Scale bars = 20 μm.*

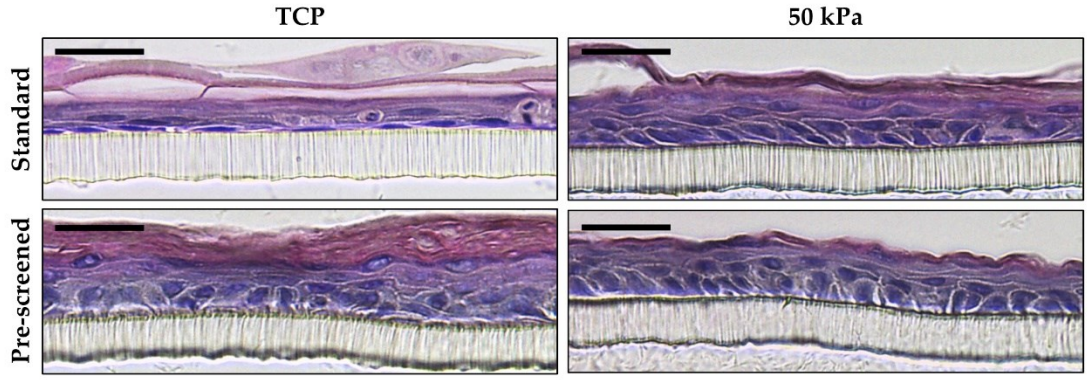

Figure 5.20 HEKn primed on 50 kPa dishes did not seem affected by pre-screening for basal cells. *HEKn were primed on TCP and 50 kPa dishes then cultured into 3D EEs following either the standard seeding protocol or the pre-screening protocol. Brightfield microscopy images of H&E stained sections show that pre-screening TCP primed HEKn produced thicker, slightly more organised models whilst pre-screening 50 kPa had little effect. Scale bars = 20 μm.*

5.5 Discussion

In this chapter the main objective was to assess whether culturing HEKn in a more *in vivo*-like mechanical environment at the 2D stage would promote the production of 3D epidermal models that better replicated native human skin. Whilst epidermal models have undergone significant improvement since their initial development in the 1990s, they are still known to exhibit abnormal expression of protein markers associated with keratinocyte activation and hyperproliferation (Simard-Bisson et al., 2018; Smiley et al., 2005; Smiley et al., 2006). Given that stiff substrates are known to promote cell proliferation (Dupont et al., 2011), it is not surprising that models produced using cells primed on TCP would be hyperproliferative. As such, one objective was to determine whether culturing HEKn on BM dishes prior to setting up epidermal models promoted a better balance between proliferation and differentiation, thus improving their appearance and expression profiles. Additionally, one of the main limitations 3D tissue models face is the time taken to produce them, which is a particular problem in a commercial setting where fast high throughput is a requirement. Another objective was therefore to assess whether priming HEKn on BM dishes could produce a better model more quickly than those made from TCP primed cells.

Whilst the objectives for this chapter targeted interesting topics of research, it has likely already been noted that the results obtained by no means fully address these early questions. As shown in multiple figures, the experiments carried out for this chapter were beset by numerous technical problems, primarily with the production of high-quality models that were a frustrating hindrance to the level of investigation desired. Consequently, it is acknowledged that this chapter is by no means as strong as it could have been, though it did yield some tantalisingly promising results that definitely warrant further research.

5.5.1 Early experiments focused on troubleshooting the development of EEs produced from TCP primed HEKn

Early experiments for this chapter focused on producing a robust epidermal model with TCP primed keratinocytes so that there was a solid foundation from which to begin further assessment. However, problems were immediately encountered due to poor epidermal assembly by the keratinocytes used. The initial batch of HEKn used were Gibco® HEKn (Cat # C-001-5C) with lot # 1776789 shown in Figure 5.2, though several lot numbers were assessed. Models created using these cells were consistently poor, exhibiting detachment from the PC membrane, poor differentiation, and parakeratosis. As mentioned in the introduction to this chapter, not all keratinocytes are able to differentiate to form a stratified epithelium *in vitro* (Eves et al., 2000; Stark et al., 1999), which could explain the inappropriate differentiation observed in the models (Figure 5.2C).

The detachment of models from the membrane was also a point of concern, suggesting poor adherence of the cells forming the basal layer. To assess whether there was a problem with the coating matric used to pre-treat the inserts, cells were seeded onto PET membranes with and without coating matrix added and stained with neutral red (Figure 5.3). It was observed that both inserts had a similar amount of adherence but there were reasonably widespread patches with weaker staining, or no staining at all, suggesting that the cells were either not fully covering the insert or that a significant proportion of them were not viable. The results of this experiment therefore suggested that it was in fact likely to be the cells that were not suitable for

in vitro model formation. Immunofluorescence analysis of the cells subsequently revealed a reasonable proportion (~20%) were binucleated, which suggested abnormality in the cells. A 2016 study on skin keratinocytes *in vitro* reportedly observed that binucleation of cells was induced by deregulation of the transcription factor Forkhead box M1 (FOXM1; responsible for a number of mitotic genes) and is commonly associated with epithelial malignancies *in vivo* (Molinuevo et al., 2016). The study concluded that FOXM1 plays a key role in epidermal cell division, and though upregulation did not prevent differentiation, it did drive nuclei division even when terminal differentiation had irreversibly blocked cytokinesis (Molinuevo et al., 2016). Whilst it is not possible to conclude the cause for binucleation in the cells used in this study without further assessment, the potential for binucleation to be associated with epithelial abnormalities and terminal differentiation makes it clear that these cells were not appropriate for further use towards 3D EE development. Following a discussion regarding the binucleation of the Gibco® HEKn (Cat # C-001-5C) with P&G, they were able to provide an alternative batch of cells that they themselves had used to successfully generate epidermal models. These were Lifeline® HEKn # FC-0007 and they were used for all subsequent experiments.

At the same time that the viability of the HEKn was being assessed, there was also concern over the suitability of the inserts being used. Early models were set up using PET membranes with 1.0 μm pores to promote greater media availability from below the model. However, it was noted that a significant number of cells appeared to be growing on the bottom of the wells after model set up despite there being no interchange between the inside of the insert and the well other than the pores in the membrane. Though it seemed unlikely given the size of the pores, the possibility that the cells may have been migrating through them and into the well was considered, and thus PET membranes with 0.4 μm were introduced. The models produced from these inserts were even poorer than the original models, with almost no evidence of proliferation having occurred, and severe parakeratosis (Figure 5.5A). Following more trial and error, it was eventually decided to use the BRAND*plates*™ system with PC membranes, 0.4 μm pores at an extremely high density, and holes within the side of the insert which increases access to the medium within the wells. EEs developed

using the Lifeline® HEKn and BRAND*plates*™ insert system were observed to be far superior to previous models, with no detachment from the membrane, more defined epidermal layers, and significantly less parakeratosis (Figure 5.5B).

Nevertheless, though the new models looked superior to the earlier attempts, they still did not replicate "gold standard" models such as EpiSkin™ and EpiDerm™ which each have around 8 to 9 cell layers between the underlying substrate and the stratum corneum (EpiSkin, 2021; MatTek Life Sciences, 2021). This raised lingering concerns that the cells were still not optimal for forming a stratified epithelium *in vitro*. However, as acknowledged in the introduction, another caveat of epidermal model development is the complex media requirements (Ng and Ikeda, 2011). In order to assess whether it was the medium that was limiting epidermal assembly, a batch of models containing Matrigel® were produced. Matrigel® is an ECM mixture that is protein rich and contains many factors found in the epidermal basement membrane such as laminin and collagen IV (Corning, 2021). Lifeline® HEKn cultured in 3D in the presence of Matrigel® were observed to differentiate fully, with a clearly defined basal and around 8 cell layers up to the stratum corneum (Figure 5.6). Consequently, it was concluded that these cells were suitable for epidermal assembly *in vitro*.

5.5.2 Culturing TCP and 4 kPa primed HEKn in hanging drops provided new insights into how 2D stiffness affects model development

Given the difficulties faced with early optimisation of EEs, it was deemed prudent to run parallel experiments using the hanging drop culture method to begin investigating the effects of BM culture on epidermal assembly. HEKn were primed on TCP and 4 kPa dishes then seeded into hanging drops and cultured for several days to observe whether they formed aggregates. Keratinocytes alone were not observed to form spheroids, though cells did appear to aggregate together in clumps; TCP primed cells forming branch-like aggregates, whilst 4 kPa primed cells aggregated more in the centre of the droplet (Figure 5.7). Not all cell types are readily able to form tight spheroids using the hanging drop system (Sargent, 2019), and keratinocytes are known to be sensitive to surface detachment, reportedly resulting

in terminal differentiation and eventually suspension-induced cell death (anoikis) (Guo and Jahoda, 2009). Given this information, it is not overly surprising that HEKn alone did not form spheroids, but the different aggregation patterns in these initial hanging drops still suggested that the stiffness of the 2D priming dish had an impact on 3D behaviour.

The next step in the hanging drop experiments was to combine HEKn with a previously formed fibroblast spheroid; the objective being to essentially use the dermal spheroid in place of an insert membrane for the keratinocytes to adhere to and assemble on top of. There was a striking difference observed between TCP and 4 kPa primed HEKn, with TCP primed cells forming an aggregate around the dermal spheroid, whilst 4 kPa did not appear to coat the dermal spheroid at all (Figure 5.8). Immunofluorescence analysis confirmed that HEKn primed on TCP did adhere to the dermal spheroid, whilst 4 kPa primed did not (Figure 5.9). It was at this stage that it began to become clear that 4 kPa hydrogels might be unsuitable for model formation. In chapters 3 and 4 we discussed the evidence that HEKn cultured on 4 kPa BM dishes are pushed more towards differentiation than those on TCP. This was shown through significant upregulation of some differentiation markers (Figures 3.19B and 3.24A) and changes in actin organisation (Figure 4.7) and LINC expression (Figures 4.15 and 4.19) that correlate to keratinocyte differentiation. Consequently, it was hypothesised that 4 kPa primed keratinocytes were too removed from the basal cell phenotype to develop a basal layer, and thus were not able to form the appropriate attachments needed to coat the dermal spheroid. This was additionally supported by the downregulation of *ITGA6* and *ITGB1* in HEKn cultured on 4 kPa BM dishes (Figure 3.21) which encode basal cell integrin proteins.

However, given that HEKn are traditionally cultured under high calcium conditions to produce 3D models, it was decided that the experiment should be repeated under high calcium conditions. Surprisingly this did result in a significant improvement, with both TCP and 4 kPa primed keratinocytes forming an aggregate around the original fibroblast spheroid (Figure 5.10). This seemed to somewhat negate the original hypothesis that 4 kPa were too differentiated to adhere to the fibroblasts.

With much frustration it was discovered that the spheroids were too fragile to embed for immunofluorescence analysis and it was therefore not possible to perform further analysis. In the epidermis, calcium forms a steep gradient that is highest in the stratum granulosum, and keratinocytes respond to increased levels by forming strong cell-cell contacts, i.e., adherens junctions, tight junctions and desmosomes (Bikle, Xie and Tu, 2012). This would obviously result in improved aggregation, which correlates with the spheroids in Figure 5.10. However, as it was not possible to perform further analysis, we cannot confirm whether the keratinocytes were actually bound to the underlying fibroblast spheroid. The fragility of the models, which even the TCP primed HEKn exhibited under high calcium conditions, suggested that the keratinocytes may have just aggregated around the dermal spheroid without binding to it. It was observed during culture that when hanging droplets were contaminated with dust or other debris, the cells would aggregate around it. Therefore, it could be that under high calcium conditions, the presence of the dermal spheroid acted to influence the surface tension and gravitational force within the droplet to promote a keratinocyte spheroid to form.

This hypothesis was somewhat supported by the appearance of HEKn aggregates in the absence of a dermal spheroid. Under high calcium conditions, TCP primed HEKn formed a single aggregate sheet, whilst 4 kPa primed formed multiple smaller aggregates (Figure 5.11). This showed that high calcium medium did in fact promote better cell aggregation, but in the absence of the dermal spheroid, HEKn were only able to form a sheet of cells rather than a spheroid structure. The fact that there was still a distinct difference in appearance between TCP and 4 kPa primed HEKn led to the idea that combining the two cells together in a spheroid may produce an interesting result. This was indeed that case, with TCP and 4 kPa primed mixed aggregates forming a single cell sheet, similar to TCP only, but with a transparent outer layer surrounding it (Figure 5.11). It was theorised that this was potentially evidence that HEKn primed on different substrates are able to organise themselves based on the phenotype of the cells. Thus, in this instance, it was hypothesised that the more differentiated 4 kPa primed HEKn were arranged to the outside of the spheroid, and that the transparent outer layer was indicative of a stratum corneum.

Again, subsequent assessment of these aggregates was hindered by the inability to embed the cell aggregates. As an alternative, new hanging drops were set up in which 4 kPa primed HEKn were labelled with a cell tracker, then the entire aggregate was stained with Hoechst in the hope that this would highlight the location of the 4 kPa primed cells. However, early images of these spheroids were not of sufficient quality due to oversaturation of the cell tracker, and the experiment required further optimisation.

Given that the main interests of P&G lay with the PC insert models, and the fact that the new BRAND*plates*™ system showed promise, it was decided to end the spheroid experiments here rather than devote time to optimising the cell tracker. This was admittedly disappointing, as the results obtained with these few experiments, whilst by no means ground-breaking, were definitely interesting and hinted at a strong connection between 2D mechanics and 3D model formation. The benefits of hanging drop experiments are the speed with which they can be set up and cultured, and the lack of a requirement for expensive equipment such as inserts and scaffolds. As such, this technique offers an excellent opportunity to pursue the effects of 2D BM dish priming on epidermal assembly, and further work would definitely be warranted in the future, particularly with regard to mixed cell aggregates.

5.5.3 HEKn primed on 50 kPa BM dishes in 2D produced far superior 3D epidermal models

As a consequence of the hanging drop experiments, it was determined that 4 kPa BM dishes were potentially too soft to replicate the epidermal basement membrane. The rationale behind why 4 and 8 kPa hydrogel-coated dishes were originally selected for this study is described in depth in the introduction to chapter 3 (3.1.4). However, following the need for a stiffer surface, a more in-depth scour of the literature was conducted, resulting in the discovery of a 2016 study that reported Young's Modulus measurements of the dermal-epidermal interface of dermal explants as being around 48.09 kPa (Kao, Connelly and Barber, 2016). Thus 50 kPa BM dishes were introduced into the study; a change that immediately yielded positive results. HEKn primed on TCP, 50 kPa and 4 kPa dishes prior to being cultured using the BRAND*plates*™

system were observed to produce drastically different epidermal models. TCP primed cells formed a stratified epidermis but with a poorly defined basal layer and parakeratosis, whilst 50 kPa primed cells produced a model that was significantly thicker, had no evidence of parakeratosis, and had more clearly defined cell layers (Figure 5.12). In contrast, 4 kPa primed models were extremely thin with only a couple of cells layers that were very flattened, suggesting limited proliferation had taken place during the submerged culture stage (Figure 5.12).

These observations were extremely exciting, supporting as they did the core hypotheses that keratinocytes grown in a more realistic 2D mechanical environment will produce more organised and *in vivo*-like epidermal models. In addition to this, the poor quality of the 4 kPa primed model supported the theory that these dishes were too soft to promote epidermal assembly in a 3D *in vitro* setting and aligned with the results of the hanging drop experiments. Finally, it should be noted that the TCP primed model was far inferior to other EEs published in the literature, in particular the models presented by Roger et al. who utilised a very similar protocol and medium composition and thus provide an appropriate comparison (Roger et al., 2019). The poor quality of the TCP models seen in this study clearly demonstrates that the protocol or cells used were ultimately not sufficient for optimal epidermal assembly. However, despite this apparent deficiency, the 50 kPa primed models are significantly improved and are much more reminiscent of those produced by Roger et al. (Roger et al., 2019). This therefore suggests that priming keratinocytes on a more suitable 2D substrate, could potentially reduce the impact of the usual limitations associated with epidermal model production *in vitro*. If this is the case, it could drastically alter the future of epidermal tissue development; potentially enabling the use of primary keratinocytes that would otherwise be unable to form a stratified epidermis *in vitro* and reducing the sensitivity of cells to their medium composition. However, in order to determine the truth behind these hypotheses a significant amount of further testing would be required, using multiple keratinocyte batches and different medium conditions to assess how big of a part 2D mechanics plays in successful 3D epidermal assembly.

Unfortunately, the time constraints of this project did not allow any investigations along that avenue, and subsequent experiments instead aimed to further characterise the models produced. Immunofluorescence analysis of CK14 and CK10 revealed that both TCP and 50 kPa primed models exhibited correct localisation of these proteins, with CK14 in the basal layer, and CK10 in the suprabasal layer through to the upper cell layers (Figure 5.13A). However, the highlighting of the basal layer by CK14 revealed that basal cells in the TCP primed models were flatter than those in the 50 kPa primed model, a fact that was confirmed by the greater number of basal cells in the 50 kPa models (Figure 5.13B).

Additional immunofluorescence analysis looked at expression of E-cadherin and p63. E-cadherin is an integral component of the epidermis, regulating tight junctions to facilitate epidermal barrier function (Tunggal et al., 2005), whilst p63 is associated with cells that have high proliferative potential and is absent from those undergoing terminal differentiation (Parsa et al., 1999). Both TCP and 50 kPa primed models had abundant p63 expression in the basal layer and some expression in the suprabasal (Figure 5.14) which aligned with *in vivo* skin (Tsujita-Kyutoku et al., 2003). However, whilst both models presented with E-cadherin staining throughout all cell layers, the staining in TCP primed models appeared more irregular and potentially cytoplasmic, whilst 50 kPa primed models showed clearly defined cell membrane staining (Figure 5.14). The results of these immunofluorescence analyses suggested that, whilst TCP primed HEKn were clearly proliferative and able to undergo differentiation in response to ALI culture and high calcium medium, it was almost as if they were remaining phenotypically 2D. It is well established that cells cultured on 2D plastic surfaces are flattened and well spread whilst those in 3D are not (Kapałczyńska et al., 2016; Soares et al., 2012). Additionally, it has been shown that human keratinocytes cultured on glass and stiff hydrogel surfaces are well spread and develop a polygonal shape, whilst those on soft hydrogels are rounder (Ya et al., 2019). Moreover, less developed cell membrane E-cadherin staining was already observed in keratinocytes cultured in 2D on glass compared to BM coverslips (Figure 4.10).

The idea that cells "remember" their mechanical environment is not a novel one; in 2010, Gilbert et al. reported that culturing muscle stem cells on a substrate with mechanical physiological relevance, greatly improved the success of *in vivo* engraftment of the cells (Gilbert et al., 2010). Additionally, Yang et al., observed that the activation of YAP/TAZ in human mesenchymal stem cells cultured on 2 kPa hydrogels was dependent on how long they had previously been cultured on TCP (Yang et al., 2014). Moreover, a more recent study involving primary human keratinocytes presented data showing that culturing cells beyond a certain threshold period of time on soft substrates produced evidence of "mechanical memory" that impacted the rate of wound healing during scratch wound assays (Mogha et al., 2019). As a result, it is likely that the flattened basal layer and less defined E-cadherin membrane staining is reflective of the 2D TCP environment on which the HEKn were primed. If so, this would go a long way to justifying the concept of a lag effect, in which cells primed on TCP must adjust to their new mechanical environment in 3D, which slows the epidermal model development process.

5.5.4 Barrier function in an unchallenged epidermis did not differ between TCP and 50 kPa primed EEs

In addition to assessing any changes to model appearance, another objective of this chapter was to see whether priming HEKn on TCP versus BM dishes had an impact on barrier function. In the section above we discussed the more defined E-cadherin staining observed in 50 kPa primed models (Figure 5.14) which is important for epidermal barrier function. However, the stratum corneum is the main barrier between epidermal cells and the external environment (van Smeden and Bouwstra, 2016), and its presence in a model is a hallmark of successful keratinocyte differentiation. Lucifer Yellow diffusion assays are routinely performed across laboratories to detect skin barrier defects in *in vitro* models (Indra and Leid, 2011). Early attempts to perform a Lucifer Yellow assay on the BRAND*plates*™ models were met with problems due to the holes in the sides of the inserts. This led to bleeding of the dye into the underlying medium which meant that the cells layers were contaminated from beneath via the pores in the PC membrane (Figure 5.15). In the

end it was necessary to remove the medium completely whilst the assay was being performed, meaning that these models could not be used for any additional analyses (e.g., protein expression etc). It was observed that Lucifer Yellow did not penetrate beyond the stratum corneum in either TCP or 50 kPa primed models (Figure 5.16).

The results of this experiment showed that TCP primed keratinocytes were able to fully differentiate to form a sufficient barrier despite the poorer appearance of the models and the presence of parakeratosis. The original plan for this part of the study was to follow-up this assay by challenging the barrier through the topical application of 0.25% and 0.5% SDS solutions and then repeating the Lucifer Yellow assay. However, once again technical problems were encountered; application of SDS solution caused models to begin to detach from the underlying PC membrane, and thus when Lucifer Yellow was added it was not contained to the upper surface and stained the model from below. In an attempt to combat this issue, experiments were repeated using cloning cylinders to try and isolate the SDS to the centre of the model, thus ensuring that the edges remained attached to the membrane. However, the cloning cylinders available in the laboratory were either too big to fit inside the insert, or significantly smaller than the inserts which made them difficult to keep in a set position when adding and removing the SDS. Unfortunately, there was no time left in the project to finalise the troubleshooting for this experiment, and thus it must be listed under recommended future work in order to ascertain whether 50 kPa primed models have better protection against barrier challenge. Additional future work of interest would be to look at the lipid content of the stratum corneum in TCP and 50 kPa primed models and directly compare this to both each other and to native skin. This would enable a more quantitative analysis of the barrier, and thus provide a more thorough comparison.

5.5.5 Suboptimal EEs produced from 50 kPa primed HEKn exhibited improved appearance following extended culture time

As touched upon in the results section, one of the most frustrating issues faced with the experiments for this chapter was the recurring production of suboptimal models. This made it difficult to perform additional experiments exploring how 50 kPa 2D

priming affected model appearance. However, even when models were not at a high standard, the differences between TCP and 50 kPa primed cells was striking. During a period where models were consistently thin regardless of 2D priming stiffness, it was decided to assess whether increasing the culture time gave models chance to develop better. Models were cultured for the usual 12 days at ALI and compared to 18 days at ALI, and it was observed that whilst TCP primed models did not really change, 50 kPa primed models became noticeably thicker and developed a clear basal layer of columnar cells (Figure 5.17). Earlier it was hypothesised that priming HEKn on 50 kPa at 2D could potentially reduce the impact of limiting factors such as HEKn batches not being suitable for model development. The fact that additional culture time was able to significantly improve the appearance of 50 kPa primed models but not TCP primed, further supports this theory. Consequently, HEKn cultured on 50 kPa substrates at 2D appear to have a superior ability for epidermal assembly even under suboptimal culture conditions.

5.5.6 The mixing of 50 kPa and 4 kPa primed cells to produce EEs requires further optimisation

One experiment performed using the hanging drop technique that yielded particularly interesting results was the mixing of TCP and 4 kPa primed cells into one aggregate. Though an in-depth analysis of these aggregates was not possible, it was hypothesised that the cells had been able to arrange themselves due to the presence of a transparent outer layer believed to be a stratum corneum. As such, a similar experiment was performed using the BRAND*plates*™ system and 50 kPa and 4 kPa primed HEKn to respectively represent the basal and differentiated layers. HEKn primed on 50 kPa dishes were seeded onto an insert and cultured at the submerged stage for 4 days. On the 4th day, 4 kPa primed HEKn were seeded on top and 24 hours later the models were raised to the ALI.

The resulting models were far inferior to 50 kPa primed alone, but slightly better in appearance than 4 kPa alone, presenting with an extra one or two cell layers and less flattened basal cells (Figure 5.18). The conclusion from this was that the 4 kPa primed cells had been added too quickly and that the models would have benefited from a

few days at the ALI for the 50 kPa primed cells to begin stratifying and forming the partially differentiated spinous layers. However, once again time constraints caused by the prolonged issues with model production meant that this experiment could not be optimised further. Consequently, this is an experiment that would benefit from further work in the future, as the success of this technique may result in even thicker epidermal models with multiple cell layers within each epidermal layer as observed in *in vivo* skin.

5.5.7 TCP primed HEKn screened for a basal phenotype prior to model set-up produced EEs similar to 50 kPa primed

It has already been mentioned that one of the key limitations of working with primary keratinocytes to produce epidermal models is that not all batches are able to form a differentiated stratified epidermis under *in vitro* conditions (Eves et al., 2000; Stark et al., 1999). One of the potential reasons for this is that primary keratinocytes extracted from the entire epidermis (Anderson et al., 2018) and are not subsequently isolated depending on their epidermal layer of origin (i.e., basal layer, spinous layer, granular layer). As a result, when primary keratinocytes are purchased from a commercial company, the pool of cells provided is a heterogenous mix of keratinocytes. As demonstrated by the 4 kPa primed cells in this study, keratinocytes that are more differentiated are not suitable for *in vitro* formation of a stratified epidermis. Therefore, if a purchased batch of cells has a particularly high number of partially or fully differentiated keratinocytes, it is not going produce optimal EEs.

In 2017, a study group published the results of two screening methods that were designed to isolate keratinocyte stem cells from transitory amplifying cells (direct progeny of keratinocyte stem cells) (Metral et al., 2017). To do this they compared both a rapid adhesion method and flow cytometry cell sorting for the stem cell phenotype $\alpha 6^{high}$/CD71^{low}. For the rapid adhesion technique, a dish was coated with collagen I and cells were seeded on top and allowed to adhere for 10 mins before low-adhesion or non-adhered cells were removed (Metral et al., 2017). Given the simplicity and speed of this technique, it was deemed a relatively easy addition to the existing EE model protocol. HEKn were primed on either TCP or 50 kPa dishes

but prior to seeding onto a PC membrane, half of the TCP cells were seeded onto a second TCP dish treated with coating matrix and allowed to adhere for 10 mins. Only the cells that adhered to this dish during the 10 mins were used to set up the TCP pre-screened models.

The results of this experiment were interesting, producing a model that was somewhere in the middle of the TCP and 50 kPa primed models. Though the TCP pre-screened models did not appear much thicker than the normal TCP models, they were better organised with no signs of parakeratosis and clearer cell layer distinction (Figure 5.19A). Moreover, immunofluorescence analysis revealed that the basal layer of cells was more cuboidal compared to the flattened TCP models, and E-cadherin staining was localised to the cell membrane in the majority of cells (Figure 5.19B). Despite the improved appearance of the TCP pre-screened models compared to the non-screened TCP, the 50 kPa primed models were still superior due to the increased thickness and more columnar basal layer. However, the similarity in appearance between the 50 kPa and TCP pre-screened models raised the question of whether 50 kPa priming already selects for basal cell phenotype keratinocytes. If this is the case, the difference in thickness could merely be an artifact of the lag period previously discussed, in which mechanical memory likely delays the development of TCP primed HEKn when they are transferred into a 3D environment.

In order to help address this question, the experiment was repeated but this time both TCP and 50 kPa primed cells were pre-screened using the rapid adhesion method. However, the resulting control (non-screened) models were far from optimal (Figure 5.20); a consistent issue with some of the latter analyses performed for this chapter. This was frustrating as it meant few conclusions could be drawn due to the compromised controls. Nonetheless, the resulting pre-screened models still provided some information which suggested that future repeats of the experiment are warranted. TCP pre-screened models were thicker and more organised than the non-screened TCP, whilst the 50 kPa primed models looked similar regardless of whether the HEKn had been pre-screened for basal cells or not (Figure 5.20). This could potentially support the theory that 50 kPa primed models already select for this

keratinocyte niche. However, this can be in no way concluded at this stage. A more thorough assessment of the connection between pre-screening and 50 kPa priming needs to be performed in the future, both through the repetition of model development, and through assessment of the cells at a 2D stage. This could include flow cytometry cell sorting for $\alpha 6^{high}$/$CD71^{low}$ cells to quantify the number following TCP and 50 kPa priming, as described by Metral et al. (Metral et al., 2017).

5.6 Conclusions

This chapter aimed to investigate whether pre-culturing HEKn on BM substrates that replicated the *in vivo* mechanical environment could improve the appearance of *in vitro* epidermal models. The secondary aim was to assess whether 50 kPa primed HEKn produced models with protein expression and barrier function that better reflected native skin. It was hypothesised that HEKn primed on TCP may exhibit a lag period as a result of mechanical memory of the 2D culture environment. As such, the final aim was to investigate whether EEs could be developed more quickly if HEKn were primed on 50 kPa dishes in 2D.

The experiments performed in order to try and meet these aims were besieged with numerous technical problems as a result of suboptimal cells and problems with the protocol despite months of troubleshooting. However, this does not mean that the chapter did not yield some promising results. It was observed that HEKn primed on 4 kPa BM dishes were unable to undergo epidermal assembly, both in hanging drop spheroid models and using the BRAND*plates*™ system. This led to the introduction of 50 kPa BM dishes, which were found to produce superior EEs that were thicker, had a less flattened basal layer composed of cuboidal/columnar keratinocytes, and improved cell membrane localisation of E-cadherin compared to TCP primed models.

Hanging drop experiments revealed that mixing of HEKn primed on different substrate stiffnesses could potentially be used to produce even better 3D models as a result of cells organising themselves based on their phenotype. However, more work needs to be done to optimise the mixing of cells in PC membrane models in order to fully investigate this.

HEKn primed on 50 kPa dishes were observed to produce superior models compared to TCP even when controls were suboptimal, and extending culture time appeared to rescue 50 kPa primed models regardless of how poor the controls were. This was hypothesised to be a sign that 50 kPa BM dishes could potentially be used to produce epidermal models from keratinocytes previously shown to be unable to undergo epidermal assembly *in vitro*. Pre-screening of HEKn for basal cell phenotypes led to the theory that 50 kPa dishes may already screen for basal keratinocytes, hence the superior epidermal models produced using these cells.

The results obtained in this chapter offer a tantalising glimpse into the potential benefits that 2D mechanical priming could have on not only skin model production, but tissue engineering as a whole. However, the technical issues faced during the completion of these experiments mean that many would benefit from repetition. As such, these data should be viewed as the foundation of a more in-depth future study into the relationship between the 2D mechanical environment and 3D tissue development.

6 Investigating the effects of *in vitro* substrate stiffness on fibroblast behaviour and senescence

6.1 Introduction

In the previous chapters of this thesis, the extent to which external mechanics play a role in keratinocyte behaviour, phenotype and genotype was the primary focus. However, the mechanical properties of *in vivo* skin are in large part a reflection of dermal composition; the dermis being the thickest compartment of the skin and composed of dense connective tissue which owes its synthesis, deposition, and turnover to a relatively small number of fibroblasts (Jepps et al., 2013; Yousef, Alhajj and Sharma, 2021). Fibroblasts have been shown to respond to physical stimuli such as stretch, compression and shear forces which leads to changes in collagen deposition (Wong, Longaker and Gurtner, 2012).

Moreover, it is well established that a hallmark of ageing in many tissues is a major alteration of the biomechanical properties due to ECM degradation and remodelling (Phillip et al., 2015). This is of particular relevance to the skin, which undergoes both intrinsic and extrinsic ageing leading to significant dermal remodelling events that alter the tissue's rigidity (Achterberg et al., 2014). In addition, another key feature of the ageing process is an accumulation of senescent cells (López-Otín et al., 2013). Senescent cells have been shown to exhibit altered expression of nuclear envelope proteins such as Lamin A, Lamin B1 and SUN1, which form part of the LINC complex; a major component of a cell's biomechanical machinery (Gilbert and Swift, 2019). Alterations to the composition of the LINC complex can have an impact on a cell's ability to sense mechanical stimuli; suggesting that senescent cells may respond differently to age-associated ECM remodelling than those still in the cell cycle. Consequently, it would have been remiss to not include some preliminary analyses into the effect of culturing fibroblasts on BM hydrogel-coated dishes within this project.

6.1.1 The dermal ECM and the mechanical changes induced by skin ageing

The dermis connects to the epidermis at the epidermal basement membrane and is composed of two layers: the thin papillary dermis, and the thicker underlying reticular dermis which is less cellularised (Yousef, Alhajj and Sharma, 2021). Collagens I and III are the most abundant ECM proteins in the dermis and co-polymerise to provide the tissue's tensile strength. In addition, skin elasticity (resilience and compliancy) is provided by the presence of an elastic fibre system, whilst the group of carbohydrates, collectively referred to as glycosaminoglycans (GAGs) help to maintain skin hydration (Naylor, Watson and Sherratt, 2011). Unlike other tissues, skin undergoes both an intrinsic and extrinsic ageing process. Intrinsic ageing of the skin over time, results in the gradual degradation of collagens I, III and IV, and the elastic fibres, and the loss of oligosaccharides, which impacts the skin's ability to retain water. In conjunction, these changes produce the aged phenotype of wrinkled, stiffened skin that is less able to recoil (Naylor, Watson and Sherratt, 2011). Extrinsic ageing is triggered as a result of exposure to UV radiation, and results in a distinctly different remodelling event, including both catabolic and anabolic mechanisms (Takeuchi and Rünger, 2013). These events are dose dependent, with severe photoageing resulting in the additional loss of collagen VII at the dermal-epidermal junction, and the increase and redistribution of GAGs to co-localise with the elastic fibre system. This elastic network is also remodelled; severe photoageing leading to the accumulation of disorganised elastic fibre proteins in the reticular dermis (Kohl et al., 2011).

It has already been noted in previous chapters that ECM stiffness is a key mechanical stimulus for cells, and the remodelling events observed in ageing skin inevitably lead to changes in its rigidity. A study by Achterberg et al. reportedly used AFM to measure the Young's Modulus of the papillary and reticular dermis of abdominal and breast skin from young and old women. Their results revealed that, overall, the stiffness gradually increased with age, before dropping suddenly between 50 and 60 years (Achterberg et al., 2014), an age range that correlates with the usual onset of menopause. It has been observed that oestrogen has an inhibitory effect on collagen

degrading matrix metalloproteases (MMPs) (Chang et al., 2010), and thus this would explain the sudden loss in stiffness, as collagen degradation is likely to have increased with the diminishment of oestrogen. In conclusion, skin ageing triggers significant remodelling of the dermal ECM which has a substantial impact on the mechanical environment.

6.1.2 Fibroblast senescence and the effects on external and internal mechanics

As mentioned previously, in addition to changes in ECM composition, another hallmark of skin ageing is the accumulation of senescent fibroblasts within the dermis. Senescence describes cells that have transitioned from a proliferative to a non-proliferative state but are still metabolically active and able to manipulate their surrounding ECM (Birch-Machin and Bowman, 2016; Toutfaire, Bauwens and Debacq-Chainiaux, 2017). The mosaic nature of skin ageing makes it difficult to conclusively ascertain the origin of fibroblast senescence, and thus the relationship between mechanical changes to the ECM and the onset of senescence is unknown. However, increased oxidative stress has been noted as a potential contributor towards cell senescence; mitochondrial-derived ROS can contribute to telomere shortening and premature senescence by generating DNA damage, including single-stranded breaks to DNA within telomeres (Passos et al., 2007). DNA damage is considered an essential driver of the senescence-associated secretory phenotype (SASP), and the presence of the DNA damage response (DDR) marker γ-H2AX is commonly used to detect senescent cells (Hernandez-Segura, Nehme and Demaria, 2018). Both intrinsic and extrinsic ageing are associated with accumulation of ROS. Moreover, not only have ROS been shown to contribute towards cell senescence, but senescent cells themselves exhibit a significant increase in ROS production in comparison to their proliferative counterparts (Kuilman et al., 2010). Accumulation of ROS triggers a cascade promoting elevated expression of MMPs and the inhibition of pro-collagen I expression (Toutfaire, Bauwens and Debacq-Chainiaux, 2017). This means that a dermis with a high senescent cell content would have elevated MMP

levels and pro-collagen I inhibition, which would have a bigger impact on the mechanical environment to which fibroblasts are exposed.

In addition to having an effect on the mechanics of the external ECM, senescence also results in internal changes that effect a cell's own biomechanics. In chapter 4, the LINC complex and its roll in cell mechanotransduction was introduced, and its relevance to keratinocyte homeostasis was explored. Actin and other cytoskeletal components are connected to the nuclear lamina via the LINC complex, which enables the communication of external mechanical cues directly to the nucleus interior (Hieda, 2019). The LINC complex is made up of two protein domains; SUN domain and the C-terminal KASH domain, which is expressed in nesprin proteins, and collectively they span the nuclear envelope (Bouzid et al., 2019). The N-termini of SUN domain proteins are bound to the nuclear lamina which in turn organises chromatin, thus providing the final link between external mechanical stimuli and the nuclear interior (Cartwright and Karakesisoglou, 2014; Chambliss et al., 2013; Hieda, 2019; Padmakumar et al., 2005).

It has been reported that senescent cells exhibit altered expression of NE proteins, with downregulation of Lamin B1 being a particular hallmark (Hernandez-Segura, Nehme and Demaria, 2018). Lamin A has also been observed to be downregulated in senescent cells, though Lamin C appears to be unaffected along with emerin, and SUN1 was observed to be increased following cellular senescence (Lenain et al., 2015). It is unsurprising that these changes in NE protein expression have deleterious effects on nuclear function, not least of which is the compromising of the barrier between the nucleus and cytoplasm; it has been shown that senescent cells show increased NE permeability, characterised by the presence of chromatin in the cytoplasm (Ivanov et al., 2013). Accumulation of DNA fragments in the cytoplasm triggers an innate immune response which promotes the SASP (Rocha, Dalgarno and Neretti, 2021). Additionally, alterations to NE protein expression alter a cell's mechanical response to external forces. This aberrant mechano-response, combined with inevitable changes to chromatin regulation as a result of Lamin downregulation, will result in

alterations in mechanically induced gene expression in senescent cells (Gilbert and Swift, 2019).

6.1.3 The effects of substrate stiffness on fibroblast activation *in vitro*

It should by now be clear that the ageing process has a significant impact on the mechanics of skin tissue, both at a cellular level and with regards to the surrounding ECM. In order to examine the effects that changes to ECM stiffness have on fibroblasts, Achterberg et al. cultured primary human dermal fibroblasts on silicone gels of differing stiffness to mimic normal (1 to 10 kPa) and fibrotic (15 to 50 kPa) dermis (Achterberg et al., 2014). It was observed that cells grown on 1.5 kPa gels were quiescent, α-smooth muscle actin (SMA) negative and produced no stress fibres. However, cells grown on gels ranging from 5 kPa upwards began to spontaneously activate; shown by the expression of α-SMA positive stress fibres. The number of active fibroblasts correlated positively with increased substrate stiffness; suggesting that even small changes to ECM stiffness could have a large impact on cell behaviour within the skin (Achterberg et al., 2014). Given that TCP has a known Young's Modulus of around 3 GPa (Landry, Rattan and Dixon, 2019), it follows that fibroblasts are likely to be maintained in a permanently active state in *in vitro* culture.

Activated myofibroblasts are a differentiated form of fibroblast involved in the inflammatory response at healing wound sites, and they are identified by their morphological similarities to smooth muscle cells (Darby et al., 2014). The transition from quiescent fibroblasts to active myofibroblasts includes a precursor stage characterised by the expression of large stress fibres, prominent microfilament bundles, and remodelling of the surrounding ECM (Hinz, 2007). Fully differentiated myofibroblasts exhibit expression of α-SMA which is usually only found in smooth muscle cells (Sandbo and Dulin, 2011). It has been shown that myofibroblast activation can be promoted by matrix stiffness and increased mechanical strain as well as higher ROS levels (Edmondson et al., 2014). Reverting to a softer substrate has been shown to reverse this phenotype (Kloxin, Benton and Anseth, 2010).

6.2 Hypotheses and Aims

This chapter aims to investigate the potential changes to fibroblast behaviour and phenotype in response to culture on BM hydrogels, with particular focus on proliferation, DDR, ROS levels and senescence. It has already been highlighted that biomechanics play an integral role in the dermal compartment of skin, particularly during the ageing process. Moreover, it is well established in the literature that fibroblasts are very responsive to changes in their mechanical environment *in vitro*. In their native environment, fibroblasts grow at low density and have a low rate of proliferation in comparison to keratinocytes; their main role being the deposition of ECM to provide the core foundation of skin tissue. During skin ageing, the integrity of the ECM is diminished and thus the mechanics of the dermis changes; a feature that is exacerbated in areas exposed to age-accelerating factors such as UV radiation which causes elevated levels of DNA damage. Additionally, skin ageing is associated with elevation of cellular ROS levels and increased numbers of senescent fibroblasts within the dermis, however, the relationship between cell senescence and ECM mechanics has not thus far been determined.

Given what is already known about fibroblasts and dermal mechanics, it was firstly hypothesised that culturing fibroblasts on a softer substrate would result in reduced proliferation and cell density, and a quiescent phenotype. The relationship between age-associated changes in dermal mechanics and fibroblast senescence is ambiguous, particularly in an *in vitro* setting where senescence is artificially induced. Thus, it was difficult to devise specific hypotheses as to the effects of substrate stiffness on DDR and senescence following *in vitro* irradiation. Consequently, it was simply hypothesised that fibroblasts cultured on BM hydrogels would exhibit altered DDR and levels of senescent markers compared to those on TCP following irradiation. Additionally, it was hypothesised that fibroblasts cultured on hydrogel-coated dishes would exhibit different ROS levels in comparison to those on TCP due to variations in quiescence versus activation.

To summarise, the key hypothesis driving this chapter was that culturing fibroblasts on soft BM dishes reflecting the dermal mechanical environment would promote a

more quiescent phenotype. This chapter therefore aimed to answer the following questions:

- Does culturing fibroblasts on soft 2D hydrogels result in changes to cell proliferation and density compared to those on TCP?
- Do fibroblasts cultured on soft hydrogels exhibit altered levels of senescence and ROS compared to those on TCP?
- Do the mechanics of the underlying 2D substrate affect the DDR of *in vitro* cultured fibroblasts?

6.3 Objectives

- Determine whether soft hydrogels promote a less active fibroblast phenotype reminiscent of their *in vivo* counterparts.
- Use irradiation to induce DNA damage and determine differences in the DDR of fibroblasts cultured on TCP versus BM dishes.
- Use irradiation to induce cell senescence and determine the prevalence of senescent fibroblasts on TCP versus BM dishes.

6.4 Results

As explained above, the main questions posed for this chapter were, what impact does culturing fibroblasts have on their appearance and behaviour? And does a softer substrate effect cell senescence and the DNA damage response? The results presented here provide a preliminary answer to these questions and offer a good foundation for further investigation along this avenue of research.

Before presenting the results, it is worth reiterating that the desired Young's Modulus for the hydrogel-coated dishes used for these experiments was 1 kPa. However, due to persistent problems with fungal infections and poor cell response to the hydrogels (discussed further in section 6.4.4), it was necessary to use both 1 kPa and 4 kPa dishes to ensure that there were enough available to carry out repeats. For this reason, samples cultured on hydrogel-coated dishes are labelled "BM" throughout the figures which encompasses both 1 kPa and 4 kPa dishes. No discernible difference

was noted between HDFn cultured on 1 kPa and 4 kPa, and comparison of repeats taken from different dishes showed no statistically significant variance.

6.4.1 HDFn cultured on BM dishes appeared more proliferative and had reduced nuclear area

The first step in investigating the HDFn response to softer substrates was to follow the same pattern as early HEKn experiments; simply culture the cells on TCP and BM dishes and observe any differences in behaviour and/or appearance. It was noted that HDFn on BM dishes three days after seeding had a slightly more 3D appearance than those on TCP (Figure 6.1A), reminiscent of the HaCaTs cultured on BM dishes (Figure 3.12A). By day five, HDFn on BM dishes were much more densely packed and appeared to have proliferated more rapidly (Figure 3.12A). Dissociating cells from the dishes and counting them revealed that a significantly greater number of cells were harvested from the BM dishes compared to TCP (Figure 6.1). Calculating the population doubling level (PDL) revealed that HDFn cultured on BM dishes had a significantly greater PDL than those on TCP (6.00 and 4.74, respectively) (Figure 6.2). PDL was calculated using the following formula:

$$PDL = PDL_0 + 3.322\ (\log C_f - \log C_i)$$

where:

PDL_0 = initial population doubling level

C_i = initial cell number seeded into vessel

C_f = final cell yield

Figure 6.1 (overleaf) HDFn cultured on 1 kPa dishes appeared denser than those on TCP after 5 days of culture. (A) *Phase contrast images show HDFn cultured on TCP and 1 kPa dishes at 3 and 5 days after seeding. At day 5, HDFn on 1 kPa dishes seemed more densely packed. Scale bars = 100 μm.* **(B)** *Quantification of the number of cells seeded versus the number of cells harvested after 5 days in culture. Data represent mean ±SEM, n = 3, statistical significance at "day harvested" was assessed using an unpaired, two-tailed t-test, *** p ≤ 0.0001.*

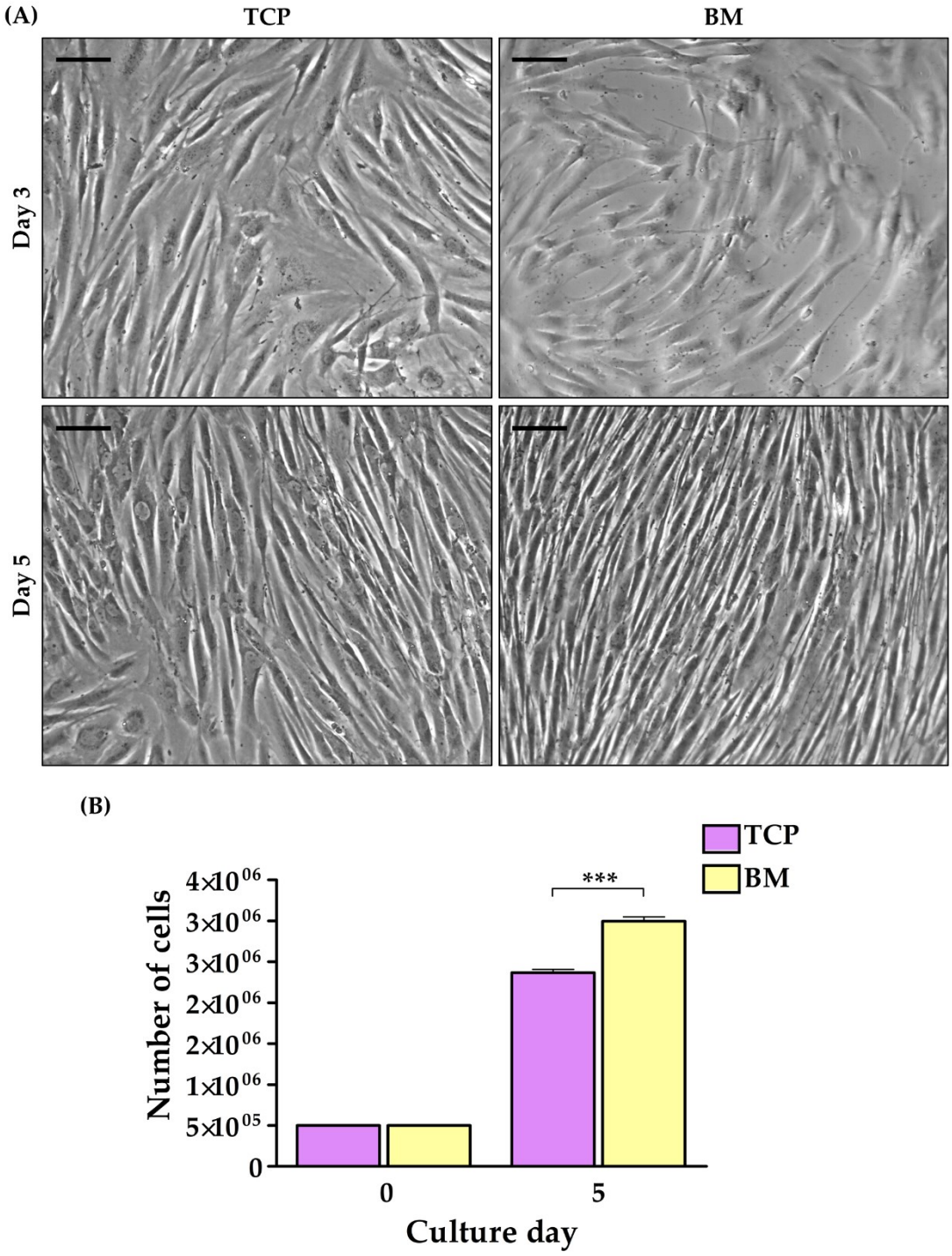
(A)
TCP
BM
Day 3
Day 5
(B)
TCP
BM
***
Number of cells
4×10^06
3×10^06
3×10^06
2×10^06
2×10^06
1×10^06
5×10^05
0
0
5
Culture day

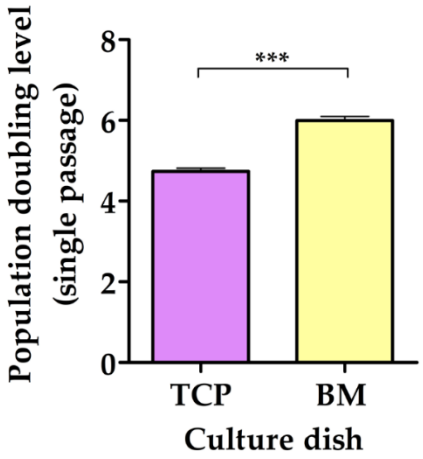

Figure 6.2 HDFn cultured on BM dishes had a greater average PDL after one passage than cells on TCP. *Quantification of the average PDL of HDFn after a single passage. Data represent mean ±SEM, n = 3, statistical significance was assessed using an unpaired, two-tailed t-test, *** $p \leq 0.0001$.*

Whilst PDL values offer a good insight into cell proliferation, they rely on cell yield and problems fully dissociating and counting cells removed from BM dishes (discussed further in section 6.4.4), meant that the PDL value presented here may be underestimating the true level of HDFn proliferation on BM dishes. As a result, it was decided that an alternative proliferation quantification should be performed through ki67 staining. HDFn were cultured on glass and BM coverslips for four days then fixed and immunofluorescently stained for the proliferation marker ki67 (Figure 6.3A). However, repeated problems were faced with this staining, and it was noted that ki67 staining was only observed at the periphery of the coverslips. This was confirmed as a technical issue rather than a true result by a decreased gradient in staining intensity from the periphery towards the centre of the coverslip, rather than a total absence of stain. This made it difficult to get an accurate measure of cell proliferation, and the resulting quantification contradicted the PDL value by suggesting that BM primed HDFn were less proliferative than those on TCP (Figure 6.3B). This analysis would therefore benefit from repetition, or the use of an EdU assay in place of ki67 staining.

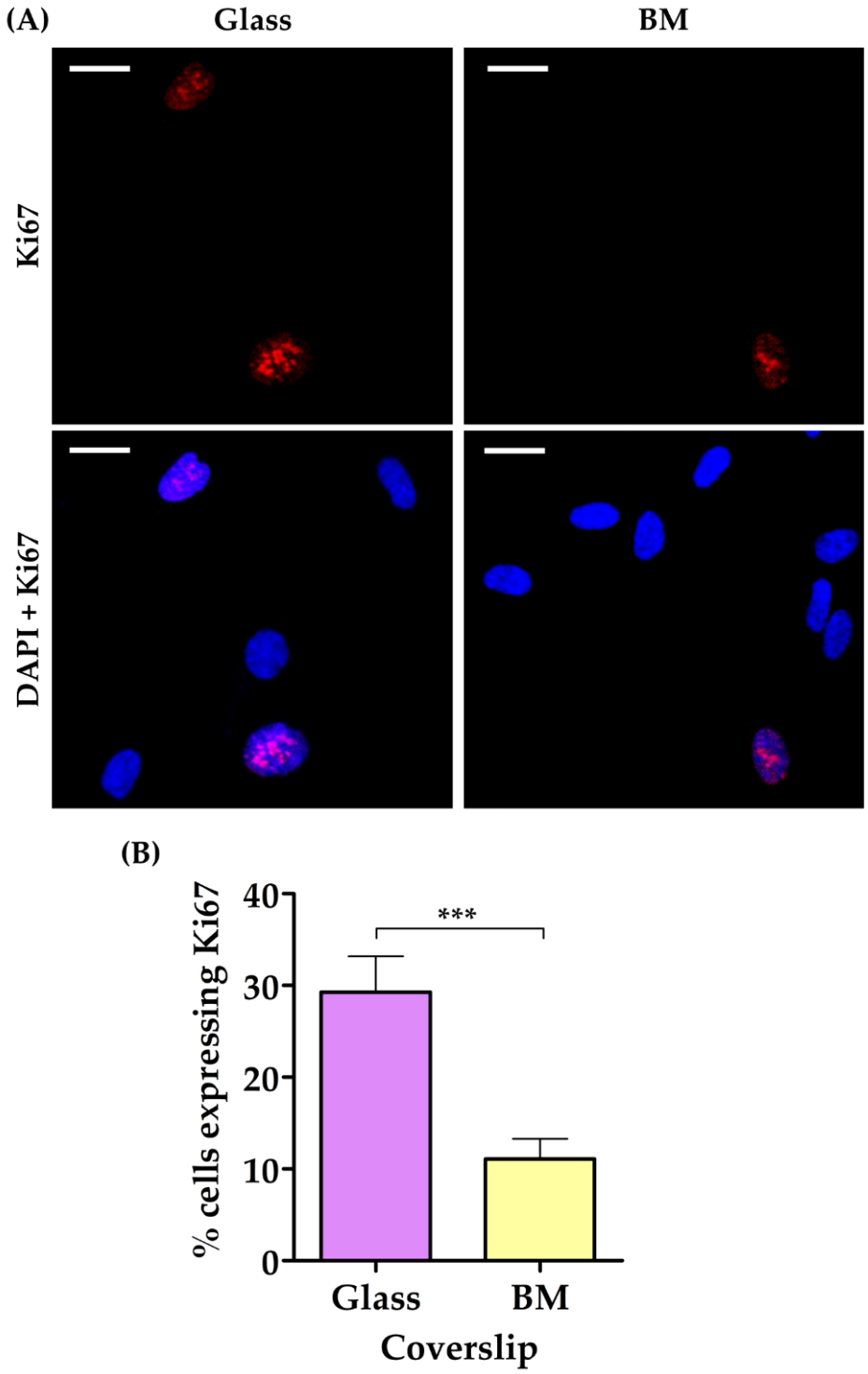

Figure 6.3 HDFn cultured on BM coverslips had fewer ki67 positive nuclei than cells on glass. HDFn were cultured on glass and BM coverslips and immunostained for the proliferation marker ki67. (A) *Confocal microscopy images show ki67 staining in the DAPI stained nuclei of HDFn.* **(B)** *Quantification of the percentage of cells expressing ki67 in their nuclei. Data represent mean ±SEM, n = 3 (3x 100 cells), statistical significance was assessed using an unpaired, two-tailed t-test, *** $p \leq 0.0001$.*

Despite the issues faced with ki67 immunofluorescence, the experiment did yield some benefit by drawing attention to the fact that the nuclei of HDFn cultured on BM coverslips appeared smaller compared to cells cultured on glass (Figure 6.4A). Quantification of nuclear area and perimeter revealed that both were significantly lower in cells cultured on BM coverslips (Figure 6.4B-C), but nuclear circularity was observed to be the same (Figure 6.4D).

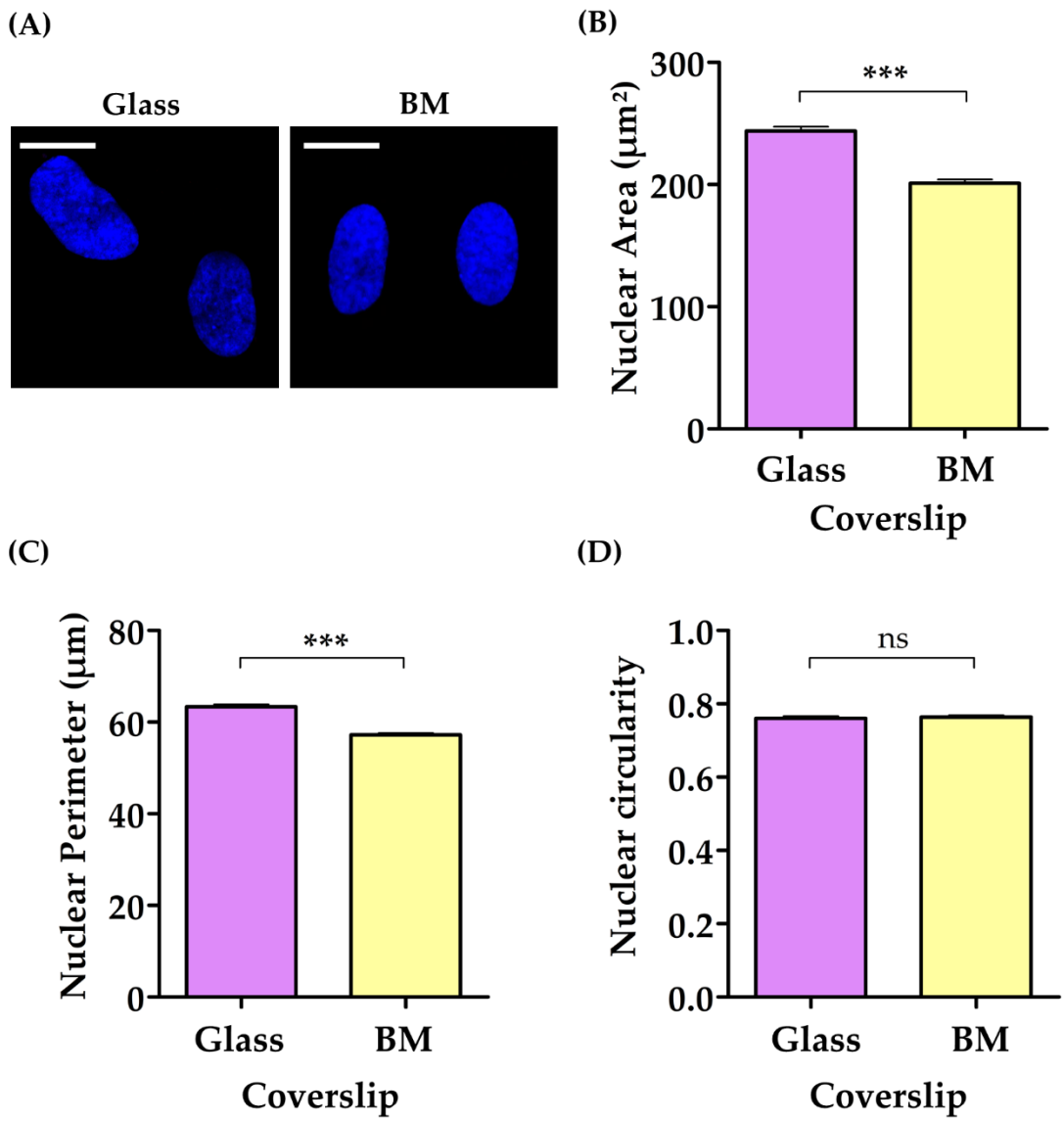

Figure 6.4 HDFn cultured on BM coverslips had reduced nuclear area and perimeter compared to those on glass. (A) *Confocal microscopy images showing DAPI stained nuclei of HDFn cultured on glass and BM coverslips. Scale bars = 20 µm.* **(B)** *Quantification of nuclear area. Data represent mean ±SEM, n = 3 (3x 100 cells), statistical significance was assessed using an unpaired, two-tailed t-test, *** p ≤ 0.0001.* **(C)** *Quantification of nuclear perimeter. Data represent mean ±SEM, n = 3 (3x 100 cells), statistical significance was assessed using an unpaired, two-tailed t-test, *** p ≤ 0.0001.* **(D)** *Quantification of nuclear circularity (1.0 = circle, 0.0 = polygon). Data represent mean ±SEM, n = 3 (3x 100 cells), statistical significance was assessed using an unpaired, two-tailed t-test, *** p ≤ 0.0001.*

6.4.2 HDFn cultured on BM dishes did not appear as susceptible to x-ray irradiation as those on TCP

One of the main points of interest for this chapter was whether HDFn cultured on BM dishes exhibited any changes in response to senescence-inducing irradiation. In order to ascertain this, HDFn were cultured on TCP and BM dishes for four days, and then exposed to an x-ray dose of either 10 Gy, to induce DNA damage, and 20 Gy to induce senescence. Cells were cultured for a further 10 days to allow senescence to take place and were then imaged to assess differences in appearance. A key feature of senescent fibroblasts is that they are often bigger than younger cells (Rani et al., 2017). Enlarged cells were observed in HDFn cultured on TCP but not in those cultured on BM dishes following irradiation (Figure 6.5).

In order to ascertain the level of DNA damage the cells experienced in response to irradiation, cells were fixed and stained for the DNA damage marker phospho-histone H2A.X both immediately after irradiation (Figure 6.6A), and 10 days later (Figure 6.7A). This experiment was therefore designed to capture both the amount of DNA damage caused by irradiation, and the level of repair that cells had undergone following 10 days back in culture. It was observed that HDFn cultured on BM dishes had significantly fewer phospho-histone H2A.X expressing nuclei compared to those on TCP immediately following an x-ray dose of either 10 Gy (50.3% and 88.3%, respectively) or 20 Gy (79.1% and 91.3%, respectively) (Figure 6.6B).

Unfortunately, due to continued problems with fungal infections it was only possible to produce one repeat of the DNA damage stain 10 days after irradiation. The results for this showed that there was no DNA damage in either TCP or hydrogel cultured cells after a dose of 10 Gy, but HDFn appeared to have more DNA damage foci after a 20 Gy dose when cultured on BM dishes compared to TCP (Figure 6.7A). Given that this experiment was n = 1 it is not possible to draw conclusions and further repeats are needed. However, an interesting observation was that after 10 days the appearance of the phospho-histone H2A.X staining was drastically different. Immediately following irradiation, nuclei possessed a high number of small foci, but

10 days after irradiation nuclei were observed to possess a very small number of larger foci (Figure 6.7B).

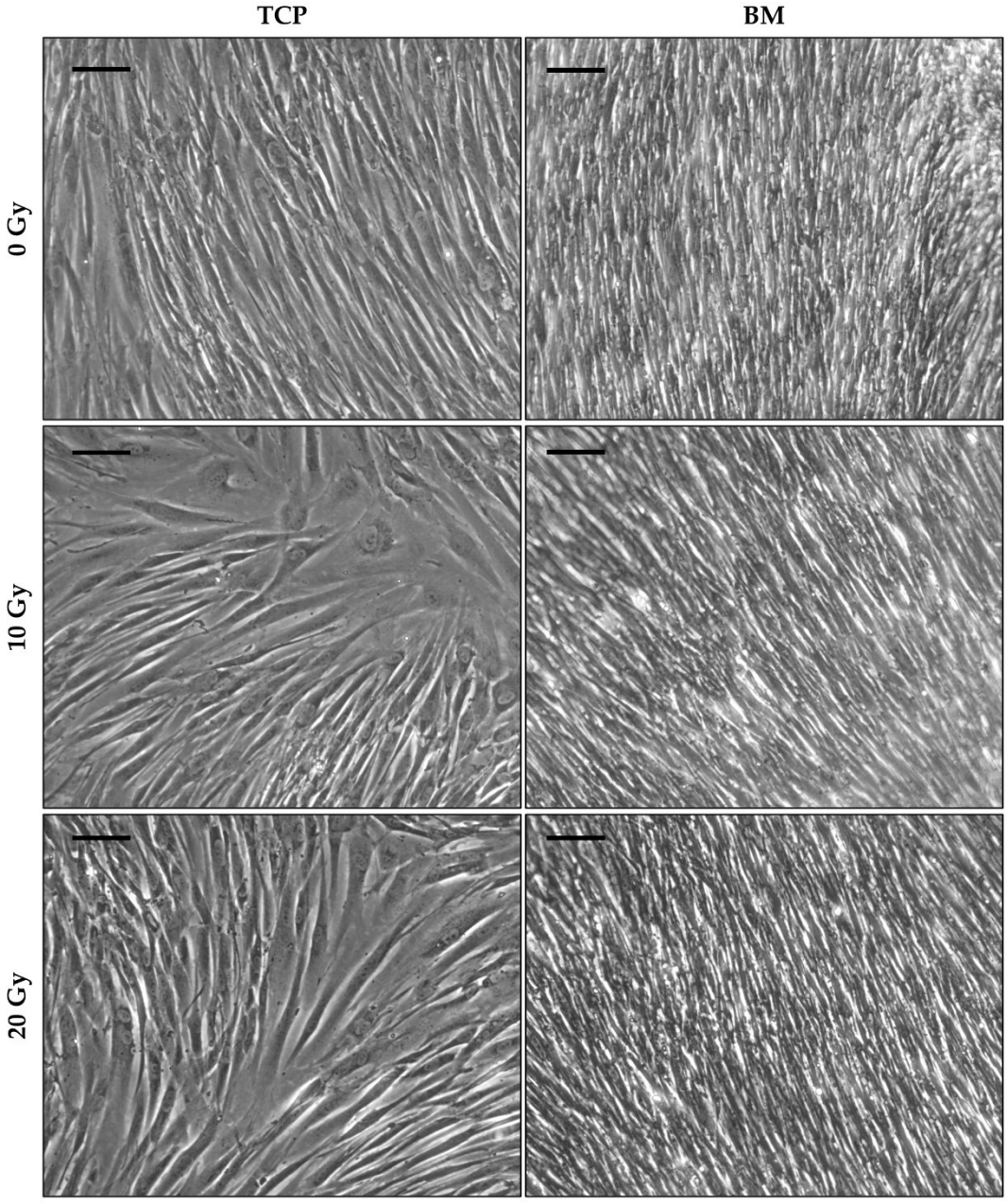

Figure 6.5 HDFn cultured on BM dishes did not appear to alter appearance following irradiation. *HDFn were cultured on TCP and BM dishes for 4 days then irradiated with an x-ray dose of 0, 10 or 20 Gy. Phase contrast images show the cells 10 days after irradiation on TCP and BM dishes.*

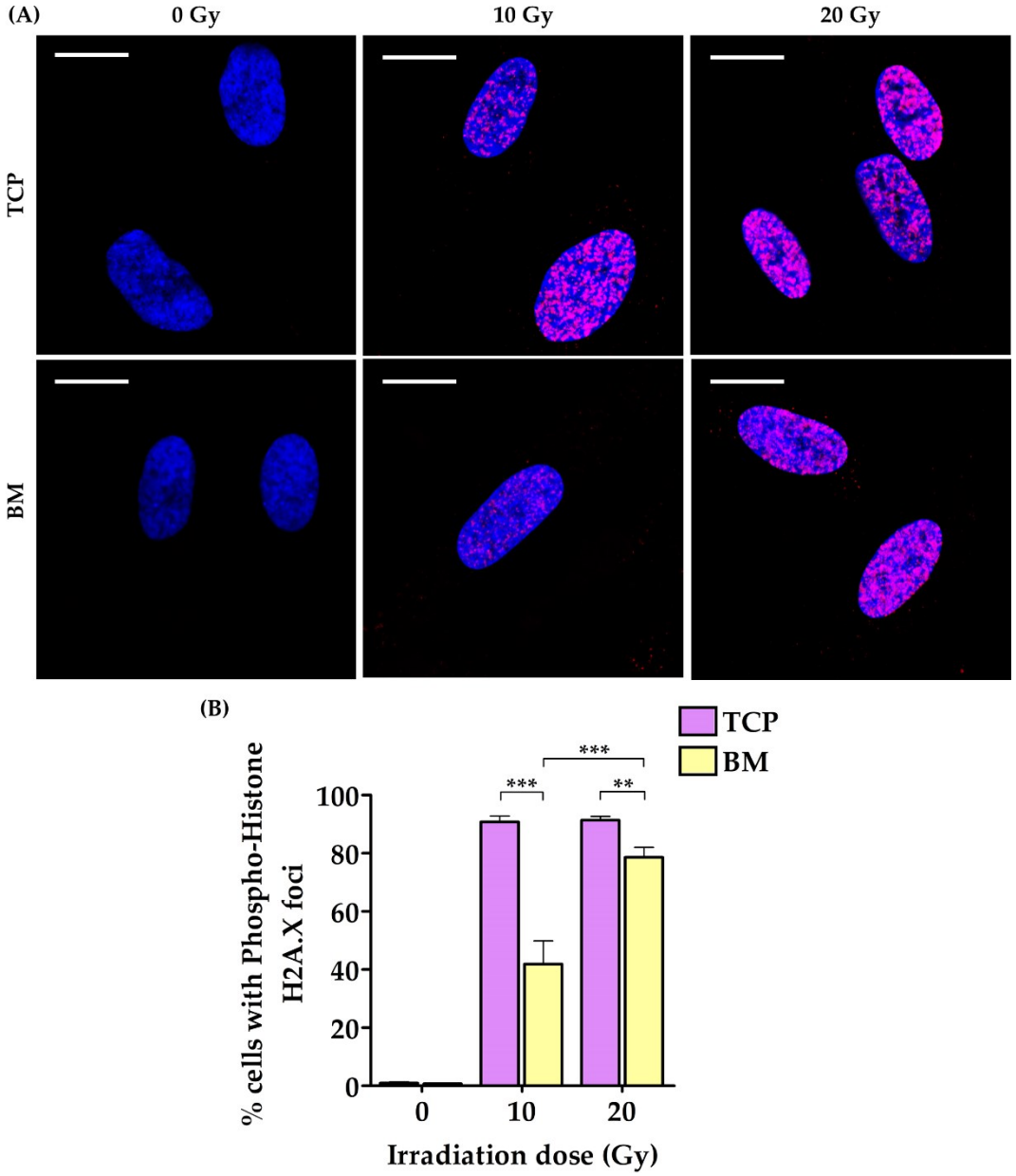

Figure 6.6 HDFn cultured on BM dishes had fewer DNA damage foci following irradiation than those on TCP. *HDFn were cultured on TCP and BM dishes for 4 days before being irradiated with 0, 10 and 20 Gy and immediately fixed and immunostained for the DNA damage marker phospho-histone H2A.X.* **(A)** *Confocal microscopy images show phospho-histone H2A.X foci in the DAPI stained nuclei of HDFn. Scale bars = 20 μm.* **(B)** *Quantification of the percentage of cells expressing nuclear phospho-histone H2A.X foci. Data represent mean ±SEM, n = 3 (3x 100 cells), statistical significance was assessed using a one-way ANOVA with Tukey's post-hoc test, ** p≤0.01, *** p ≤ 0.0001.*

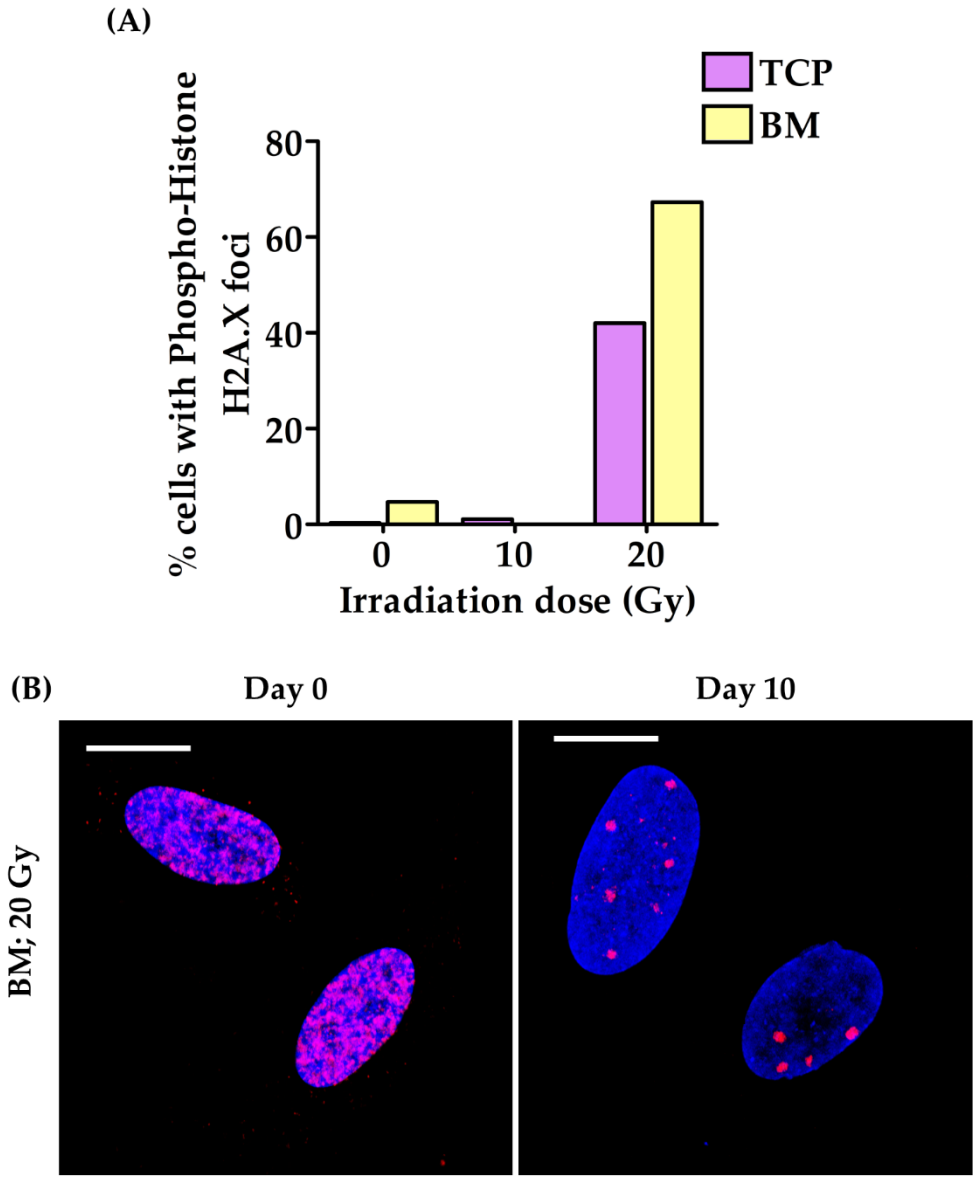

Figure 6.7 HDFn cultured on BM dishes may have had more DNA damage foci than TCP 10 days after irradiation. *HDFn were cultured on TCP and BM dishes for 4 days before being irradiated with 0, 10 and 20 Gy and cultured for 10 days. Cells were then fixed and immunostained for the DNA damage marker Phospho-Histone H2A.X.* **(A)** *Quantification of the percentage of cells expressing nuclear Phospho-Histone H2A.X foci. Data represent mean ±SEM, n = 1 (1x 100 cells).* **(B)** *Confocal microscopy images show Phospho-Histone H2A.X foci in the DAPI stained nuclei of BM cultured HDFn immediately after (day 0) and 10 days after an x-ray dose of 20 Gy. Scale bars = 20 μm.*

As highlighted at the start of this section, a key focus of these experiments was to investigate whether culturing HDFn on BM dishes had an impact on senescence. Fibroblast senescence is a key contributor of skin ageing (Weinmüllner et al., 2020),

and irradiating cells with a dose of 20 Gy has been proven to induce senescence after 10 days in an *in vitro* setting (Nelson et al., 2018). In order to assess HDFn for senescence, cells were stained for the senescence markers p21 and pl6 10 days after irradiation. However, again only one repeat was possible so full conclusions cannot be drawn from the results. The number of p21 positive cells was observed to be higher in HDFn on BM dishes for all conditions, even in the absence of irradiation (Figure 6.8). This result seemed questionable, particularly given the fact that the number of p21 positive cells was higher without irradiation than with for BM cultured cells. However, a comparison stain with p16 was not possible due to consistent problems with various p16 antibodies that showed cell-wide non-specific staining, with particular localisation in the nucleoli and vesicle structures (Figure 6.9). Consequently, drawing conclusions regarding the connection between culture substrate stiffness and senescence would require significant further work.

Figure 6.8 (overleaf) HDFn cultured on BM dishes may have had higher p21 expression than TCP 10 days after irradiation. *HDFn were cultured on TCP and BM dishes for 4 days before being irradiated with 0, 10 and 20 Gy and cultured for 10 days. Cells were then fixed and immunostained for the senescence marker p21.* **(A)** *Confocal microscopy images show nuclear p21 staining in HDFn cultured on TCP and BM dishes 10 days after an x-ray dose of 20 Gy. Scale bars = 20 μm.* **(B)** *Quantification of the percentage of cells expressing nuclear p21. Data represent mean ±SEM, n = 1 (1x 100 cells).*

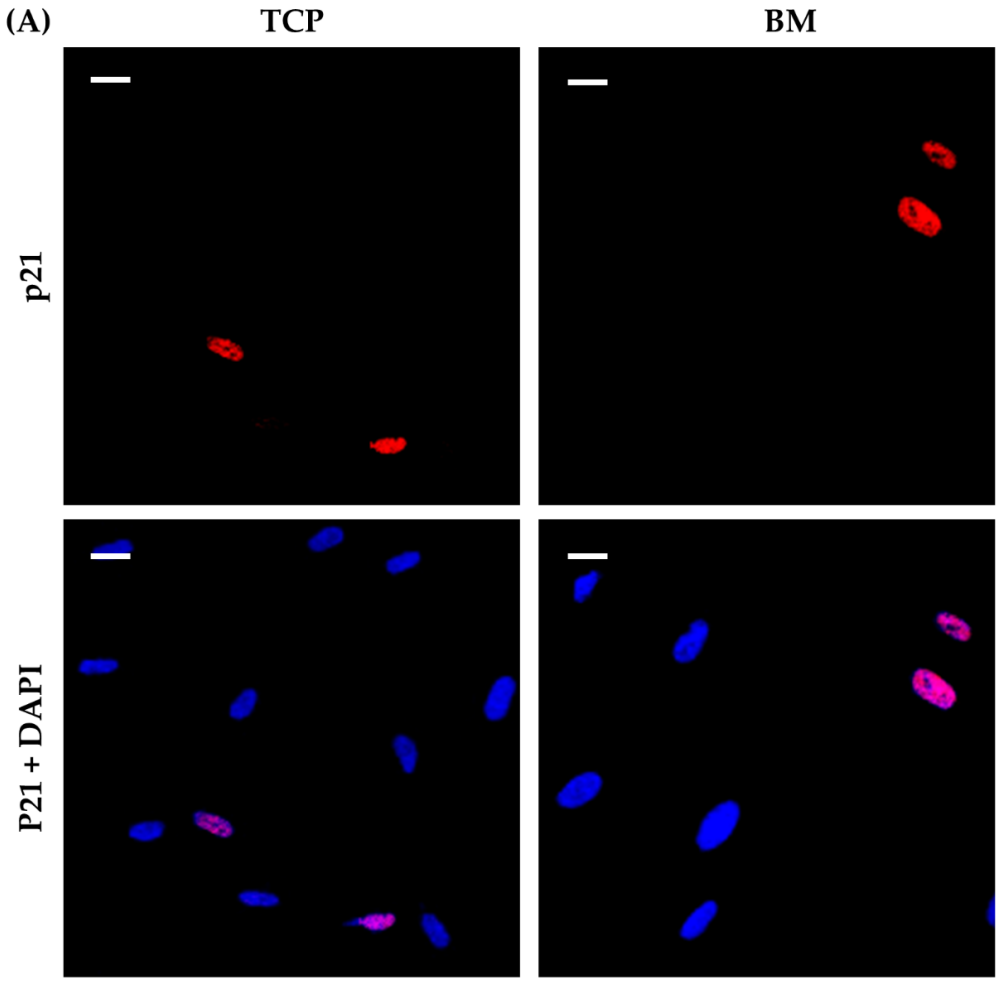
(A)
TCP
BM
p21
P21 + DAPI

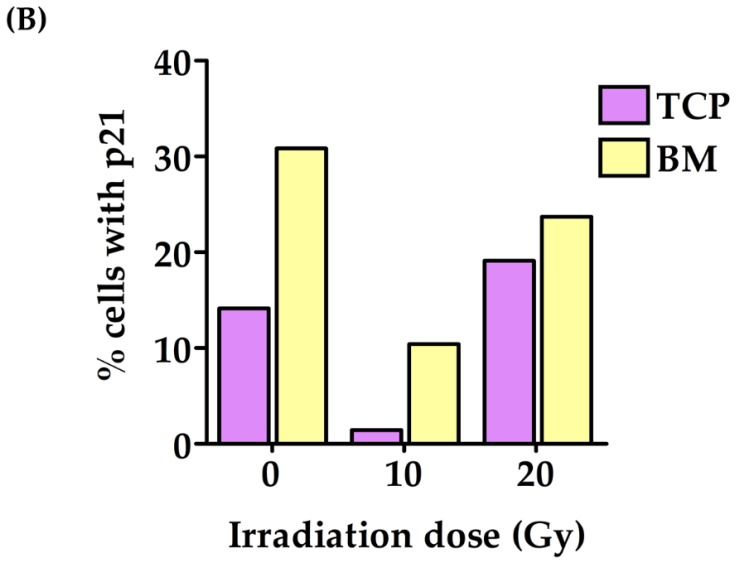
(B)
% cells with p21
40
30
20
10
0
0
10
20
Irradiation dose (Gy)
TCP
BM

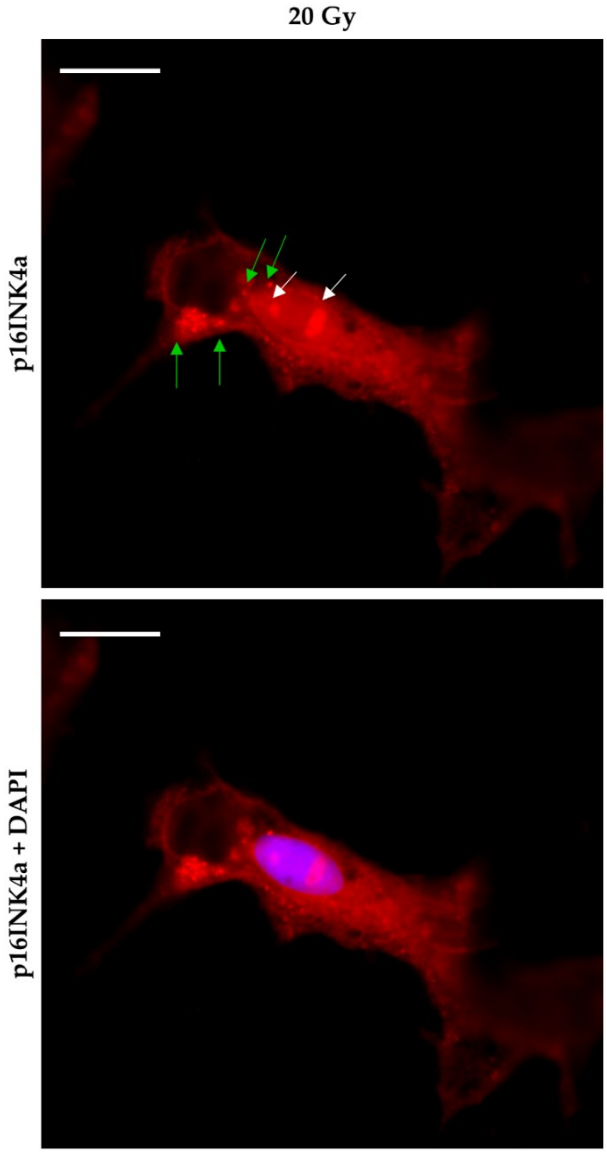

Figure 6.9 Immunofluorescence staining of p16INK4a could not be optimised. *Confocal microscopy images show non-specific staining of p16INK4a antibody in HDFn dosed with 20 Gy x-ray 10 days prior to fixation. White arrows highlight strong localisation in the nucleoli, green arrows highlight vesicle structures. Scale bars = 20 μm.*

6.4.3 HDFn cultured on BM dishes were observed to have fewer ROS

Mitochondrial ROS are both effectors and an effect of cell senescence (Pole, Dimri and Dimri, 2016), and as such it was important to investigate ROS levels in HDFn cultured on TCP and BM dishes both before and after irradiation. Due to the issue of maintaining cultures up to 10 days after irradiation without infection, there was an initial concern that there would be only one repeat. However, it was observed that

there was no apparent trend associated with culture dish stiffness and irradiation, but there was a noticeable difference between TCP and BM cultured dishes prior to irradiation. As such, the experiment was repeated with comparisons between cells on TCP and BM dishes following four days of culture with no irradiation. Flow cytometry analysis revealed that HDFn cultured on BM dishes produced less autofluorescence than those on TCP (Figure 6.10A) and had significantly lower mitochondrial mass (Figure 6.10C) and superoxide levels (Figure 6.10D). Levels of overall ROS were also observed to be significantly lower in HDFn on BM dishes when normalised to the TCP control (Figure 6.10E). These observations provide a striking insight into how significantly TCP cultureware may be associated with cellular stress *in vitro*.

Figure 6.10 (overleaf) HDFn cultured on BM dishes exhibited reduced mitochondrial mass and ROS compared to TCP. *HDFn were cultured on TCP and BM dishes for 4 days before being stained for mitochondrial mass and ROS and assessed through flow cytometry.* **(A)** *Quantification of FL3 autofluorescence using unstained control HDFn.* **(B)** *Quantification of cellular ROS using MitoSOX™ fluorescent probe.* **(C)** *Quantification of mitochondrial mass using NAO fluorogenic dye.* **(D)** *Quantification of superoxides using DHE fluorescent probe.* **(E)** *Quantification of ROS using DHR fluorogenic dye. All data* **(A – E)** *represent mean ±SEM, n = 3, statistical significance was assessed using an unpaired, two-tailed t-test, * $p \leq 0.05$, *** $p \leq 0.0001$.*

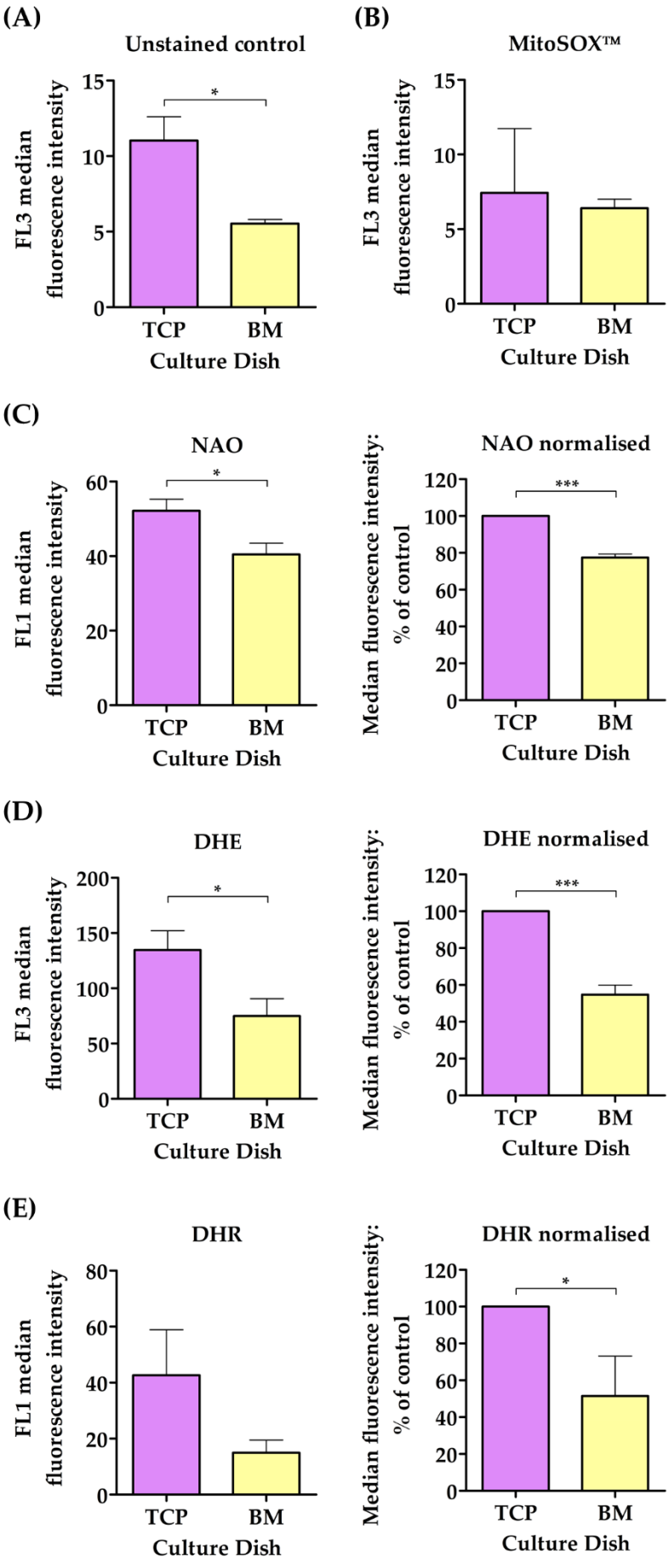
(A)
Unstained control
FL3 median fluorescence intensity
15
10
5
0
*
TCP
BM
Culture Dish
(B)
MitoSOX™
FL3 median fluorescence intensity
15
10
5
0
TCP
BM
Culture Dish
(C)
NAO
FL1 median fluorescence intensity
60
40
20
0
*
TCP
BM
Culture Dish
NAO normalised
Median fluorescence intensity: % of control
120
100
80
60
40
20
0
***
TCP
BM
Culture Dish
(D)
DHE
FL3 median fluorescence intensity
200
150
100
50
0
*
TCP
BM
Culture Dish
DHE normalised
Median fluorescence intensity: % of control
120
100
80
60
40
20
0
***
TCP
BM
Culture Dish
(E)
DHR
FL1 median fluorescence intensity
80
60
40
20
0
TCP
BM
Culture Dish
DHR normalised
Median fluorescence intensity: % of control
120
100
80
60
40
20
0
*
TCP
BM
Culture Dish

6.4.4 Technical challenges arose when culturing HDFn on hydrogel-coated dishes

It has already been mentioned earlier in this section that significant problems were faced with fungal infections during these experiments which made it difficult to obtain repeats for the irradiated samples. Whilst this was in some part due to prevalent problems with incubator contamination, it was also exacerbated by the practicalities of the irradiation process itself. In order to transport the cells to the x-ray machine they had to be carried a significant distance and the loose-lid nature of the dishes sometimes led to spillage of the medium. This was difficult to clean up without compromising the sterility of the dishes and often led to fungal growth at the sides of the dish which then spread to the inside due to the loose lid.

However, this was not the only problem faced when using BM dishes to culture HDFn. As with the keratinocytes, problems were encountered when attempting to dissociate the cells from the dishes, though in this instance it was not due to serum retention in the medium as TrypLE™ was still used to dissociate the cells. Instead, issues arose as a result of high density of cells by the end of the four-day culture period, with the HDFn often forming several layers on top of the dish. This made it difficult for the TrypLE™ to reach all of the cells even after prolonged exposure (Figure 6.11) and they often detached in large clumps that were then difficult to count. Using a cell scraper did help improve the removal of cells from the dish but did not help with the cell clumping, thus cell counting for all experiments could not be relied on to be wholly accurate.

The other main difficulty encountered when culturing HDFn on BM dishes was the frequent presentation of a "stained" region on the hydrogel that was observed on a significant number of dishes. The stain was visible to the naked eye as a white cloudiness within the hydrogel itself, and examination under a high microscopic objective ruled out an infection. Instead, the stain appeared grainy under the microscope and within this region there was very little cell growth, with abnormal cell appearance (Figure 6.12). In instances where this stain appeared the dishes were deemed compromised and were not used for experiments. This therefore contributed

to the loss of further samples and hindered a deeper investigation into fibroblast behaviour on hydrogel-coated BM dishes.

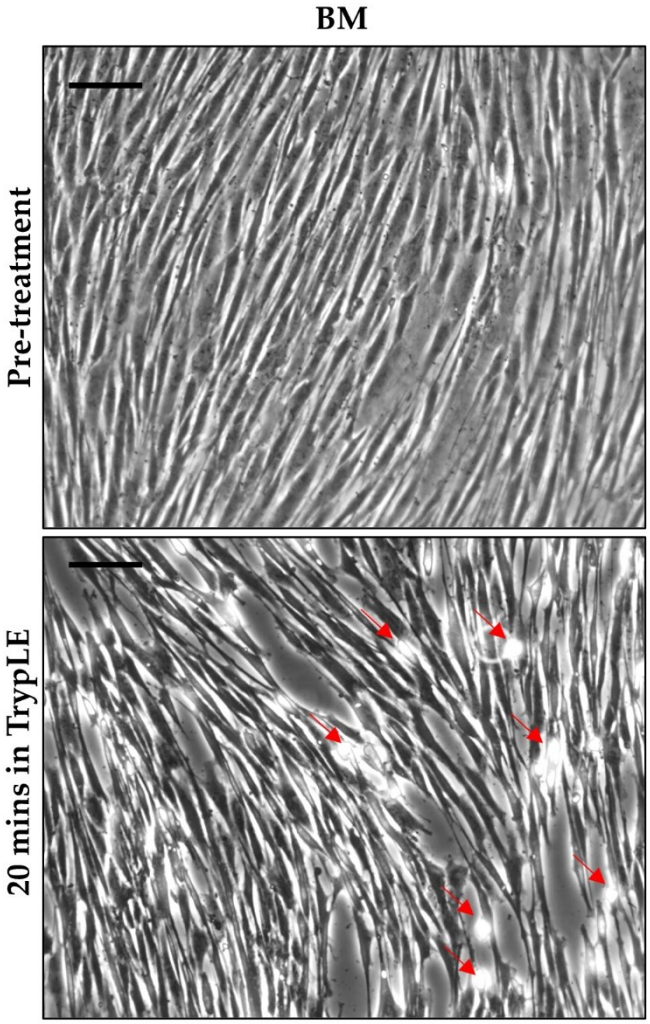

Figure 6.11 HDFn were difficult to dissociate from BM dishes. *HDFn cultured on BM dishes were difficult to dissociate using TrypLE™ due to high cell density and layering of cells. Phase contrast images show HDFn prior to treatment with TrypLE™ and 20 mins in TrypLE™. Red arrows highlight dissociating cells. Scale bars = 100 μm.*

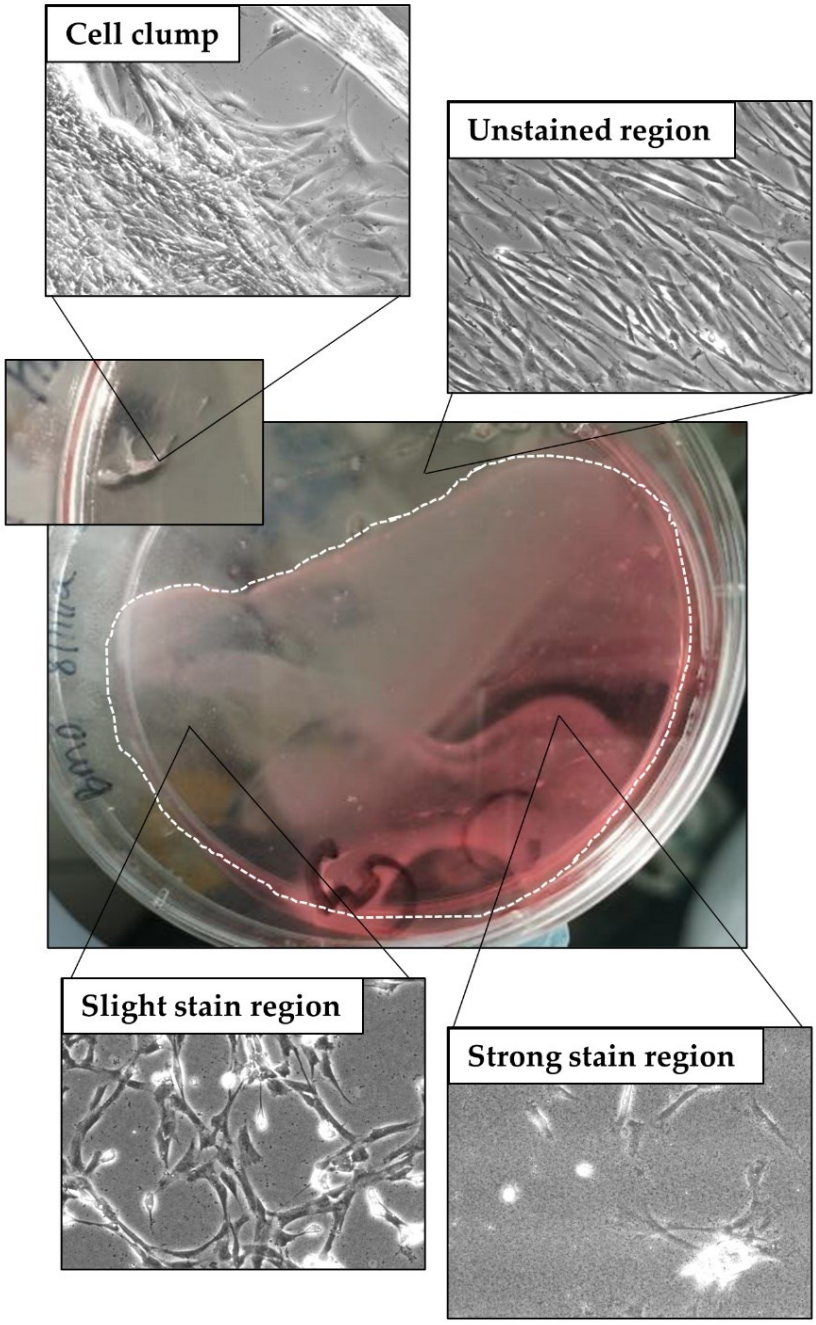

Figure 6.12 A significant proportion of BM dishes developed a stain within the hydrogel on which HDFn would not grow. *HDFn were cultured on BM dishes and in a significant proportion the hydrogel developed a stain. HDFn did not grow within these stained regions. Photographs show a stained BM dish and a clump of cells in the non-stained region. Dotted white line highlights the edge of the stain. Phase contrast images show HDFn within unstained, slightly stained, and strongly stained regions of the dish.*

6.5 Discussion

In this chapter, the main objective was to ascertain how fibroblasts were affected when cultured on hydrogel-coated dishes instead of TCP. In the literature, it has been shown that fibroblast expression of the myofibroblast marker α-SMA positively correlates to increased stiffness of the culture surface and moving the cells to a softer surface can reverse this expression (Achterberg et al., 2014; Kloxin, Benton and Anseth, 2010). Given that TCP is known to be up to one million times stiffer than *in vivo* skin, with a reported Young's Modulus of 3 GPa (Landry, Rattan and Dixon, 2019), it follows that fibroblasts grown on plastic cultureware are likely in a permanently activated state more reminiscent of wounded than quiescent skin. This is interesting as it has already been discussed in chapter 5 that TCP is known to have a similar impact on keratinocytes, with activation markers such as keratins 6, 16 and 17 often observed in 3D epidermal models cultured from TCP primed cells (Smiley et al., 2006).

Whilst for keratinocytes the interest in external mechanics related to its role in balancing proliferation and differentiation *in vivo*, for fibroblasts changes to external mechanical stimuli are associated with skin ageing. Dermal ageing is associated with remodelling of the ECM as well as the accumulation of senescent fibroblasts. The direct relationship between external mechanics and senescence is not yet understood, and thus another objective of this chapter was to ascertain whether culturing HDFn on a softer substrate impacted the level of cell senescence and the DDR following irradiation.

However, it should be noted that the results presented above only just begin to answer the questions raised at the start of this chapter, and further work would need to be done to fully meet the objectives. It has already been mentioned that persistent problems with fungal infections and presentation of a growth-impacting "stained" region on the hydrogels were a big hindrance to obtaining sufficient repeats and optimising experiments to produce the desired data. The initial placement in the Newcastle laboratory was only three months running through autumn of 2019. It was planned to extend this placement and spend another couple of months in 2020 tying

up some of the loose ends. However, due to the COVID-19 pandemic and the implementation of a national lockdown in March 2020 there was unfortunately no opportunity to do this. Once the laboratories were reopened it was with limited access and it was deemed more realistic to spend the final months focusing on the keratinocyte experiments rather than having to travel to Newcastle University whilst restrictions were still in place. This was disappointing as some of the data presented in this chapter is truly interesting, in particular the differences in expression of DNA damage markers following irradiation, and levels of ROS in fibroblasts cultured on BM dishes versus TCP. The potential implications of these findings are discussed in greater depth below, along with descriptions of experiments that could not be completed and would be an ideal starting point for future work on this topic.

6.5.1 Early differences observed between HDFn on hydrogel-coated dishes versus TCP

The first step in assessing fibroblasts on soft hydrogel-coated dishes was to simply seed the cells onto the dishes and observe any differences in cell appearance and behaviour. It has already been mentioned that initially 1 kPa dishes were the desired stiffness for the fibroblast work. However, due to problems with infection, "stained" dishes, and slow delivery time it was necessary to incorporate both 1 kPa and 4 kPa dishes which were referred to collectively as BM dishes throughout the results section. As reported earlier, there were no statistically significant differences noted between 1 kPa and 4 kPa cultured fibroblasts, and in their 2014 study Achterberg et al. used 1 kPa to 10 kPa substrates to replicate normal dermis (Achterberg et al., 2014).

As discussed with relation to the keratinocytes, a stiff external environment is known to induce proliferation in cells as a result of the Hippo signalling pathway (Dupont et al., 2011), and as such it was hypothesised that HDFn cultured on BM dishes would proliferate more slowly than those on TCP. This was found to be the case for HEKn, as discussed in chapter 3, but for HDFn the opposite was observed. HDFn cultured on BM dishes exhibited high proliferative capacity that was comparable to TCP in the first two to three days, but which rapidly surpassed TCP by day five after seeding (Figure 6.1A). This was confirmed by comparing the number of cells seeded against

the number of cells harvested, the latter of which was significantly greater for HDFn on BM dishes (Figure 6.1B). The number of population doublings was also observed to be significantly higher in cells cultured on BM dishes (Figure 6.2). It must also be noted that HDFn cultured on BM dishes were very difficult to dissociate due to the density of the cells (Figure 6.11), and as such these may actually be underestimates of the true proliferative capacity of HDFn on BM dishes. The one contradictory result in this batch of experiments was the ki67 immunostaining which revealed that HDFn on BM dishes possessed significantly less nuclei with the proliferation marker (Figure 6.3). However, as mentioned previously (section 6.4.1), persistent problems with ki67 staining being limited to the periphery of coverslips throws into doubt the accuracy of this result, and further work would need to be done to either optimise the antibody or to test an alternative proliferation marker.

Comparing these observations to the literature it is of no surprise that they largely fail to correlate, with other studies reporting that an increase in hydrogel or matrix stiffness resulted in an increase in fibroblast proliferation (Lin et al., 2021; Wahlsten et al., 2021; Wang, Chung and Kurisawa, 2012). Nonetheless, one study using 3D poly(ethylene glycol) (PEG) based hydrogels did report that the proliferation rate of human dermal fibroblasts increased with decreasing material stiffness (Bott et al., 2010). Given that this study used 3D hydrogels, it is not directly comparable to the experiments performed here as the fibroblasts were cultured within the gel itself. As such, the difference in proliferation was attributed to variations in the amount of cross-linking within the low and high stiffness PEG-hydrogels which impacted the amount of space cells had to move into (Bott et al., 2010). However, in its discussion the study did highlight the importance of gel viscoelastic characteristics and response to cell activities in manipulating cell behaviour. It was noted that collagen gels with a similar stiffness to the PEG-gels underwent a matrix shrinkage that was not observed in the PEG-gels despite them possessing a greater number of cells. Collagen contraction in the presence of fibroblasts is well documented *in vitro* (Berry, Shelton and Lee, 2009; Bullard et al., 1999; Meshel et al., 2005) and is attributed to the free movement of collagen molecules against one another, making them easy to displace and enabling macroscopic contraction of the material (Bott et al., 2010). Proliferation

on the collagen gels in the study performed by Bott et al. was observed to rapidly increase in the first seven days of culture but did not vary between days 14 and 21 (Bott et al., 2010).

Given the information above, it should be noted that the hydrogels purchased for this project were coated with collagen I to improve cell adherence in culture. Whilst this likely had no impact on the keratinocytes, in hindsight it should have been anticipated that the fibroblasts would have a more significant interaction with this collagen layer. As such, it is possible that the HDFn cultured on the BM dishes were contracting the underlying collagen fibres, thus increasing the level of mechanical strain the cells encountered, and potentially explaining the observation of a higher proliferation rate than anticipated. Additionally, the collagen-derived dipeptide proline-hydroxyproline (Pro-Hyp) has been shown to increase fibroblast proliferation *in vitro* (Ohara et al., 2010), which means the elevated proliferation rate could also be a result of the HDFn breaking down the collagen I coating into peptides during remodelling. In order to draw any definitive conclusions regarding the elevated proliferation of HDFn cultured on BM dishes, it would be necessary to perform an in-depth investigation into both the gene and protein expression of the cells and their interaction with the collagen coating. The localisation of YAP1 would be of specific interest, but this may be hard to visualise given the densely packed nature of HDFn cultured on BM dishes. It would also be interesting to culture the cells on dishes without the collagen I coating which are available to purchase from the same source (Cell Guidance Systems), and thus a direct comparison between the two could be performed.

In addition to the highly proliferative nature of the HDFn when cultured on BM dishes, it was also noted that the appearance of the cells was very different to those on TCP. At day five of culture, the HDFn on TCP appeared heterogenous in size and shape and were not all orientated in the same direction. However, those on the BM dishes were observed to have taken on the characteristic spindle shape of *in vivo* fibroblasts and were all orientated in parallel to one another (Figure 6.1A). The stellate morphology observed in some of the TCP HDFn is indicative of fibroblast

activation (Ravikanth et al., 2011), thus the spindle shape of the HDFn on BM dishes suggests that these cells are more morphologically similar to the quiescent fibroblasts found in normal *in vivo* dermis despite the increased proliferation rate. In a 2017 study, computational modelling was used to understand the mechanism of long-range alignment patterns in fibroblasts, such as that observed in HDFn on BM dishes in this project. The results of this study suggested that recapitulating long-range alignment critically relies on the mutual alignment of fibroblasts and collagen fibres, and that modification of the underlying ECM network is necessary to reproduce this morphology (Li et al., 2017). Consequently, this further consolidates the hypothesis that HDFn on BM dishes were interacting with the collagen I coating, and suggests that this influenced HDFn appearance and behaviour beyond the scope of the mechanical properties of the hydrogel alone.

The final observation made during the early stages of HDFn culture was that cells propagated on BM dishes appeared to have smaller nuclei. Quantification of HDFn cultured on BM and glass coverslips confirmed that the nuclear area and nuclear perimeter was lower for cells on BM coverslips to a statistically significant degree (Figure 6.4B-C). However, this was deemed a result of the smaller, spindle cell morphology of HDFn on BM dishes, as nuclear size is known to correlate with cytoplasmic volume (Katiyar et al., 2019).

6.5.2 HDFn cultured on BM dishes differed to those on TCP following irradiation

Following the initial assessment of HDFn in standard cell culture, the next step was to induce DNA damage and senescence in order to simulate dermal ageing. This was achieved through irradiating the HDFn using an x-ray machine. The first difference noted between TCP and BM cultured cells 10 days after irradiation was in their appearance; following doses of either 10 Gy or 20 Gy, HDFn cultured on TCP exhibited an increased number of large cells, whilst the fibroblasts cultured on BM dishes remained small and spindle shaped across all conditions (Figure 6.5). Senescent fibroblasts are larger, flattened, and have an irregular shape (Rani et al., 2017), suggesting that the bigger cells observed on the TCP dishes following

irradiation may have been indicative of cell senescence. Given that the cells on BM dishes retained the same appearance regardless of irradiation dose, it was hypothesised that these cells were perhaps not as susceptible to damage from x-ray exposure. This appeared to be further consolidated following immunofluorescence analysis of HDFn fixed immediately after irradiating the cells. HDFn were stained for the DDR marker phospho-histone H2A.X, and cells cultured on TCP were observed to have significantly greater foci positive nuclei than those on BM dishes, particularly following a 10 Gy dose (Figure 6.6).

A recent study by Dos Santos et al. reported that treatment of HeLa cells with cisplatin to induce DNA damage resulted in the significant reduction of nuclear stiffness as a result of chromatin decondensation. Additional reduction of nuclear tension as a result of cytoskeletal relaxation was observed to have a protective effect on the cells, and in fact reduced the accumulation of DNA damage (Dos Santos et al., 2021). Their hypothesis was that nuclear softening reduced the rate of DNA replication, and thus limited the number of double-stranded breaks induced by cisplatin. The idea that nuclear softening is a protective mechanism against DNA damage does offer some hint as to why HDFn cultured on BM dishes might have exhibited fewer DDR markers immediately following irradiation; it is well documented that cell stiffness correlates with that of the external environment (Liu, Sun and Simmons, 2013; Rianna and Radmacher, 2017; Solon et al., 2007), and keratinocytes cultured on BM dishes were observed to have softer nuclei than those on TCP (Figure 4.24). However, it has already been discussed above that these cells were more proliferative than those on TCP, so the hypothesis of Dos Santos et al. would not align with the observations made in this study. Additionally, without AFM analysis, it cannot be confirmed that HDFn on BM dishes did exhibit nuclear softening.

Another potential explanation for this protective effect is that HDFn cultured on BM dishes appeared much smaller, were much more densely packed, and had smaller nuclei. In 2019, a study reported that NIH3T3 fibroblasts cultured on silicone elastic membranes exhibited significantly decreased fluorescence intensity of phospho-

histone γ-H2A.X following UV radiation when the membranes had been stretched and nuclei were under greater tension (Nagayama and Fukuei, 2019). Cells on stretched membranes had dramatically compressed nuclei as a result of actin reorganisation in response to the greater tension, and it was hypothesised that the resulting force-induced condensation of chromatin provided resistance to UV radiation-induced DNA damage (Nagayama and Fukuei, 2019). Consequently, given the smaller nuclear size and densely packed cells on BM dishes, it is possible that the same hypothesis applies to this study; increased nuclear tension as a result of high cell confluency, and smaller nuclear, acted together to increase chromatin condensation which provided a protective resistance to irradiation.

Given the highly proliferative nature of the HDFn on BM dishes, it was difficult to balance obtaining a reduced cell density whilst ensuring the cells were in culture long enough to enable them to fully acclimatise to their mechanical environment. Nonetheless, in order to assess whether the high cell density is responsible for the protective effect against DNA damage, it would be necessary to repeat the irradiation experiment on cells that are at a significantly lower confluency. Thus, at this stage it cannot be concluded why HDFn cultured on BM dishes had fewer DDR markers immediately following irradiation.

However, in contradiction to these early observations, further assessment of the HDFn 10 days after irradiation suggested that cells exposed to a 20 Gy dose had less DNA damage when cultured on the TCP dishes (Figure 6.7A); a noticeable difference in contrast to the diffuse staining observed immediately after irradiation was that the nuclei now possessed discrete phospho-histone H2A.X foci (Figure 6.7B). A potential reason for this could be that DNA damage repair is facilitated by a delay in cell cycle progression (Meng et al., 2005), and the increased proliferative capacity of HDFn on BM dishes could have resulted in a slower repair process, even though fewer cells encountered DNA damage immediately following irradiation. However, the biggest of this experiment was that it only had one repeat due to issues with carrying enough samples through to the 10 day time point without infection. Consequently, additional

repeats would be required before conclusions could be drawn about the long-term DDR of HDFn on TCP and BM dishes following irradiation.

Another contradictory result came from the immunofluorescence analysis of the senescence marker p21, which suggested that HDFn had a greater percentage of p21 positive cells (Figure 6.8). However, once again this experiment only had one repeat and therefore cannot be relied upon to draw conclusions from, particularly given the questionable data point suggesting that >30% of HDFn on BM dishes had positive staining in the control sample that was not irradiated. This directly contradicts the high proliferation rate and morphological appearance of the cells in culture, and thus it was attempted to repeat this experiment using the alternative senescence marker p16INK4a. However, problems were encountered when trying to optimise numerous p16INK4a antibodies, with all of them producing non-specific staining (Figure 6.9).

As a result of these problems, further investigation would be required in order to assess the level of cell senescence in HDFn cultured on TCP versus BM dishes 10 days after irradiation. It should be noted that it had been planned to return to the Newcastle laboratory and run western blots for p21 and p16 in case the antibodies were better suited for this technique. Additionally, another planned experiment was to take samples of the medium from HDFn 10 days after a 20 Gy x-ray dose and send them off for analysis of SASP content. However, it was not possible to complete these experiments due to the COVID-19 pandemic which prevented a return to the Newcastle laboratory, and as such they must recommended as a starting point for any future research into this aspect of the project.

6.5.3 HDFn cultured on BM dishes exhibited reduced levels of ROS

One of the main contributors towards skin ageing is the accumulation of ROS, with skin possessing the highest ROS load of any organ in the body (Rinnerthaler et al., 2015). Consequently, levels of ROS were considered an important aspect of fibroblast biology to compare in HDFn cultured on TCP and BM dishes. Differences in ROS levels in irradiated HDFn were not found to be significant, however there was a striking difference in ROS levels in the control cells that had not been irradiated. It

was observed through flow cytometry analysis that the fluorescence intensity for ROS, superoxides, and mitochondrial mass were all significantly lower for HEKn cultured on BM dishes compared to TCP (Figure 6.10). Increased mitochondrial mass is indicative of a stress response to mitochondrial dysfunction, with cells increasing their number of mitochondria as a compensation method (Nugent et al., 2007). Cellular ROS such as superoxides and hydrogen peroxide are produced as a result of mitochondrial oxidative metabolism, but accumulation of ROS within a cell can result in oxidative damage to nucleic acids, proteins, and lipids (Ray, Huang and Tsuji, 2012). Therefore, the result of the flow cytometry analysis suggests that HDFn cultured on BM dishes may have had superior mitochondrial function and a better antioxidant defence system than those on TCP. This is particularly interesting due to the role that mitochondrial ROS play in regulating cell proliferation as they are required for mitogenic signalling (Diebold and Chandel, 2016). Given that HDFn on BM dishes exhibited higher proliferation but lower ROS levels than those on TCP, it can be hypothesised that HDFn cultured on TCP exhibit ROS levels that surpass the requirement for cell proliferation, putting them at greater risk of oxidative stress.

6.5.4 The use of BM dishes presented technical problems that hindered the culture of HDFn

As mentioned in chapter 3, one of the primary objectives of this project was to ascertain whether culturing cells on hydrogel-coated cultureware facilitated the ease of use with which 2D culture is normally associated. In chapter 3, it was highlighted that there were a number of technical issues encountered during the culturing of HEKn on BM dishes. One of these problems was a difficulty with dissociating the cells, which was eventually solved through the introduction of TrypLE™ which was not neutralised by the retention of serum from the medium by the hydrogel. However, despite the use of TrypLE™ to dissociate HDFn, problems were still encountered as a result of the extreme density to which the fibroblasts grew to when cultured on BM dishes. As a result, even after 20 minutes of exposure to TrypLE™ there were still a large number of cells stuck to the dishes as the reagent was unable to penetrate through the cell layers (Figure 6.11).

In an attempt to combat this, a cell scraper was gently used to help dislodge cells that had been incubated with TrypLE™ but this led to issues with cell clumping which made it hard to count the cell number and isolate cells for further analysis such as immunostaining or flow cytometry. It may have been possible to get around this by adjusting the initial seeding density, but as mentioned earlier, it was important to ensure that the cells were exposed to the dishes for long enough to adjust to their mechanical environment, and the high proliferation rate of cells on the BM dishes meant that they easily reached confluency during this period.

Nevertheless, whilst the difficulties with dissociating cells from the dishes was frustrating, it was not a major hindrance to the overall study of HDFn on BM cultureware. In contrast, one persistent issue which did have a severe impact on the ability to produce data for this chapter was the appearance of a white "stain" on numerous hydrogels, over which the cells either grew abnormally or died (Figure 6.12). This phenomenon was never witnessed during keratinocyte culture, and no reference to similar experiences could be found in the literature but it was a consistent problem encountered across dishes from separate batches and with different gel stiffnesses. As such, the only potential hypothesis thought of at the time was that the fibroblasts were interacting with the underlying hydrogel in a way that altered it in a way that made it toxic to the cells.

Microorganisms have been shown to hydrolyse polyacrylamide using amidase enzymes (Xiong et al., 2018; Yu et al., 2015), which are a large group of proteins found in both prokaryotes and eukaryotes that share a highly conserved Ser-Ser-Lys catalytic triad used for amide hydrolysis, though the substrate specificity and function varies widely (InterPro, 2021). N-acylethanolamine acid amidase is an enzyme found in numerous human cell types, including dermal fibroblasts (The Human Protein Atlas, 2020) but whether the enzyme is close enough in function to bacterial amidases to be able to hydrolyse polyacrylamide, and whether it is secreted extracellularly by fibroblasts, are two uncertainties that throw doubt on the likelihood of this being the reason behind the "stain". As such, it is still unknown what the cause of this phenomenon was, and the only apparent way to avoid it would

be to change the composition of the gel. However, given that there is so much literature available in which fibroblasts have been cultured on polyacrylamide hydrogels with no mention of similar experiences, the cause of this issue begs further investigation.

6.5.5 Additional experiments that could not be completed

As mentioned at the start of this discussion, the combination of persistent infections and problems with the "stain" phenomenon, as well as the COVID-19 pandemic, meant that not all of the experiments originally planned for this chapter were able to be completed. One of these, as has already been discussed, was a more in-depth investigation into fibroblast senescence when cultured on TCP and BM dishes. The original plan for this aspect of the study was to take samples of medium from the dishes 10 days after irradiation and send these off to be assessed for SASP content. This would have been an interesting experiment that would have provided a much more detailed insight into any senescence differences between the two conditions. Additionally, western blot analysis of senescence markers combined with LINC proteins would have been of interest given what is known about changes to the LINC protein content in response to cell senescence (6.1.2).

Moreover, another key aspect of fibroblast biology is cell activation which is associated with wound healing *in vivo*. It has been shown that myofibroblast activation can be promoted by matrix stiffness and increased mechanical strain (Achterberg et al., 2014) as well as higher ROS levels (Edmondson et al., 2014). Given the stiffness of TCP and the higher levels of ROS HDFn cultured on TCP exhibited, combined with the more quiescent morphology of HDFn on BM dishes, another planned experiment was to investigate the expression of α-SMA in order to assess whether a myofibroblast phenotype was promoted by TCP culture.

6.6 Conclusions

This chapter aimed to investigate whether culturing HDFn on BM substrates mimicking dermal mechanics would result in changes to cell activation under normal conditions, and to the DDR and senescence following irradiation. It was hypothesised

that cell activation and proliferation would be decreased in HDFn on BM dishes, but the unknown link between extracellular mechanics and senescence made it difficult to predict how cells would respond to irradiation.

Whilst the experimental results obtained for this chapter were extremely interesting, they by no means provided a full answer to the original questions raised. Moreover, the experiments were beset by hindrances such as fungal infections, the presentation of a stained region in numerous dishes upon which cells would not grow, and the COVID-19 pandemic which prevented a return to the Newcastle laboratory to perform additional experiments and to obtain final repeats.

Nonetheless, it was evident from the early stages of culture that BM dishes had an impact on fibroblast behaviour, though this presented itself as an unexpected increase in proliferative capacity that was attributed to potential interactions with the collagen coating on top of the hydrogel layer. Additionally, HDFn on BM dishes were observed to have smaller nuclei and the cells themselves appeared smaller and more spindle shaped, making them more morphologically reminiscent of quiescent cells *in vivo* in contrast to the active stellate morphology observed on TCP dishes. Flow cytometry analysis revealed that HDFn on TCP dishes had greater mitochondrial mass and higher levels of ROS and superoxides than those on BM dishes. This suggested that fibroblasts on TCP might have inferior antioxidant and mitochondrial function compared to those on hydrogel-coated dishes. Moreover, elevated ROS levels has been linked to myofibroblast activation, further suggesting that TCP promoted an activated phenotype and BM dishes promoted quiescence.

Finally, it was observed that HDFn cultured on BM dishes exhibited reduced DNA damage marker expression immediately following irradiation, suggesting a protective effect that was hypothetically attributed to increased cell density and smaller nuclei resulting in force-induced condensing of chromatin. Repetition of this analysis 10 days after irradiation revealed the opposite, with HDFn on BM dishes expressing a greater number of phospho-histone H2A.X foci. This result was hypothesised to be due to the high proliferative capacity of HDFn on BM dishes which resulted in delayed DNA damage repair which is usually associated with a

delay in cell cycle progression. However, further repeats would be needed in order to confirm this difference in the DDR 10 days after irradiation. Similarly inconclusive were the experiments designed to assess differences in cell senescence following irradiation, though HDFn cultured on TCP exhibited an increase in the number of large, irregular-shaped cells that are a hallmark of senescence and were notably absent from the BM dishes.

To conclude, the results of this experiment provide a solid foundation for further investigation into the effects of substrate stiffness on 2D fibroblast culture. These early analyses offer promising evidence that BM hydrogels reduce the prevalence of the activated fibroblast phenotype usually observed *in vitro*, though contradictions such as the increased proliferation show that further work is required to fully understand the response of HDFn to substrate stiffness. Moreover, the tantalising hints at reduced ROS, protection from DNA damage, and fewer morphologically senescent fibroblasts when HDFn are cultured on BM dishes could have implications that are much more far-reaching than the future of *in vitro* fibroblast culture. As such, these data are only the starting point of what could be a fascinating study into the effects of external mechanics on fibroblast phenotype and behaviour.

7 Summary and Final Discussion

7.1 Skin cells cultured on BM dishes could be more reflective of their *in vivo* counterparts

The main aim of this project was to replicate the mechanical environment of the epidermal and dermal compartments of human skin in 2D, and observe any differences between keratinocytes and fibroblasts cultured on standard TCP versus those on a BM substrate. The data presented and discussed throughout this thesis demonstrate that the stiffness of TCP has a significant impact on the behaviour and gene and protein expression of HEKn and HDFn. It has been reported in the literature that both keratinocytes and fibroblasts cultured on TCP exhibit an activated and hyperproliferative phenotype that is reminiscent of cells found at wound healing sites rather than normal quiescent skin (Smiley et al., 2005; Smiley et al., 2006; Darby et al., 2014; Edmondson et al., 2014). In this comparison of cells cultured on TCP and BM dishes, it was observed that BM substrates appeared to promote a more quiescent phenotype.

In keratinocytes this presented as a reduced proliferation rate, downregulation of proliferation markers, reduced nuclear YAP1, and reorganisation of the actin cytoskeleton to have fewer stress fibres. Fibroblasts cultured on BM dishes appeared to contradict the understood relationship between substrate stiffness and proliferation and were in fact more proliferative than those on TCP. However, conversely the HDFn on BM dishes were observed to exhibit reduced ROS and a smaller, spindle morphology, making them more reminiscent of quiescent fibroblasts than the stellate cells observed on TCP dishes. Further work should focus on confirming this active versus quiescent cell phenotype through the analysis of keratin markers associated with wound healing in keratinocytes, and α-SMA expression in fibroblasts.

However, reduced proliferative capacity was not the limit of the changes observed in HEKn when cultured on BM dishes. One of the main hallmarks of the epidermis is the homeostatic balance between proliferation and differentiation. *In vivo*, the

external mechanical environment plays a critical role in keratinocyte differentiation as cells move away from the stiff basement membrane (Biggs et al., 2020). In this study, it was observed that HEKn cultured on soft 4 kPa hydrogels exhibited upregulated differentiation markers, suggesting that this mechanical environment was more reminiscent of the suprabasal layers of the epidermis. Additionally, colony density was increased on soft BM dishes, and HEKn were observed to express E-cadherin localised linearly at the cell membrane, suggesting tighter cell-cell connections which are again reminiscent of higher epidermal layers. Consequently, by manipulating the stiffness of BM dishes in 2D culture, it may be possible to facilitate more focused research into the gene expression, protein localisation, and behaviour of keratinocytes at various stages of terminal differentiation, thus reflecting the different epidermal layers.

What is ultimately demonstrated through the results of this thesis is that the mechanical strength of TCP cultureware impacts cells in ways that should not be ignored during subsequent analyses. AFM measurements of HEKn showed that *in vitro* cells alter their entire mechanical stiffness to correlate with that of their underlying substrate, and the striking downregulation of cytoskeletal and LINC protein components exhibited on softer substrates will inevitably have more widespread implications than could be investigated here.

Additionally, HDFn exposed to irradiation exhibited significantly reduced expression of the DNA damage marker phospho-histone H2A.X, and lacked the presentation of large, irregular-shaped cells indicative of cellular senescence. Whilst both the HEKn and HDFn observations require significant further investigation in order to fully understand the full impact of *in vitro* substrate stiffness, they throw into stark relief the potential for TCP to skew the results of a study. It should be a point of concern that so much literature in the public domain fails to acknowledge the potential limitations of TCP culture. Whilst studies specifically focused on biomechanics clearly recognise the implications of using TCP or glass cultureware *in vitro*, it is important that all studies utilizing standard 2D cell culture techniques, regardless of whether biomechanics is a focus, begin to draw attention to the

limitations that this inappropriate mechanical environment engenders, and acknowledge that this might be reflected in their data.

7.2 Priming skin cells in a more realistic mechanical environment could be used to produce superior 3D skin models

The secondary significant aim of this project was to assess whether culturing skin cells on a BM substrate in 2D facilitated superior 3D model development; superior models were defined as a physical organisation and protein expression profile more reminiscent of *in vivo* skin. For this section of the project, keratinocytes were the focus, and it was observed after some trial and error that HEKn cultured on 50 kPa dishes in 2D produced epidermal models that were thicker and had more defined layers that better represented the epidermis in human skin. HEKn cultured on 4 kPa dishes produced thin, poorly assembled models that were attributed to the dishes being too soft and therefore promoting too differentiated a phenotype to mimic the proliferative basal layer. In contrast, the TCP primed cells were known to be highly proliferative in 2D but were deemed too stiff to support the balance between proliferation and differentiation required for epidermal assembly. Additionally, it was hypothesised that cells harvested from TCP dishes were subject to a lag period in which the cells had to adjust to their new, softer mechanical environment which impacted epidermal assembly and led to thinner, less organised models.

Whilst the data presented in chapter 5 offer a tantalising glimpse as to how altering the mechanical environment of 2D culture could improve 3D models, there remains a significant amount of more in-depth work to be done. With this in mind, future work should focus on a thorough analysis of protein expression and localisation within EEs formed from TCP and 50 kPa primed dishes, and directly compare them to the human epidermis. Moreover, further experiments should be done to assess the impact of 50 kPa dishes in 2D on barrier function in 3D. Finally, it would be beneficial to perform further work to combine HEKn primed on 50 kPa and 4 kPa dishes to see whether this would improve model organisation still further.

Branching out beyond the EEs, future work stemming from this project should focus on the production of dermal models using fibroblasts primed on BM dishes in 2D. The results of the few analyses performed on HDFn cultured on BM dishes were striking, and it would be interesting to see how the changes in physical appearance, proliferative capacity, ROS levels, and DDR affect ECM deposition and composition within a dermal equivalent. Viewing this project in hindsight, it would perhaps have been better to focus the 3D model work on the fibroblasts rather than the keratinocytes. Epidermal models are notoriously difficult to produce *in vitro* given the donor variability of primary HEKn which impacts the ability of some cells to form a stratified epidermis in culture (Eves et al., 2000; Stark et al., 1999). Moreover, keratinocytes are sensitive to terminal differentiation at any time in culture as a result of cues as simple as increased cell density due to high confluency (Poumay and Pittelkow, 1995), which would also impact their capacity for epidermal assembly. In contrast, dermal models are relatively easy to produce using scaffolds such as Alvetex® onto which HDFn can be seeded and where they can then secrete ECM components to form their own external environment (Roger et al., 2019). These models can be easily assessed through immunofluorescence and western blotting techniques.

To conclude, whilst the results of the EEs provided a promising correlation between using a BM substrate in 2D and improved 3D appearance, the experiments were hindered by persistent problems with inconsistency in the quality of the models that was more to do with the cells than the dishes on which they were cultured. As such, whilst further work does need to be done on the EEs to consolidate these early findings, it would be prudent to focus a significant amount of future time producing dermal models and characterising the effects that BM priming have on fibroblasts once transferred to a 3D setting.

7.3 Culturing HEKn and HDFn on BM cultureware required adaptation of standard 2D cell culture techniques

Perhaps one if the most important considerations for this project was to provide a natural mechanical environment in a 2D format that would not compromise the ease of use and cost-effective nature of standard cell culture. The chosen format of culture dishes and coverslips coated with a thin hydrogel seemed to meet this objective, and the ability to purchase the cultureware in batches of different stiffnesses offered an element of product control. However, whilst the dishes were significantly easier to work with compared to 3D tissue models, issues did arise that meant they were still not wholly comparable with TCP culture.

The first problem encountered was that the hydrogel layer absorbed growth medium that could not be removed by washing with PBS. This made it difficult to dissociate the cells using standard trypsin and led to the unavoidable contamination of protein and RNA lysates with medium components. Additionally, for the HEKn it was not possible to propagate the cells on the softer dishes beyond a single passage meaning that long-term maintenance of the cells in a BM environment was not possible. Further difficulties included the BM coverslips being too thick to image when mounted onto slides and the hydrogels being too fragile for a cell scraper resulting in inferior protein yields for western blot analysis.

However, whilst initially frustrating, most of these issues were relatively easy to adapt to through the implementation of small changes e.g., using a different reagent for dissociating cells, lysing cells using a rocker rather than a cell scraper, and using microscope objectives with a greater free working distance to image coverslips. The issue with cell propagation on softer dishes was not one that could be readily fixed, but it should be noted that this was in no way a negative reflection on the dishes themselves; softer dishes pushed HEKn towards differentiation and as such it is likely that they were unable to re-form attachments to a new dish following dissociation. Consequently, if longer-term culture on BM dishes was desired, it would be more appropriate to culture HEKn on 50 kPa dishes which were shown to promote

propagation as well as superior epidermal assembly, thus implying that they more appropriately represented the mechanical environment of the epidermal basement membrane.

In contrast to these relatively minor setbacks, the biggest hindrance to working with the hydrogel-coated dishes were persistent problems with cells not growing properly on the dishes. When culturing HEKn, it was observed that occasional batches of BM dishes did not support cell growth, and HEKn would either fail to proliferate, or die and detach following seeding. It was noted that when this occurred, all dishes with the same lot number were affected, suggesting that the issue was specific to the dishes purchased, and that their production was not as standardised as first assumed. Moreover, HDFn were observed to also fail to grow on some dishes, though in this instance the problem arose following the presentation of a white stained area within the hydrogel and did not seem to correlate with batch number but occurred randomly. Given that the dishes were expensive, took a long time to arrive when ordered, and could only be purchased in packs of 10, it is clear that buying dishes such as this from companies would in no way be a cost-effective equivalent to using TCP cultureware. The decision to purchase BM dishes for this project stemmed largely from a desire to not devote a large amount of time to optimising recipes to produce hydrogels of specific stiffnesses. However, polyacrylamide gels are easy to make and the ingredients to do so already exist in many laboratories where western blotting takes places. As such, future work may wish to consider focusing on the development of a protocol for making hydrogels in the laboratory. This would not only be a significantly more cost-effective option, but it would also enable the production of a much greater number of dishes to facilitate bigger experimental set-ups and long-term culture of cells on BM substrates.

To conclude, whilst not as easy to work with as standard TCP cultureware, replacing TCP with hydrogel-coated dishes would only require minimal adaptations to current culture techniques in order to implement their wider use. Cell culture in a 2D format has long been the gold standard of *in vitro* cell work, but it would be to science's detriment to rigidly hold on to a technique that it is becoming increasingly apparent

offers a grossly inappropriate mechanical environment for mammalian cells. Given the findings of both this project and the numerous published studies investigating cell biomechanics, it is clear that the future of cell culture research relies on a field-wide willingness to focus attention away from past techniques and towards BM cultureware. Until mammalian cells are routinely cultured in a mechanical environment that reflects their native tissue, the results of *in vitro* cell culture will never truly capture the behaviour, genotype and phenotype of *in vivo* cells.

8 References

Abe, Y. and Tanaka, N. (2017). Roles of the Hedgehog Signaling Pathway in Epidermal and Hair Follicle Development, Homeostasis, and Cancer. *Journal of Developmental Biology*, [online] 5(4), p.12. Available at: https://www.ncbi.nlm.nih.gov/pmc/articles/PMC5831796/#!po=7.81250.

Achterberg, V.F., Buscemi, L., Diekmann, H., Smith-Clerc, J., Schwengler, H., Meister, J.-J., Wenck, H., Gallinat, S. and Hinz, B. (2014). The Nano-Scale Mechanical Properties of the Extracellular Matrix Regulate Dermal Fibroblast Function. *Journal of Investigative Dermatology*, [online] 134(7), pp.1862–1872. Available at: https://www.sciencedirect.com/science/article/pii/S0022202X15368949.

Akiyama, Y., Yamamoto, Y., Doi, Y., Izumi, Y., Nishijima, S. and Kimura, H. (2008). Analysis of Viscoelasticity of Human Skin for Prevention of Pressure Ulcers. *Journal of Mechanics in Medicine and Biology*, 08(01), pp.33–43.

Alam, H., Sehgal, L., Kundu, S.T., Dalal, S.N. and Vaidya, M.M. (2011). Novel function of keratins 5 and 14 in proliferation and differentiation of stratified epithelial cells. *Molecular Biology of the Cell*, [online] 22(21), pp.4068–4078. Available at: https://www.ncbi.nlm.nih.gov/pmc/articles/PMC3204069/.

Almeida, F.V., Walko, G., McMillan, J.R., McGrath, J.A., Wiche, G., Barber, A.H. and Connelly, J.T. (2015). The cytolinker plectin regulates nuclear mechanotransduction in keratinocytes. *Journal of Cell Science*. [online] Available at: https://journals.biologists.com/jcs/article/128/24/4475/55383/The-cytolinker-plectin-regulates-nuclear.

Anderson, E.D., Sastalla, I., Earland, N.J., Mahnaz, M., Moore, I.N., Otaizo-Carrasquero, F., Myers, T.G., Myles, C.A., Datta, S.K. and Myles, I.A. (2018). Prolonging culture of primary human keratinocytes isolated from suction blisters with the Rho kinase inhibitor Y-27632. *PLoS ONE*, [online] 13(9), p.e0198862. Available at: https://www.ncbi.nlm.nih.gov/pmc/articles/PMC6135349/.

Balzac, F., Avolio, M., Degani, S., Kaverina, I., Torti, M., Silengo, L., Small, J.V. and Retta, S.F. (2005). E-cadherin endocytosis regulates the activity of Rap1: a traffic light GTPase at the crossroads between cadherin and integrin function. *Journal of Cell Science*, [online] 118(20), pp.4765–4783. Available at: https://journals.biologists.com/jcs/article/118/20/4765/28514/E-cadherin-endocytosis-regulates-the-activity-of.

Banerjee, S., Utuje, K.J. C. and Marchetti, M.C. (2015). Propagating Stress Waves During Epithelial Expansion. *Physical Review Letters*, [online] 114(22). Available at: https://journals.aps.org/prl/abstract/10.1103/PhysRevLett.114.228101.

Berger, J. and Sellke, T. (1987). Testing a Point Null Hypothesis: The Irreconcilability of P Values and Evidence. *Journal of the American Statistical Association*. [online] Available at: https://www.tandfonline.com/doi/abs/10.1080/01621459.1987.10478397.

Berry, C.C., Shelton, J.C. and Lee, D.A. (2009). Cell-generated forces influence the viability, metabolism and mechanical properties of fibroblast-seeded collagen gel constructs. *Journal of Tissue Engineering and Regenerative Medicine*, [online] 3(1), pp.43–53. Available at: https://pubmed.ncbi.nlm.nih.gov/19039798/.

Bertolero, F., Kaighn, M.Edward., Gonda, M.A. and Saffiotti, U. (1984). Mouse epidermal keratinocytes. *Experimental Cell Research*, [online] 155(1), pp.64–80. Available at: https://pubmed.ncbi.nlm.nih.gov/6208047/.

Biggs, C.L., Kim, C.S., Miroshnikova, Y.A. and Wickström, S.A. (2020). Mechanical Forces in the Skin: Roles in Tissue Architecture, Stability, and Function. *Journal of Investigative Dermatology*, [online] 140(2), pp.284–290. Available at: https://eurekamag.com/research/069/166/069166963.php.

Bikle, D.D., Xie, Z. and Tu, C.-L. (2012). Calcium regulation of keratinocyte differentiation. *Expert Review of Endocrinology & Metabolism*, [online] 7(4), pp.461–472. Available at: https://www.ncbi.nlm.nih.gov/pmc/articles/PMC3491811/.

Bio-rad. (2021). Western Blot DoctorTM — Protein Band Size and Pattern Problems | LSR | Bio-Rad. [online] Available at: https://www.bio-rad.com/en-

uk/applications-technologies/western-blot-doctor-protein-band-size-pattern-problems?ID=MIW4MCKG4#significantlyhighermw [Accessed 12 Jul. 2021].

Birch-Machin, M.A. and Bowman, A. (2016). Oxidative stress and ageing. *British Journal of Dermatology*, [online] 175(S2), pp.26–29. Available at: https://onlinelibrary.wiley.com/doi/full/10.1111/bjd.14906?casa_token=pwcJIA2HjN4AAAAA%3A6mmWZwC0LT8ZQZir5Ziq5wetBRI-rt78CobWWuX1-em_FVFujIlq5heA1Vy4F7cWaUn_T3XRT8Tc4rw.

Bordeleau, F., Myrand Lapierre, M.-E., Sheng, Y. and Marceau, N. (2012). Keratin 8/18 Regulation of Cell Stiffness-Extracellular Matrix Interplay through Modulation of Rho-Mediated Actin Cytoskeleton Dynamics. *PLoS ONE*, [online] 7(6), p.e38780. Available at: https://journals.plos.org/plosone/article?id=10.1371/journal.pone.0038780.

Bose, A., Teh, M.-T., Mackenzie, I. and Waseem, A. (2013). Keratin K15 as a Biomarker of Epidermal Stem Cells. *International Journal of Molecular Sciences*, [online] 14(10), pp.19385–19398. Available at: https://www.ncbi.nlm.nih.gov/pmc/articles/PMC3821562/.

Bott, K., Upton, Z., Schrobback, K., Ehrbar, M., Hubbell, J.A., Lutolf, M.P. and Rizzi, S.C. (2010). The effect of matrix characteristics on fibroblast proliferation in 3D gels. *Biomaterials*, [online] 31(32), pp.8454–8464. Available at: https://pubmed.ncbi.nlm.nih.gov/20684983/.

Bouameur, J.-E., Favre, B., Fontao, L., Lingasamy, P., Begré, N. and Borradori, L. (2014). Interaction of Plectin with Keratins 5 and 14: Dependence on Several Plectin Domains and Keratin Quaternary Structure. *Journal of Investigative Dermatology*, [online] 134(11), pp.2776–2783. Available at: https://www.sciencedirect.com/science/article/pii/S0022202X15365180.

Bouzid, T., Kim, E., Riehl, B.D., Esfahani, A.M., Rosenbohm, J., Yang, R., Duan, B. and Lim, J.Y. (2019). The LINC complex, mechanotransduction, and mesenchymal stem cell function and fate. *Journal of Biological Engineering*, [online] 13(1). Available at: https://jbioleng.biomedcentral.com/articles/10.1186/s13036-019-0197-9.

Broussard, J.A., Yang, R., Huang, C., Nathamgari, S.S.P., Beese, A.M., Godsel, L.M., Hegazy, M.H., Lee, S., Zhou, F., Sniadecki, N.J., Green, K.J. and Espinosa, H.D. (2017). The desmoplakin–intermediate filament linkage regulates cell mechanics. *Molecular Biology of the Cell*, [online] 28(23), pp.3156–3164. Available at: https://www.ncbi.nlm.nih.gov/pmc/articles/PMC5687018/.

Bullard, K.M., Mudgett, J., Scheuenstuhl, H., Hunt, T.K. and Banda, M.J. (1999). Stromelysin-1-Deficient Fibroblasts Display Impaired Contractionin Vitro. *Journal of Surgical Research*, [online] 84(1), pp.31–34. Available at: https://pubmed.ncbi.nlm.nih.gov/10334885/.

Butler, T.A.J., Paul, J.W., Chan, E.-C., Smith, R. and Tolosa, J.M. (2019). Misleading Westerns: Common Quantification Mistakes in Western Blot Densitometry and Proposed Corrective Measures. *BioMed Research International*, [online] 2019, pp.1–15. Available at: https://www.hindawi.com/journals/bmri/2019/5214821/.

Cai, X., Wang, K.-C. and Meng, Z. (2021). Mechanoregulation of YAP and TAZ in Cellular Homeostasis and Disease Progression. *Frontiers in Cell and Developmental Biology*, [online] 9. Available at: https://www.frontiersin.org/articles/10.3389/fcell.2021.673599/full.

Caliari, S.R. and Burdick, J.A. (2016). A practical guide to hydrogels for cell culture. *Nature Methods*, [online] 13(5), pp.405–414. Available at: https://www.ncbi.nlm.nih.gov/pmc/articles/PMC5800304/.

Candi, E., Schmidt, R. and Melino, G. (2005). The cornified envelope: a model of cell death in the skin. *Nature Reviews Molecular Cell Biology*, [online] 6(4), pp.328–340. Available at: https://pubmed.ncbi.nlm.nih.gov/15803139/.

Carley, E., Stewart, R.K., Zieman, A., Jalilian, I., King, Diane.E., Zubek, A., Lin, S., Horsley, V. and King, M.C. (2020). The LINC complex transmits integrin-dependent tension to the nuclear lamina and represses epidermal differentiation. *bioRxiv*. [online] Available at: https://www.biorxiv.org/content/10.1101/2020.05.03.075085v2.

Carthew, J. (2015). Characterising LINC Complex Roles in 3D Epithelial Migration and Breast Cancer Metastasis. [PhD Thesis] Available at: http://etheses.dur.ac.uk/11453/.

Cartwright, S. and Karakesisoglou, I. (2014). Nesprins in health and disease. *Seminars in Cell & Developmental Biology*, [online] 29, pp.169–179. Available at: https://pubmed.ncbi.nlm.nih.gov/24374011/.

Castañón, M.J., Walko, G., Winter, L. and Wiche, G. (2013). Plectin–intermediate filament partnership in skin, skeletal muscle, and peripheral nerve. *Histochemistry and Cell Biology*, [online] 140(1), pp.33–53. Available at: https://link.springer.com/article/10.1007/s00418-013-1102-0.

Chambliss, A.B., Khatau, S.B., Erdenberger, N., Robinson, D.K., Hodzic, D., Longmore, G.D. and Wirtz, D. (2013). The LINC-anchored actin cap connects the extracellular milieu to the nucleus for ultrafast mechanotransduction. *Scientific Reports*, [online] 3(1). Available at: https://www.nature.com/articles/srep01087.

Chang, K.C.N., Wang, Y., Oh, I.G., Jenkins, S., Freedman, L.P., Thompson, C.C., Chung, J.H. and Nagpal, S. (2010). Estrogen Receptor β Is a Novel Therapeutic Target for Photoaging. *Molecular Pharmacology*, [online] 77(5), pp.744–750. Available at: https://pubmed.ncbi.nlm.nih.gov/20110405/.

Chang, W., Antoku, S., Östlund, C., Worman, H.J. and Gundersen, G.G. (2015). Linker of nucleoskeleton and cytoskeleton (LINC) complex-mediated actin-dependent nuclear positioning orients centrosomes in migrating myoblasts. *Nucleus*, [online] 6(1), pp.77–88. Available at: https://www.ncbi.nlm.nih.gov/pmc/articles/PMC4615731/.

Chang, Y.-C., Wu, J.-W., Wang, C.-W. and Jang, A.C.-C. . (2020). Hippo Signaling-Mediated Mechanotransduction in Cell Movement and Cancer Metastasis. *Frontiers in Molecular Biosciences*, [online] 6. Available at: https://www.frontiersin.org/articles/10.3389/fmolb.2019.00157/full.

Chari, N.S., Romano, R.A., Koster, M.I., Jaks, V., Roop, D., Flores, E.R., Teglund, S., Sinha, S., Gruber, W., Aberger, F., Medeiros, L.J., Toftgard, R. and McDonnell, T.J.

(2013). Interaction between the TP63 and SHH pathways is an important determinant of epidermal homeostasis. *Cell Death & Differentiation*, [online] 20(8), pp.1080–1088. Available at: https://www.nature.com/articles/cdd201341.

Coleman, A.K., Joca, H.C., Shi, G., Lederer, W.J. and Ward, C.W. (2021). Tubulin acetylation increases cytoskeletal stiffness to regulate mechanotransduction in striated muscle. *Journal of General Physiology*, [online] 153(7). Available at: https://rupress.org/jgp/article-abstract/153/7/e202012743/211904/Tubulin-acetylation-increases-cytoskeletal.

Collin, C., Moll, R., Kubicka, S., Ouhayoun, J.-P. and Franke, W.W. (1992). Characterization of human cytokeratin 2, an Epidermal cytoskeletal protein synthesized late during differentiation. *Experimental Cell Research*, [online] 202(1), pp.132–141. Available at: https://www.sciencedirect.com/science/article/abs/pii/0014482792904122.

Collins, C., Denisin, A.K., Pruitt, B.L. and Nelson, W.J. (2017). Changes in E-cadherin rigidity sensing regulate cell adhesion. *Proceedings of the National Academy of Sciences*, [online] 114(29), pp.E5835–E5844. Available at: https://www.pnas.org/content/pnas/114/29/E5835.full.pdf.

Colombo, I., Sangiovanni, E., Maggio, R., Mattozzi, C., Zava, S., Corbett, Y., Fumagalli, M., Carlino, C., Corsetto, P.A., Scaccabarozzi, D., Calvieri, S., Gismondi, A., Taramelli, D. and Dell'Agli, M. (2017). HaCaT Cells as a Reliable In Vitro Differentiation Model to Dissect the Inflammatory/Repair Response of Human Keratinocytes. *Mediators of Inflammation*, [online] 2017, pp.1–12. Available at: https://www.hindawi.com/journals/mi/2017/7435621/.

Connelly, J. (2019). Biophysical regulation of epidermal fate and function. *Advances in Stem Cells and their Niches*, [online]. Available at: https://www.semanticscholar.org/paper/Biophysical-regulation-of-epidermal-fate-and-Connelly/bac4554fc060308bfff7cce67fda453f8ee9f51a.

Cooper, G.M. (2000). *The Cell: A Molecular Approach*. 2nd ed. Sunderland (MA): Sinauer Associates. Available at: https://www.ncbi.nlm.nih.gov/books/NBK9932/.

Cornelissen, L.H., Oomens, C.W.J., Huyghe, J.M. and Baaijens, F.P.T. (2007). Mechanisms that play a role in the maintenance of the calcium gradient in the epidermis. *Skin Research and Technology*, [online] 13(4), pp.369–376. Available at: https://pubmed.ncbi.nlm.nih.gov/17908187/.

Corning. (2021). Corning® Matrigel® Matrix. [online] Available at: https://www.corning.com/emea/en/products/life-sciences/products/surfaces/matrigel-matrix.html [Accessed 2 Aug. 2021].

D'Angelo, Maximiliano A., Gomez-Cavazos, J. Sebastian, Mei, A., Lackner, Daniel H. and Hetzer, Martin W. (2012). A Change in Nuclear Pore Complex Composition Regulates Cell Differentiation. *Developmental Cell*, [online] 22(2), pp.446–458. Available at: https://www.sciencedirect.com/science/article/pii/S1534580711005314.

Dainichi, T., Hayden, Matthew S., Park, S.-G., Oh, H., Seeley, John J., Grinberg-Bleyer, Y., Beck, Kristen M., Miyachi, Y., Kabashima, K., Hashimoto, T. and Ghosh, S. (2016). PDK1 Is a Regulator of Epidermal Differentiation that Activates and Organizes Asymmetric Cell Division. *Cell Reports*, [online] 15(8), pp.1615–1623. Available at: https://www.sciencedirect.com/science/article/pii/S2211124716304788.

Darby, I.A., Laverdet, B., Bonté, F. and Desmoulière, A. (2014). Fibroblasts and myofibroblasts in wound healing. *Clinical, Cosmetic and Investigational Dermatology*, [online] 7, pp.301–311. Available at: https://www.ncbi.nlm.nih.gov/pmc/articles/PMC4226391/#!po=59.0909.

Daulagala, A.C., Yost, J., Yeganegi, A., Richardson, W.J., Yost, M.J. and Kourtidis, A. (2020). A Simple Method to Test Mechanical Strain on Epithelial Cell Monolayers Using a 3D-Printed Stretcher. *Methods in Molecular Biology*, [online] pp.235–247. Available at: https://link.springer.com/protocol/10.1007/7651_2020_314.

Diebold, L. and Chandel, N.S. (2016). Mitochondrial ROS regulation of proliferating cells. *Free Radical Biology and Medicine*, [online] 100, pp.86–93. Available at: https://www.sciencedirect.com/science/article/pii/S0891584916302180?casa_token=Qy7SyGe7PuIAAAAA:9h_n0kol1awh_6XXOfADw5W1TzzydvwH2PDxTrnmHG_jyU1oG7nQQYe7gKSkB64s4jhj4kij.

Donnaloja, F., Jacchetti, E., Soncini, M. and Raimondi, M.T. (2019). Mechanosensing at the Nuclear Envelope by Nuclear Pore Complex Stretch Activation and Its Effect in Physiology and Pathology. *Frontiers in Physiology*, [online] 10. Available at: https://www.frontiersin.org/articles/10.3389/fphys.2019.00896/full.

Dos Santos, Á., Cook, A.W., Gough, R.E., Schilling, M., Olszok, N., Brown, I., Wang, L., Aaron, J., Martin-Fernandez, M.L., Rehfeldt, F. and Toseland, C.P. (2021). DNA damage alters nuclear mechanics through chromatin reorganization. *Nucleic Acids Research*, [online] 49(1), pp.340–353. Available at: https://academic.oup.com/nar/article/49/1/340/6039924?login=true.

Duning, K., Schurek, E.-M., Schlüter, M., Bayer, M., Reinhardt, H.-C., Schwab, A., Schaefer, L., Benzing, T., Schermer, B., Saleem, M.A., Huber, T.B., Bachmann, S., Kremerskothen, J., Weide, T. and Pavenstädt, H. (2008). KIBRA Modulates Directional Migration of Podocytes. *Journal of the American Society of Nephrology*, [online] 19(10), pp.1891–1903. Available at: https://pubmed.ncbi.nlm.nih.gov/18596123/.

Duperret, E. and Ridky, T.W. (2013). Focal adhesion complex proteins in epidermis and squamous cell carcinoma. *Cell Cycle*, [online] 12(20), pp.3272–3285. Available at: https://www.ncbi.nlm.nih.gov/pmc/articles/PMC3885638/.

Dupont, S., Morsut, L., Aragona, M., Enzo, E., Giulitti, S., Cordenonsi, M., Zanconato, F., Le Digabel, J., Forcato, M., Bicciato, S., Elvassore, N. and Piccolo, S. (2011). Role of YAP/TAZ in mechanotransduction. *Nature*, [online] 474(7350), pp.179–183. Available at: https://www.nature.com/articles/nature10137.

Eaglstein, W.H. and Falanga, V. (1997). Tissue engineering and the development of Apligraf®, a human skin equivalent. *Clinical Therapeutics*, [online] 19(5), pp.894–905. Available at: https://www.sciencedirect.com/science/article/abs/pii/S0149291897800434.

EC (European Commission) (2010). Directive 2010/63/EU of the European Parliament and of the council of 22 September 2010 on the protection of animals used for scientific purposes. *Official Journal of the European Union*, [online] 276,

pp.33–79. Available at: https://eur-lex.europa.eu/LexUriServ/LexUriServ.do?uri=OJ:L:2010:276:0033:0079:EN:PDF.

EC (European Commission). (2017). Skin Irritation: EpiDerm Skin Irritation Test (SIT). [online] Available at: https://ec.europa.eu/jrc/en/eurl/ecvam/alternative-methods-toxicity-testing/validated-test-methods/skin-irritation/epiderm.

Edmondson, R., Broglie, J.J., Adcock, A.F. and Yang, L. (2014). Three-Dimensional Cell Culture Systems and Their Applications in Drug Discovery and Cell-Based Biosensors. *ASSAY and Drug Development Technologies*, [online] 12(4), pp.207–218. Available at: https://www.ncbi.nlm.nih.gov/pmc/articles/PMC4026212/#!po=44.6429.

Elias, P.M., Brown, B.E., Crumrine, D., Feingold, K.R. and Ahn, S.K. (2002). Origin of the Epidermal Calcium Gradient: Regulation by Barrier Status and Role of Active vs Passive Mechanisms. *Journal of Investigative Dermatology*, [online] 119(6), pp.1269–1274. Available at: https://www.sciencedirect.com/science/article/pii/S0022202X1530083X.

Elosegui-Artola, A., Andreu, I., Beedle, A.E.M., Lezamiz, A., Uroz, M., Kosmalska, A.J., Oria, R., Kechagia, J.Z., Rico-Lastres, P., Le Roux, A.-L., Shanahan, C.M., Trepat, X., Navajas, D., Garcia-Manyes, S. and Roca-Cusachs, P. (2017). Force Triggers YAP Nuclear Entry by Regulating Transport across Nuclear Pores. *Cell*, [online] 171(6), pp.1397-1410.e14. Available at: https://www.cell.com/cell/fulltext/S0092-8674(17)31192-3?_returnURL=https%3A%2F%2Flinkinghub.elsevier.com%2Fretrieve%2Fpii%2FS0092867417311923%3Fshowall%3Dtrue.

Enyedi, B. and Niethammer, P. (2017). Nuclear membrane stretch and its role in mechanotransduction. *Nucleus*, [online] 8(2), pp.156–161. Available at: https://pubmed.ncbi.nlm.nih.gov/28112995/.

EpiSkin (2021). EpiSkin / Human Epidermis. [online] https://www.episkin.com/Episkin. Available at: https://www.episkin.com/Episkin.

Eves, P., Layton, C., Hedley, S., Dawson, R.A., Wagner, M., Morandini, R., Ghanem, G. and Mac Neil, S. (2000). Characterization of an in vitro model of human

melanoma invasion based on reconstructed human skin. *British Journal of Dermatology*, [online] 142(2), pp.210–222. Available at: https://pubmed.ncbi.nlm.nih.gov/10730751/.

Ezratty, Ellen J., Stokes, N., Chai, S., Shah, Alok S., Williams, Scott E. and Fuchs, E. (2011). A Role for the Primary Cilium in Notch Signaling and Epidermal Differentiation during Skin Development. *Cell*, [online] 145(7), pp.1129–1141. Available at: https://www.sciencedirect.com/science/article/pii/S0092867411005915.

Faller, C. and Bracher, M. (2002). Reconstructed Skin Kits: Reproducibility of Cutaneous Irritancy Testing. *Skin Pharmacology and Physiology*, [online] 15(1), pp.74–91. Available at: https://pubmed.ncbi.nlm.nih.gov/12476011/.

Fentem, J.H., Archer, G.E.B., Balls, M., Botham, P.A., Curren, R.D., Earl, L.K., Esdaile, D.J., Holzhütter, H.-G. . and Liebsch, M. (1998). The ECVAM International Validation Study on In Vitro Tests for Skin Corrosivity. *Toxicology in Vitro*, [online] 12(4), pp.483–524. Available at: https://www.sciencedirect.com/science/article/abs/pii/S0887233398000198.

Fletcher, D.A. and Mullins, R.D. (2010). Cell mechanics and the cytoskeleton. *Nature*, [online] 463(7280), pp.485–492. Available at: https://www.nature.com/articles/nature08908.

Flitney, E.W., Kuczmarski, E.R., Adam, S.A. and Goldman, R.D. (2009). Insights into the mechanical properties of epithelial cells: the effects of shear stress on the assembly and remodeling of keratin intermediate filaments. *The FASEB Journal*, [online] 23(7), pp.2110–2119. Available at: https://www.ncbi.nlm.nih.gov/pmc/articles/PMC2704593/.

Fuchs, E. and Green, H. (1980). Changes in keratin gene expression during terminal differentiation of the keratinocyte. *Cell*, [online] 19(4), pp.1033–1042. Available at: https://pubmed.ncbi.nlm.nih.gov/6155214/.

Furukawa, F., Fujii, K., Horiguchi, Y., Matsuyoshi, N., Fujita, M., Toda, K.-I., Imamura, S., Wakita, H., Shirahama, S. and Takigawa, M. (1997). Roles of E- and P-cadherin in the human skin. *Microscopy Research and Technique*, [online] 38(4),

pp.343–352. Available at: https://analyticalsciencejournals.onlinelibrary.wiley.com/doi/10.1002/(SICI)1097-0029(19970815)38:4%3C343::AID-JEMT2%3E3.0.CO;2-K.

Gassmann, M., Grenacher, B., Rohde, B. and Vogel, J. (2009). Quantifying western blots: Pitfalls of densitometry. *ELECTROPHORESIS*, [online] 30(11), pp.1845–1855. Available at: https://analyticalsciencejournals.onlinelibrary.wiley.com/doi/full/10.1002/elps.200800720?casa_token=YwlxCbAw8sYAAAAA%3AB-39Q9wv3fwVy9R7x_YzWA9renB3dBWPSKjG2PMbaYMuVz9MAfvj18_NwLpc23jcl9682hc3nTO_eoE.

Gdula, M.R., Poterlowicz, K., Mardaryev, A.N., Sharov, A.A., Peng, Y., Fessing, M.Y. and Botchkarev, V.A. (2013). Remodeling of Three-Dimensional Organization of the Nucleus during Terminal Keratinocyte Differentiation in the Epidermis. *Journal of Investigative Dermatology*, [online] 133(9), pp.2191–2201. Available at: https://www.ncbi.nlm.nih.gov/pmc/articles/PMC4135477/.

Ghassemi, S., Meacci, G., Liu, S., Gondarenko, A.A., Mathur, A., Roca-Cusachs, P., Sheetz, M.P. and Hone, J. (2012). Cells test substrate rigidity by local contractions on submicrometer pillars. *Proceedings of the National Academy of Sciences*, [online] 109(14), pp.5328–5333. Available at: https://www.pnas.org/content/pnas/109/14/5328.full.pdf.

Gilbert, H.T.J. and Swift, J. (2019). The consequences of ageing, progeroid syndromes and cellular senescence on mechanotransduction and the nucleus. *Experimental Cell Research*, [online] 378(1), pp.98–103. Available at: https://pubmed.ncbi.nlm.nih.gov/30836065/.

Gilbert, P.M., Havenstrite, K.L., Magnusson, K.E.G., Sacco, A., Leonardi, N.A., Kraft, P., Nguyen, N.K., Thrun, S., Lutolf, M.P. and Blau, H.M. (2010). Substrate Elasticity Regulates Skeletal Muscle Stem Cell Self-Renewal in Culture. *Science*, [online] 329(5995), pp.1078–1081. Available at: https://science.sciencemag.org/content/329/5995/1078.full.

Gittes, F., Mickey, B., Nettleton, J. and Howard, J. (1993). Flexural rigidity of microtubules and actin filaments measured from thermal fluctuations in shape. *Journal of Cell Biology*, [online] 120(4), pp.923–934. Available at: https://rupress.org/jcb/article/120/4/923/28578.

Gomez, J.M., Chumakova, L., Bulgakova, N.A. and Brown, N.H. (2016). Microtubule organization is determined by the shape of epithelial cells. *Nature Communications*, [online] 7(1). Available at: https://www.nature.com/articles/ncomms13172.

Gonzales, K.A.U. and Fuchs, E. (2017). Skin and Its Regenerative Powers: An Alliance between Stem Cells and Their Niche. *Developmental Cell*, [online] 43(4), pp.387–401. Available at: https://www.sciencedirect.com/science/article/pii/S1534580717308146.

Graham, H.K., McConnell, J.C., Limbert, G. and Sherratt, M.J. (2019). How stiff is skin? *Experimental Dermatology*, [online] 28, pp.4–9. Available at: https://onlinelibrary.wiley.com/doi/full/10.1111/exd.13826.

Grose, R., Hutter, C., Wilhelm Bloch, Thorey, I., Watt, F.M., Reinhard Fässler, Cord Brakebusch and Werner, S. (2002). A crucial role of β1 integrins for keratinocyte migration in vitro and during cutaneous wound repair. *Development*, [online] 129(9), pp.2303–2315. Available at: https://dev.biologists.org/content/129/9/2303.long.

Guilluy, C., Osborne, L.D., Van Landeghem, L., Sharek, L., Superfine, R., Garcia-Mata, R. and Burridge, K. (2014). Isolated nuclei adapt to force and reveal a mechanotransduction pathway in the nucleus. *Nature Cell Biology*, [online] 16(4), pp.376–381. Available at: https://www.ncbi.nlm.nih.gov/pmc/articles/PMC4085695/#!po=8.33333.

Guo, A. and Jahoda, C.A.B. (2009). An improved method of human keratinocyte culture from skin explants: cell expansion is linked to markers of activated progenitor cells. *Experimental Dermatology*, [online] 18(8), pp.720–726. Available at: https://onlinelibrary.wiley.com/doi/full/10.1111/j.1600-0625.2009.00900.x.

Gupta, M., Doss, B.L., Kocgozlu, L., Pan, M., Mège, R.-M., Callan-Jones, A., Voituriez, R. and Ladoux, B. (2019). Cell shape and substrate stiffness drive actin-based cell polarity. *Physical Review E*, [online] 99(1). Available at: https://journals.aps.org/pre/abstract/10.1103/PhysRevE.99.012412.

Gupta, M., Sarangi, B.R., Deschamps, J., Nematbakhsh, Y., Callan-Jones, A., Margadant, F., Mège, R.-M., Lim, C.T., Voituriez, R. and Ladoux, B. (2015). Adaptive rheology and ordering of cell cytoskeleton govern matrix rigidity sensing. *Nature Communications*, [online] 6(1). Available at: https://www.nature.com/articles/ncomms8525.

Guyot, Y., Papantoniou, I., Chai, Y.C., Van Bael, S., Schrooten, J. and Geris, L. (2014). A computational model for cell/ECM growth on 3D surfaces using the level set method: a bone tissue engineering case study. *Biomechanics and Modeling in Mechanobiology*, [online] 13(6), pp.1361–1371. Available at: https://link.springer.com/article/10.1007%2Fs10237-014-0577-5.

Hamant, O., Inoue, D., Bouchez, D., Dumais, J. and Mjolsness, E. (2019). Are microtubules tension sensors? *Nature Communications*, [online] 10(1). Available at: https://www.nature.com/articles/s41467-019-10207-y.

Hashizume, C., Moyori, A., Kobayashi, A., Yamakoshi, N., Endo, A. and Wong, R.W. (2013). Nucleoporin Nup62 maintains centrosome homeostasis. *Cell Cycle*, [online] 12(24), pp.3804–3816. Available at: https://www.ncbi.nlm.nih.gov/pmc/articles/PMC3905072/.

Haycock, J.W. (2010). 3D Cell Culture: A Review of Current Approaches and Techniques. *Methods in Molecular Biology*, [online] pp.1–15. Available at: https://pubmed.ncbi.nlm.nih.gov/21042962/.

Hennings, H., Michael, D., Cheng, C., Steinert, P., Holbrook, K. and Yuspa, S.H. (1980). Calcium regulation of growth and differentiation of mouse epidermal cells in culture. *Cell*, [online] 19(1), pp.245–54. Available at: https://www.ncbi.nlm.nih.gov/pubmed/6153576.

Hernandez-Segura, A., Nehme, J. and Demaria, M. (2018). Hallmarks of Cellular Senescence. *Trends in Cell Biology*, [online] 28(6), pp.436–453. Available at: https://www.sciencedirect.com/science/article/abs/pii/S0962892418300205.

Hieda, M. (2019). Signal Transduction across the Nuclear Envelope: Role of the LINC Complex in Bidirectional Signaling. *Cells*, [online] 8(2), p.124. Available at: https://www.ncbi.nlm.nih.gov/pmc/articles/PMC6406650/.

Higgins, C.A., Chen, J.C., Cerise, J.E., Jahoda, C.A.B. and Christiano, A.M. (2013). Microenvironmental reprogramming by three-dimensional culture enables dermal papilla cells to induce de novo human hair-follicle growth. *Proceedings of the National Academy of Sciences*, [online] 110(49), pp.19679–19688. Available at: https://pubmed.ncbi.nlm.nih.gov/24145441/.

Hinz, B. (2007). Formation and Function of the Myofibroblast during Tissue Repair. *Journal of Investigative Dermatology*, [online] 127(3), pp.526–537. Available at: https://www.sciencedirect.com/science/article/pii/S0022202X15332863.

Hollister, S.J., Maddox, R.D. and Taboas, J.M. (2002). Optimal design and fabrication of scaffolds to mimic tissue properties and satisfy biological constraints. *Biomaterials*, [online] 23(20), pp.4095–4103. Available at: https://www.sciencedirect.com/science/article/abs/pii/S0142961202001485?via%3Dihub.

Hong, W. and Guan, K.-L. (2012). The YAP and TAZ transcription co-activators: Key downstream effectors of the mammalian Hippo pathway. *Seminars in Cell & Developmental Biology*, [online] 23(7), pp.785–793. Available at: https://pubmed.ncbi.nlm.nih.gov/22659496/.

Hsu, C.-Y., Lecland, N., Pendaries, V., Viodé, C., Redoulès, D., Paul, C., Merdes, A., Simon, M. and Bierkamp, C. (2018). Stabilization of microtubules restores barrier function after cytokine-induced defects in reconstructed human epidermis. *Journal of Dermatological Science*, [online] 91(1), pp.87–96. Available at: https://www.sciencedirect.com/science/article/pii/S0923181118301646?casa_token=L

uYlvxvhw_8AAAAA:uZ_l4SayidPpGJ8RebMqmIes5rMGqSDJU_cXagduOgPt-kAXpFnKDncJkK79hROHlqhId1yte6E.

Hunter-Featherstone, E., Young, N., Chamberlain, K., Cubillas, P., Hulette, B., Wei, X., Tiesman, J.P., Bascom, C.C., Benham, A.M., Goldberg, M.W., Saretzki, G. and Karakesisoglou, I. (2021). Culturing Keratinocytes on Biomimetic Substrates Facilitates Improved Epidermal Assembly In Vitro. *Cells*, [online] 10(5), p.1177. Available at: https://www.mdpi.com/2073-4409/10/5/1177.

Hussain, S.H., Limthongkul, B. and Humphreys, T.R. (2013). The Biomechanical Properties of the Skin. *Dermatologic Surgery*, [online] 39(2), pp.193–203. Available at: https://journals.lww.com/dermatologicsurgery/Abstract/2013/02000/The_Biomechanical_Properties_of_the_Skin.4.aspx.

Indra, A.K. and Leid, M. (2011). Epidermal Permeability Barrier Measurement in Mammalian Skin. *Methods in Molecular Biology*, [online] pp.73–81. Available at: https://www.ncbi.nlm.nih.gov/pmc/articles/PMC3306247/.

InterPro. (2021). Amidase, conserved site. [online] Available at: https://www.ebi.ac.uk/interpro/entry/InterPro/IPR020556/ [Accessed 25 Sep. 2021].

Ito, Y. (1999). Surface micropatterning to regulate cell functions. *Biomaterials*, [online] 20(23-24), pp.2333–2342. Available at: https://www.sciencedirect.com/science/article/abs/pii/S0142961299001623?casa_token=YRsSVygSugoAAAAA:O_dpYDylzX-IYIllxZ7zwPGObhoka7chD7PK-jUWFvX1QaGWJhdxcD-uClfbugzZbEPolBU.

Ivanov, A., Pawlikowski, J., Manoharan, I., van Tuyn, J., Nelson, D.M., Rai, T.S., Shah, P.P., Hewitt, G., Korolchuk, V.I., Passos, J.F., Wu, H., Berger, S.L. and Adams, P.D. (2013). Lysosome-mediated processing of chromatin in senescence. *Journal of Cell Biology*, [online] 202(1), pp.129–143. Available at: https://rupress.org/jcb/article/202/1/129/37371/Lysosome-mediated-processing-of-chromatin-in.

Jacob, J.T., Coulombe, P.A., Kwan, R. and Omary, M.B. (2018). Types I and II Keratin Intermediate Filaments. *Cold Spring Harbor Perspectives in Biology*, [online]

10(4), p.a018275. Available at: https://cshperspectives.cshlp.org/content/10/4/a018275.

Jean, J., Garcia-Pérez, M.E. and Pouliot, R. (2011). Bioengineered Skin: The Self-Assembly Approach. *Journal of Tissue Science & Engineering*, 5(1).

Jepps, O.G., Dancik, Y., Anissimov, Y.G. and Roberts, M.S. (2013). Modeling the human skin barrier — Towards a better understanding of dermal absorption. *Advanced Drug Delivery Reviews*, [online] 65(2), pp.152–168. Available at: https://www.sciencedirect.com/science/article/pii/S0169409X12001226?casa_token=dB522zS_s_MAAAAA:lW4hJBNEmVn7RGfleFUQuWP0bg8EmI3cjaxhvNl3J1c27ui_6sel102ppntXEpyeRDor89yP.

Jiang, Y., Lee, A., Chen, J., Cadene, M., Chait, B.T. and MacKinnon, R. (2002). Crystal structure and mechanism of a calcium-gated potassium channel. *Nature*, [online] 417(6888), pp.515–522. Available at: https://pubmed.ncbi.nlm.nih.gov/12037559/.

Johnson, D.H. (1999). The Insignificance of Statistical Significance Testing. *The Journal of Wildlife Management*, 63(3), p.763.

Julian, L. and Olson, M.F. (2014). Rho-associated coiled-coil containing kinases (ROCK). *Small GTPases*, [online] 5(2), p.e29846. Available at: https://www.ncbi.nlm.nih.gov/pmc/articles/PMC4114931/.

Jung, H.-J., Tatar, A., Tu, Y., Nobumori, C., Yang, S.H., Goulbourne, C.N., Herrmann, H., Fong, L.G. and Young, S.G. (2014). An Absence of Nuclear Lamins in Keratinocytes Leads to Ichthyosis, Defective Epidermal Barrier Function, and Intrusion of Nuclear Membranes and Endoplasmic Reticulum into the Nuclear Chromatin. *Molecular and Cellular Biology*, [online] 34(24), pp.4534–4544. Available at: https://pubmed.ncbi.nlm.nih.gov/25312645/.

Kahn-Kirby, A.H., Dantzker, J.L.M., Apicella, A.J., Schafer, W.R., Browse, J., Bargmann, C.I. and Watts, J.L. (2004). Specific Polyunsaturated Fatty Acids Drive TRPV-Dependent Sensory Signaling In Vivo. *Cell*, [online] 119(6), pp.889–900. Available at: https://pubmed.ncbi.nlm.nih.gov/15607983/.

Kanoldt, V., Fischer, L. and Grashoff, C. (2018). Unforgettable force – crosstalk and memory of mechanosensitive structures. *Biological Chemistry*, [online] 400(6), pp.687–698. Available at: https://www.degruyter.com/document/doi/10.1515/hsz-2018-0328/html.

Kao, A.P., Connelly, J.T. and Barber, A.H. (2016). 3D nanomechanical evaluations of dermal structures in skin. *Journal of the Mechanical Behavior of Biomedical Materials*, [online] 57, pp.14–23. Available at: https://pubmed.ncbi.nlm.nih.gov/26703362/.

Kapałczyńska, M., Kolenda, T., Przybyła, W., Zajączkowska, M., Teresiak, A., Filas, V., Ibbs, M., Bliźniak, R., Łuczewski, Ł. and Lamperska, K. (2016). 2D and 3D cell cultures – a comparison of different types of cancer cell cultures. *Archives of Medical Science*, [online] 14(4). Available at: https://www.ncbi.nlm.nih.gov/pmc/articles/PMC6040128/.

Kassianidou, E., Kalita, J. and Lim, R.Y.H. (2019). The role of nucleocytoplasmic transport in mechanotransduction. *Experimental Cell Research*, [online] 377(1-2), pp.86–93. Available at: https://www.sciencedirect.com/science/article/pii/S0014482718310577?casa_token=di-QBMt_DosAAAAA:PNWFyHhLpDmA67c5-ileM7mYRYgg3DPRW1q5-rylTUvgQrO32vY_HxNBzCo4o_tlvtyBUOnEaVc.

Katiyar, A., Tocco, V.J., Li, Y., Aggarwal, V., Tamashunas, A.C., Dickinson, R.B. and Lele, T.P. (2019). Nuclear size changes caused by local motion of cell boundaries unfold the nuclear lamina and dilate chromatin and intranuclear bodies. *Soft Matter*, [online] 15(45), pp.9310–9317. Available at: https://pubs.rsc.org/en/content/articlelanding/2019/sm/c9sm01666j/unauth.

Kazi, G.A.S., Yamanaka, T. and Osamu, Y. (2019). Chitosan Coating an Efficient Approach to Improve the Substrate Surface for In Vitro Culture System. *Journal of The Electrochemical Society*, [online] 166(9), pp.B3025–B3030. Available at: https://iopscience.iop.org/article/10.1149/2.0051909jes.

Kenny, F.N. and Connelly, J.T. (2014). Integrin-mediated adhesion and mechano-sensing in cutaneous wound healing. *Cell and Tissue Research*, [online] 360(3),

pp.571–582. Available at: https://link.springer.com/article/10.1007/s00441-014-2064-9.

Kerr, J.P., Robison, P., Shi, G., Bogush, A.I., Kempema, A.M., Hexum, J.K., Becerra, N., Harki, D.A., Martin, S.S., Raiteri, R., Prosser, B.L. and Ward, C.W. (2015). Detyrosinated microtubules modulate mechanotransduction in heart and skeletal muscle. *Nature Communications*, [online] 6(1). Available at: https://www.nature.com/articles/ncomms9526.

Ketema, M., Kreft, M., Secades, P., Janssen, H. and Sonnenberg, A. (2013). Nesprin-3 connects plectin and vimentin to the nuclear envelope of Sertoli cells but is not required for Sertoli cell function in spermatogenesis. *Molecular Biology of the Cell*. Molecular Biology of the Cell. [online] Available at: https://www.molbiolcell.org/doi/10.1091/mbc.e13-02-0100.

Kleinschmidt, E.G. and Schlaepfer, D.D. (2017). Focal adhesion kinase signaling in unexpected places. *Current Opinion in Cell Biology*, [online] 45, pp.24–30. Available at: https://www.sciencedirect.com/science/article/abs/pii/S0955067417300145.

Klezovitch, O. and Vasioukhin, V. (2015). Cadherin signaling: keeping cells in touch. *F1000Research*, [online] 4, p.550. Available at: https://www.ncbi.nlm.nih.gov/pmc/articles/PMC4544379/.

Kloxin, A.M., Benton, J.A. and Anseth, K.S. (2010). In situ elasticity modulation with dynamic substrates to direct cell phenotype. *Biomaterials*, [online] 31(1), pp.1–8. Available at: https://pubmed.ncbi.nlm.nih.gov/19788947/.

Kobielak, A. and Fuchs, E. (2004). α-catenin: at the junction of intercellular adhesion and actin dynamics. *Nature Reviews Molecular Cell Biology*, [online] 5(8), pp.614–625. Available at: https://www.ncbi.nlm.nih.gov/pmc/articles/PMC2475680/#!po=1.66667.

Kohl, E., Steinbauer, J., Landthaler, M. and Szeimies, R.-M. . (2011). Skin ageing. *Journal of the European Academy of Dermatology and Venereology*, [online] 25(8), pp.873–884. Available at: https://pubmed.ncbi.nlm.nih.gov/21261751/.

Kose, O., Erkekoglu, P., Sabuncuoglu, S. and Kocer-Gumusel, B. (2018). Evaluation of skin irritation potentials of different cosmetic products in Turkish market by reconstructed human epidermis model. *Regulatory Toxicology and Pharmacology*, [online] 98, pp.268–273. Available at: https://www.sciencedirect.com/science/article/pii/S0273230018302216?casa_token=nfm9FxRK_1AAAAAA:sZUZzyCV4FxGKBNsRqbn5nT8GR3wGyFKwelcQqudfcd5kzxUf_j_03Av_-gnO1EF8Rbpr0l3Fw#bib11.

Koster, M.I. (2010). p63 in Skin Development and Ectodermal Dysplasias. *Journal of Investigative Dermatology*, [online] 130(10), pp.2352–2358. Available at: https://www.sciencedirect.com/science/article/pii/S0022202X15345838.

Kremerskothen, J., Plaas, C., Büther, K., Finger, I., Veltel, S., Matanis, T., Liedtke, T. and Barnekow, A. (2003). Characterization of KIBRA, a novel WW domain-containing protein. *Biochemical and Biophysical Research Communications*, [online] 300(4), pp.862–867. Available at: https://pubmed.ncbi.nlm.nih.gov/12559952/.

Kühn, S., Erdmann, C., Kage, F., Block, J., Schwenkmezger, L., Steffen, A., Rottner, K. and Geyer, M. (2015). The structure of FMNL2–Cdc42 yields insights into the mechanism of lamellipodia and filopodia formation. *Nature Communications*, [online] 6(1). Available at: https://www.nature.com/articles/ncomms8088?origin=ppub.

Kuilman, T., Michaloglou, C., Mooi, W.J. and Peeper, D.S. (2010). The essence of senescence. *Genes & Development*, [online] 24(22), pp.2463–2479. Available at: http://genesdev.cshlp.org/content/24/22/2463.full#ref-183.

Kvistedal, Y.A. and Nielsen, P.M.F. (2007). Estimating material parameters of human skin in vivo. *Biomechanics and Modeling in Mechanobiology*, [online] 8(1), pp.1–8. Available at: https://pubmed.ncbi.nlm.nih.gov/18040732/.

Lachowski, D., Cortes, E., Robinson, B., Rice, A., Rombouts, K. and Del Río Hernández, A.E. (2018). FAK controls the mechanical activation of YAP, a transcriptional regulator required for durotaxis. *The FASEB Journal*, [online] 32(2),

pp.1099–1107. Available at: https://faseb.onlinelibrary.wiley.com/doi/full/10.1096/fj.201700721R.

Laly, A.C., Sliogeryte, K., Pundel, O.J., Ross, R., Keeling, M.C., Avisetti, D., Waseem, A., Gavara, N. and Connelly, J.T. (2021). The keratin network of intermediate filaments regulates keratinocyte rigidity sensing and nuclear mechanotransduction. *Science Advances*, [online] 7(5), p.eabd6187. Available at: https://advances.sciencemag.org/content/7/5/eabd6187?elqTrackId=d6f7775f792546fa8cd1bf67ce1217b8.

Landry, N.M., Rattan, S.G. and Dixon, I.M.C. (2019). An Improved Method of Maintaining Primary Murine Cardiac Fibroblasts in Two-Dimensional Cell Culture. *Scientific Reports,* [online] 9(1). Available at: https://www.nature.com/articles/s41598-019-49285-9.

Last, J.A., Thomasy, S.M., Croasdale, C.R., Russell, P. and Murphy, C.J. (2012). Compliance profile of the human cornea as measured by atomic force microscopy. *Micron*, [online] 43(12), pp.1293–1298. Available at: https://www.ncbi.nlm.nih.gov/pmc/articles/PMC3622051/.

Lechler, T. and Fuchs, E. (2007). Desmoplakin: an unexpected regulator of microtubule organization in the epidermis. *Journal of Cell Biology*, [online] 176(2), pp.147–154. Available at: https://rupress.org/jcb/article/176/2/147/44710.

LeMasurier, M. and Gillespie, P.G. (2005). Hair-Cell Mechanotransduction and Cochlear Amplification. *Neuron*, [online] 48(3), pp.403–415. Available at: https://pubmed.ncbi.nlm.nih.gov/16269359/.

Lenain, C., Gusyatiner, O., Douma, S., van den Broek, B. and Peeper, D.S. (2015). Autophagy-mediated degradation of nuclear envelope proteins during oncogene-induced senescence. *Carcinogenesis*, [online] 36(11), pp.1263–1274. Available at: https://academic.oup.com/carcin/article/36/11/1263/370607.

Levy, L., Broad, S., Diekmann, D., Evans, R.D. and Watt, F.M. (2000). β1 Integrins Regulate Keratinocyte Adhesion and Differentiation by Distinct Mechanisms.

Molecular Biology of the Cell, [online] 11(2), pp.453–466. Available at: https://www.ncbi.nlm.nih.gov/pmc/articles/PMC14785/.

Li, X., Balagam, R., He, T.-F., Lee, P.P., Igoshin, O.A. and Levine, H. (2017). On the mechanism of long-range orientational order of fibroblasts. *Proceedings of the National Academy of Sciences*, [online] 114(34), pp.8974–8979. Available at: https://www.pnas.org/content/114/34/8974#F3.

Limbert, G. (2017). Mathematical and computational modelling of skin biophysics: a review. Proceedings. *Mathematical, Physical, and Engineering Sciences*, [online] 473(2203). Available at: https://www.ncbi.nlm.nih.gov/pmc/articles/PMC5549575/.

Lin, F.-S., Lee, J.-J., Lee, A.K.-X., Ho, C.-C., Liu, Y.-T. and Shie, M.-Y. (2021). Calcium Silicate-Activated Gelatin Methacrylate Hydrogel for Accelerating Human Dermal Fibroblast Proliferation and Differentiation. *Polymers*, [online] 13(1), p.70. Available at: https://www.mdpi.com/2073-4360/13/1/70#cite.

Liu, H., Sun, Y. and Simmons, C.A. (2013). Determination of local and global elastic moduli of valve interstitial cells cultured on soft substrates. *Journal of Biomechanics*, [online] 46(11), pp.1967–1971. Available at: https://www.sciencedirect.com/science/article/pii/S0021929013002108?casa_token=Slg7lF-030UAAAAA:E0ee_jfPpGEKI8j9feZqKD-jJa8mi4kHipywL5Q_8Jf9UqRaQB6O9yi-aQbrmxamwFeftYMt-a8.

Lloyd-Lewis, B., Mourikis, P. and Fre, S. (2019). Notch signalling: sensor and instructor of the microenvironment to coordinate cell fate and organ morphogenesis. *Current Opinion in Cell Biology*, [online] 61, pp.16–23. Available at: https://www.sciencedirect.com/science/article/pii/S0955067418301790?casa_token=p5fiFJT4_EIAAAAA:Ab7ixPgnDnBkI9evib48Jf9B4mCedw8qWpLfafvtZqbZd8ZgtgH0cyuyAkgBX7_4ctPLnQQU.

Lobo, J., Petronilho, S., Newell, A.H., Coach, J., Harlow, G., Cruz, A., Lopes, P., Antunes, L., Bai, I., Walker, E. and Henrique, R. (2019). E-cadherin clone 36 nuclear staining dictates adverse disease outcome in lobular breast cancer patients. *Modern*

Pathology, [online] 32(11), pp.1574–1586. Available at: https://www.nature.com/articles/s41379-019-0294-9.

Lock, F.E. and Hotchin, N.A. (2009). Distinct Roles for ROCK1 and ROCK2 in the Regulation of Keratinocyte Differentiation. *PLoS ONE*, [online] 4(12), p.e8190. Available at: https://journals.plos.org/plosone/article?id=10.1371/journal.pone.0008190.

Lopez-Otín, C., Blasco, M.A., Partridge, L., Serrano, M. and Kroemer, G. (2013). The Hallmarks of Aging. *Cell*, [online] 153(6), pp.1194–1217. Available at: https://pubmed.ncbi.nlm.nih.gov/23746838/.

Lumpkin, E.A. and Caterina, M.J. (2007). Mechanisms of sensory transduction in the skin. *Nature*, [online] 445(7130), pp.858–865. Available at: https://www.nature.com/articles/nature05662.

Lutolf, M.P. and Hubbell, J.A. (2005). Synthetic biomaterials as instructive extracellular microenvironments for morphogenesis in tissue engineering. *Nature Biotechnology*, [online] 23(1), pp.47–55. Available at: https://www.nature.com/articles/nbt1055.

Madison, K.C. (2003). Barrier Function of the Skin: "La Raison d'Être" of the Epidermis. *Journal of Investigative Dermatology*, [online] 121(2), pp.231–241. Available at: https://www.sciencedirect.com/science/article/pii/S0022202X15303560.

Maeda, K. (2017). New Method of Measurement of Epidermal Turnover in Humans. *Cosmetics*, [online] 4(4), p.47. Available at: https://www.mdpi.com/2079-9284/4/4/47/htm.

Maier, T., Güell, M. and Serrano, L. (2009). Correlation of mRNA and protein in complex biological samples. *FEBS Letters*, [online] 583(24), pp.3966–3973. Available at: https://febs.onlinelibrary.wiley.com/doi/10.1016/j.febslet.2009.10.036.

Mancini, M., Lena, A.M., Saintigny, G., Mahé, C., Di Daniele, N., Melino, G. and Candi, E. (2014). MicroRNAs in human skin ageing. *Ageing Research Reviews*, [online] 17, pp.9–15. Available at: https://pubmed.ncbi.nlm.nih.gov/24784027/.

Mansfeld, J., Güttinger, S., Hawryluk-Gara, L.A., Panté, N., Mall, M., Galy, V., Haselmann, U., Mühlhäusser, P., Wozniak, R.W., Mattaj, I.W., Kutay, U. and Antonin, W. (2006). The Conserved Transmembrane Nucleoporin NDC1 Is Required for Nuclear Pore Complex Assembly in Vertebrate Cells. *Molecular Cell*, [online] 22(1), pp.93–103. Available at: https://www.sciencedirect.com/science/article/pii/S1097276506001171.

Martínez-Abraín, A. (2008). Statistical significance and biological relevance: A call for a more cautious interpretation of results in ecology. *Acta Oecologica*, [online] 34(1), pp.9–11. Available at: https://www.sciencedirect.com/science/article/pii/S1146609X08000337?casa_token=t4z0bJcsKKsAAAAA:ozzGBgNoDT3EiYxkOQbPqh_UBI1pkAiQZv0RjQsjdB3eLbo9fGJAm6tw_nh37gLoe5ZXkEJb.

Martino, F., Perestrelo, A.R., Vinarský, V., Pagliari, S. and Forte, G. (2018). Cellular Mechanotransduction: From Tension to Function. *Frontiers in Physiology*, [online] 9. Available at: https://www.frontiersin.org/articles/10.3389/fphys.2018.00824/full.

MatTek Life Sciences (2021). EpiDerm. [online] MatTek A BICO Company. Available at: https://www.mattek.com/products/epiderm/.

Maurer, M. and Lammerding, J. (2019). The Driving Force: Nuclear Mechanotransduction in Cellular Function, Fate, and Disease. *Annual Review of Biomedical Engineering*, 21(1), pp.443–468.

McMullan, R., Lax, S., Robertson, V.H., Radford, D.J., Broad, S., Watt, F.M., Rowles, A., Croft, D.R., Olson, M.F. and Hotchin, N.A. (2003). Keratinocyte Differentiation Is Regulated by the Rho and ROCK Signaling Pathway. *Current Biology*, [online] 13(24), pp.2185–2189. Available at: https://www.sciencedirect.com/science/article/pii/S0960982203009060.

Melchels, F.P.W., Tonnarelli, B., Olivares, A.L., Martin, I., Lacroix, D., Feijen, J., Wendt, D.J. and Grijpma, D.W. (2011). The influence of the scaffold design on the distribution of adhering cells after perfusion cell seeding. *Biomaterials*, [online]

32(11), pp.2878–2884. Available at: https://www.sciencedirect.com/science/article/pii/S0142961211000366?via%3Dihub.

Mellad, J.A., Warren, D.T. and Shanahan, C.M. (2011). Nesprins LINC the nucleus and cytoskeleton. *Current Opinion in Cell Biology*, [online] 23(1), pp.47–54. Available at: https://www.sciencedirect.com/science/article/abs/pii/S0955067410002127?via%3Dihub.

Meng, L., Kohlhagen, G., Liao, Z., Antony, S., Sausville, E. and Pommier, Y. (2005). DNA-Protein Cross-links and Replication-Dependent Histone H2AX Phosphorylation Induced by Aminoflavone (NSC 686288), a Novel Anticancer Agent Active against Human Breast Cancer Cells. *Cancer Research*, [online] 65(12), pp.5337–5343. Available at: https://cancerres.aacrjournals.org/content/65/12/5337.

Meshel, A.S., Wei, Q., Adelstein, R.S. and Sheetz, M.P. (2005). Basic mechanism of three-dimensional collagen fibre transport by fibroblasts. *Nature Cell Biology*, [online] 7(2), pp.157–164. Available at: https://pubmed.ncbi.nlm.nih.gov/15654332/.

Metral, E., Bechetoille, N., Demarne, F., Rachidi, W. and Damour, O. (2017). α6 Integrin (α6high)/Transferrin Receptor (CD71)low Keratinocyte Stem Cells Are More Potent for Generating Reconstructed Skin Epidermis Than Rapid Adherent Cells. *International Journal of Molecular Sciences*, [online] 18(2), p.282. Available at: https://pubmed.ncbi.nlm.nih.gov/28134816/.

Mills, A.A., Zheng, B., Wang, X.-J., Vogel, H., Roop, D.R. and Bradley, A. (1999). p63 is a p53 homologue required for limb and epidermal morphogenesis. *Nature*, [online] 398(6729), pp.708–713. Available at: https://www.nature.com/articles/19531.

Moers, K., Steinberg, T., Schlunck, G., Reinhard, T., Tomakidi, P. and Eberwein, P. (2013). Substrate elasticity as biomechanical modulator of tissue homeostatic parameters in corneal keratinocytes. *Experimental Cell Research*, [online] 319(12), pp.1889–1901. Available at: https://www.sciencedirect.com/science/article/abs/pii/S0014482713001961?via%3Dihub.

Mogha, P., Srivastava, A., Kumar, S., Das, S., Kureel, S., Dwivedi, A., Karulkar, A., Jain, N., Sawant, A., Nayak, C., Majumder, A. and Purwar, R. (2019). Hydrogel scaffold with substrate elasticity mimicking physiological-niche promotes proliferation of functional keratinocytes. *RSC Advances*, [online] 9(18), pp.10174–10183. Available at: https://pubs.rsc.org/en/content/articlehtml/2019/ra/c9ra00781d#imgfig4.

Molinuevo, R., Freije, A., de Pedro, I., Stoll, S.W., Elder, J.T. and Gandarillas, A. (2016). FOXM1 allows human keratinocytes to bypass the oncogene-induced differentiation checkpoint in response to gain of MYC or loss of p53. *Oncogene*, [online] 36(7), pp.956–965. Available at: https://www.nature.com/articles/onc2016262.

Moll, R., Divo, M. and Langbein, L. (2008). The human keratins: biology and pathology. *Histochemistry and Cell Biology*, [online] 129(6), pp.705–733. Available at: https://link.springer.com/article/10.1007%2Fs00418-008-0435-6.

Moore, S.W., Roca-Cusachs, P. and Sheetz, M.P. (2010). Stretchy Proteins on Stretchy Substrates: The Important Elements of Integrin-Mediated Rigidity Sensing. *Developmental Cell*, [online] 19(2), pp.194–206. Available at: https://pubmed.ncbi.nlm.nih.gov/20708583/.

Müller, E.J., Williamson, L., Kolly, C. and Suter, M.M. (2008). Outside-in Signaling through Integrins and Cadherins: A Central Mechanism to Control Epidermal Growth and Differentiation? *Journal of Investigative Dermatology*, [online] 128(3), pp.501–516. Available at: https://www.sciencedirect.com/science/article/pii/S0022202X1533760X.

Müller, I. and Kulms, D. (2018). A 3D Organotypic Melanoma Spheroid Skin Model. *Journal of Visualized Experiments*, [online] (135). Available at: https://www.ncbi.nlm.nih.gov/pmc/articles/PMC6101273/.

Murphy, R.M. and Lamb, G.D. (2013). Important considerations for protein analyses using antibody based techniques: down-sizing western blotting up-sizes outcomes.

The Journal of Physiology, [online] 591(23), pp.5823–5831. Available at: https://physoc.onlinelibrary.wiley.com/doi/10.1113/jphysiol.2013.263251.

Naeem, A.S., Zhu, Y., Di, W.L., Marmiroli, S. and O'Shaughnessy, R.F.L. (2015). AKT1-mediated Lamin A/C degradation is required for nuclear degradation and normal epidermal terminal differentiation. *Cell Death & Differentiation*, [online] 22(12), pp.2123–2132. Available at: https://www.ncbi.nlm.nih.gov/pmc/articles/PMC4816115/.

Nagayama, K. and Fukuei, T. (2019). Cyclic stretch-induced mechanical stress to the cell nucleus inhibits ultraviolet radiation-induced DNA damage. *Biomechanics and Modeling in Mechanobiology*, [online] 19(2), pp.493–504. Available at: https://link.springer.com/article/10.1007/s10237-019-01224-3.

Nanba, D., Toki, F., Matsushita, N., Matsushita, S., Higashiyama, S. and Barrandon, Y. (2013). Actin filament dynamics impacts keratinocyte stem cell maintenance. *EMBO Molecular Medicine*, [online] 5(4), pp.640–653. Available at: https://www.ncbi.nlm.nih.gov/pmc/articles/PMC3628097/.

Naylor, E.C., Watson, R.E.B. and Sherratt, M.J. (2011). Molecular aspects of skin ageing. *Maturitas*, [online] 69(3), pp.249–256. Available at: https://pubmed.ncbi.nlm.nih.gov/21612880/.

Nekrasova, O., Harmon, R.M., Broussard, J.A., Koetsier, J.L., Godsel, L.M., Fitz, G.N., Gardel, M.L. and Green, K.J. (2018). Desmosomal cadherin association with Tctex-1 and cortactin-Arp2/3 drives perijunctional actin polymerization to promote keratinocyte delamination. *Nature Communications*, [online] 9(1). Available at: https://www.nature.com/articles/s41467-018-03414-6.

Nelson, G., Kucheryavenko, O., Wordsworth, J. and von Zglinicki, T. (2018). The senescent bystander effect is caused by ROS-activated NF-κB signalling. *Mechanisms of Ageing and Development*, [online] 170, pp.30–36. Available at: https://www.ncbi.nlm.nih.gov/pmc/articles/PMC5861994/.

Ng, W. and Ikeda, S. (2011). Standardized, Defined Serum-free Culture of a Human Skin Equivalent on Fibroblast-populated Collagen Scaffold. *Acta Dermato*

Venereologica, [online] 91(4), pp.387–391. Available at: https://pubmed.ncbi.nlm.nih.gov/21461550/.

Nguyen, B.-C. . (2006). Cross-regulation between Notch and p63 in keratinocyte commitment to differentiation. *Genes & Development*, [online] 20(8), pp.1028–1042. Available at: http://genesdev.cshlp.org/content/20/8/1028.short.

Nugent, S.M.E., Mothersill, C.E., Seymour, C., McClean, B., Lyng, F.M. and Murphy, J.E.J. (2007). Increased Mitochondrial Mass in Cells with Functionally Compromised Mitochondria after Exposure to both Direct γ Radiation and Bystander Factors. *Radiation Research*, [online] 168(1), pp.134–142. Available at: https://pubmed.ncbi.nlm.nih.gov/17722997/.

Ohara, H., Ichikawa, S., Matsumoto, H., Akiyama, M., Fujimoto, N., Kobayashi, T. and Tajima, S. (2010). Collagen-derived dipeptide, proline-hydroxyproline, stimulates cell proliferation and hyaluronic acid synthesis in cultured human dermal fibroblasts. *The Journal of Dermatology*, [online] 37(4), pp.330–338. Available at: https://onlinelibrary.wiley.com/doi/full/10.1111/j.1346-8138.2010.00827.x.

Omary, M.B., Coulombe, P.A. and McLean, W.H.I. (2004). Intermediate Filament Proteins and Their Associated Diseases. *New England Journal of Medicine*, [online] 351(20), pp.2087–2100. Available at: https://www.nejm.org/doi/full/10.1056/NEJMra040319.

Padmakumar, V.C., Libotte, T., Lu, W., Zaim, H., Abraham, S., Noegel, A.A., Gotzmann, J., Foisner, R. and Karakesisoglou, I. (2005). The inner nuclear membrane protein Sun1 mediates the anchorage of Nesprin-2 to the nuclear envelope. *Journal of Cell Science*, [online] 118(15), pp.3419–3430. Available at: https://pubmed.ncbi.nlm.nih.gov/16079285/.

Pailler-Mattei, C., Bec, S. and Zahouani, H. (2008). In vivo measurements of the elastic mechanical properties of human skin by indentation tests. *Medical Engineering & Physics*, [online] 30(5), pp.599–606. Available at: https://pubmed.ncbi.nlm.nih.gov/17869160/.

Parks, D.H. and Beiko, R.G. (2010). Identifying biologically relevant differences between metagenomic communities. *Bioinformatics*, [online] 26(6), pp.715–721. Available at: https://academic.oup.com/bioinformatics/article/26/6/715/245265?login=true.

Parsa, R., Yang, A., McKeon, F. and Green, H. (1999). Association of p63 with Proliferative Potential in Normal and Neoplastic Human Keratinocytes. *Journal of Investigative Dermatology*, [online] 113(6), pp.1099–1105. Available at: https://www.sciencedirect.com/science/article/pii/S0022202X15407043.

Passos, J.F., Saretzki, G., Ahmed, S., Nelson, G., Richter, T., Peters, H., Wappler, I., Birket, M.J., Harold, G., Schaeuble, K., Birch-Machin, M.A., Kirkwood, T.B.L. and von Zglinicki, T. (2007). Mitochondrial Dysfunction Accounts for the Stochastic Heterogeneity in Telomere-Dependent Senescence. *PLoS Biology*, [online] 5(5), p.e110. Available at: https://journals.plos.org/plosbiology/article?id=10.1371/journal.pbio.0050110.

Pastar, I., Stojadinovic, O., Yin, N.C., Ramirez, H., Nusbaum, A.G., Sawaya, A., Patel, S.B., Khalid, L., Isseroff, R.R. and Tomic-Canic, M. (2014). Epithelialization in Wound Healing: A Comprehensive Review. *Advances in Wound Care*, [online] 3(7), pp.445–464. Available at: https://www.ncbi.nlm.nih.gov/pmc/articles/PMC4086220/.

Pellegrini, G., Dellambra, E., Golisano, O., Martinelli, E., Fantozzi, I., Bondanza, S., Ponzin, D., McKeon, F. and De Luca, M. (2001). p63 identifies keratinocyte stem cells. *Proceedings of the National Academy of Sciences*, [online] 98(6), pp.3156–3161. Available at: https://pubmed.ncbi.nlm.nih.gov/11248048/.

Peppas, N. A., Hilt, J. Z., Khademhosseini, A. and Langer, R. (2006). Hydrogels in Biology and Medicine: From Molecular Principles to Bionanotechnology. *Advanced Materials*, [online] 18(11), pp.1345–1360. Available at: https://onlinelibrary.wiley.com/doi/epdf/10.1002/adma.200501612.

Phillip, J.M., Aifuwa, I., Walston, J. and Wirtz, D. (2015). The Mechanobiology of Aging. *Annual Review of Biomedical Engineering*, [online] 17(1), pp.113–141. Available at: https://pubmed.ncbi.nlm.nih.gov/26643020/.

Piccolo, S., Dupont, S. and Cordenonsi, M. (2014). The biology of YAP/TAZ: hippo signaling and beyond. *Physiological reviews*, [online] 94(4), pp.1287–312. Available at: https://www.ncbi.nlm.nih.gov/pubmed/25287865.

Pole, A., Dimri, M. and Dimri, G. (2016). Oxidative stress, cellular senescence and ageing. *AIMS Molecular Science*, 3(3), pp.300–324.

Poumay, Y. and Coquette, A. (2007). Modelling the human epidermis in vitro: tools for basic and applied research. *Archives of Dermatological Research*, [online] 298(8), pp.361–369. Available at: https://www.ncbi.nlm.nih.gov/pmc/articles/PMC1705521/.

Poumay, Y. and Pittelkow, M.R. (1995). Cell Density and Culture Factors Regulate Keratinocyte Commitment to Differentiation and Expression of Suprabasal K1/K10 Keratins. *Journal of Investigative Dermatology*, 104(2), pp.271–276.

Prager-Khoutorsky, M., Lichtenstein, A., Krishnan, R., Rajendran, K., Mayo, A., Kam, Z., Geiger, B. and Bershadsky, A.D. (2011). Fibroblast polarization is a matrix-rigidity-dependent process controlled by focal adhesion mechanosensing. *Nature Cell Biology*, [online] 13(12), pp.1457–1465. Available at: https://www.nature.com/articles/ncb2370.

Preece, D. (1990). Fisher and Experimental design: a Review. *Biometrics*, 46, pp.925–993.

Prosser, S.L. and Pelletier, L. (2017). Mitotic spindle assembly in animal cells: a fine balancing act. *Nature Reviews Molecular Cell Biology*, [online] 18(3), pp.187–201. Available at: https://www.nature.com/articles/nrm.2016.162.

Ramirez, R.D. (2001). Putative telomere-independent mechanisms of replicative aging reflect inadequate growth conditions. *Genes & Development*, [online] 15(4), pp.398–403. Available at: https://www.ncbi.nlm.nih.gov/pmc/articles/PMC312628/.

Rani, S., Bhardwaj, S., Srivastava, N., Sharma, V.L., Parsad, D. and Kumar, R. (2017). Senescence in the lesional fibroblasts of non-segmental vitiligo patients. *Archives of Dermatological Research*, [online] 309(2), pp.123–132. Available at:

https://pubmed.ncbi.nlm.nih.gov/28078437/#:~:text=Senescence%20in%20the%20dermal%20fibroblasts,fibroblasts%20in%20the%20vitiligo%20pathogenesis..

Rapisarda, V., Malashchuk, I., Asamaowei, I.E., Poterlowicz, K., Fessing, M.Y., Sharov, A.A., Karakesisoglou, I., Botchkarev, V.A. and Mardaryev, A. (2017). p63 Transcription Factor Regulates Nuclear Shape and Expression of Nuclear Envelope-Associated Genes in Epidermal Keratinocytes. *Journal of Investigative Dermatology*, [online] 137(10), pp.2157–2167. Available at: https://www.sciencedirect.com/science/article/pii/S0022202X17315531.

Ravikanth, M., Manjunath, K., Ramachandran, C., Soujanya, P. and Saraswathi, T. (2011). Heterogenecity of fibroblasts. *Journal of Oral and Maxillofacial Pathology*, [online] 15(2), p.247. Available at: https://www.ncbi.nlm.nih.gov/pmc/articles/PMC3329689/.

Ray, P.D., Huang, B.-W. and Tsuji, Y. (2012). Reactive oxygen species (ROS) homeostasis and redox regulation in cellular signaling. *Cellular Signalling*, [online] 24(5), pp.981–990. Available at: https://www.ncbi.nlm.nih.gov/pmc/articles/PMC3454471/#:~:text=Reactive%20oxygen%20species%20(ROS)%20are,mount%20an%20effective%20antioxidant%20response..

Rheinlaender, J., Dimitracopoulos, A., Wallmeyer, B., Kronenberg, N.M., Chalut, K.J., Gather, M.C., Betz, T., Charras, G. and Franze, K. (2020). Cortical cell stiffness is independent of substrate mechanics. *Nature Materials*, [online] 19(9), pp.1019–1025. Available at: https://www.nature.com/articles/s41563-020-0684-x.

Rianna, C. and Radmacher, M. (2017). Comparison of viscoelastic properties of cancer and normal thyroid cells on different stiffness substrates. *European Biophysics Journal*, [online] 46(4), pp.309–324. Available at: https://pubmed.ncbi.nlm.nih.gov/27645213/.

Rinnerthaler, M., Bischof, J., Streubel, M., Trost, A. and Richter, K. (2015). Oxidative Stress in Aging Human Skin. *Biomolecules,* [online] 5(2), pp.545–589. Available at: https://www.ncbi.nlm.nih.gov/pmc/articles/PMC4496685/.

Robison, P., Caporizzo, M.A., Ahmadzadeh, H., Bogush, A.I., Chen, C.Y., Margulies, K.B., Shenoy, V.B. and Prosser, B.L. (2016). Detyrosinated microtubules buckle and bear load in contracting cardiomyocytes. *Science*, [online] 352(6284), pp.aaf0659–aaf0659. Available at: https://science.sciencemag.org/content/352/6284/aaf0659.abstract?casa_token=VYHHEK3ro-EAAAAA:W5m8gjJeXVVLDos9A2-S6tzptpRTwJQeLtnhopuTqBVI5DAyw2L4wzPj-CSBuAj-h2PD7miac-ooqBs.

Rocha, A., Dalgarno, A. and Neretti, N. (2021). The functional impact of nuclear reorganization in cellular senescence. *Briefings in Functional Genomics*. [online] Available at: https://academic.oup.com/bfg/advance-article/doi/10.1093/bfgp/elab012/6182491?login=true.

Roger, M., Fullard, N., Costello, L., Bradbury, S., Markiewicz, E., O'Reilly, S., Darling, N., Ritchie, P., Määttä, A., Karakesisoglou, I., Nelson, G., von Zglinicki, T., Dicolandrea, T., Isfort, R., Bascom, C. and Przyborski, S. (2019). Bioengineering the microanatomy of human skin. *Journal of Anatomy*, [online] 234(4), pp.438–455. Available at: https://pubmed.ncbi.nlm.nih.gov/30740672/.

Rogerson, C. and O'Shaughnessy, R.F.L. (2018). Protein kinases involved in epidermal barrier formation: The AKT family and other animals. *Experimental Dermatology*, [online] 27(8), pp.892–900. Available at: https://onlinelibrary.wiley.com/doi/full/10.1111/exd.13696.

Rogerson, C., Wotherspoon, D.J., Tommasi, C., Button, R.W. and O'Shaughnessy, R.F.L. (2021). Akt1-associated actomyosin remodelling is required for nuclear lamina dispersal and nuclear shrinkage in epidermal terminal differentiation. *Cell Death & Differentiation*. [online] Available at: https://www.nature.com/articles/s41418-020-00712-9.

Rognoni, E. and Walko, G. (2019). The Roles of YAP/TAZ and the Hippo Pathway in Healthy and Diseased Skin. *Cells*, [online] 8(5), p.411. Available at: https://www.ncbi.nlm.nih.gov/pmc/articles/PMC6562585/.

Rosińczuk, J., Taradaj, J., Dymarek, R. and Sopel, M. (2016). Mechanoregulation of Wound Healing and Skin Homeostasis. *BioMed Research International*, [online] 2016, pp.1–13. Available at: https://www.hindawi.com/journals/bmri/2016/3943481/.

Roux, K.J., Crisp, M.L., Liu, Q., Kim, D., Kozlov, S., Stewart, C.L. and Burke, B. (2009). Nesprin 4 is an outer nuclear membrane protein that can induce kinesin-mediated cell polarization. *Proceedings of the National Academy of Sciences*, [online] 106(7), pp.2194–2199. Available at: https://www.pnas.org/content/106/7/2194.short.

Rübsam, M., Broussard, J.A., Wickström, S.A., Nekrasova, O., Green, K.J. and Niessen, C.M. (2017a). Adherens Junctions and Desmosomes Coordinate Mechanics and Signaling to Orchestrate Tissue Morphogenesis and Function: An Evolutionary Perspective. *Cold Spring Harbor Perspectives in Biology*, [online] 10(11), p.a029207. Available at: https://cshperspectives.cshlp.org/content/10/11/a029207.full.

Rübsam, M., Mertz, A.F., Kubo, A., Marg, S., Jüngst, C., Goranci-Buzhala, G., Schauss, A.C., Horsley, V., Dufresne, E.R., Moser, M., Ziegler, W., Amagai, M., Wickström, S.A. and Niessen, C.M. (2017b). E-cadherin integrates mechanotransduction and EGFR signaling to control junctional tissue polarization and tight junction positioning. *Nature Communications*, [online] 8(1). Available at: https://www.nature.com/articles/s41467-017-01170-7.

Ryu, N.-E., Lee, S.-H. and Park, H. (2019). Spheroid Culture System Methods and Applications for Mesenchymal Stem Cells. *Cells*, [online] 8(12), p.1620. Available at: https://www.ncbi.nlm.nih.gov/pmc/articles/PMC6953111/.

Saha, K., Pollock, J.F., Schaffer, D.V. and Healy, K.E. (2007). Designing synthetic materials to control stem cell phenotype. *Current Opinion in Chemical Biology*, [online] 11(4), pp.381–387. Available at: https://www.ncbi.nlm.nih.gov/pmc/articles/PMC1993842/?report=reader.

Sandbo, N. and Dulin, N. (2011). Actin cytoskeleton in myofibroblast differentiation: Ultrastructure defining form and driving function. *Translational Research*, [online] 158(4), pp.181–196. Available at: https://www.sciencedirect.com/science/article/pii/S1931524411001873?casa_token=N

vPCzEaYdnUAAAAA:e6ftm2JjDYRxeDXFSxNhjYqm_P2dhQ5R2gxYtusgK4P_iS1tiYyyW87FPSngTRi4fe1h7z8.

Sargent, B. (2019). Spheroid Cell Culture – Practical solutions for frequently asked questions... [online] Cell Culture Dish. Available at: https://cellculturedish.com/spheroid-cell-culture-practical-solutions-for-frequently-asked-questions/.

Scalia, C.R., Boi, G., Bolognesi, M.M., Riva, L., Manzoni, M., DeSmedt, L., Bosisio, F.M., Ronchi, S., Leone, B.E. and Cattoretti, G. (2016). Antigen Masking During Fixation and Embedding, Dissected. Journal of Histochemistry & Cytochemistry, [online] 65(1), pp.5–20. doi:10.1369/0022155416673995.

Schlegelmilch, K., Mohseni, M., Kirak, O., Pruszak, J., Rodriguez, J. Renato, Zhou, D., Kreger, Bridget T., Vasioukhin, V., Avruch, J., Brummelkamp, Thijn R. and Camargo, Fernando D. (2011). Yap1 Acts Downstream of α-Catenin to Control Epidermal Proliferation. *Cell*, 144(5), pp.782–795.

Schmitz, A., Lazi'ć, E., Koumaki, D., Kuonen, F., Verykiou, S. and Rübsam, M. (2015). Assessing the In Vivo Epidermal Barrier in Mice: Dye Penetration Assays. *Journal of Investigative Dermatology*, [online] 135(2), pp.1–4. Available at: https://pubmed.ncbi.nlm.nih.gov/25573050/.

Schneider, M., Lu, W., Neumann, S., Brachner, A., Gotzmann, J., Noegel, A.A. and Karakesisoglou, I. (2010). Molecular mechanisms of centrosome and cytoskeleton anchorage at the nuclear envelope. *Cellular and Molecular Life Sciences*, [online] 68(9), pp.1593–1610. Available at: https://pubmed.ncbi.nlm.nih.gov/20922455/.

Ścieżyńska, A., Nogowska, A., Sikorska, M., Konys, J., Karpińska, A., Komorowski, M., Ołdak, M. and Malejczyk, J. (2018). Isolation and culture of human primary keratinocytes – a methods review. *Experimental Dermatology*. [online] Available at: https://onlinelibrary.wiley.com/doi/full/10.1111/exd.13860.

Seetharaman, S., Vianay, B., Roca, V., De Pascalis, C., Boëda, B., Dingli, F., Loew, D., Vassilopoulos, S., Théry, M. and Etienne-Manneville, S. (2020). *Microtubules tune*

mechanosensitive cell responses. [online] Available at: https://www.biorxiv.org/content/10.1101/2020.07.22.205203v1.abstract.

Seo, M.-D., Kang, T.-J., Lee, C.-H., Lee, A.-Y. and Noh, M.-S. (2012). HaCaT Keratinocytes and Primary Epidermal Keratinocytes Have Different Transcriptional Profiles of Cornified Envelope-Associated Genes to T Helper Cell Cytokines. *Biomolecules and Therapeutics*, [online] 20(2), pp.171–176. Available at: https://www.ncbi.nlm.nih.gov/pmc/articles/PMC3792214/.

Shi, R., Xu, L., Huang, L. and Cheng, J.-X. (2020). Nucleoporin 107 Promotes the Survival of Tumor Cells in Cervical Cancers. *Gynecologic and Obstetric Investigation*, [online] 85(1), pp.41–52. Available at: https://www.karger.com/Article/Abstract/502788.

Sigma-Aldrich. (2021). Bovine Serum Albumins - Albumin | Sigma-Aldrich. [online] Available at: https://www.sigmaaldrich.com/life-science/biochemicals/biochemical-products.html?TablePage=103994915#:~:text=Bovine%20serum%20albumin%20(BSA)%20is,of%20interference%20within%20biological%20reactions.&text=BSA%20is%20a%20single%20polypeptide,acid%20residues%20and%20no%20carbohydrates..

Simard-Bisson, C., Parent, L.A., Moulin, V.J. and Fruteau de Laclos, B. (2018). Characterization of Epidermal Lipoxygenase Expression in Normal Human Skin and Tissue-Engineered Skin Substitutes. *Journal of Histochemistry & Cytochemistry*, [online] 66(11), pp.813–824. Available at: https://www.ncbi.nlm.nih.gov/pmc/articles/PMC6213569/.

Simpson, C.L., Patel, D.M. and Green, K.J. (2011). Deconstructing the skin: cytoarchitectural determinants of epidermal morphogenesis. *Nature Reviews Molecular Cell Biology*, [online] 12(9), pp.565–580. Available at: https://www.nature.com/articles/nrm3175.

Sivaramakrishnan, S., DeGiulio, J.V., Lorand, L., Goldman, R.D. and Ridge, K.M. (2008). Micromechanical properties of keratin intermediate filament networks. *Proceedings of the National Academy of Sciences*, [online] 105(3), pp.889–894. Available at: https://www.pnas.org/content/105/3/889.short.

Smiley, A.K., Klingenberg, J.M., Aronow, B.J., Boyce, S.T., Kitzmiller, Wj. and Supp, D.M. (2005). Microarray Analysis of Gene Expression in Cultured Skin Substitutes Compared with Native Human Skin. *Journal of Investigative Dermatology*, [online] 125(6), pp.1286–1301. Available at: https://pubmed.ncbi.nlm.nih.gov/16354201/.

Smiley, A.K., Klingenberg, J.M., Boyce, S.T. and Supp, D.M. (2006). Keratin expression in cultured skin substitutes suggests that the hyperproliferative phenotype observed in vitro is normalized after grafting. *Burns*, [online] 32(2), pp.135–138. Available at: https://pubmed.ncbi.nlm.nih.gov/16455203/.

Smits, J.P.H., Niehues, H., Rikken, G., van Vlijmen-Willems, I.M.J.J., van de Zande, G.W.H.J.F., Zeeuwen, P.L.J.M., Schalkwijk, J. and van den Bogaard, E.H. (2017). Immortalized N/TERT keratinocytes as an alternative cell source in 3D human epidermal models. *Scientific Reports*, [online] 7(1). Available at: https://www.nature.com/articles/s41598-017-12041-y.

Soares, C.P., Midlej, V., Oliveira, M.E.W. de, Benchimol, M., Costa, M.L. and Mermelstein, C. (2012). 2D and 3D-Organized Cardiac Cells Shows Differences in Cellular Morphology, Adhesion Junctions, Presence of Myofibrils and Protein Expression. *PLoS ONE*, [online] 7(5), p.e38147. Available at: https://journals.plos.org/plosone/article?id=10.1371/journal.pone.0038147#s1.

Soares, E. and Zhou, H. (2017). Master regulatory role of p63 in epidermal development and disease. *Cellular and Molecular Life Sciences*, [online] 75(7), pp.1179–1190. Available at: https://www.ncbi.nlm.nih.gov/pmc/articles/PMC5843667/#:~:text=In%20summary%2C%20p63%20is%20likely,to%20shape%20the%20chromatin%20and.

Solon, J., Levental, I., Sengupta, K., Georges, P.C. and Janmey, P.A. (2007). Fibroblast Adaptation and Stiffness Matching to Soft Elastic Substrates. *Biophysical Journal*, [online] 93(12), pp.4453–4461. Available at: https://www.sciencedirect.com/science/article/pii/S000634950771696X.

Sosnova-Netukova, M., Kuchynka, P. and Forrester, J.V. (2007). The suprabasal layer of corneal epithelial cells represents the major barrier site to the passive

movement of small molecules and trafficking leukocytes. *British Journal of Ophthalmology*, [online] 91(3), pp.372–378. Available at: https://www.ncbi.nlm.nih.gov/pmc/articles/PMC1857692/.

Sotiropoulou, P.A. and Blanpain, C. (2012). Development and Homeostasis of the Skin Epidermis. *Cold Spring Harbor Perspectives in Biology*, [online] 4(7), pp.a008383–a008383. Available at: https://cshperspectives.cshlp.org/content/4/7/a008383.full.pdf+html.

Stark, H.-J., Baur, M., Breitkreutz, D., Mirancea, N. and Fusenig, N.E. (1999). Organotypic Keratinocyte Cocultures in Defined Medium with Regular Epidermal Morphogenesis and Differentiation. *Journal of Investigative Dermatology*, [online] 112(5), pp.681–691. Available at: https://pubmed.ncbi.nlm.nih.gov/10233757/.

Stewart, R.M., Zubek, A.E., Rosowski, K.A., Schreiner, S.M., Horsley, V. and King, M.C. (2015). Nuclear–cytoskeletal linkages facilitate cross talk between the nucleus and intercellular adhesions. *Journal of Cell Biology*, [online] 209(3), pp.403–418. Available at: https://pdfs.semanticscholar.org/f5c4/33df5cd50c29f374f12ef7ff643bfce891fe.pdf.

Stroud, M.J. (2018). Linker of nucleoskeleton and cytoskeleton complex proteins in cardiomyopathy. *Biophysical Reviews*, [online] 10(4), pp.1033–1051. Available at: https://link.springer.com/article/10.1007/s12551-018-0431-6#Sec3.

Sumigray, K.D., Foote, H.P. and Lechler, T. (2012). Noncentrosomal microtubules and type II myosins potentiate epidermal cell adhesion and barrier formation. *Journal of Cell Biology*, [online] 199(3), pp.513–525. Available at: https://rupress.org/jcb/article/199/3/513/37038/Noncentrosomal-microtubules-and-type-II-myosins.

Swift, J., Ivanovska, I.L., Buxboim, A., Harada, T., Dingal, P.C.D.P., Pinter, J., Pajerowski, J.D., Spinler, K.R., Shin, J.-W., Tewari, M., Rehfeldt, F., Speicher, D.W. and Discher, D.E. (2013). Nuclear Lamin-A Scales with Tissue Stiffness and Enhances Matrix-Directed Differentiation. *Science*, [online] 341(6149), p.1240104. Available at: https://science.sciencemag.org/content/341/6149/1240104/tab-pdf.

Takeuchi, H. and Rünger, T.M. (2013). Longwave UV Light Induces the Aging-Associated Progerin. *Journal of Investigative Dermatology*, [online] 133(7), pp.1857–1862. Available at: https://pubmed.ncbi.nlm.nih.gov/23392295/.

Thakar, K., May, C.K., Rogers, A. and Carroll, C.W. (2017). Opposing roles for distinct LINC complexes in regulation of the small GTPase RhoA. *Molecular Biology of the Cell*, [online] 28(1), pp.182–191. Available at: https://pubmed.ncbi.nlm.nih.gov/28035049/.

The Human Protein Atlas. (2020). NAAA - Cell Type Atlas. [online] Available at: https://www.proteinatlas.org/ENSG00000138744-NAAA/celltype [Accessed 25 Sep. 2021].

Tibbitt, M.W. and Anseth, K.S. (2009). Hydrogels as extracellular matrix mimics for 3D cell culture. *Biotechnology and Bioengineering*, [online] 103(4), pp.655–663. Available at: https://www.ncbi.nlm.nih.gov/pmc/articles/PMC2997742/?report=reader#!po=19.4444.

Totaro, A., Castellan, M., Battilana, G., Zanconato, F., Azzolin, L., Giulitti, S., Cordenonsi, M. and Piccolo, S. (2017). YAP/TAZ link cell mechanics to Notch signalling to control epidermal stem cell fate. *Nature Communications*, [online] 8(1). Available at: https://www.nature.com/articles/ncomms15206.

Toutfaire, M., Bauwens, E. and Debacq-Chainiaux, F. (2017). The impact of cellular senescence in skin ageing: A notion of mosaic and therapeutic strategies. *Biochemical Pharmacology*, [online] 142, pp.1–12. Available at: https://www.sciencedirect.com/science/article/pii/S0006295217302009?casa_token=soKdLRo6qQQAAAAA:_jQft-yWXftml53YktjZMqbShm-5VZ5JvTbYp1yc2d_D58HEv_RtwuQZPJMk1UgHGkNHo_yr#b0070.

Trappmann, B., Gautrot, J.E., Connelly, J.T., Strange, D.G.T., Li, Y., Oyen, M.L., Cohen Stuart, M.A., Boehm, H., Li, B., Vogel, V., Spatz, J.P., Watt, F.M. and Huck, W.T.S. (2012). Extracellular-matrix tethering regulates stem-cell fate. *Nature*

Materials, [online] 11(7), pp.642–649. Available at: https://pubmed.ncbi.nlm.nih.gov/22635042/.

Truong, A.B., Kretz, M., Ridky, T.W., Kimmel, R. and Khavari, P.A. (2006). p63 regulates proliferation and differentiation of developmentally mature keratinocytes. *Genes & Development*, [online] 20(22), pp.3185–3197. Available at: https://pubmed.ncbi.nlm.nih.gov/17114587/.

TrypLE Express User Guide. (2020). [online] Thermo Fisher Scientific. Available at: https://assets.thermofisher.com/TFS-Assets/LSG/manuals/tryplE_man.pdf.

Tsujita-Kyutoku, M., Kiuchi, K., Danbara, N., Yuri, T., Senzaki, H. and Tsubura, A. (2003). p63 expression in normal human epidermis and epidermal appendages and their tumors. *Journal of Cutaneous Pathology*, [online] 30(1), pp.11–17. Available at: https://pubmed.ncbi.nlm.nih.gov/12534798/.

Tunggal, J.A., Helfrich, I., Schmitz, A., Schwarz, H., Günzel, D., Fromm, M., Kemler, R., Krieg, T. and Niessen, C.M. (2005). E-cadherin is essential for in vivo epidermal barrier function by regulating tight junctions. *The EMBO Journal*, [online] 24(6), pp.1146–1156. Available at: https://www.ncbi.nlm.nih.gov/pmc/articles/PMC556407/.

Van Bael, S., Chai, Y.C., Truscello, S., Moesen, M., Kerckhofs, G., Van Oosterwyck, H., Kruth, J.-P. . and Schrooten, J. (2012). The effect of pore geometry on the in vitro biological behavior of human periosteum-derived cells seeded on selective laser-melted Ti6Al4V bone scaffolds. *Acta Biomaterialia*, [online] 8(7), pp.2824–2834. Available at: https://www.sciencedirect.com/science/article/abs/pii/S1742706112001481?via%3Dihub.

van Smeden, J. and Bouwstra, J.A. (2016). Stratum Corneum Lipids: Their Role for the Skin Barrier Function in Healthy Subjects and Atopic Dermatitis Patients. *Current Problems in Dermatology*, [online] 49, pp.8–26. Available at: https://www.karger.com/Article/Abstract/441540#:~:text=The%20skin%20barrier%20is%20located,the%20body%20via%20the%20epidermis..

Wagner, B., Tharmann, R., Haase, I., Fischer, M. and Bausch, A.R. (2006). Cytoskeletal polymer networks: The molecular structure of cross-linkers determines macroscopic properties. *Proceedings of the National Academy of Sciences*, [online] 103(38), pp.13974–13978. Available at: https://pubmed.ncbi.nlm.nih.gov/16963567/.

Wahlsten, A., Rütsche, D., Nanni, M., Giampietro, C., Biedermann, T., Reichmann, E. and Mazza, E. (2021). Mechanical stimulation induces rapid fibroblast proliferation and accelerates the early maturation of human skin substitutes. *Biomaterials*, [online] 273, p.120779. Available at: https://www.sciencedirect.com/science/article/pii/S0142961221001356.

Wälde, S., Thakar, K., Hutten, S., Spillner, C., Nath, A., Rothbauer, U., Wiemann, S. and Kehlenbach, R.H. (2011). The Nucleoporin Nup358/RanBP2 Promotes Nuclear Import in a Cargo- and Transport Receptor-Specific Manner. *Traffic,* [online] 13(2), pp.218–233. Available at: https://onlinelibrary.wiley.com/doi/full/10.1111/j.1600-0854.2011.01302.x.

Walko, G., Castañón, M.J. and Wiche, G. (2015). Molecular architecture and function of the hemidesmosome. *Cell and Tissue Research*, [online] 360(3), pp.529–544. Available at: https://www.ncbi.nlm.nih.gov/pmc/articles/PMC4452579/.

Wang, F., Zhan, R., Chen, L., Dai, X., Wang, W., Guo, R., Li, X., Li, Z., Wang, L., Huang, S., Shen, J., Li, S. and Cao, C. (2017). RhoA promotes epidermal stem cell proliferation via PKN1-cyclin D1 signaling. *PLoS ONE*, [online] 12(2), p.e0172613. Available at: https://www.ncbi.nlm.nih.gov/pmc/articles/PMC5319766/.

Wang, L.-S., Chung, J.E. and Kurisawa, M. (2012). Controlling Fibroblast Proliferation with Dimensionality-Specific Response by Stiffness of Injectable Gelatin Hydrogels. *Journal of Biomaterials Science, Polymer Edition*, [online] 23(14), pp.1793–1806. Available at: https://pubmed.ncbi.nlm.nih.gov/21943785/.

Wang, W., Zuidema, A., te Molder, L., Nahidiazar, L., Hoekman, L., Schmidt, T., Coppola, S. and Sonnenberg, A. (2020). Hemidesmosomes modulate force generation via focal adhesions. *Journal of Cell Biology*, [online] 219(2). Available at:

https://rupress.org/jcb/article/219/2/e201904137/133567/Hemidesmosomes-modulate-force-generation-via-focal.

Watt, F.M. (2002). NEW EMBO MEMBER'S REVIEW: Role of integrins in regulating epidermal adhesion, growth and differentiation. *The EMBO Journal*, [online] 21(15), pp.3919–3926. Available at: https://www.embopress.org/doi/full/10.1093/emboj/cdf399.

Weaver, V.M., Petersen, O.W., Wang, F., Larabell, C.A., Briand, P., Damsky, C. and Bissell, M.J. (1997). Reversion of the Malignant Phenotype of Human Breast Cells in Three-Dimensional Culture and In Vivo by Integrin Blocking Antibodies. *Journal of Cell Biology*, [online] 137(1), pp.231–245. Available at: https://rupress.org/jcb/article/137/1/231/15446/Reversion-of-the-Malignant-Phenotype-of-Human.

Weinmüllner, R., Zbiral, B., Becirovic, A., Stelzer, E.M., Nagelreiter, F., Schosserer, M., Lämmermann, I., Liendl, L., Lang, M., Terlecki-Zaniewicz, L., Andriotis, O., Mildner, M., Golabi, B., Waidhofer-Söllner, P., Schedle, K., Emsenhuber, G., Thurner, P.J., Tschachler, E., Gruber, F. and Grillari, J. (2020). Organotypic human skin culture models constructed with senescent fibroblasts show hallmarks of skin aging. *npj Aging and Mechanisms of Disease*, [online] 6(1). Available at: https://www.nature.com/articles/s41514-020-0042-x.

Wilhelm, M., Schlegl, J., Hahne, H., Gholami, A.M., Lieberenz, M., Savitski, M.M., Ziegler, E., Butzmann, L., Gessulat, S., Marx, H., Mathieson, T., Lemeer, S., Schnatbaum, K., Reimer, U., Wenschuh, H., Mollenhauer, M., Slotta-Huspenina, J., Boese, J.-H., Bantscheff, M. and Gerstmair, A. (2014). Mass-spectrometry-based draft of the human proteome. *Nature*, [online] 509(7502), pp.582–587. Available at: https://www.nature.com/articles/nature13319.

Wilhelmsen, K., Litjens, S.H.M., Kuikman, I., Tshimbalanga, N., Janssen, H., van den Bout, I., Raymond, K. and Sonnenberg, A. (2005). Nesprin-3, a novel outer nuclear membrane protein, associates with the cytoskeletal linker protein plectin.

Journal of Cell Biology, [online] 171(5), pp.799–810. Available at: https://www.ncbi.nlm.nih.gov/pmc/articles/PMC2171291/.

Wilson, V.G. (2013). Growth and Differentiation of HaCaT Keratinocytes. *Methods in Molecular Biology*, [online] pp.33–41. Available at: https://link.springer.com/protocol/10.1007/7651_2013_42.

Woappi, Y., Altomare, D., Creek, K.E. and Pirisi, L. (2020). Self-assembling 3D spheroid cultures of human neonatal keratinocytes have enhanced regenerative properties. *Stem Cell Research*, [online] 49, p.102048. Available at: https://www.sciencedirect.com/science/article/pii/S1873506120303494.

Wong, C.-W., LeGrand, C.F., Kinnear, B.F., Sobota, R.M., Ramalingam, R., Dye, D.E., Raghunath, M., Lane, E.B. and Coombe, D.R. (2019). In Vitro Expansion of Keratinocytes on Human Dermal Fibroblast-Derived Matrix Retains Their Stem-Like Characteristics. Scientific Reports, [online] 9(1). Available at: https://www.nature.com/articles/s41598-019-54793-9.

Wong, V.W., Longaker, M.T. and Gurtner, G.C. (2012). Soft tissue mechanotransduction in wound healing and fibrosis. Seminars in Cell & Developmental Biology, [online] 23(9), pp.981–986. Available at: https://www.sciencedirect.com/science/article/pii/S1084952112001759.

Wood, A., Sun, H., Jones, M., Percival, H., Broadberry, E., Zindy, E., Lawless, C., Streuli, C., Swift, J., Brennan, K. and Gilmore, A.P. (2020). Increased microenvironment stiffness leads to altered aldehyde metabolism and DNA damage in mammary epithelial cells through a RhoA-dependent mechanism. [online] Available at: https://www.biorxiv.org/content/10.1101/2020.10.06.327726v1.article-info.

Wu, N., Rollin, J., Masse, I., Lamartine, J. and Gidrol, X. (2012). p63 Regulates Human Keratinocyte Proliferation via MYC-regulated Gene Network and Differentiation Commitment through Cell Adhesion-related Gene Network. Journal of Biological Chemistry, [online] 287(8), pp.5627–5638. Available at: https://pubmed.ncbi.nlm.nih.gov/22184109/.

Xiong, B., Loss, R.D., Shields, D., Pawlik, T., Hochreiter, R., Zydney, A.L. and Kumar, M. (2018). Polyacrylamide degradation and its implications in environmental systems. npj Clean Water, [online] 1(1). Available at: https://www.nature.com/articles/s41545-018-0016-8.

Ya, C., Carrancá, M., Sigaudo-Roussel, D., Faure, P., Fromy, B. and Debret, R. (2019). Substrate softness promotes terminal differentiation of human keratinocytes without altering their ability to proliferate back into a rigid environment. Archives of Dermatological Research, [online] 311(10), pp.741–751. Available at: https://pubmed.ncbi.nlm.nih.gov/31392392/.

Yang, A., Kaghad, M., Wang, Y., Gillett, E., Fleming, M.D., Dötsch, V., Andrews, N.C., Caput, D. and McKeon, F. (1998). p63, a p53 Homolog at 3q27–29, Encodes Multiple Products with Transactivating, Death-Inducing, and Dominant-Negative Activities. *Molecular Cell*, [online] 2(3), pp.305–316. Available at: https://www.cell.com/molecular-cell/fulltext/S1097-2765(00)80275-0?_returnURL=https%3A%2F%2Flinkinghub.elsevier.com%2Fretrieve%2Fpii%2FS1097276500802750%3Fshowall%3Dtrue.

Yang, A., Schweitzer, R., Sun, D., Kaghad, M., Walker, N., Bronson, R.T., Tabin, C., Sharpe, A., Caput, D., Crum, C. and McKeon, F. (1999). p63 is essential for regenerative proliferation in limb, craniofacial and epithelial development. *Nature*, [online] 398(6729), pp.714–718. Available at: https://www.nature.com/articles/19539.

Yang, C., Tibbitt, M.W., Basta, L. and Anseth, K.S. (2014). Mechanical memory and dosing influence stem cell fate. *Nature Materials*, [online] 13(6), pp.645–652. Available at: https://www.nature.com/articles/nmat3889.

Yang, Y., Nguyen, E., Narayana, G.H.N.S., Heuzé, M., Mège, R.-M., Ladoux, B. and Sheetz, M.P. (2018). Local Contractions Regulate E-Cadherin Adhesions, Rigidity Sensing and Epithelial Cell Sorting. *bioRxiv*. [online] Available at: https://www.biorxiv.org/content/10.1101/318642v2.full.pdf+html.

Yi-Lei Zhang, Ruo-Chen Wang, Cheng, K., Ring, B.Z. and Su, L. (2016). Roles of Rap1 signaling in tumor cell migration and invasion. *Cancer Biology & Medicine*,

[online] 14(1), pp.90–99. Available at: http://www.cancerbiomed.org/index.php/cocr/article/view/1012/1128.

Young, P. (2003). E-cadherin controls adherens junctions in the epidermis and the renewal of hair follicles. *The EMBO Journal*, [online] 22(21), pp.5723–5733. Available at: https://www.ncbi.nlm.nih.gov/pmc/articles/PMC275417/.

Yousef, H., Alhajj, M. and Sharma, S. (2021). Anatomy, Skin (Integument), *Epidermis*. [online] StatPearls. Available at: https://www.ncbi.nlm.nih.gov/books/NBK470464/.

Yu, F., Fu, R., Xie, Y. and Chen, W. (2015). Isolation and Characterization of Polyacrylamide-Degrading Bacteria from Dewatered Sludge. *International Journal of Environmental Research and Public Health*, [online] 12(4), pp.4214–4230. Available at: https://www.ncbi.nlm.nih.gov/pmc/articles/PMC4410243/.

Yu, F.-X. . and Guan, K.-L. . (2013). The Hippo pathway: regulators and regulations. *Genes & Development*, [online] 27(4), pp.355–371. Available at: https://pubmed.ncbi.nlm.nih.gov/23431053/.

Zarkoob, H., Bodduluri, S., Ponnaluri, S.V., Selby, J.C. and Sander, E.A. (2015). Substrate Stiffness Affects Human Keratinocyte Colony Formation. *Cellular and Molecular Bioengineering*, [online] 8(1), pp.32–50. Available at: https://www.ncbi.nlm.nih.gov/pmc/articles/PMC4442095/.

Zeltinger, J., Landeen, L.K., Alexander, H.G., Kidd, I.D. and Sibanda, B. (2001). Development and Characterization of Tissue-Engineered Aortic Valves. *Tissue Engineering*, [online] 7(1), pp.9–22. Available at: https://pubmed.ncbi.nlm.nih.gov/11224920/.

Zhong, S.P., Zhang, Y.Z. and Lim, C.T. (2010). Tissue scaffolds for skin wound healing and dermal reconstruction. *WIREs Nanomedicine and Nanobiotechnology*, [online] 2(5), pp.510–525. Available at: https://wires.onlinelibrary.wiley.com/doi/full/10.1002/wnan.100.

Zhu, R., Antoku, S. and Gundersen, G.G. (2017). Centrifugal Displacement of Nuclei Reveals Multiple LINC Complex Mechanisms for Homeostatic Nuclear Positioning. *Current Biology*, [online] 27(20), pp.3097-3110.e5. Available at: https://www.sciencedirect.com/science/article/pii/S0960982217311132.